



**SCIENTIFIC COMMITTEE
SEVENTEENTH REGULAR SESSION
ELECTRONIC MEETING
11-19 August 2021**

Input data for the 2021 South Pacific blue shark (*Prionace glauca*) stock assessment

WCPFC-SC17-2021/SA-IP-18

**Philip Neubauer¹, Kath Large¹, Stephen Brouwer², Mikihiko Kai³ and
Wen-Pei Tasi⁴ and Kwang-Ming Liu⁵**

¹ Dragonfly Data Science

² Saggittus Consulting

³ Fisheries Resources Institutes, Japan Fisheries Research and Education Agency

⁴ National Kaohsiung University of Science and Technology

⁵ National Taiwan Ocean University



Input data for the 2021 South Pacific Blue Shark stock assessment

Authors:

Philipp Neubauer
Kath Large
Stephen Brouwer
Mikihiko Kai
Wen - Pei Tsai
Kwang - Ming Liu





Cover Notes

To be cited as:

Neubauer, Philipp; Large, Kath; Brouwer, Stephen; Kai, Mikihiko; Tsai, Wen-Pei; Liu, Kwang-Ming (2021). Input data for the 2021 South Pacific Blue Shark stock assessment, 158 pages. WCPFC-SC17-2021/SA-IP-18. Report to the WCPFC Scientific Committee. Seventeenth Regular Session, 13–20 August 2018.

CONTENTS

EXECUTIVE SUMMARY	3
1 INTRODUCTION	4
2 METHODS	4
2.1 Description of datasets	4
2.2 Length frequency for assessments	6
2.3 Catch reconstruction	6
2.3.1 Prediction of catch rates from observed sets	6
2.3.2 Extrapolation of observed catch rates to WCPO - wide effort	8
2.3.3 Adjusting for discarding and condition at release	8
2.3.4 CPUE from observer catch - rate model	9
2.3.5 CPUE from Chinese - Taipei observer data	10
2.4 Logsheets CPUE standardisation	10
3 RESULTS	11
3.1 Length frequency data	11
3.2 Models of catch rates based on observer data	12
3.2.1 Observer data	12
3.2.2 Historical catch reconstructions	12
3.2.3 Estimates of discard fate	13
3.2.4 Standardised CPUE from observer data	13
3.2.5 Standardised CPUE from observer data - Chinese - Taipei	14
3.3 CPUE standardisation for logsheets CPUE data	14
3.3.1 Japanese catch and effort data	14
3.3.2 Chinese Taipei catch and effort data	15
3.3.3 Standardisation of logsheets data	15
4 DISCUSSION	18
5 REFERENCES	19
TABLES	21

FIGURES	23
A OBSERVER MODEL DIAGNOSTICS	50
B LOGSHEET CPUE STANDARDISATION DIAGNOSTICS	57
B.1 New Zealand fleet high latitude CPUE	57
B.2 EU fleet CPUE	71
B.3 Japan low latitude CPUE	84
B.4 Alternative CPUE standardisations	105
B.4.1 Chinese Taipei low latitude CPUE	105
B.4.2 Australian low latitude CPUE	118
B.4.3 Australian high latitude CPUE	132
B.4.4 Combined low latitude CPUE	145

EXECUTIVE SUMMARY

Blue shark (*Prionace glauca*) are targeted and caught as bycatch in tuna and billfish fisheries in the WCPFC and globally. The present report details data inputs for the South Pacific stock assessment for blue shark, including length frequency information from regional observer programmes, reconstructed catch histories, and a number of alternative catch-rate (CPUE) series.

Length frequencies showed a substantial difference between high latitude (south of 35°South) and low latitude fisheries, with high latitude fisheries catching both juveniles (approx. 50 cm+) and mature animals (≤ 200 cm), whereas lower latitude fisheries encounter mostly large animals (around 200 cm). The EU longline fleet appear to also catch the largest size animals (250 cm+), which do not appear in any other fishery. Based on the length frequency analysis, subsequent analyses were structured latitudinally, or included appropriate standardisation variables to account for spatial and temporal differences in trends among these fisheries.

Catch was reconstructed from observer data using a Bayesian implementation of a spatial GLMM, including a term for non-linear effects of total effect by latitude. The model produced good diagnostics, and led to trend estimates that were comparable to previous analyses, albeit at lower median estimated total catches than previous analysis. Nevertheless, the Bayesian model also produced high uncertainties in catches between the mid 1990s and early 2000s, with overall catches ranging between 100 000 and 1 million sharks per year (90% confidence).

CPUE trends from observer models were found to be dominated by observer effort in a restricted area before the mid-2000s, leading us to question their usefulness as indices of abundance for the larger area. Logsheet CPUE series were attempted, using delta-lognormal GLM models, for a number of areas and fleets, including New Zealand, Australian, Japanese and Chinese-Taipei fleets. Grooming for vessels with consistent reporting attempted to remove vessels with poor reporting rates, and we retained only series from positive observations, discarding presence absence components as potentially biased due to changes in reporting. Although there was some variability among series, there were also consistent trends: all series showed some level of increase in CPUE in the recent decade. In addition, when accounting for ontogeny, high latitude trends align well with low-latitude trends for larger individuals. Disagreements among indices arose mainly for early CPUE (late 1990s), where both the Australian and Japanese indices showed declines between the mid-1990s and early-2000s, while the high latitude indices did not show corresponding declines.

Our results show a reasonable amount of consistency among datasets in recent trends, suggesting that blue shark may have been increasing after fishing mortality dropped in the early 2000s. Trends in the 1990s are less certain, due to poor observer coverage, and poor reporting of sharks in logsheet data. Nevertheless, there is some evidence that the adult spawning stock declined during the late 1990s and early 2000s in low latitudes, but catch rates may have been less affected in high latitudes.

1. INTRODUCTION

Blue shark (*Prionace glauca*) are caught in association with tuna and billfish in global pelagic longline fisheries. In the pacific, they are thought to be divided into two stocks at the Equator. South Pacific blue sharks are caught in large numbers off New Zealand, Southern Australia and the high seas to the north and east of New Zealand, but catches are observed throughout the Western and Central Pacific Fisheries Commission Convention Area (WCPFC-CA), albeit at lower catch rates (Brouwer et al. 2021). Despite their prevalence in longline catch, the catch history and recent trends remain highly uncertain (e.g., Tremblay-Boyer & Takeuchi 2016).

In order to track changes in stock abundance through time, estimates of catch are required to undertake a meaningful stock assessment. Catch reporting of sharks in the Pacific Ocean has been relatively poor prior to, and since, the inception of the Western and Central Pacific Fisheries Commission (WCPFC). While catch reporting on logsheets and observer coverage has improved in Western and Central Pacific Ocean (WCPO) longline fisheries in recent years (Brouwer et al. 2021), accurate catch records for all WCPFC Key Sharks is generally poor prior to about 2015 (Brouwer and Hamer 2020). An additional complication for elucidating shark catch, is the change to regulations within the WCPFC that not only require reporting, but also the release in unwanted sharks (WCPFC 2019 and its predecessors). These changes have both increased reported landings and decreased landing frequency of WCPFC Key Sharks including blue sharks (Brouwer et al. 2021). These changes and the resulting variability of shark reporting has resulted in a lack of confidence in the shark data overall.

In order to overcome problematic shark reporting WCPO shark catch reconstruction has been undertaken to estimate shark catch using observed catch data (Lawson 2011, Rice 2012, Tremblay-Boyer and Takeuchi 2016, Peatman et al. 2018) or fin trade information (Clarke 2009). In addition, a range of approaches were trialled to elucidate relative abundance indices that may be useful indicators of abundance in various regions across the South Pacific (Tremblay-Boyer and Takeuchi 2016). However, these indices were found to be variable among data sources, and potentially in conflict.

Here we build on previous analyses to reconstruct catch histories and develop standardised catch per unit of effort (CPUE) indices as inputs for stock assessment (Neubauer et al. 2021).

2. METHODS

2.1 Description of datasets

We used a range of data-sources supplied by Members, Cooperating Non-Members and Participating Territories (CCMs) of the WCPFC to the Pacific community. These datasets were extracted by SPC upon request, and analysed by the assessment team. In addition, scientists from Japan, Korea and Chinese Taipei were contacted with the intention of working collaboratively to develop blue shark CPUE indices from their longline fleets. A summary of the Japan and Chinese Taipei longline fleets and the resulting CPUE analyses are provided

below. Upon review of the Korean data summaries it was decided not to pursue the development of a CPUE index from that fleet as the data series was short and restricted spatially, and these data were not further progressed for this assessment.

For Japan and Chinese Taipei the assessment team supplied standardised scripts for CPUE to ensure that analyses were comparable between datasets. In summary, the following datasets were used for analysis:

- **L_BEST:** SPC's best (raised) estimates of longline catch and effort (in hooks) for fleets in the WCPFC Convention Area (WCPFC-CA), available at the $5^\circ \times$ month \times year \times flag \times fleet resolution for key species of tuna and billfish, and sharks in some years.
- **Observer programmes for the WCPO longline fleet:** The full observer dataset for the WCPFC longline fleet available to SPC was used for the analysis, including data from the SPC's Regional Observer Programme and national observer programmes. Records collected by longline observers that are relevant to this assessment are key fishing event attributes (including date and time, location), as well as information on gear and catch:
 - Gear/set characteristics (hooks between floats, total number of hooks fished);
 - species;
 - fate code of the catch (e.g., discarded or retained);
 - condition at capture and at release (if not retained);
 - length and the sex of the individual.

The quality and coverage for most variables changes over time and between programmes.

- **Operational logsheet data:** Operational (logsheet) catch and effort data, by day, flag, Exclusive Economic Zone (EEZ), latitude and longitude, set type, catch and effort. Note that logsheet data is not a complete reflection of fishing effort (as estimated in L-BEST), and shark reporting is variable among vessels, fleets, and years (Brouwer and Hamer 2020).

Further detail on datasets and characteristics of the fisheries landing South Pacific blue sharks can be found in Brouwer et al. 2021.

Data preparation largely followed protocols in Tremblay-Boyer and Neubauer 2019. All datasets were filtered to retain records south of the equator within the WCPFC-CA only, over the period of the stock assessment from 1995 to 2020. For the longline observer datasets, when the number of hooks was missing, the number of hooks observed was estimated from the product of hooks-between-floats and the number of baskets observed. Oceanography covariates (sea surface temperature, chlorophyll-*a*, and distance from the coast) were extracted at the lowest resolution possible and aggregated to match the resolution of each dataset. Species targeting clusters were applied following k-means clustering of observed catch proportions as described in Tremblay-Boyer and Neubauer 2019.

2.2 Length frequency for assessments

Length-frequency information as extracted from observer records. All measurements were standardised to fork-length using $FL = 0.8313 \cdot TL - 1.3900$. Fork length distributions were plotted in space and time, by flag and target fishery in order to elicit commonalities and differences between fisheries that catch blue shark.

2.3 Catch reconstruction

Overall fishing related mortality was estimated as the product of overall catch and discarding and fish condition (Figure 1). For each of these components of catch, data were variable in the geographical coverage and information content, and we employed a series of models for these different components in order to estimate total fishing related mortality.

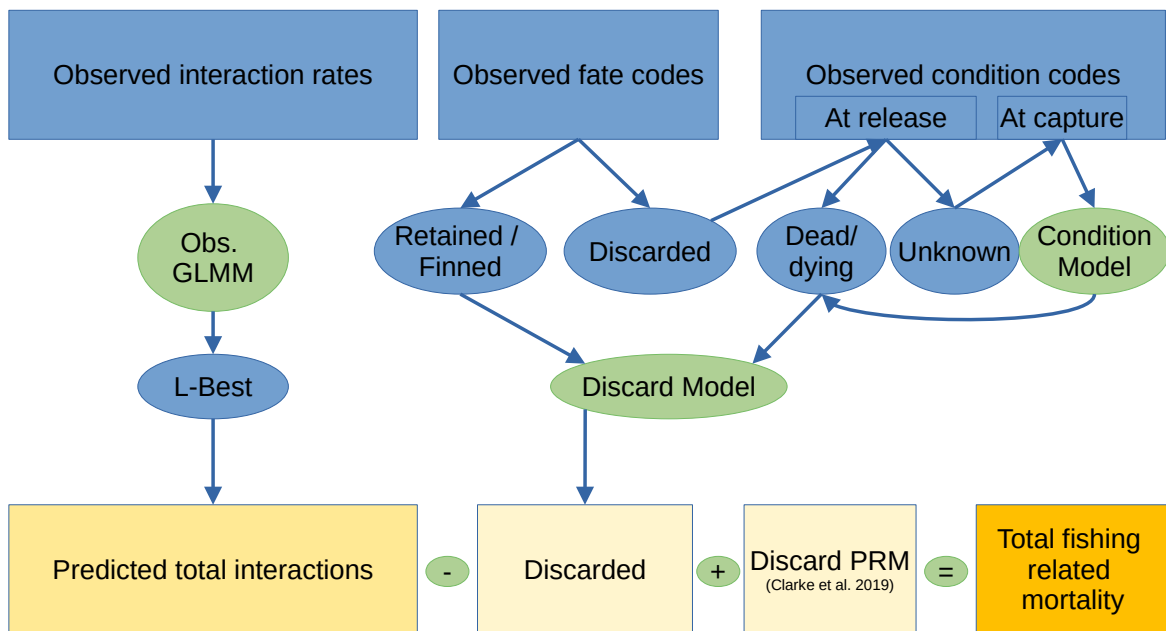


Figure 1: Illustration of the over-all approach used to reconstruct fishing related mortality. Data sources are shown in blue, models and assumptions in green, resulting estimated catch components are shown in orange. Observer catches (interactions) were estimated from observer data, then scaled to overall predicted interactions using the L-Best dataset. These estimates were then scaled by estimates of live discards based on observer discard and condition information, as well by post-release mortality estimates for blue shark.

2.3.1 Prediction of catch rates from observed sets

Overall catches (interactions) were estimated from observer catch rates using generalised linear mixed model. Previous approaches to reconstruct catches for this species have also been based on observer catch data (see Tremblay-Boyer and Takeuchi 2016, Peatman et al. 2018). The basis for these methods is similar: a model of catch-per-unit-effort (CPUE) is built based on observed

sets and relevant covariates, and the model is then used to predict catches based on total effort by fleet across the assessment region.

The previous approaches differ in the modelling framework used to build the catch rate model, and the covariates considered. Tremblay-Boyer and Takeuchi 2016 used generalised linear models (GLMs) with splines for oceanographic covariates to predict catches in unobserved strata. Peatman et al. 2018 used Generalised Estimating Equations (GEEs) to model catch rates, also with a delta-log-normal model structure. The GEE framework allows for the correlation between observed sets in the same observer trips to be accounted for. Catch predictions and uncertainty were estimated with a Monte Carlo simulation approach drawing samples from modelled catch distributions.

We used a similar approach to Tremblay-Boyer and Takeuchi 2016 to model catch rates of blue shark in observer data. We employed generalised linear mixed models with splines for oceanographic predictors, estimated within the general Bayesian framework “*brms*” (Bürkner 2017). We used delta-lognormal models throughout this assessment for catch rates. Although negative binomial error distributions are generally well suited at representing catch rates of bycatch species (Tremblay-Boyer and Neubauer 2019), and are often preferred for highly skewed distributions with large amounts of zeros, blue shark catch rates appear more like those of target species. We found the negative-binomial to produce generally worse diagnostics than the delta-lognormal approach, where initial model runs with negative binomial and zero-inflated negative binomial models showed consistent bias in predictions (i.e., annual capture predictions; Figure A-1).

All models were run using CPUE aggregated to the resolution of the L-Best dataset (i.e., $5^\circ \times 5^\circ$, flag, month) as the response, while allowing for non-linearity in CPUE with effort by including a non-linear term for the number of hooks set per stratum. While it is generally more common to model catch directly as a function of a non-linear term of effort, this can lead to poorly behaving diagnostics for continuous models applied to discrete data. By applying the model to CPUE, we obtain an equivalent model¹ that often shows better behaviour for diagnostics.

All models included spline formulations (estimated as random effects in *brms*) for oceanographic habitat predictors. In addition to oceanographic and geographic predictors, the model included a random effect for the vessel flag (Table 1), allowing the prediction of a distribution for flag effects, which can then be used to predict catches for countries without any observer coverage. Month was fitted as a random effect in the model, and targeting cluster was fitted as a fixed effect. A spline by month and longitude and latitude was used to adjust for within-season spatio-temporal trend in habitat preference (Kai et al. 2017) that are not well described by the predictors in the model. The same linear predictor structure was used for positive catches as well as the presence absence component of the delta-lognormal model.

The final model was written as:

¹The models are strictly equivalent except for the estimated effect for effort: models are related as $\log(Catch) = \alpha + \beta * \log(Effort) \Leftrightarrow \log(Catch/Effort) = \alpha + (\beta - 1) * \log(Effort)$. Therefore, if catch increases less than proportionally to effort, CPUE will decline with increasing effort.

```
f(y) ~ s(log(hooks), by=Lat5) + (1|month) + s(SST) + s(Lon5, Lat5, by=month) +
s(CHLa) + target_cluster + (1 | flag_id)+ (1 | year:flag_id)
```

for $f(y)$ the transformed response, i.e., $\log(\text{CPUE})$ and $\text{logit}(\text{CPUE}>1)$ for the lognormal and binomial component of the delta-lognormal model, respectively.

Models were fitted with eight separate Markov Chain Monte Carlo chains with 3000 iterations each, including 1000 iterations burn-in period that was discarded from posterior samples. Model selection was performed on the basis of model diagnostics. Delta-lognormal models provided reasonable fits (Appendix A) and convergence, as judged by marginal and multivariate scale reduction factors (SRF) across 8 chains (at convergence of MCMC runs, the MSRF (or Rhat) is one).

2.3.2 Extrapolation of observed catch rates to WCPO-wide effort

Predictions to the L-BEST dataset were performed on the basis of available variables in the L-Best dataset. Targeting practice was assumed to be described by the inferred targeting clusters. We avoided predicting on the basis of additional gear characteristics, such as HBF, as these are not consistently available, and uncertainty from imputing such values on the basis of other characteristics cannot be straightforwardly propagated to catch estimates.

We found that predictions (in terms of total numbers, not trends) were highly sensitive to the assumed effect of effort in the model. We compared our model to a version of the model that did not include a non-linear effect for effort (which is more aligned with previously published model predictions that did not employ non-linear scaling).

Models were formally compared using leave-one-out model selection ($LOO - IC = -2 * EPLD$; where the $EPLD$ is the expected log-posterior density under leave one out cross-validation; Vehtari et al. 2016a, 2016b), a measure of the model's predictive accuracy. The LOO-IC is akin to the Akaike Information Criterion (AIC) metric that balances additional complexity in model structure against the improvement in model performance, however, it more strongly penalises model complexity.

2.3.3 Adjusting for discarding and condition at release

Predicted catches are in the form of total interactions - i.e., some of the catch is not retained and released alive, such that fishing related mortality may be substantially different than interactions might suggest. This is especially relevant since recent CMMs for non-retention of sharks have lead to noticeable increases in sharks being cut free and/or discarded (Brouwer and Hamer 2020).

We assumed 100% mortality for retained and/or finned sharks. In addition, for discarded sharks, any sharks that had a condition at release of 'Dead' or 'Alive - dying' were classified as retained. Although information about condition at release is frequently recorded in

recent years, records prior to 2015 often had fate codes indicating discard (e.g., Discarded - other reason; or Discarded, shark damage), but had missing condition-at-release information. Nevertheless, these data often had information on the condition at capture. In order to obtain a better picture of discard mortality prior to 2015, we used a binomial GLMM to infer the condition at release (i.e., dead or likely dying vs. alive and healthy) from the condition at release (cond code), sex, vessel and flag. The latter two effects were fitted as random effects, and the final model for the expected number of mortalities for a given number of records in each stratum was then:

```
condD.num | trials(records) ~ (1 | flag_id) + (1 | vessel_id) + sex_code + cond_code
```

Note that we do not use a temporal variable in this model as most of the data (>53 000 records) with both condition at release and condition at recapture recorded occurs post 2015 (>47 000 of all records). This temporal split in the dataset largely precludes any strong inferences on changes in handling mortality over time for a given condition at capture. Nevertheless, the model above allows us to predict the expected condition of over 112 000 discarded individuals for which the condition at release was not recorded.

To estimate trends in discarding, we used the recorded and imputed discard status to estimate trends in live-discarded individual by flag and latitudinal stratum. The model for blue shark fate was similar, therefore, to the condition model. However, its main purpose was to estimate a rate by year, fleet and latitudinal stratum (LL) that could be applied to estimated catches. The model was written as:

```
FateD.num | trials(records) ~ (1 | flag_id) + (1 | vessel_id) + LL + s(year, by = LL)
```

Models were fitted using MCMC sampling in ‘brms’ as outlined above. We applied the 25%, 50% (median) and 75% percentiles of the posterior distribution of predicted live-discards, discounted by a 17% post-release mortality (Common Oceans (ABNJ) Tuna Project 2019), to predicted catches (posterior median and 90th percentile of predicted catches) to derive the total fishing related mortality used in the stock assessment.

2.3.4 CPUE from observer catch-rate model

In order to improve comparisons of observer CPUE with log-sheet CPUE series, we used the observer catch-reconstruction model to further investigate and standardise trends. In order to derive CPUE that is more comparable to log-sheet CPUE, we adjusted the model above to account for vessel effects (random effect), and replaced the flag ID random effect (which is largely confounded with vessel) with a spatial area effect. Based on length-frequency information, we divided the over-all assessment area into six separate areas to investigate if trends in observer catch-rates differ spatially among the east- and western-WCPO, as well as among latitudinal strata (Figure 2).

2.3.5 CPUE from Chinese-Taipei observer data

To align our analysis with previous attempts at deriving CPUE, we also conducted a stand-alone analysis of the Chinese-Taipei observer data for their high seas fishery. In particular, Tremblay-Boyer and Takeuchi 2016 used predictions for Chinese-Taipei catch rates from an over-all observer CPUE model across flags. We found, however, that due to a lack of observer coverage in that fishery pre-2007, early trends in this series were due to trends in other fisheries (i.e., the over-all year effect in the observer data) rather than observed high-seas CPUE. We therefore constrained our analysis to this dataset post-2007. In addition, flag-based CPUE for Chinese-Taipei includes a large amount of observed effort in Fijian waters which dominates the analysis over the more widespread high-seas fishery (Figure 3). The analysis therefore differs from our analysis of flag-based catch-rates for catch the reconstruction in that it excludes the localised effort and focuses on the high-seas fleet.

The analysis was conducted using a delta-lognormal model for catch-rates, using Area (high vs low latitudes), hooks per basket (HPB) quarter as well as interaction terms for both the log-normal and binomial components of the model.

$$\begin{aligned}\log(\text{CPUE}) &\sim \text{Year} + \text{Quarter} + \text{Area} + \text{HPB} + \text{Quarter*Area} + \text{Quarter*HPB} \\ P(\text{CPUE}>0) &\sim \text{Year} + \text{Quarter} + \text{Area} + \text{HPB} + \text{Quarter*Area} + \text{Quarter*HPB} + \text{Area*HPB}\end{aligned}$$

2.4 Logsheets CPUE standardisation

Log-sheet CPUE was standardised using a standard set of grooming rules and models across a number of fleets. Specifically, based on predicted catches, we conducted independent standardisation analyses for New Zealand ($> 35^{\circ}\text{S}$), Australia (split at 35°S), Japan, Chinese Taipei, and a combination of logsheet data from a range of flags operating in the high seas (FJ, CN, VU, TW, KR). We included TW in this set because a stand-alone standardisation of their logsheet CPUE provided highly variable trends that were not easily interpreted.

All analyses used a set of common grooming rules:

- vessels had to have reported positive BSH catches for at least 3 years;
- vessels had to have reported at least 10 events with BSH captures; and,
- only vessel-years with at least one positive catch were retained.

We compared reporting rates (i.e., proportion of positive sets) between observer records and logsheet data where possible, using predictions from the observer catch-reconstruction to compare with operational reporting. In most cases, this comparison suggested that logsheet reporting rates were lower than predicted probabilities of catch based on observer catch (see results). However, this bias was not evident in the positive catches, and we therefore used a log-normal GLM model for positive catch rates, ignoring the binomial aspect of the data.

We tested that this assumption does not unduly bias our inference by attempting negative-binomial and zero-inflated negative-binomial models on the same datasets. Relatively simple GLM models were chosen for these standardisation in order to facilitate rapid iterations on the models across all analyses and collaborators.

A standard set of predictors was prepared for all analyses, including oceanographic predictors (SST, CHL-a, distance from nearest land). The latter entered the model as splines, while vessel effects, target cluster and month effects were fixed effects in the model. We excluded CHL-a and distance from coast as these variables were highly correlated with SST in some analyses, and we aimed to keep analyses as consistent as possible.

All analyses were diagnosed using tools outlined in Bentley et al. 2012. These include detailed analyses on the fleet composition and its effect on CPUE trends, as well as standard model fit diagnostics for GLMs.

3. RESULTS

3.1 Length frequency data

Length frequencies were highly variable among years, fisheries and fleets. Large individuals (>250cm) were mainly caught in albacore and swordfish target sets, although their occurrence was variable among years (Figure 4). Small blue sharks were largely caught in southern bluefin target sets, although they sporadically appear in other target fisheries (i.e., bigeye, yellowfin) in the mid 1990s, including albacore and swordfish target sets .

Spatially, the largest individuals were caught along the eastern Australian coast between 15°S and 35°S, while the mean lengths were consistently small south of 35°S for most fleets (Figure 5). Distant water fishing fleets, other than the EU and JP, consistently caught larger individuals even south of 35°S, suggesting that juveniles may not be vulnerable to all fleets in these latitudes.

Temporally, most samples initially came from observers on Australian and Japanese vessels mainly operating in the southern Tasman Sea (1990-2000; Figure 6). Between 2000 and the late 2010s, most samples came from NZ observers on New Zealand and Japanese charter vessels operating in NZ waters. Since the mid 2010s, TW, CN and EU (ES) have supplied length frequency samples.

Spatial length frequency patterns are reflected in patterns by flag (Figures 7, 8), with Australian and Japanese samples from Tasmanian and Victorian waters being small, with peaks around ~100 cm. Larger individuals were mainly sampled from lower latitudes (Figure 5). Similar sizes are found in the NZ fishery, however, large individuals make up a greater proportion of fish in this fishery (i.e., fish between 100 and 200 cm). The EU fleet catches slightly larger fish in high latitudes, and TW samples are consistently large, even at high latitudes (~200cm).

At intermediate latitudes (<35°S and >20°S), individuals are larger, and a second peak appears

between 200 and 300cm for the EU fleet. Other samples are mainly around 200cm, which is consistent with the size of sharks captured at low latitudes.

Comparing samples grown according to the Manning and Francis 2005 growth curve for 5 years (orange histograms in Figure 7 and Figure 8), NZ samples appear to align with the common fishery peak at 200cm in lower latitudes. However, small fish in the Australian and Japanese samples appear mostly smaller than this peak, suggesting a lag of >5 years from those areas before fish appear in lower latitude fisheries. Samples from Chinese Taipei, already larger at around 200cm at high latitudes, are consistent with the larger peak in EU catches in intermediate latitudes.

3.2 Models of catch rates based on observer data

3.2.1 Observer data

Observer records were highly heterogeneous in space and time, with early observer effort concentrated in high-latitude fisheries around South-Eastern Australian waters (Figures 10, 12), and a subsequent shift to New Zealand waters for much of the 2000s. Since the late 2010s, a large number of hooks have been observed in higher latitudes on Fijian, Chinese Taipei and Japanese-flagged vessels.

Observed blue-shark captures largely mirror trends in observer coverage, with large numbers of observed BSH captures in Australian and New Zealand waters in the 1990s and 2000s, respectively (Figures 13, 15). Recent observer coverage in fleets from Fiji and Chinese Taipei lead to an increase in reported blue shark in those fisheries. However, their catch rates are still comparatively low, and about an order of magnitude lower than catch rates in higher latitudes (Figures 16, 18, 19).

3.2.2 Historical catch reconstructions

Models based on catch-rate surfaces were necessarily driven by data availability over time. The model corrected overall trends in catch-rates by adjusting for trends in observer effort by countries with different magnitude in catch rates (Figure 20), as well as fishing in areas of preferred habitat at lower sea surface temperatures early on in the time-series (Figure 21). Changes in targeting did not appear to influence overall CPUE (Figure 22).

Although predicted blue shark occurrence from the model was ubiquitous across the South Pacific, the influence of SST and CHL-a (Figure A-5) lead to predictions of highest habitat suitability and CPUE in Tasmanian/South Australian and New Zealand waters (Figure 23), with an over-all higher abundance at latitudes $\geq 35^{\circ}\text{S}$. Consequently, predicted catch rates were about an order of magnitude higher than those in lower latitudes.

Based on L-BEST estimated hooks (Figure 24), we predicted the number of blue-shark by flag and compared total capture against published catch reconstructions for blue shark. For nearly

all years and flags, estimated catches either lined up closely with reported catches (NZ, AU) or exceeded those in logsheets (JP, TW, CN). Recent catches by the FJ, TW, and AU fleets exceeded predictions, suggesting that the model has no information to reproduce these trends (Figure 25).

Total predicted catches were lower than those for previous models, by a factor of about 2/3. This difference almost entirely due to the inclusion of non-linear effects of effort on catch-rates of blue shark: The model with non-linear effects had substantially lower LOO-IC (LOO-IC -11310.1 SE 329.7), indicating clearly improved predictive capacity of the model (LOO-IC -9440.2 [SE 319.9] for the model without non-linear scaling; LOO-IC difference: 1870; SE 40); suggesting that CPUE declines substantially with effort applied within monthly 5x5 strata in the chosen model (Figure 27). The model with non-linear latitudinal effects was also substantially better than a comparable model without latitudinal effects (LOO-IC difference 102.8; SE 27.2). However, relative trends are very similar to previous models. Predictions from our model suggested an increase in BSH catches in the early 1990s, followed by steady catches around 300 thousand individuals per year. Our model also predicts declining catches predicted between the early 2000s and about 2008, but contrary to previous models, shows a relatively small increase in captures between 2008 and 2012, with a subsequent decline. The model also showed substantial uncertainty in predicted catches in the 1990s and early 2000s, with the potential for large captures of up to 1 million animals annually during that period.

3.2.3 Estimates of discard fate

Discard fate based on reported discarding, and discard conditions, together with inferred condition from the condition code model (Figure A-7), was modeled as a smooth term as a function of time. The model inferred low live-discard rates before 2010, with a steady increase in live discards since then, in both high and low latitudes (Figure 28). Data was sparse for most fleets, and discarding trends by flag have a high degree of uncertainty. Nevertheless, for fleets with high catches and catch rates, inferred trends were relatively well modeled (Figure 29). While discarding in NZ and AU was predicted to follow the more general trend, other fisheries, like JP and TW, had high retention rates even in recent years.

Applying discard estimates and their uncertainty to estimated total interactions, leads to a range of scenarios for total fishing related mortality (Figures 30, 31, 32, 33). With a high discard scenario, fishing related deaths in both high and low latitudes declined rapidly since ~ 2012, leading to a steady decline since the late 1990s in low latitudes. In comparison, with the low discard scenario, fishing related mortality remains nearly unchanged, and may have increased in high latitudes in recent years.

3.2.4 Standardised CPUE from observer data

Observer CPUE was high and increasing for many fleets in the 1990s, such as AU, JP and sporadic observations from other flags (Figure 34); these high estimates were largely due to

fishing in southern Tasman sea waters during the period (Figure 17). CPUE for AU and JP dropped sharply in the early 2000s with highly reduced observer coverage and shifting of fishing effort to higher latitudes. In absolute terms (Figure 35), these CPUE trends were small compared with those seen in New Zealand waters, where a substantial increase was estimated. Most other flag-year effects were relatively stable but highly variable, especially in early years (i.e., late 1990s, early 2000s).

The alternative CPUE model showed a strong regional pattern, with high early CPUE in Eastern areas (Figures 36–38). That pattern was reflected at western low latitudes, but those trends were highly uncertain.

3.2.5 Standardised CPUE from observer data - Chinese-Taipei

Standardised observer data from the Chinese-Taipei observer programme alone suggested a strong increase in CPUE in recent years (Figure 39; Figures A-9, A-10). The model also suggested large differences in catch probabilities by latitudinal stratum (Tables 2 & 3).

3.3 CPUE standardisation for logsheet CPUE data

3.3.1 Japanese catch and effort data

The data from the Japanese fleet was analysed at the Fisheries Resources Institutes (FRI), Japan Fisheries Research and Education Agency. These data are from longline logsheets from vessels fishing between 1994 and 2019, and from the equator South to 60°S within the WCPFC-CA (Figure B-40). The data were split into a tropical component, defined as catch occurring between the equator and 30°S; and a temperate area (30–60°S). The tropical fishery is dominated by catch of albacore, yellowfin and bigeye, while the temperate catch is dominated by albacore and, to a lesser extent, southern bluefin tuna (Figure B-41). The vessels tend to fish across the WCPO north of 10°S. But, south of 10°S they generally fished west of the 180° line of longitude.

Logsheets reporting has changed throughout this time due to changes in regulations (e.g. WCPFC 2019 and its predecessors) governing the retention of sharks. This has reduced the number of sharks retained, which declined after 2011 and has remained relatively low (particularly from 2015 onwards). But, at that time, the number of hooks set and a spatial distribution of fishing operations south of the Equator in the WCPFC-CA, also dropped appreciably (Figure B-42; Figure B-43). It is considered that these changes are the main contributor to the strong decline in reporting rates of sharks from 2016 onwards, particularly in the tropics (Figure B-44).

The number of hooks between floats for this fleet has remained relatively consistent in the tropical waters at around 15 hooks between floats, but in the temperate waters has increased from <10 prior to 2000, to around 10 hooks between floats in the last two decades (Figure B-45). Branchline length has remained relatively consistent at about 40m both in the tropical and temperate fisheries (Figure B-46). The median floatline length is longer in the tropical fishery

(~40m) than the temperate fishery (~20m), suggesting that the vessels set deeper sets targeting bigeye tuna in the tropics compared to the temperate regions.

The positive catch ratios of blue shark for the Japanese fleet were relatively steady (Figure B-47). In the tropics between 50 and 60% of vessels recorded shark catch from 1994-2011, this dropped to about 40% in 2012-2014, and dropped again to 20% or less from 2015 onwards. Sets recording the positive catch of blue shark were lower in the tropics at 20-30% prior to 2015 and 10% or less from 2016 onwards.

3.3.2 Chinese Taipei catch and effort data

The data from the Chinese Taipei fleet were analysed at the National Kaohsiung University of Science and Technology and National Chinese Taipei Ocean University. These data are from longline logsheets for vessels fishing between 2007 and 2019, and from the equator South to 45°S within the WCPFC Convention Area. The fleet has fished mostly on the high seas across the Convention Area from the equator to about 10°S, on the high seas in the eastern extreme of the Convention area from the equator south to 35°S, and across the southern high seas of the convention area between 25°S and 45°S.

The number of sets and hooks set increased from 2007-2012, and declined after that through to 2016, and then increased slightly in the most recent few years. Total blue shark catch, however, has increased through time from 2007 to 2019. The resulting nominal CPUE is relatively flat from 2007 to 2013 and increases almost continuously over the most recent six years. The vessels target tuna and have low shark catch rates with a high proportion of zero blue shark catch events.

3.3.3 Standardisation of logsheet data

General observations Most log-normal standardisation models performed well by standard model-fit diagnostics (see Appendix B). Negative binomial models and their zero-inflated counterparts did not always converge, and did not improve diagnostics or show substantially different trends.

Generally, we found habitat preferences that mirror those found in the northern hemisphere (Kai et al. 2017), i.e., increased abundance for temperatures around 15°C during the Austral summer (January to March).

New Zealand CPUE Comparison with observer data suggests that until recently, logsheets did not report blue sharks as frequently as they were observed, with BSH observed on nearly all strata (month/vessel/year) (Figure B-13). However, we must also take into account that these patterns arise from bias in observer coverage towards charter vessels operating in NZ waters. When blue sharks are reported, raw logsheet CPUE closely matched observed nominal CPUE, especially in high latitudes where most of the NZ effort occurs (Figure B-14).

The standardised CPUE is slightly adjusted relative to the unstandardised series (Figure 40; Figure B-15), but shows a strongly increasing trend since the early 2000s after an initial increase and subsequent decline in the late 1990s. The main standardising factor is SST (Figure B-21), with a large effect leading to a downward adjustment of recent CPUE. A key observation for the NZ CPUE is the inconsistency of the fleet prior to about 2005, when swordfish entered the New Zealand quota management system (Figure B-18). Prior to 2000, a relatively small number of vessels were making up the fleet, with a large influx of vessels between 2001 and 2005, and a subsequent reduction in the fleet. It is unclear if these epochs in the fishery bias the resulting CPUE.

EU CPUE For the EU fleet, Tremblay-Boyer and Takeuchi 2016 assumed accurate catch reporting by vessels. Our analysis suggests that blue sharks were caught and reported on nearly all sets (Figure B-28), with nominal CPUE on positive sets increasing substantially since 2004 (Figure B-30). Given the similarity among latitudinal bands in raw CPUE trends we did not separate the CPUE analysis into latitudinal bands. The resulting standardised CPUE index closely matched the unstandardised CPUE, with very little standardisation (Figure B-30).

Japanese low-latitude CPUE Grooming of Japanese logsheet data lead to a large change in the proportion of strata with non-zero catch (Figure B-48), suggesting that only a subset of vessels regularly report blue shark catch. This proportion increased notably in recent years (since 2010), but declined between 1998-2010. Prior to 1998, catch reporting appears to have been lower.

Nominal CPUE in the JP fleet was highly variable in high latitudes, but both high and low latitude CPUE broadly reflected trends in the proportion of positive catch records, with a decline in nominal CPUE before 2010 and a near 3-fold increase since (Figure B-49).

Standardised CPUE was adjusted down relative to unstandardised CPUE in recent years (Figure B-50), but broadly reflected trends in nominal CPUE from positive catch records. Vessel ID and SST had the strongest standardisation impact (Figure B-52), both slightly reducing recent CPUE. Alternative CPUE models had trends more similar to unstandardised CPUE (negative binomial) or the standardised series (zero-inflated negative binomial). A standardisation for Japanese high latitude CPUE was discarded due to the limited number of vessels and limited overlap.

Chinese Taipei CPUE The proportion of strata with reported blue shark catch increased notably over the whole time-series (Figure B-61), irrespective of the applied grooming, although this proportion was highly variable in lower latitudes. Nominal CPUE showed similar trends of steady increase, yet high variability in low latitudes (Figure B-62).

We initially attempted to split the CPUE series between high and low latitudes, however, the variability in the resulting CPUE lead us to consider a single time-series. This standardised

time-series is still highly variable (Figure B-63) and dominated by high variability in lower latitudes. Strong standardising effects of vessel ID (Figure B-65, and Figure B-66) suggest that much of the variability is due to vessels in the dataset.

Australian CPUE The proportion of events reporting blue shark catch in Australian fleet events increased since the early 2000s (Figure B-76). The proportion of positive catch events largely mirrors that of observer-reported events, although with a slightly more attenuated increase since the early 2000s.

Nominal CPUE was highly variable in high latitudes, although fluctuations were less pronounced in the observer CPUE (Figure B-77). The retained fleet had initially declining nominal CPUE in both high and low latitudes, with the modes increase since about 2006.

Standardisation attenuated initial declines in unstandardised CPUE in lower latitudes, but accentuated recent increases since 2006 (Figure B-78). In addition, the negative binomial index, reflecting both trends in proportions of positive catch events and positive catch-rates, showed more extreme trends in declines and increases. Standardisation effects were largely due to increases in the number of hooks set per stratum (i.e., increases in over-all effort) and the non-linear effect of CPUE with effort (Figure B-83): While prior to 2006, relatively few hooks were set by stratum, a steady increase in hooks per stratum lead to a pivot of the CPUE index about this year.

In high latitudes, CPUE standardisation lead to a similar downwards standardising of CPUE in early years (1995-2002; Figure B-91), and a strong upwards correction post 2006. Here, the trend was largely driven by shifts in vessel keys (Figure B-94) and their associated estimated vessel effects from vessels with higher catch-rates to vessels with lower catch rates.

Combined Distant Water CPUE A combined distant water CPUE was attempted due to high variability in the TW index described above. The retained fleet showed similar high catch proportions in high latitudes to those calculated from observer records (Figure B-104). In low latitudes, the increasing trends in reported positive catch strata did not mirror observer records, which showed consistently higher proportions of non-zero strata up until 2017. Nominal CPUE in these latitudes increased over the last decade (Figure B-105), mirroring increases in observer CPUE. In low latitudes, the recent increase in nominal CPUE was less pronounced, but was still higher than increases in observed nominal catch rates.

The estimated CPUE index showed high variability early in the time series, with 2011 standing out as a high, and highly uncertain year (Figure B-106). Standardisation attenuated variability in recent years, and the resulting index showed a steady increase since 2012.

Comparing CPUE series Comparing candidate CPUE series for the assessment shows considerable similarities between indices (Figure 40, Figure 41), with a consistent pattern of initial declines and subsequent increases since the mid-2000s. However, some difference in

the scale and timing of these patterns are evident. Increases in CPUE are evident in some time series (NZ-lagged, AU-low latitudes) since about 2007. However, the CPUE series from JP and EU, for example, showed increases only from 2010/2011. There was also some discrepancy in the magnitude of increases for the recent decade, with some indices (NZ, TW observer, and EU) showing 3-fold increases in recent catch rates, with about 2-fold increases in most low-latitude indices (JP, AU, DW, TW). Observer indices from the catch-reconstruction model showed high similarity for NZ, although an initial peak in logsheet-CPUE was not seen as clearly in the observer CPUE. Comparing other observer indices (e.g., AU, JP, or the High Seas Area North-West of NZ [HS.NW.of.NZ]) showed increasing CPUE in the 1990s, with a peak in the mid-to-late 1990s, and substantial declines thereafter.

4. DISCUSSION

Our combined analysis supports the notion of nursery habitats in high latitudes: Smaller individuals are mainly caught south of 35 °S. Catch-rates in these areas are also substantially higher, and all models, whether log-sheet or observer data, show a clear temperature preference for temperatures around 15 °Celsius. In addition, catch-rates in New Zealand, and to a lesser degree, the south Tasman around Tasmania and South Australia, support catch rates that are an order of magnitude higher than elsewhere in the South Pacific. Together with tracking results, our results support the hypothesis that the New Zealand and South Australian fisheries, fish juvenile and adult fish, while other fisheries to the north of New Zealand catch nearly twice the number of blue sharks, albeit at much lower catch rates.

Although our catch-reconstruction model adjusted the overall number of blue shark catch predictions downward with regards to previous studies, our catch reconstruction lines up, in relative terms, with other recent catch reconstruction models based on similar principles (i.e., predictions from observer catch-rate models). Non-linear effects of catch and effort can be explained by fishing out of local biomass within relatively short time-frames (i.e., monthly strata; Large 2015).

Although the Bayesian models employed here allowed us to readily use the full uncertainty across the delta-log-normal model for our predictions, large structural uncertainties remain with this approach. Observer coverage was biased towards South Australian waters early on in the time series (i.e., early to late 1990s), with a bias towards New Zealand samples between the late 1990s and early 2000s (Figure 20). Although the model corrects for fishing in areas of high CPUE, especially during the period of dominance of the New Zealand data, the model does not have any information about trends from other areas during that period. This means that CPUE is not representative and should not be used to represent overall abundance trends. This trend in sampling explains seemingly contradictory trends in CPUE found in the previous assessment (20), where the observer predictions for the Chinese Taipei fleet index declined despite increasing trends in South Pacific observer, and New Zealand operational data. Early trends in the Chinese Taipei index were likely driven by overall catch rates inferred from Japanese and Australian fisheries operating in south Tasman waters. Our analysis of observer

data held by Chinese Taipei observer programme suggested a strongly increasing trend in blue shark CPUE in their distant water fleet.

It is unclear to what degree latitudinal representation in observer data affects catch reconstruction models used for shark assessments. For blue shark, much of the early catch was predicted to have come from high latitude fisheries, especially during the mid-late 1990s. As these fisheries dominate observer effort during this period, high latitude catches may be relatively accurate compared to low-latitude catches at the time. The latter may be unduly inferred from CPUE trends in higher latitudes. Our model shows high uncertainties in predicted captures in this early period, but it is unclear to what degree the model can capture fundamental uncertainties associated with observer coverage.

In addition to the representation issues with observer data, it is unknown how well shark species were recorded by different observer programmes over time. It is possible the CPUE from observer records in early periods is biased by non-identification of shark species. It may be possible to extend the current approach by imputing shark species for records with unknown species identification. This would essentially combine approaches taken in the previous assessment (Tremblay-Boyer and Takeuchi 2016). In addition, logsheet reported catch could be used to provide lower bounds on estimates for poorly observed areas (i.e., via a left-censored data approach). Such an integrated catch-reconstruction model may overcome deficiencies in the present and past attempts at reconstructing catch time-series for under-reported sharks or rays. In summary, we recommend further targeted work on reconstructing shark and other catch histories based on observer data (and, potentially, other data sources), in order to better understand and quantify key uncertainties in catch histories.

ACKNOWLEDGEMENTS

The authors would like to thank Dr Sung Il Lee from the Korean National Institute of Fisheries Science for providing a detailed summary of the Korean longline fleet and the data held by the National Institute of Fisheries Science. The authors would also like to thank the SPC for providing the funding for this work through the WCPFC project 107. We would also like to thank Paul Hamer and Nicholas Ducharme-Barth from the SPC for constructive discussions throughout this work, as well as Sam McKechnie for reviewing an earlier draft of this report.

5. REFERENCES

- Bentley, N.; Kendrick, T. H.; Starr, P. J., & Breen, P. A. (2012). Influence plots and metrics: Tools for better understanding fisheries catch-per-unit-effort standardizations. *ICES Journal of Marine Science*, 69(1), 84–88.
- Brouwer, S. & Hamer, P. (2020). 2021-2025 *Shark Research Plan* (tech. rep. No. EB-IP-01 Rev1). WCPFC.

- Brouwer, S.; Large, K., & Neubauer, P. (2021). *Characterisation of the fisheries catching South Pacific blue sharks (*Prionace glauca*) in the Western and Central Pacific Ocean* (tech. rep. No. SC17-2021/SA-IP-06). WCPFC.
- Bürkner, P.-C. (2017). brms: An R package for Bayesian multilevel models using Stan. *Journal of Statistical Software*, 80, 1–28. doi:10.18637/jss.v080.i01
- Clarke, S. (2009). *An alternative estimate of catches of five species of sharks in the Western and Central Pacific Ocean based on shark fin trade data* (tech. rep. No. SC5-EB-WP-08). WCPFC.
- Common Oceans (ABNJ) Tuna Project (2019). Joint analysis of shark post-release mortality tag results. *Western and Central Pacific Fisheries Commission*.
- Kai, M.; Thorson, J. T.; Piner, K. R., & Maunder, M. N. (2017). Predicting the spatio-temporal distributions of pelagic sharks in the western and central north pacific. *Fisheries Oceanography*, 26(5), 569–582.
- Large, K. (2015). *Fine-scale spatio-temporal catch trends of blue sharks in southern bluefin target sets in the surface longline fishery* (tech. rep. No. New Zealand Fisheries Assessment Report 2015/32). WCPFC.
- Lawson, T. (2011). *Estimation of catch rates and catches of Key Shark Species in tuna fisheries of the Western and Central Pacific Ocean using observer data* (tech. rep. No. SC7-EB-IP-02). WCPFC.
- Manning, M. J. & Francis, M. P. (2005). *Age and growth of blue shark (*Prionace glauca*) from the New Zealand Economic Exclusive Zone* (tech. rep. No. New Zealand Fisheries Assessment Report 2005/26). New Zealand Ministry of Fisheries.
- Neubauer, P.; Large, K., & Brouwer, S. (2021). *Stock assessment for south Pacific blue shark in the Western and Central Pacific Ocean* (tech. rep. No. WCPFC-SC17-2021/SA-WP-03). WCPFC.
- Peatman, T.; Bell, L.; Allain, V.; Caillot, S.; Williams, P.; Tuiloma, I.; Panizza, A.; Tremblay-Boyer, L.; Fukofuka, S., & Smith, N. (2018). *Summary of longline fishery bycatch at a regional scale, 2003-2017*. WCPFC-SC14-2018/ST-WP-03.
- Rice, J. (2012). *Alternate catch estimates for silky and oceanic whitetip sharks in Western and Central Pacific Ocean* (tech. rep. No. SC8-SA-IP-12). WCPFC.
- Tremblay-Boyer, L. & Neubauer, P. (2019). *Historical catch reconstruction and CPUE standardization for the stock assessment of oceanic whitetip shark in the Western and Central Pacific Ocean* (tech. rep. No. WCPFC-SC15-2019/SA-IP-17). WCPFC.
- Tremblay-Boyer, L. & Takeuchi, Y. (2016). *Catch and CPUE inputs to the South Pacific blue shark stock assessment* (tech. rep. No. SC12-SA-WP-09). WCPFC.
- Vehtari, A.; Gelman, A., & Gabry, J. (2016a). *loo: Efficient leave-one-out cross-validation and WAIC for Bayesian models*. R package version 0.1.6. Retrieved from <https://github.com/jgabry/loo>
- Vehtari, A.; Gelman, A., & Gabry, J. (2016b). Practical Bayesian model evaluation using leave-one-out cross-validation and WAIC. *Statistics and Computing*, 1–20.
- WCPFC (2019). *Conservation and Management Measure for Sharks* (tech. rep. No. CMM2019-04). WCPFC.

TABLES

Table 1: Model covariates of operational fishing features likely to influence catch rates of oceanic whitetip shark and environmental variables that may represent habitat of this species (LBEST are databases of the SPC for longline and purse - seine fisheries, respectively).

Covariate	Description
Year	Year when the fishing set occurred, treated as categorical .
Flag	Country-assignation for the vessel performing the fishing set.
Cluster	Predicted targeting strategy for longline fishing set based on k-means clustering of the proportion in the total catch in number of albacore, bigeye, yellowfin, swordfish and other billfish (for the analysis of Japanese logsheet data, bluefin tuna was included as a category). Cluster composition was predicted based on LBEST records and assuming 4(5) centres, resulting in a categorical variable with values from 1 to 4(5). Longline observed set targeting strategy was predicted according to the LBEST classification.
SST	Sea surface temperature aggregated at 5-degree scale for LBEST, obtained from NOAA (https://www.esrl.noaa.gov/psd/data/gridded/data.noaa.oisst.v2.html).
Chl- α	Sea surface chlorophyll- α concentration aggregated at 5-degree scale for LBEST (https://coastwatch.pfeg.noaa.gov/erddap/griddap/erdMH1chlamday).
Dist2Coast	Distance of the set to the nearest coastline, aggregated at 5-degree scale for LBEST and 1-degree scale for SBEST.

Table 2: Deviance table for lognormal component of the delta - lognormal model of blue sharks from the Chinese - Taipei large - scale tuna longline fishery in the South Pacific Ocean.

Term	Df	Deviance	Resid. Df	Resid. Dev	F	Pr(>F)	
Intercept			6401.00	3145.10			
yy	12.00	405.76	6389.00	2739.30	79.65	< 2.2e-16	***
Q	3.00	11.78	6386.00	2727.60	9.25	4.23E-06	***
A	1.00	0.12	6385.00	2727.40	0.29	0.59041	
HPB	1.00	0.27	6384.00	2727.20	0.64	0.425083	
Q:A	3.00	13.08	6381.00	2714.10	10.27	9.63E-07	***
Q:HPB	3.00	6.35	6378.00	2707.70	4.99	0.001869	**

Table 3: Deviance table for the binomial component of the delta - lognormal model of blue sharks from the Chinese - Taipei large - scale tuna longline fishery in the South Pacific Ocean.

Term	Df	Deviance	Resid. Df	Resid. Dev	F	Pr(>F)
Intercept			15031.00	20507.00		
yy	12.00	800.27	15019.00	19707.00	66.69	< 2.2e-16 ***
Q	3.00	151.63	15016.00	19555.00	50.54	< 2.2e-16 ***
A	1.00	981.74	15015.00	18574.00	981.74	< 2.2e-16 ***
HPB	1.00	2.78	15014.00	18571.00	2.78	0.095638 .
Q:A	3.00	77.93	15011.00	18493.00	25.98	< 2.2e-16 ***
Q:HPB	3.00	14.25	15008.00	18479.00	4.75	0.002582 **
A:HPB	1.00	10.78	15007.00	18468.00	10.78	0.001025 **

FIGURES

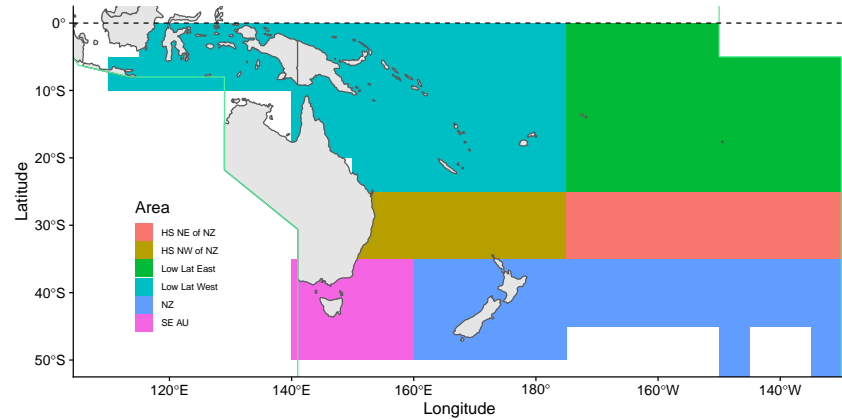


Figure 2: Areas definition used for observer catch rate modelling.

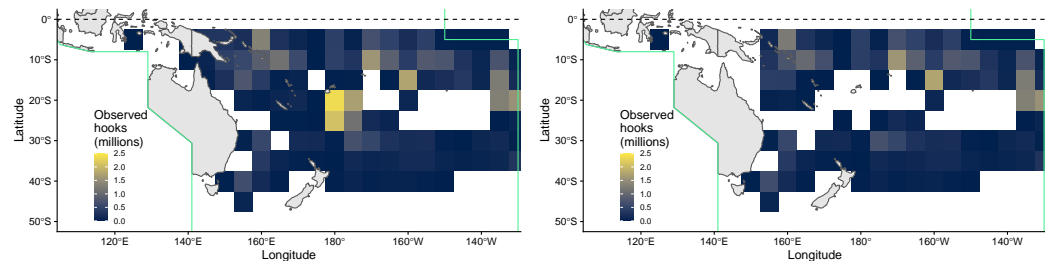


Figure 3: Comparison of observed effort distribution for (left) the Chinese-Taipei fleet and (right) the Chinese-Taipei high seas observer programme

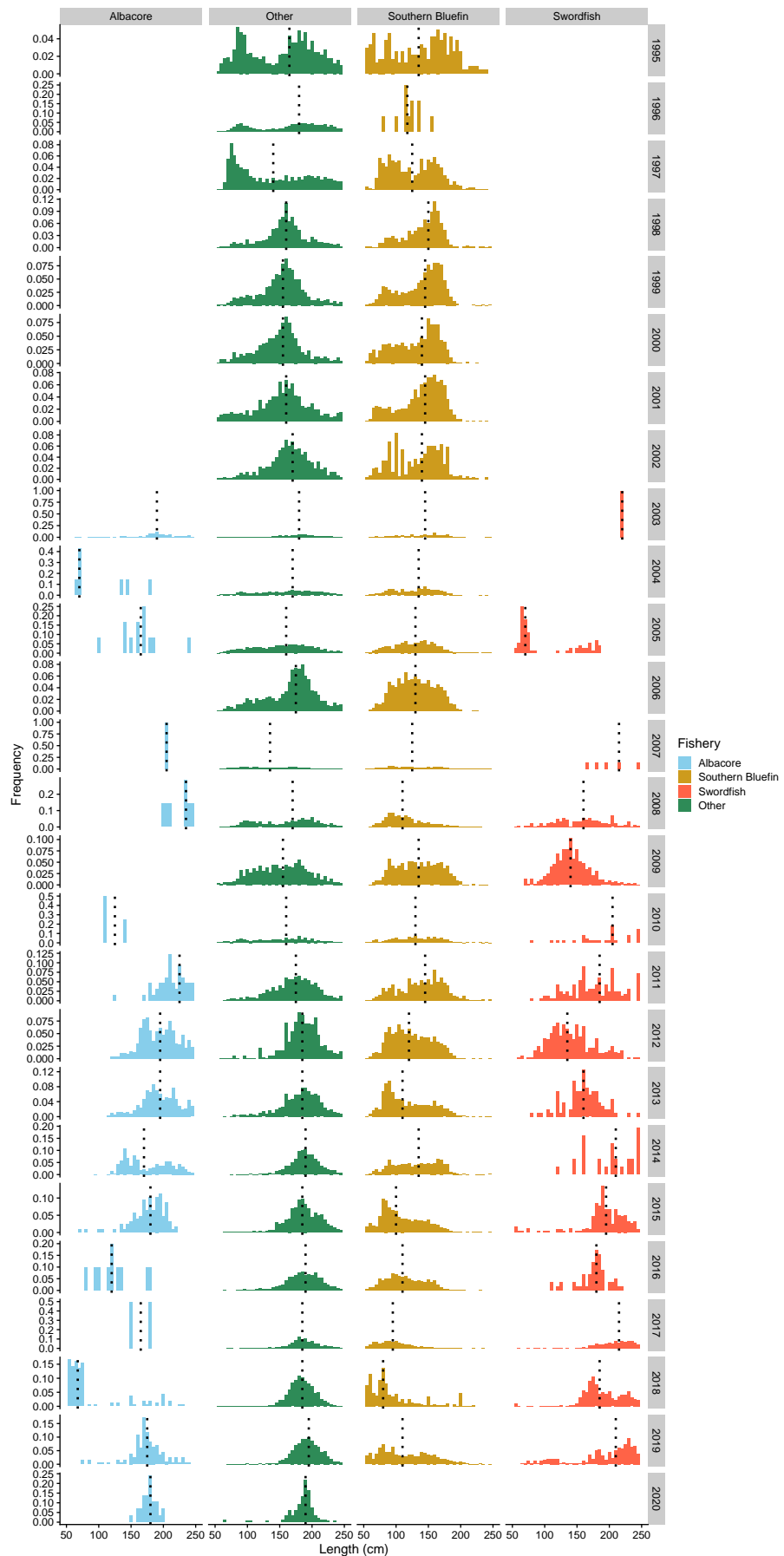


Figure 4: Length frequencies of observer-sampled blue shark in four target fisheries by year. The median length for each year is indicated with the dashed vertical line.

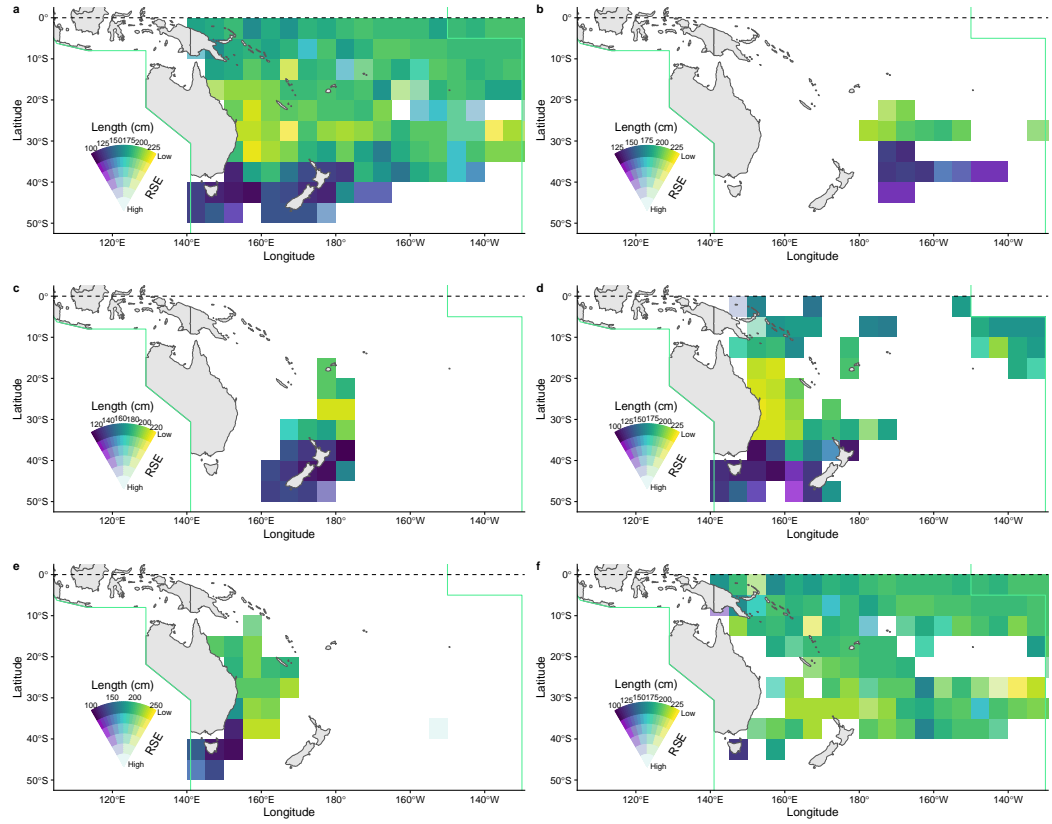


Figure 5: Maps of average length shaded by variability in lengths (SE of mean length). Samples are from a) Combined dataset, b) EU, c) New Zealand d) Japanese, e) Australian and f) distant water (TW, KR, FJ, CN, VU).

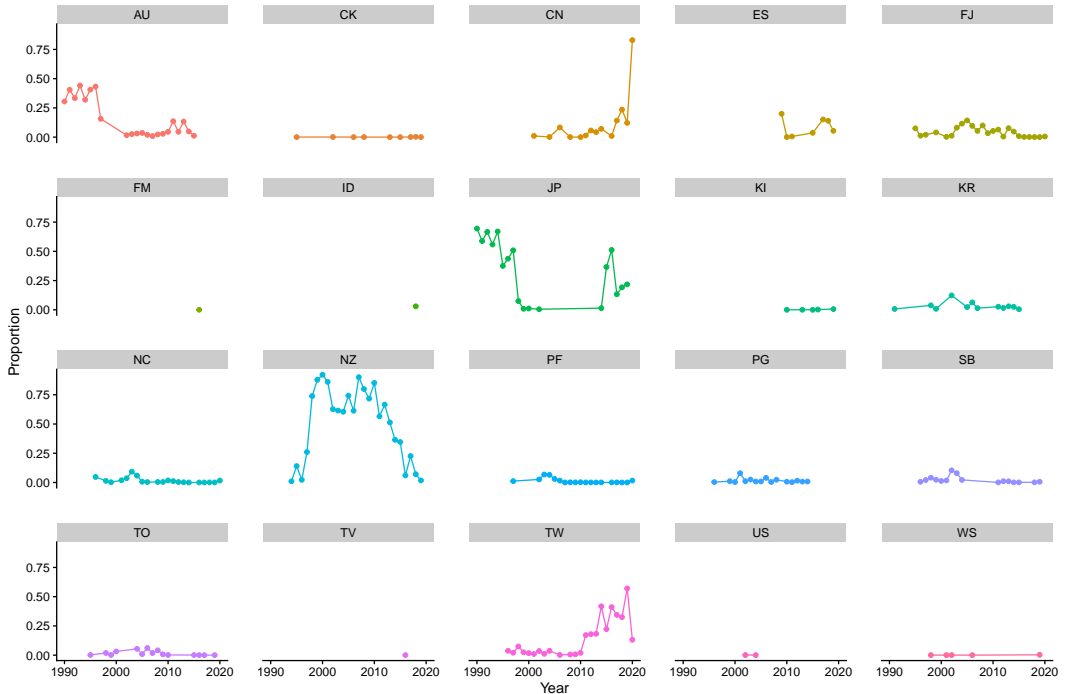


Figure 6: Sampling effort over time by flag in the observer dataset. Note that data for the 2020 year is preliminary.

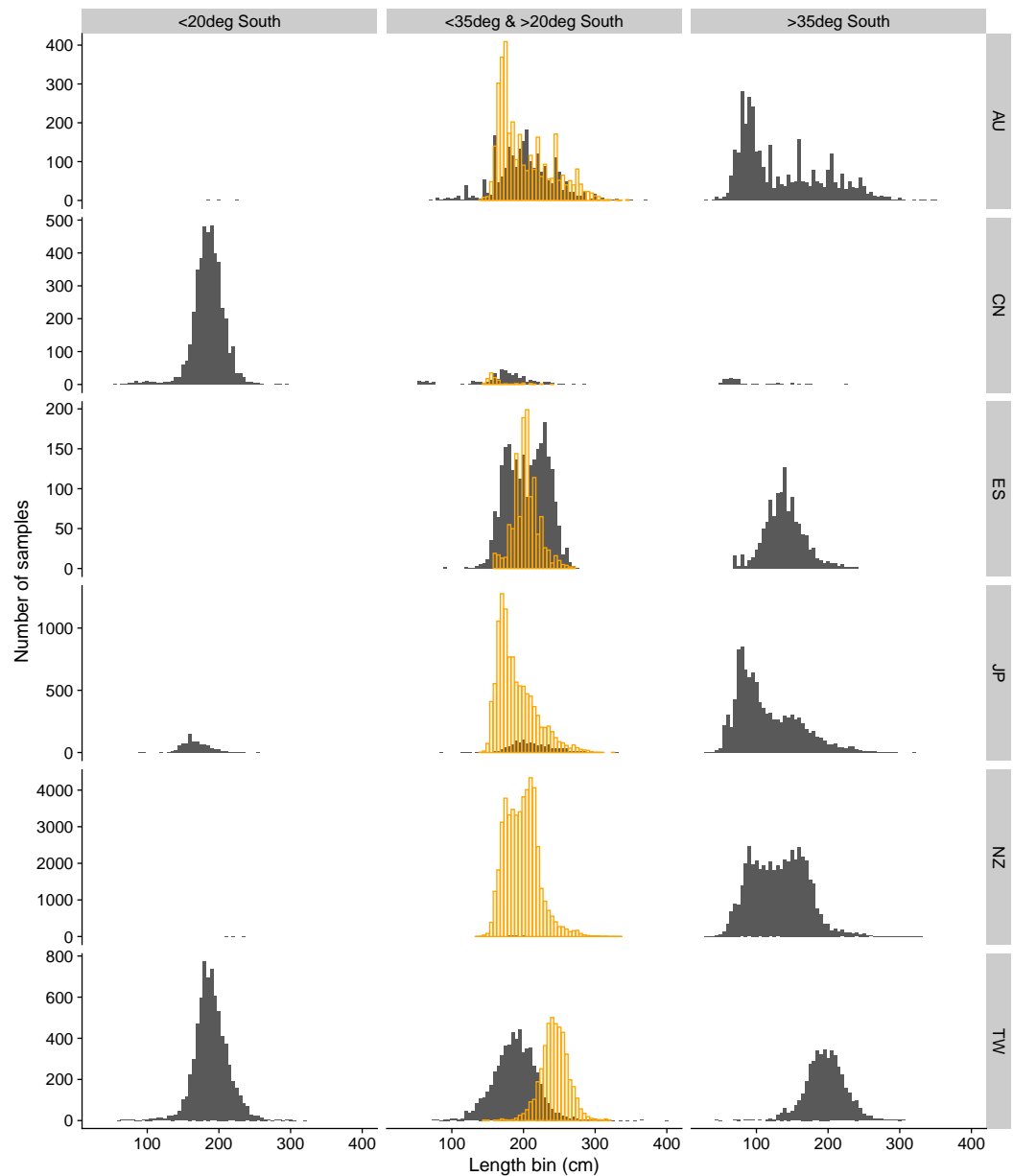


Figure 7: Length frequency by flag for flags with reasonable amounts of samples. Orange histograms show samples grown according to Manning and Francis 2005 over 5 years

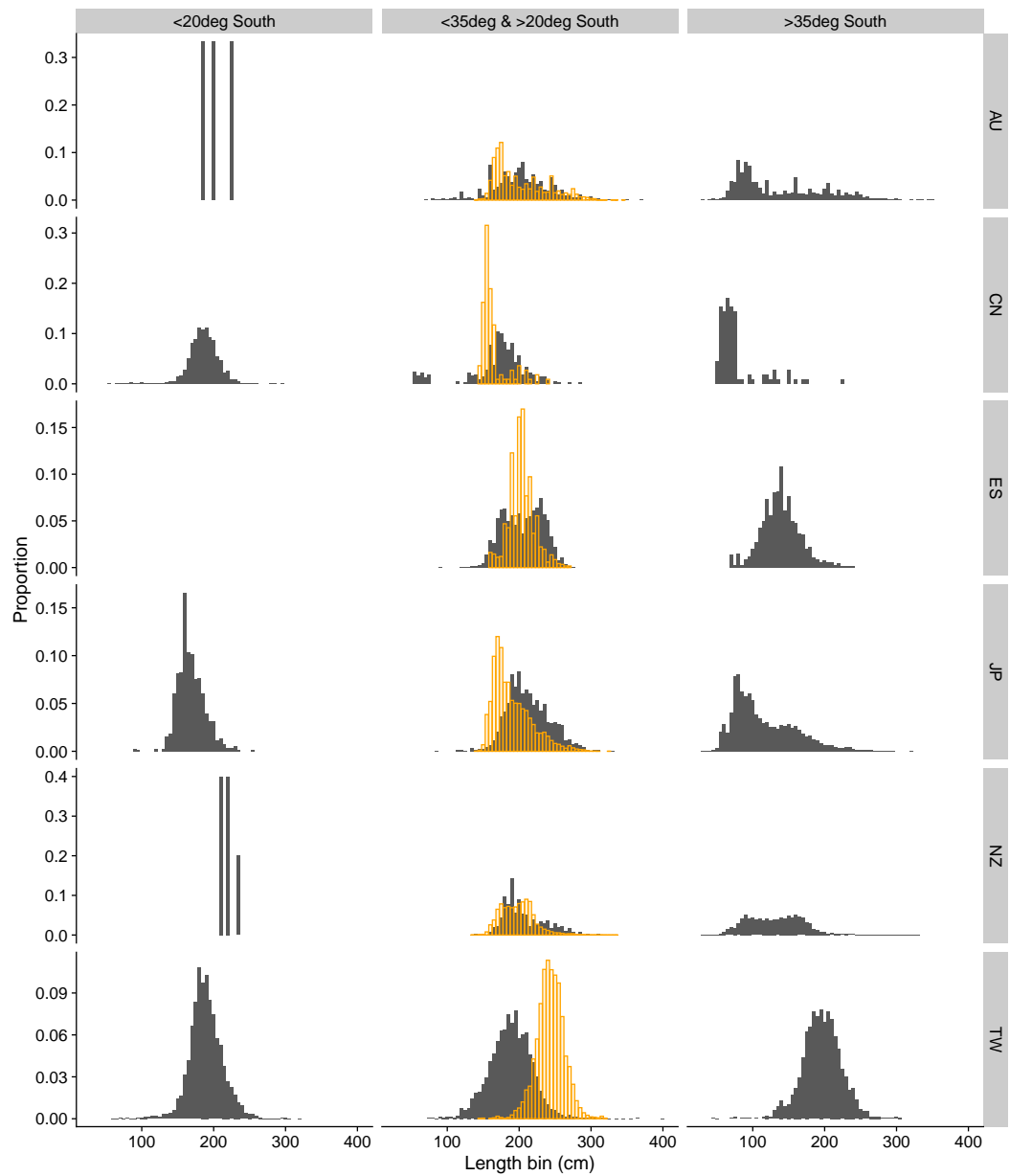


Figure 8: Length proportions by flag for flags with reasonable amounts of samples. Orange histograms show samples grown according to Manning and Francis 2005 over 5 years

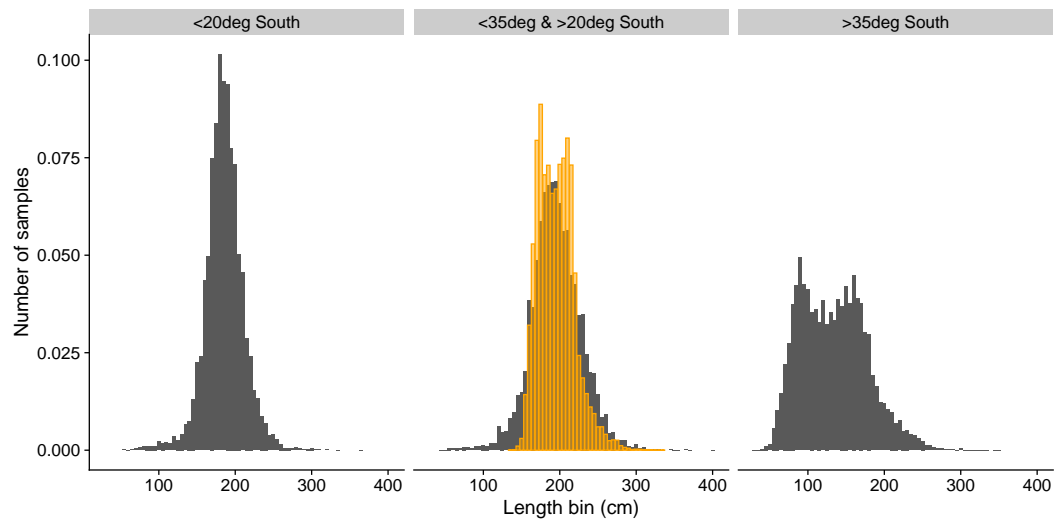


Figure 9: Length proportions by latitudinal strata for flags with reasonable amounts of samples. Orange histograms show samples grown according to Manning and Francis 2005 over 5 years

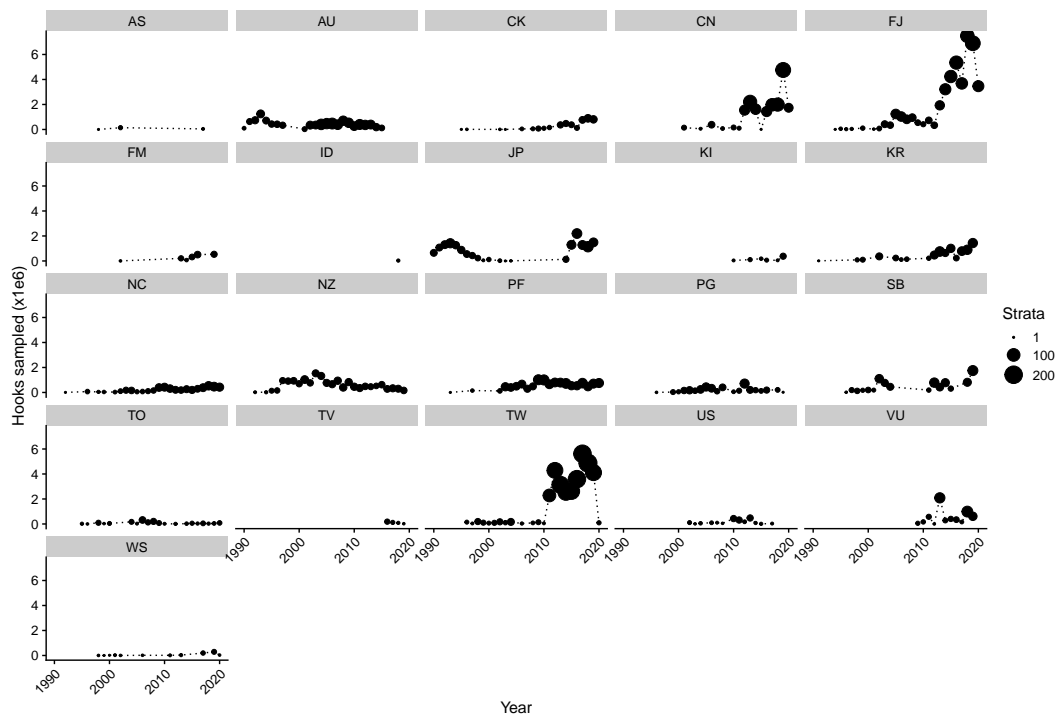


Figure 10: Number of observed hooks by fleet.

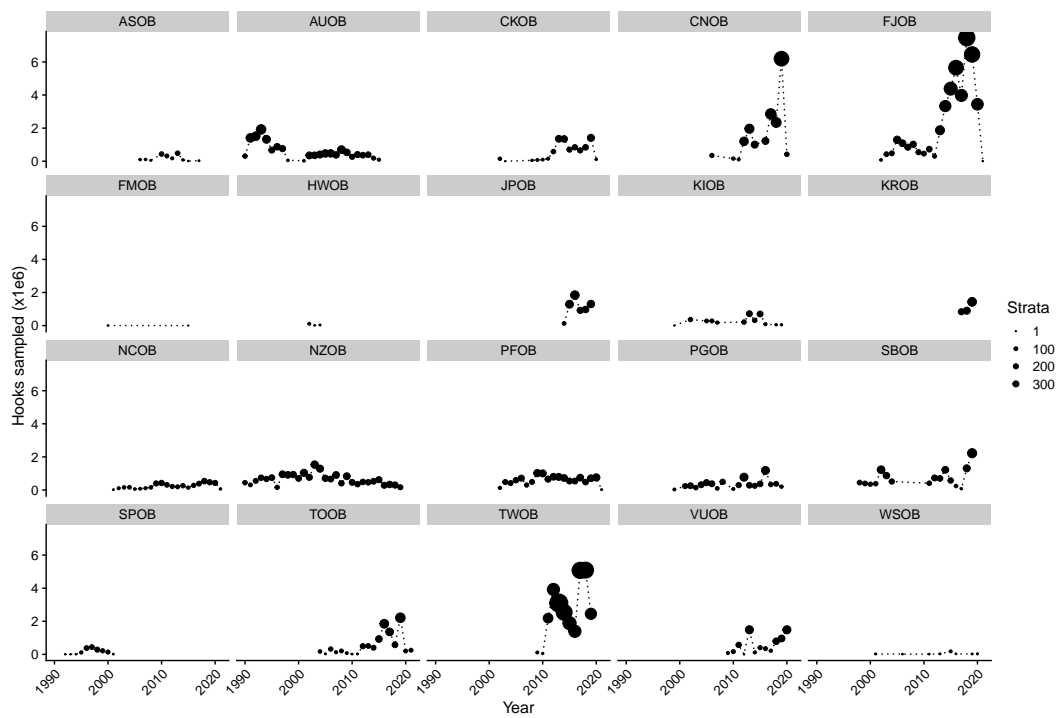


Figure 11: Observed hooks by observer programme.

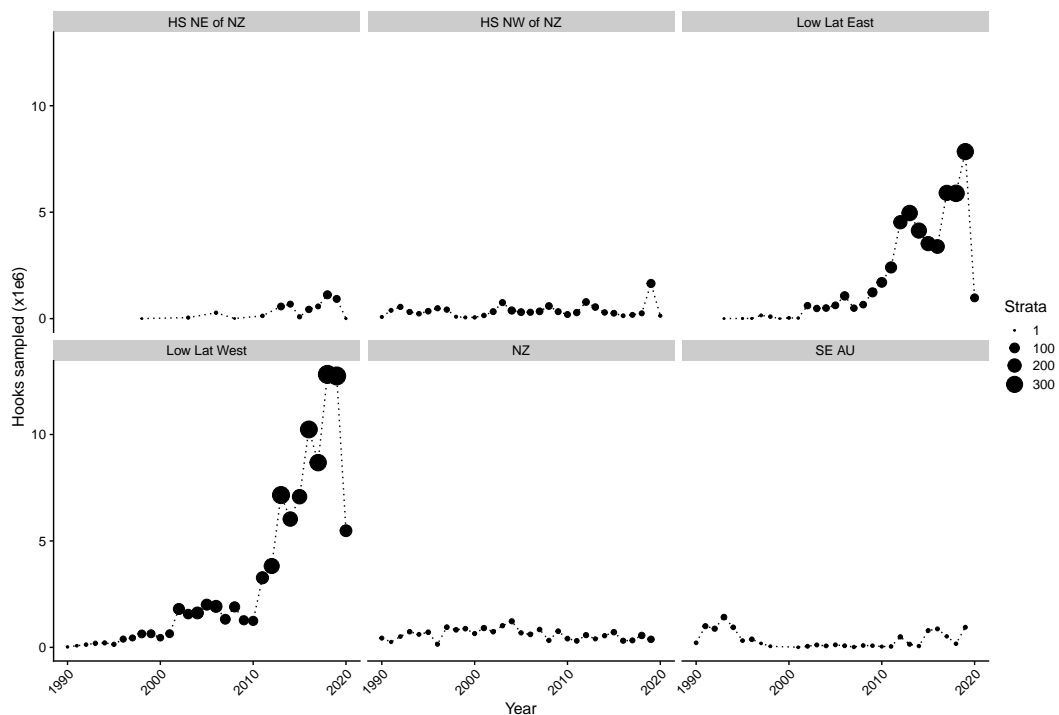


Figure 12: Number of observed hooks by area.

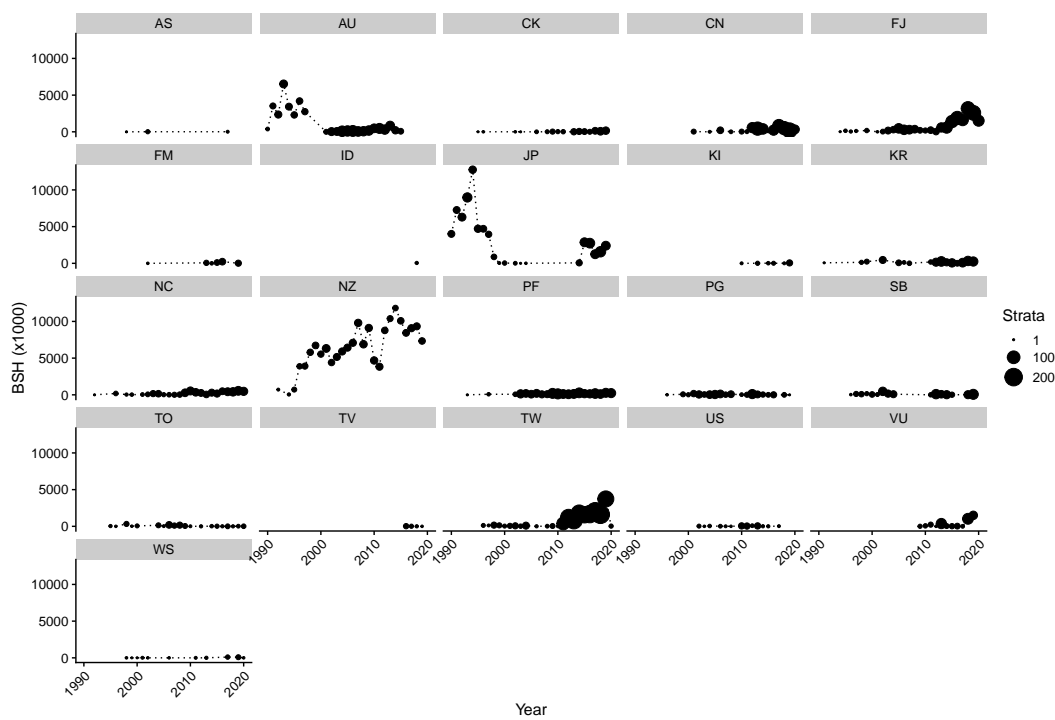


Figure 13: Observed blueshark captures by fleet.

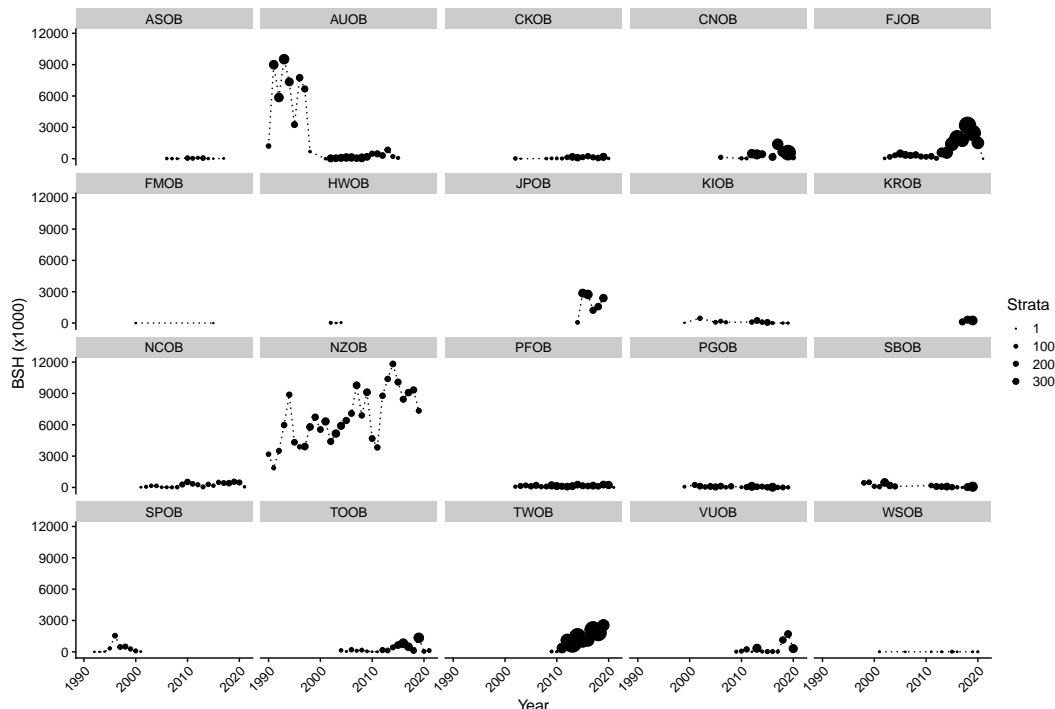


Figure 14: Observed blueshark captures by observer programme.

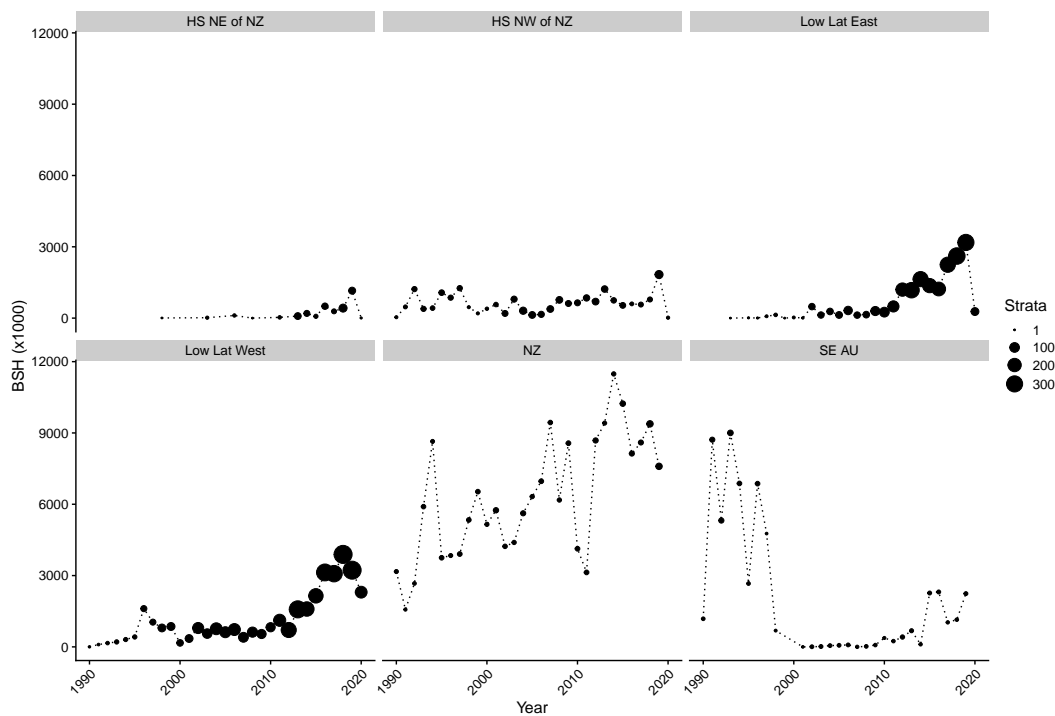


Figure 15: Observed blueshark captures by area.

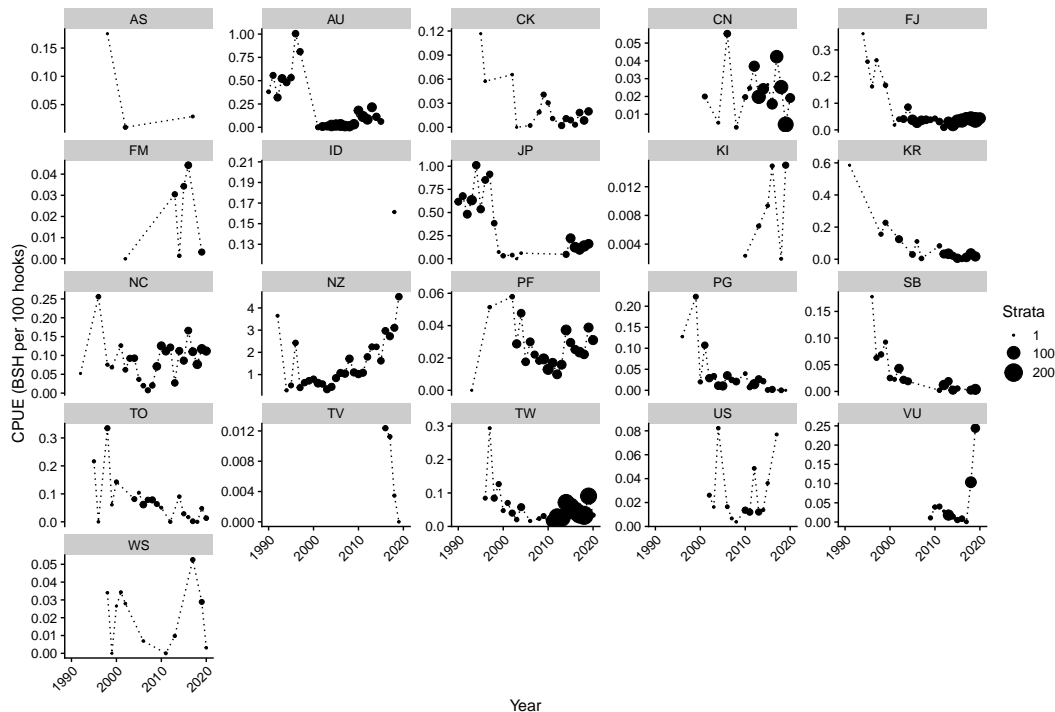


Figure 16: Nominal observed CPUE by fleet.

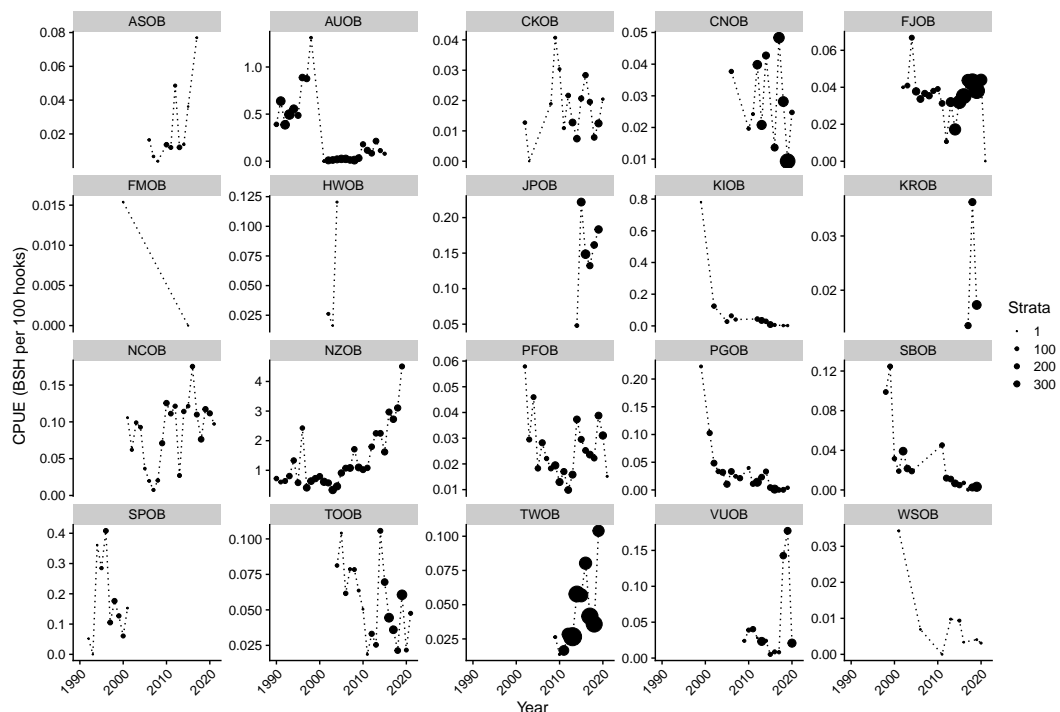


Figure 17: Nominal observed CPUE by observer programme.

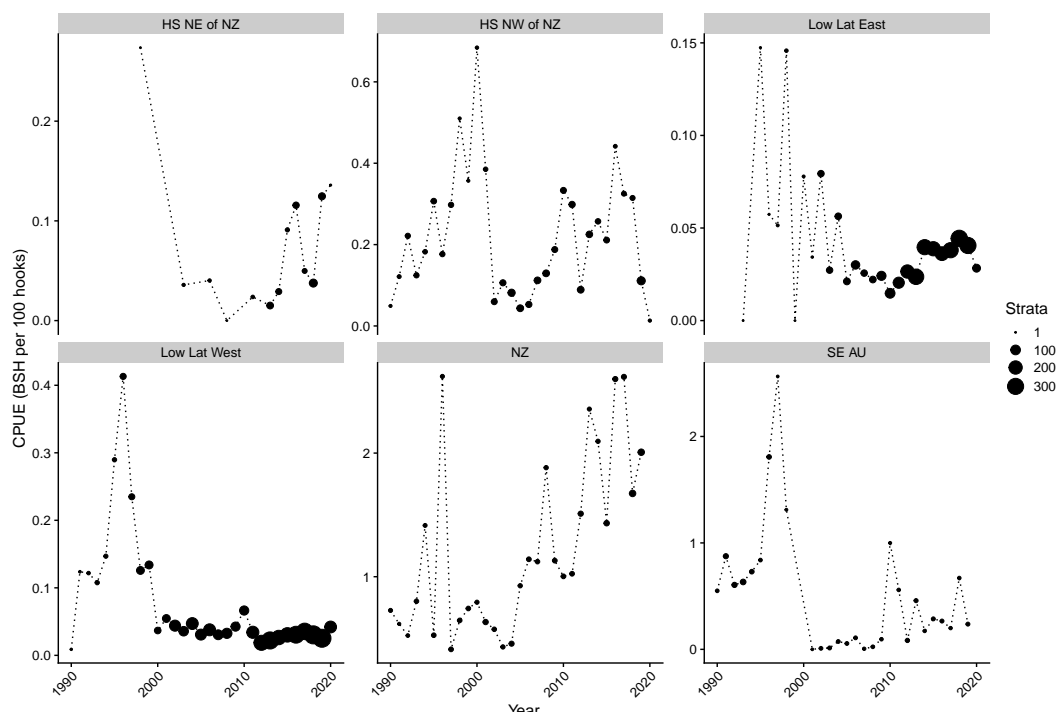


Figure 18: Nominal observed CPUE by area.

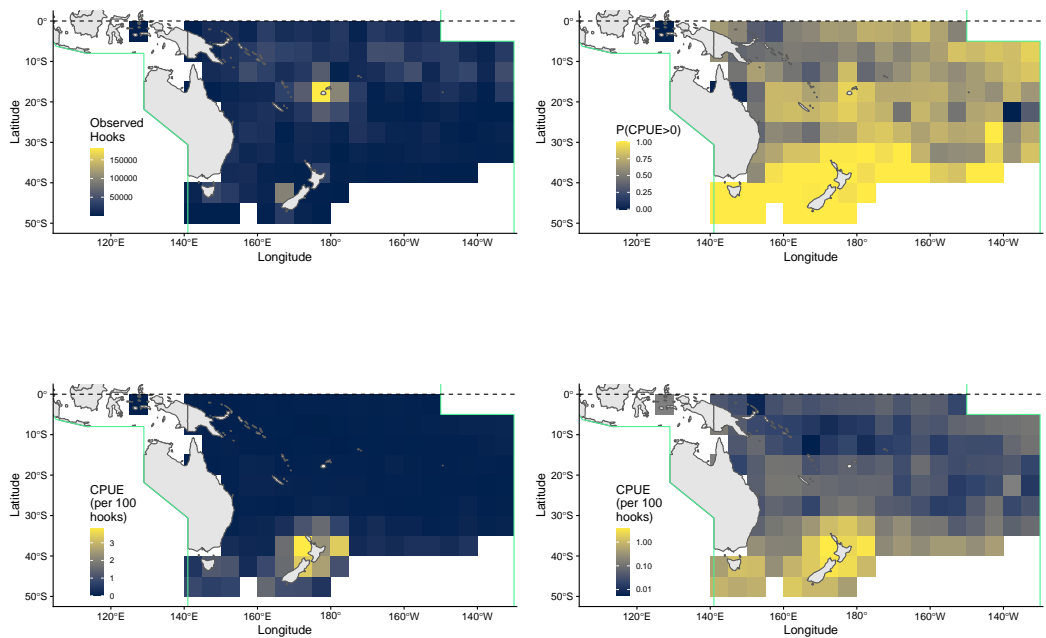


Figure 19: Observed CPUE: (Top left) Number of observed hooks by $5' \times 5'$ degree grid with non-zero blueshark catch; (top right) Proportion of observed strata ($5' \times 5'$, fleet, month) with non-zero blueshark catch; (bottom left) arithmetic mean CPUE across observed strata ($5' \times 5'$, fleet, month); (bottom right) log scale plot of arithmetic mean CPUE across observed strata ($5' \times 5'$, fleet, month).

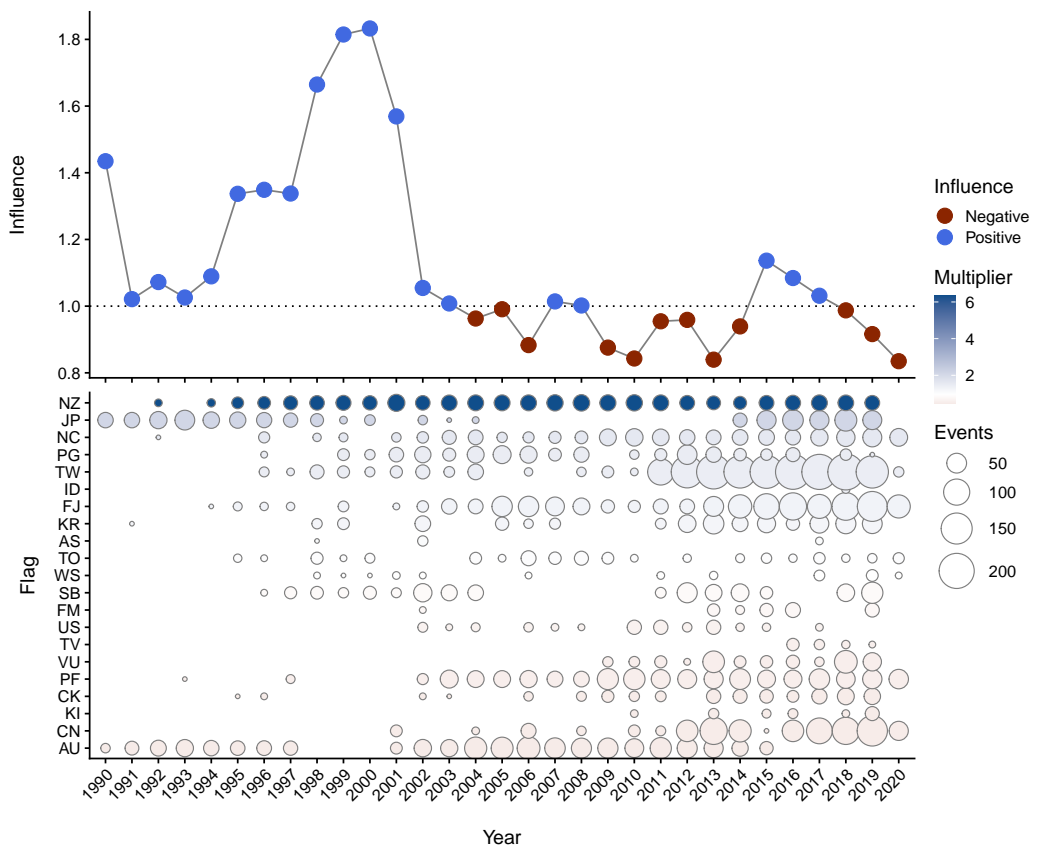


Figure 20: Influence of flag ID on inferred over-all observer catch-rates, with positive influence showing years where the over-all catch-rate in the model was standardised downward by the corresponding amount to account for differences in catch rates among flags. Individual flag influence is shown in colour as a multiplier on average catch rates, with circle size corresponding to the amount of unique strata (i.e., lines of data) for each flag entering the model. Note that data for the 2020 year is preliminary.

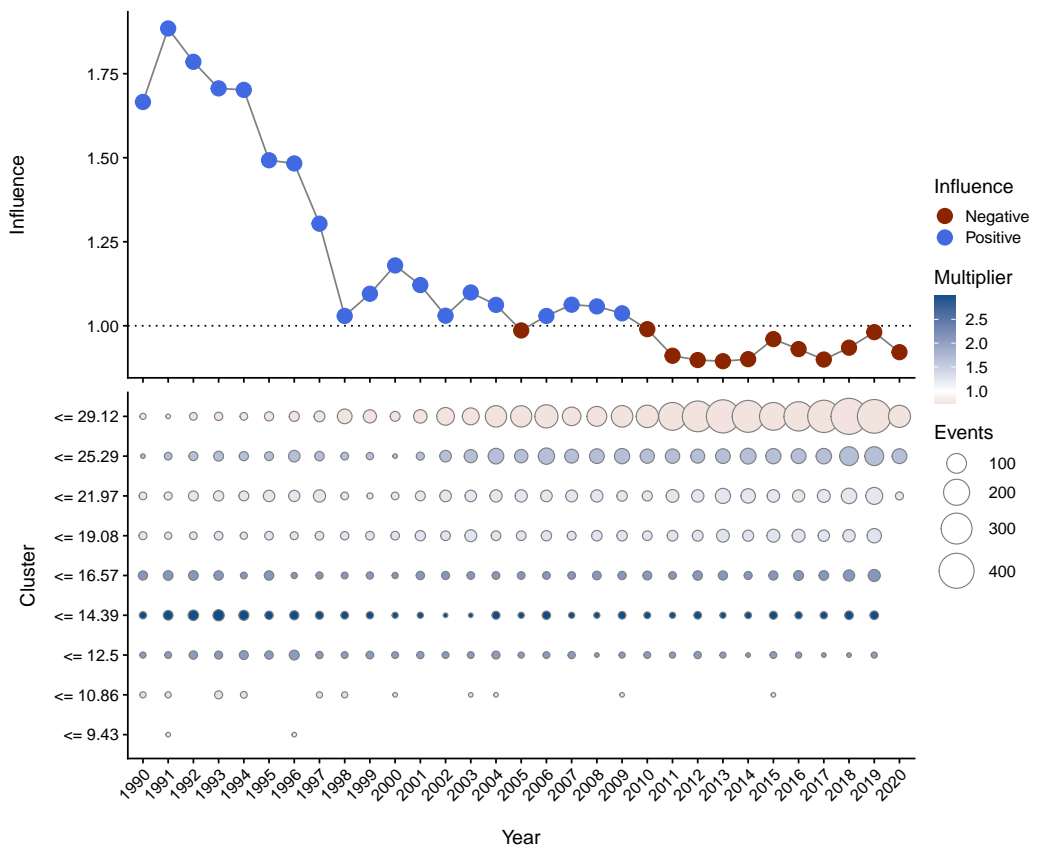


Figure 21: Influence of SST within model strata on inferred over - all observer catch - rates, with positive influence showing years where the over - all catch - rate in the model was standardised downward by the corresponding amount to account for differences in catch rates among flags. Individual SST class influence is shown in colour as a multiplier on average catch rates, with circle size corresponding to the amount of unique strata (i.e., lines of data) for each SST class entering the model. Note that data for the 2020 year is preliminary.

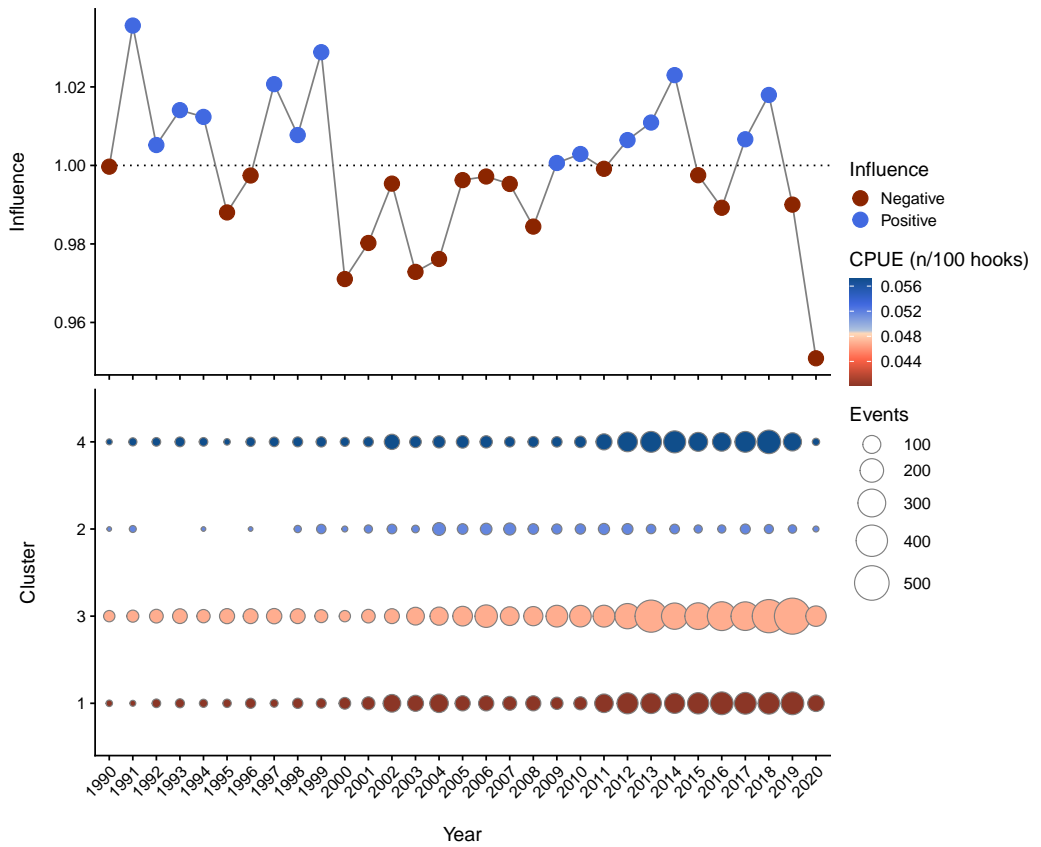


Figure 22: Influence of targeting clusters on inferred over-all observer catch-rates, with positive influence showing years where the over-all catch-rate in the model was standardised downward by the corresponding amount to account for differences in catch rates among clusters. Individual cluster influence is shown in colour as a multiplier on average catch rates, with circle size corresponding to the amount of unique strata (i.e., lines of data) for each clusters entering the model. Note that data for the 2020 year is preliminary.

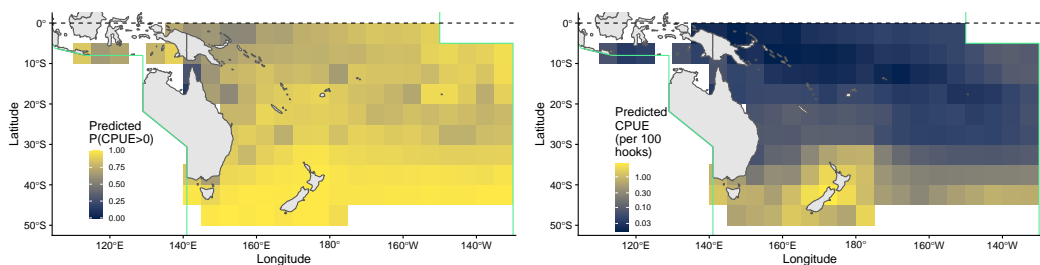


Figure 23: Predicted CPUE surface in terms of (left) predicted proportion of non-zero catch strata given observed hook numbers and (right) mean predicted CPUE from the observer catch rate GLMM.

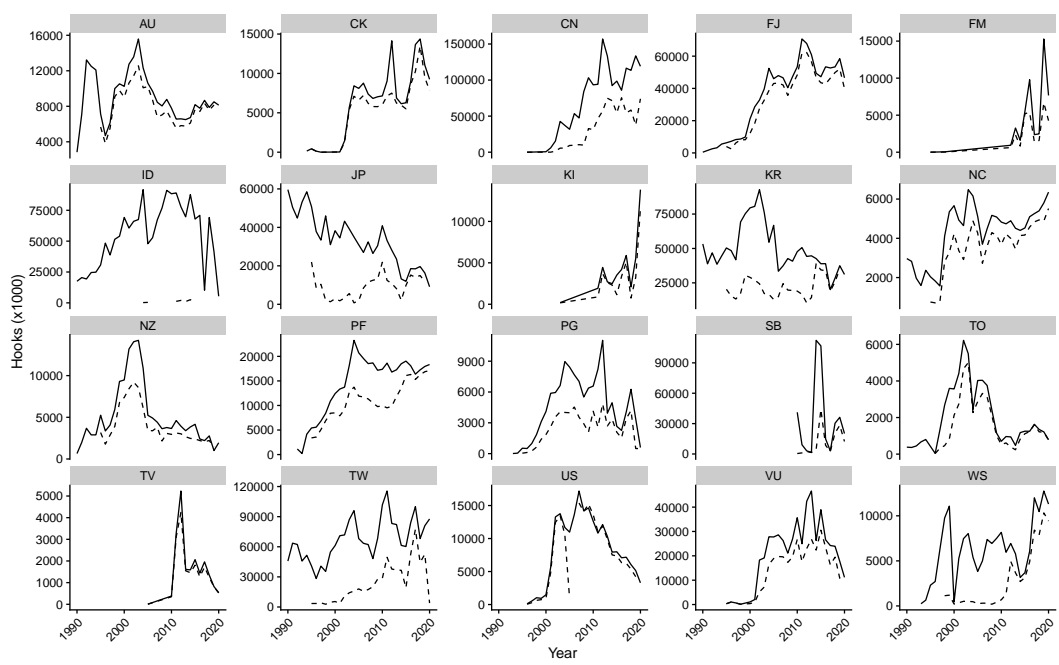


Figure 24: Estimated total hooks by fleet in L-BEST used for predictions of over-all catches of blue shark, with reported hooks in the operational log-sheet data shown for comparison (dashed lines).

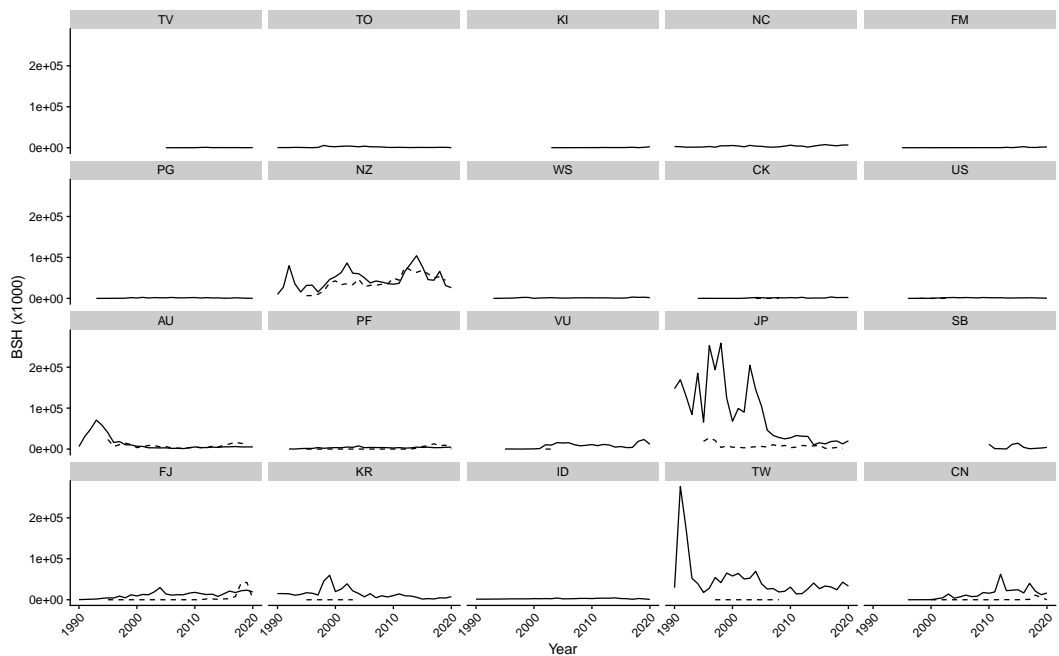


Figure 25: Predicted total blueshark captures by fleet using the observer catch-rate GLMM in conjunction with L-BEST effort. Reported numbers of blue shark from the operational log-sheet data shown for comparison (dashed lines).

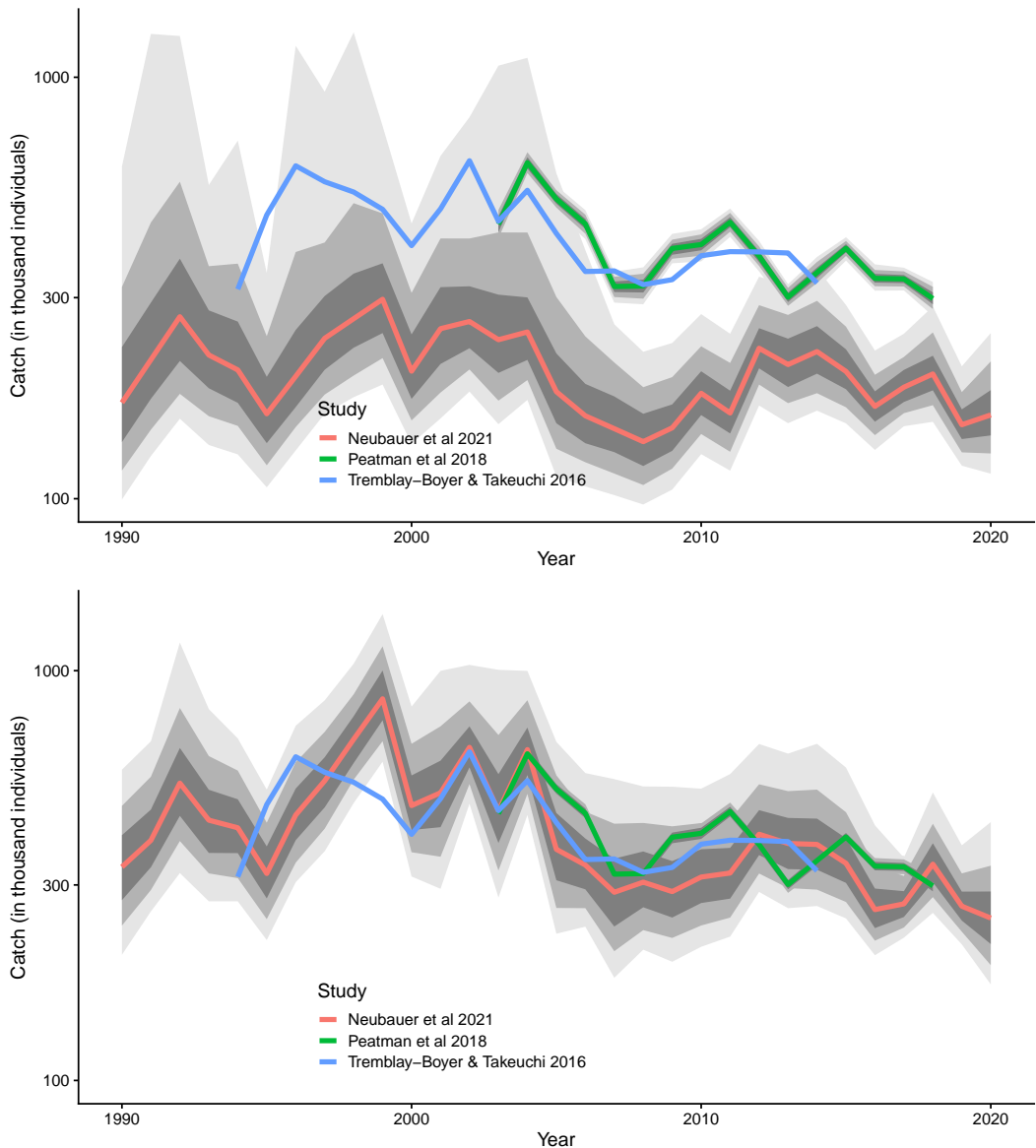


Figure 26: Predicted total blueshark captures (posterior median (red); 75% confidence (dark grey) and 80% confidence (light grey)) using the observer catch-rate GLMM in conjunction with L-BEST effort. (Top) Selected model as determined by the LOO-IC predictive model selection; (Bottom) alternative model with linear scaling of CPUE (Catch) with effort. The alternative model had substantially lower predictive power. Previous catch - reconstruction totals are shown for comparison. 2016 figures were corrected from initial published figures post SC12 re-calculated total captures from the 2016 analysis are shown for comparison.

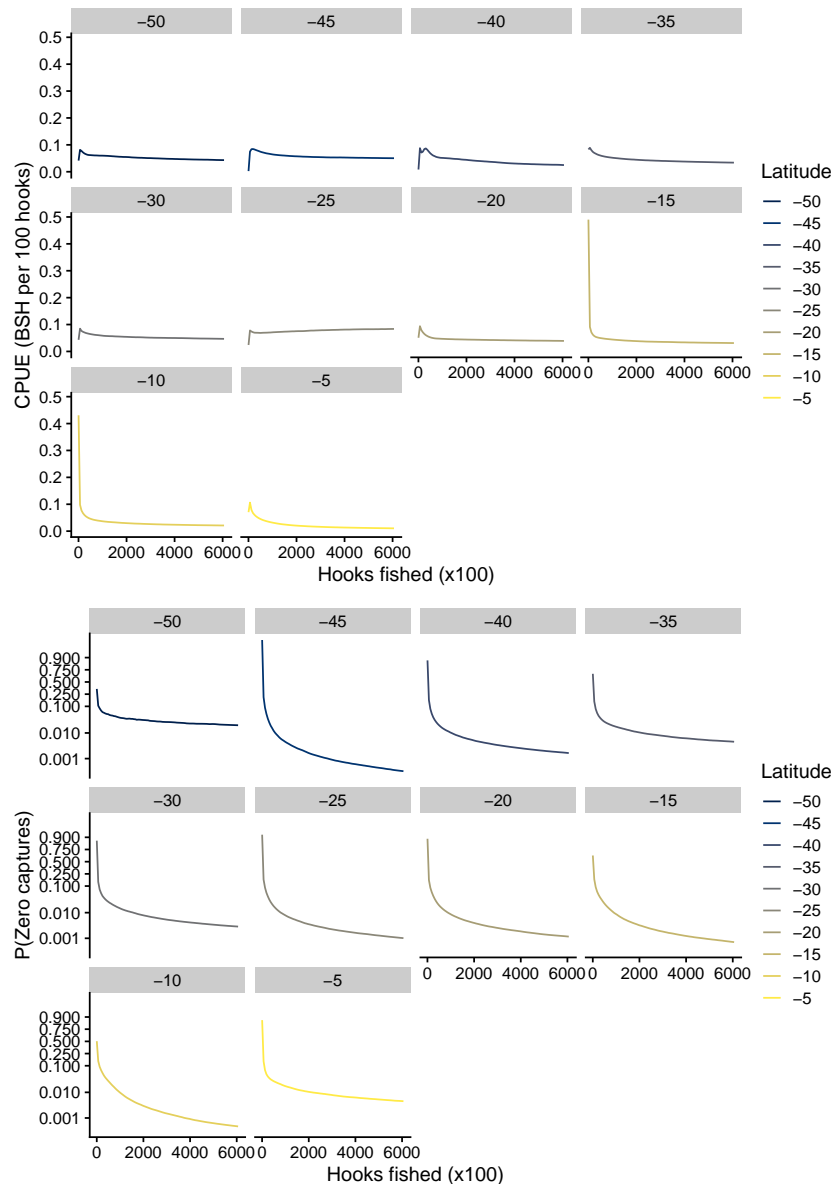


Figure 27: Conditional effects of the number of hooks fished on (top) CPUE and (bottom) probability of zero catch per stratum in the observer catch-prediction model.

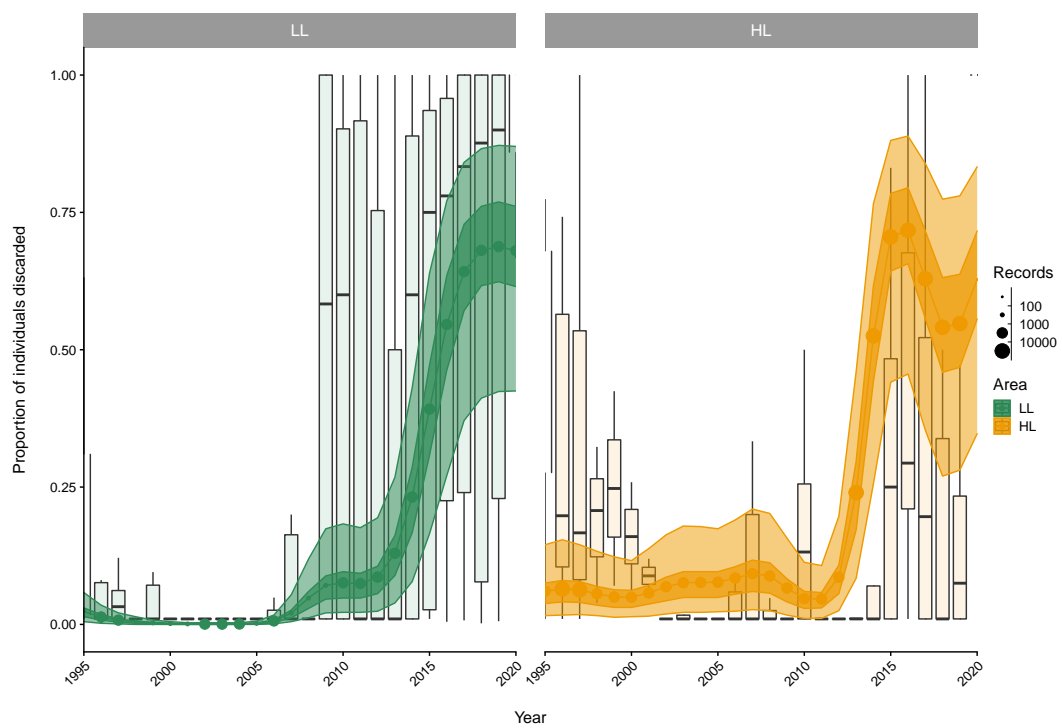


Figure 28: Estimated year effects (expected proportion discarded) for low-latitude and high-latitude (≥ 35 degree South), showing the posterior median, and 75% (dark shade) and 95% (light shade) posterior confidence. The distribution of input data is shown by underlying boxplots.

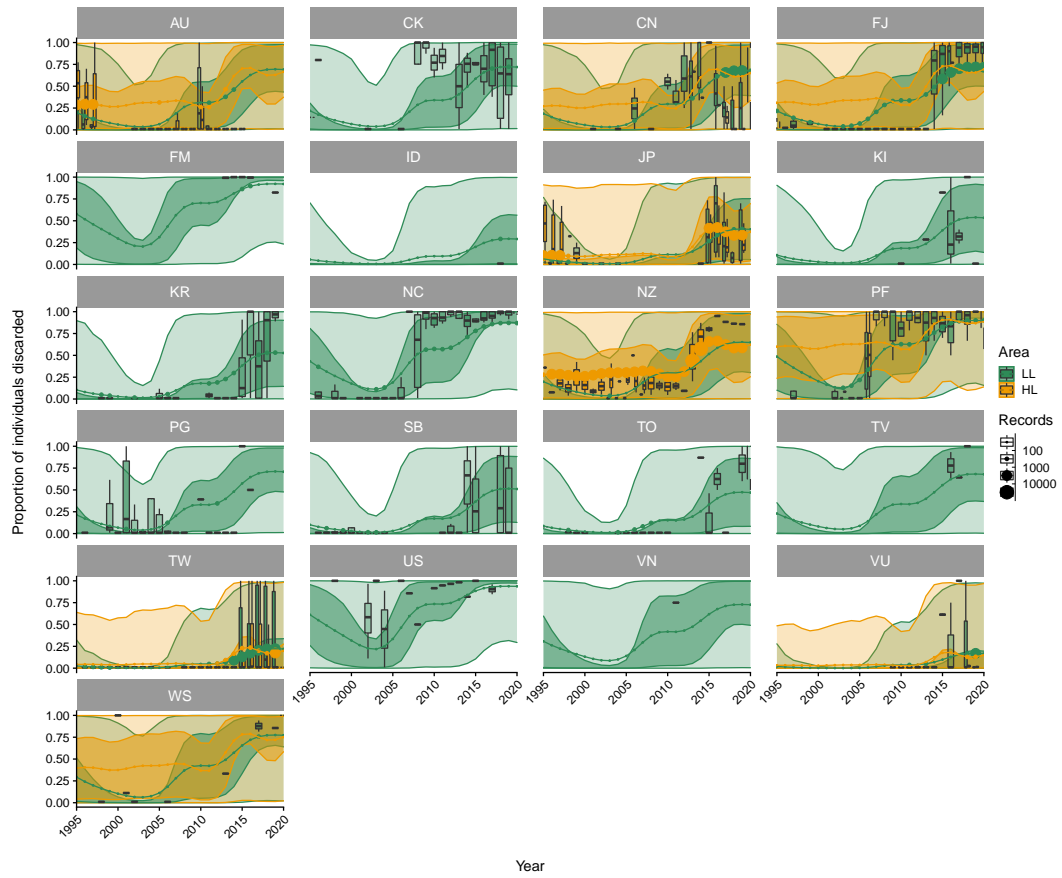


Figure 29: Estimated flag-year effects (expected proportion discarded) for flags in the observer dataset, split along low-latitude and high latitude ($>= 35$ degree South), showing the posterior median, 75% (dark shade) and 95% (light shade) posterior confidence. The distribution of input data is shown by underlying boxplots.

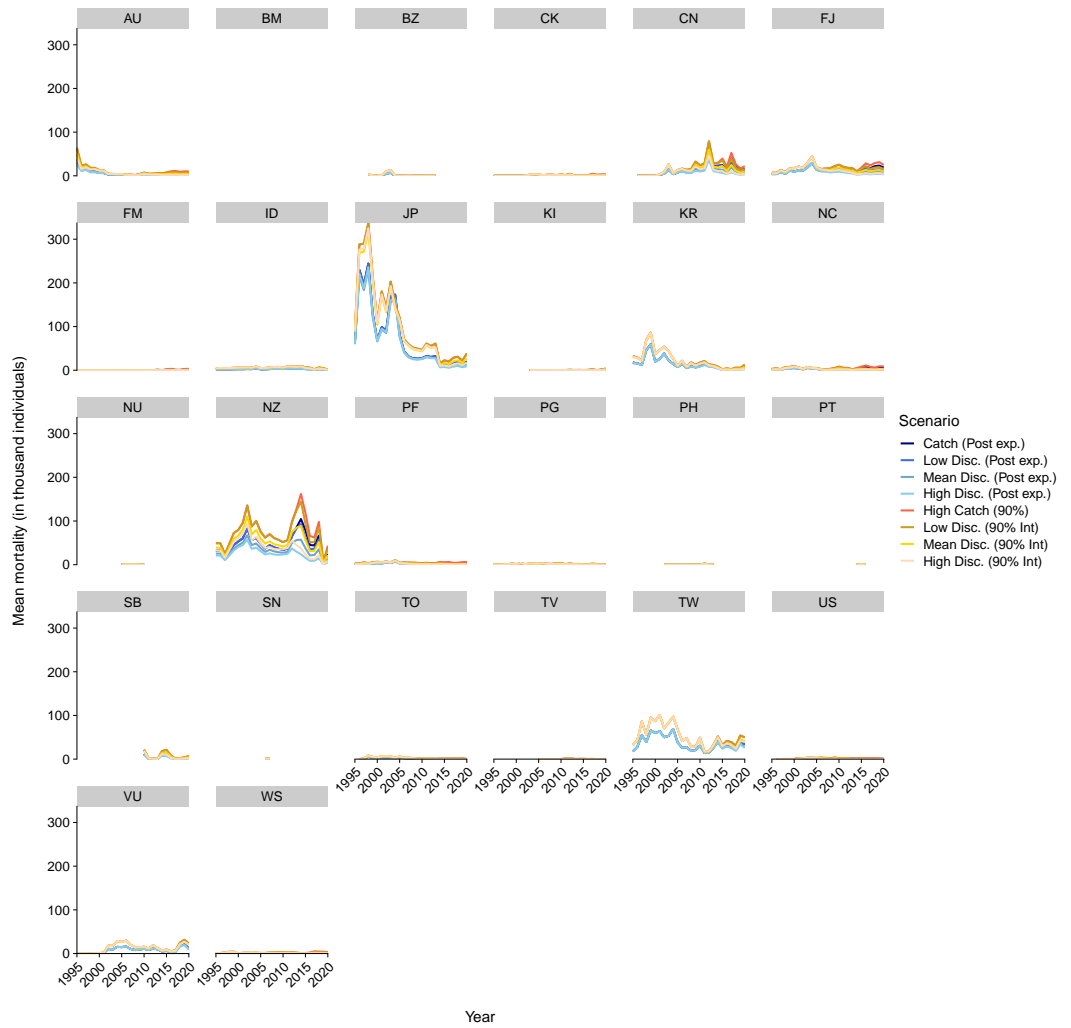


Figure 30: Predicted total fishing related mortality by flag, including 17% post release mortality for live-discarded blue sharks. Catch refers to the posterior median (50%) and 90th percentile (90%) of the predicted catch from the observer catch rate model, low, median and high discard scenarios refer to the 25%, 50% (median) and 75% discard estimates.

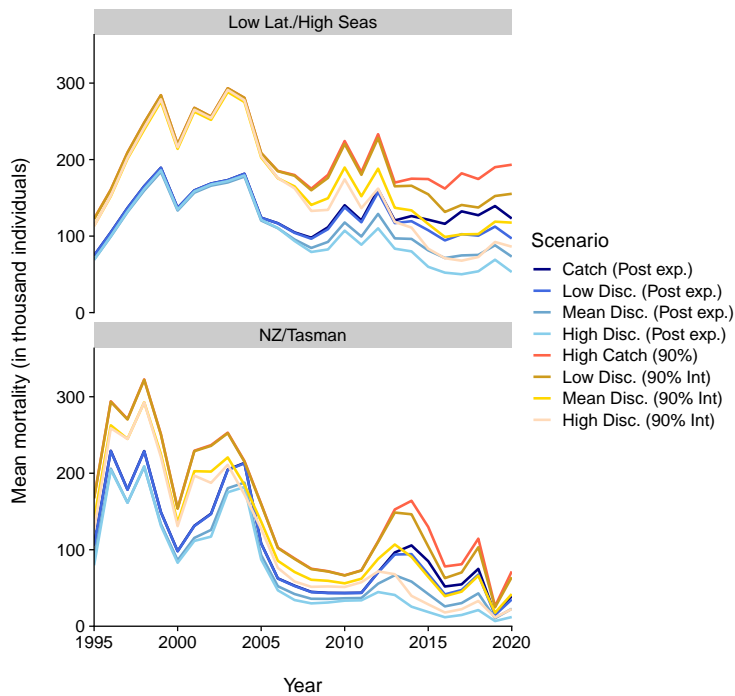


Figure 31: Predicted total fishing related mortality by latitudinal stratum (high [≥ 35 degree South] and low latitude [≥ 35 degree South]), including 17% post release mortality for live - discarded blue sharks. Catch refers to the posterior median (50%) and 90th percentile (90%) of the predicted catch from the observer catch rate model, low, median and high discard scenarios refer to the 25%, 50% (median) and 75% discard estimates. All discard estimates were applied at flag and latitudinal stratum level to over - all interactions.

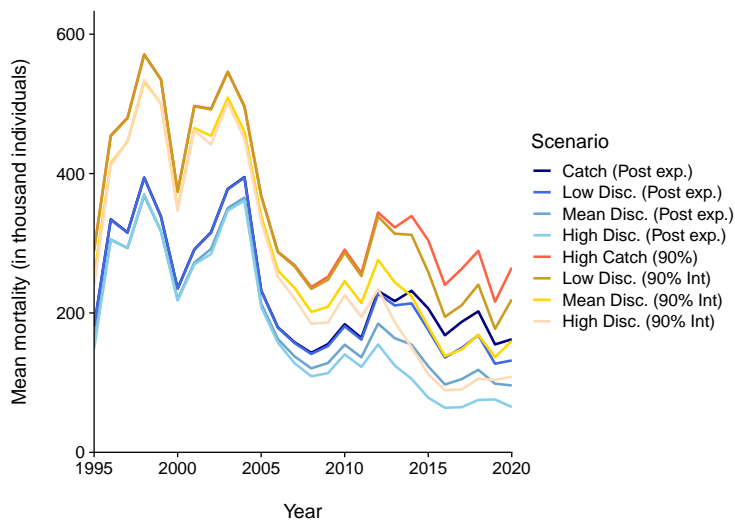


Figure 32: Predicted total fishing related mortality, including 17% post release mortality for live - discarded blue sharks. Catch refers to the posterior median (50%) and 90th percentile (90%) of the predicted catch from the observer catch rate model, low, median and high discard scenarios refer to the 25%, 50% (median) and 75% discard estimates. All discard estimates were applied at flag and latitudinal stratum level to over - all interactions.

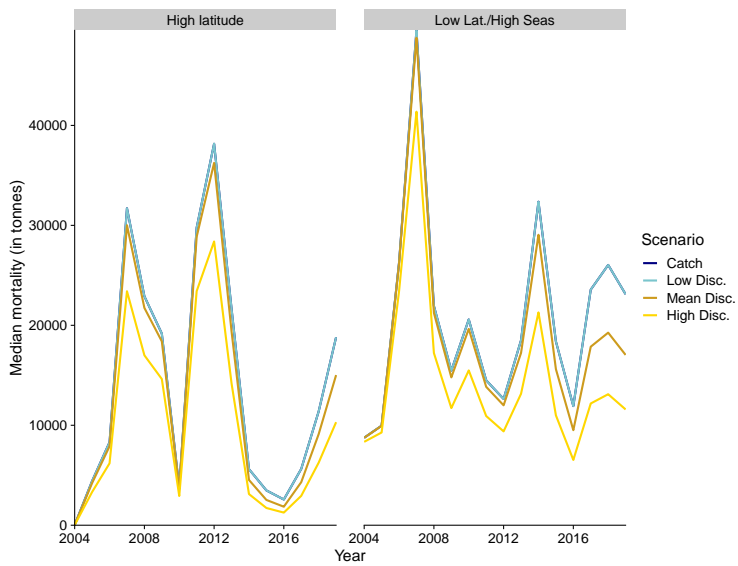


Figure 33: Predicted total fishing related mortality for the EU-ES fleet, including 17% post release mortality for live-discarded blue sharks. Interactions refer to log-sheet-reported catches; low, median and high discard scenarios refer to the 25%, 50% (median) and 75% discard estimates.

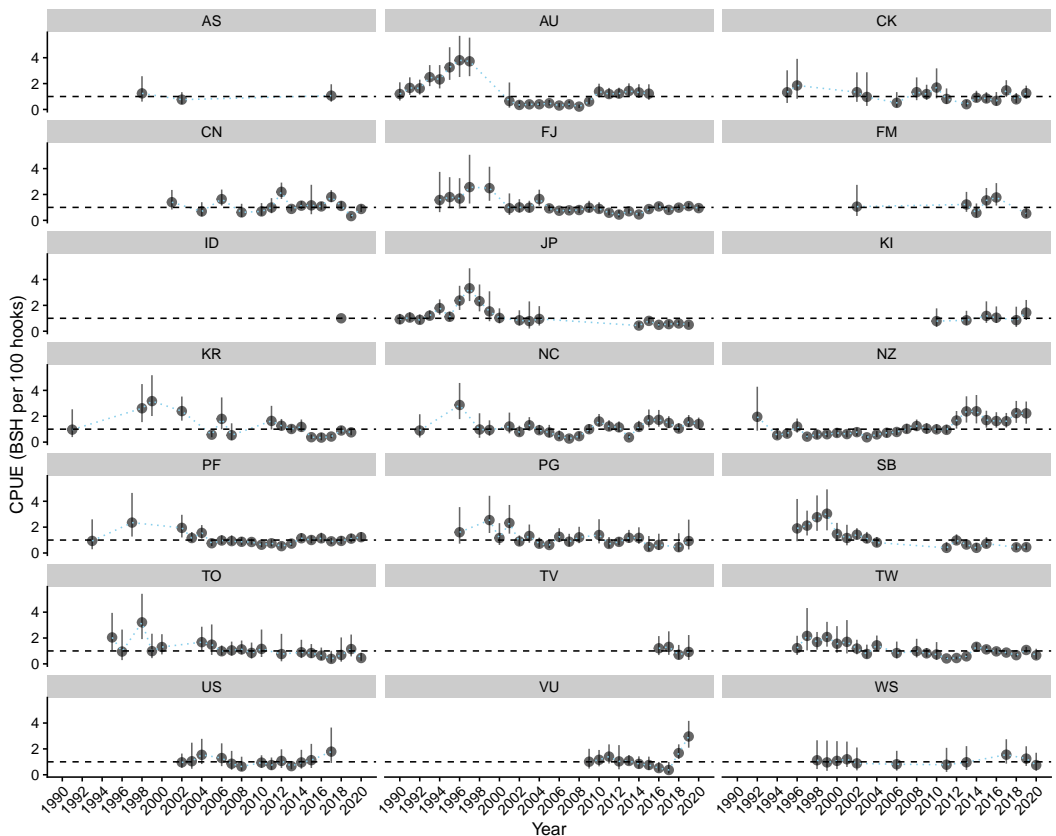


Figure 34: Indexed catch rates (posterior median and 95% percent confidence) by flag in the catch reconstruction model.

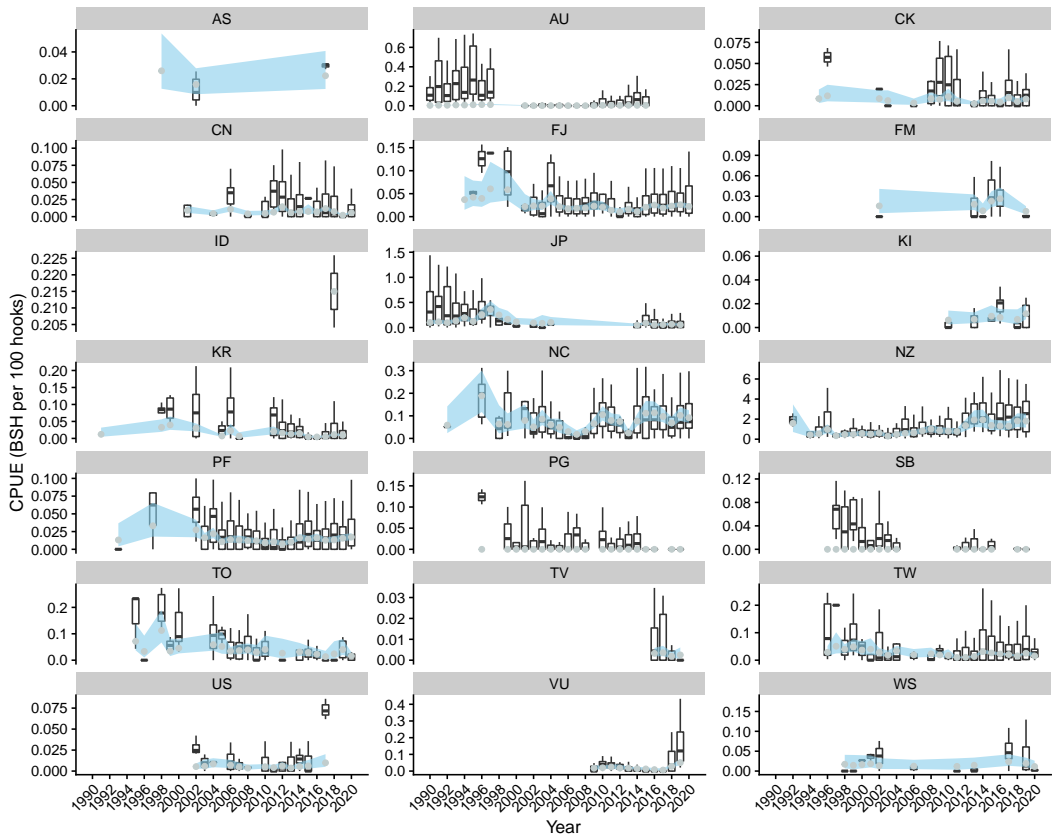


Figure 35: Estimated catch rates (posterior median and 95% percent confidence; in numbers of BSH per 100 hooks) for flags in the catch reconstruction model.

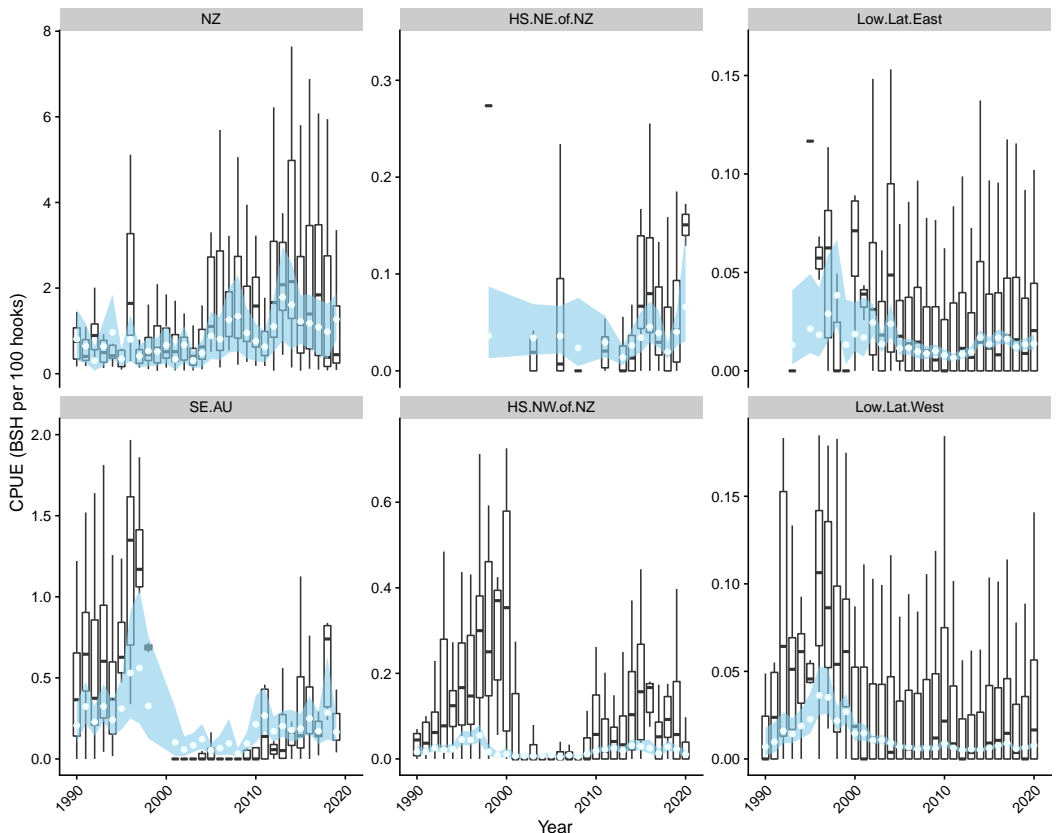


Figure 36: Estimated catch rates (posterior median and 95% percent confidence; in numbers of BSH per 100 hooks) for area in the observer CPUE standardisation model.

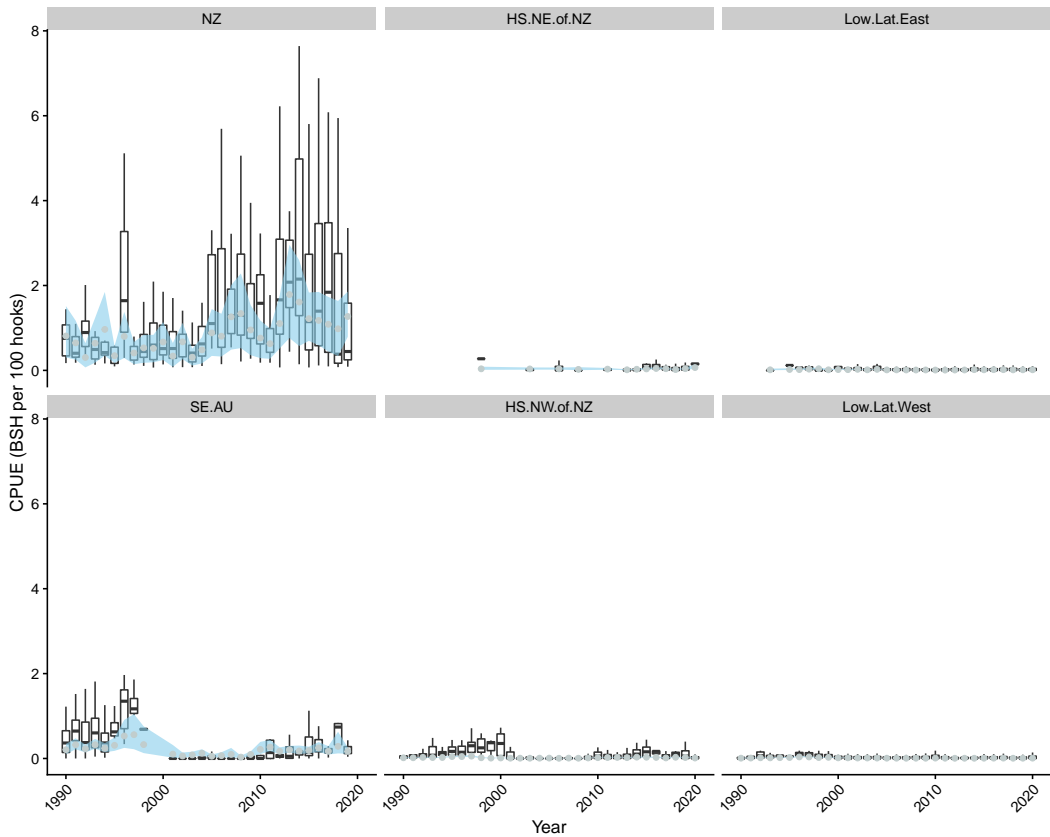


Figure 37: Estimated catch rates (posterior median and 95% percent confidence; in numbers of BSH per 100 hooks) for area in the observer CPUE standardisation model.

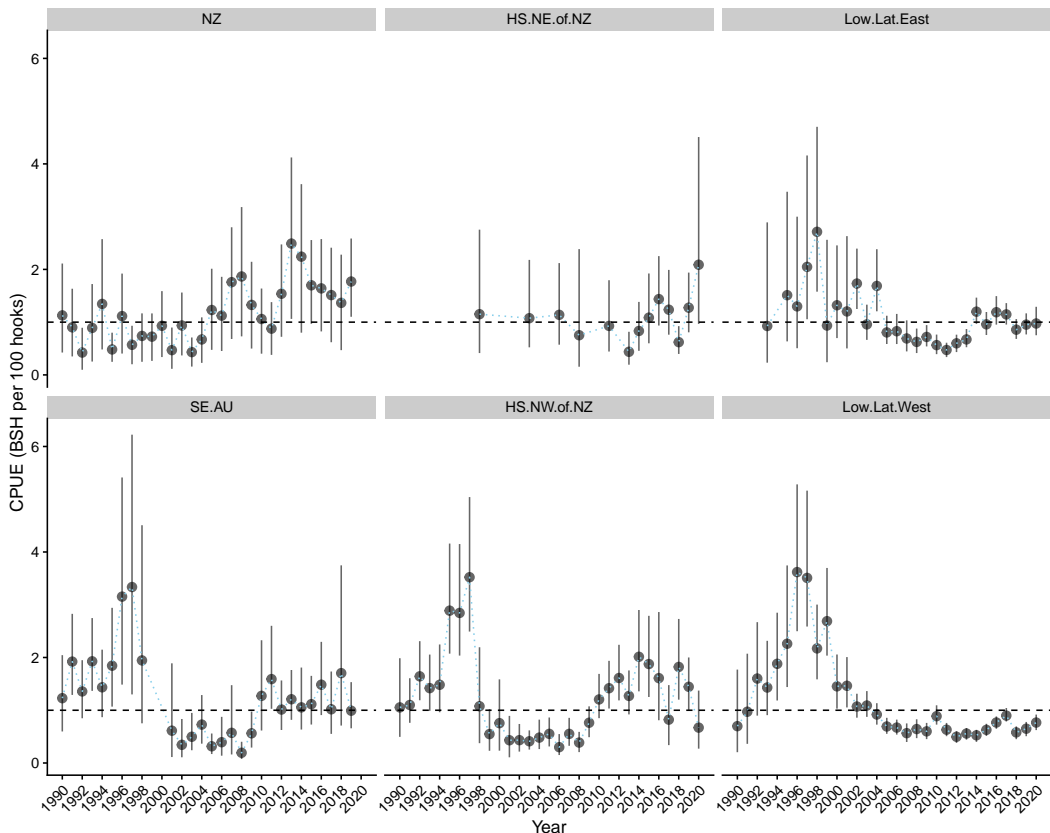


Figure 38: Indexed catch rates (posterior median and 95% percent confidence) by area in the observer CPUE standardisation reconstruction model.

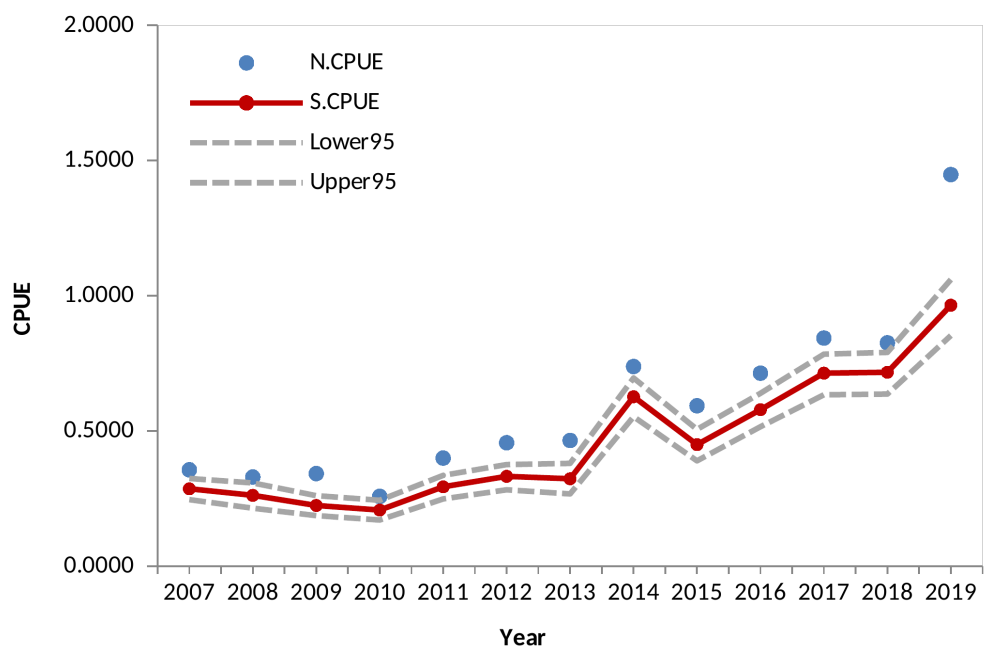


Figure 39: Standardised CPUE from the Chinese - Taipei observer programme.

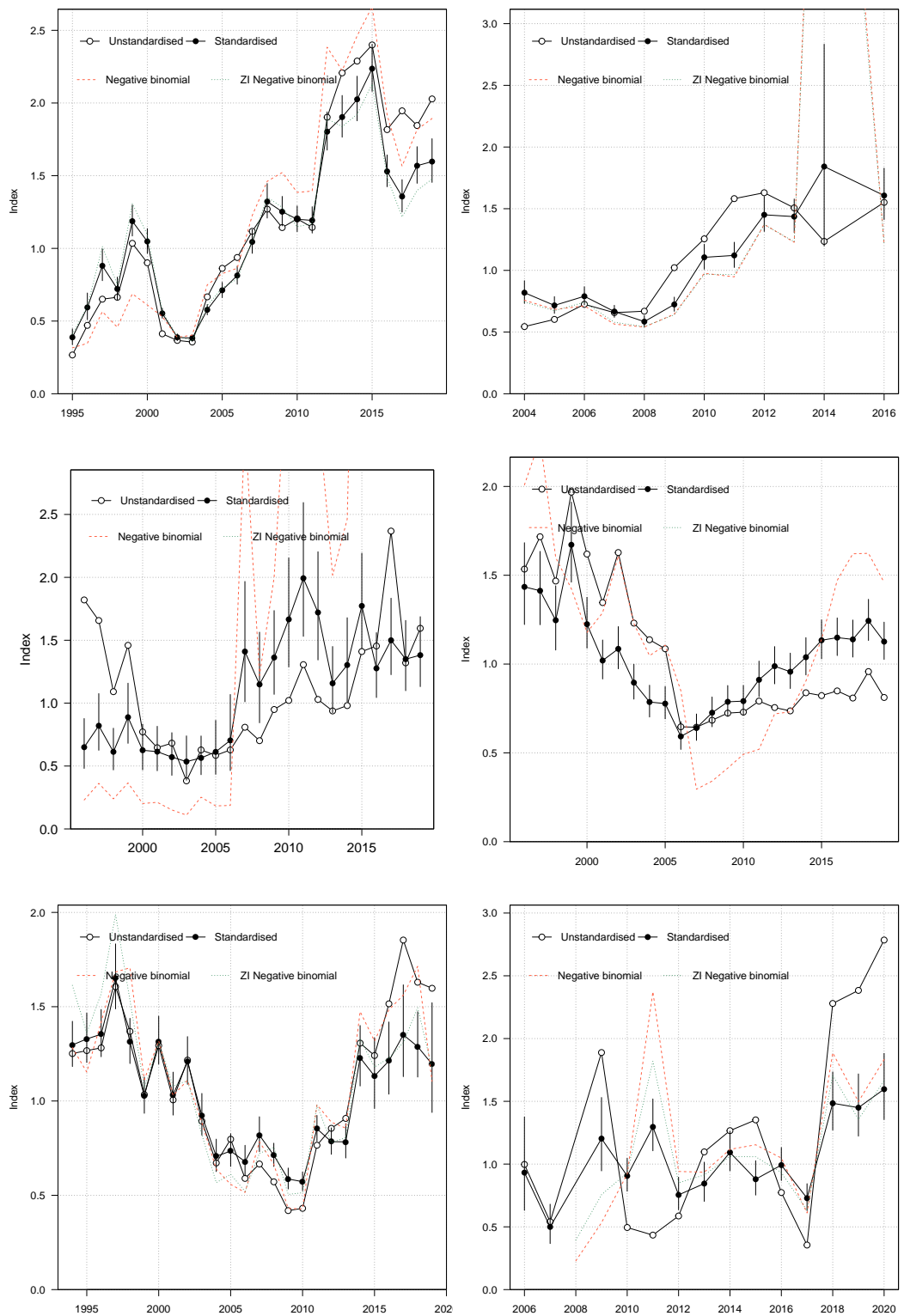


Figure 40: Standardised (closed black circles with standard error) and un-standardised (open circles) CPUE indices for New Zealand (top left), EU (top right), Australian high-latitude (middle-left) and low-latitude (middle-right), Japanese (bottom left) and Chinese-Taipei (bottom right) fleets, for strata with positive catch. Where successful (i.e., converged), standardised trends from a negative-binomial and zero-inflated negative binomial model run over the full dataset (including strata with zero values) are also shown for comparison. Note that any data for the 2020 year is preliminary.

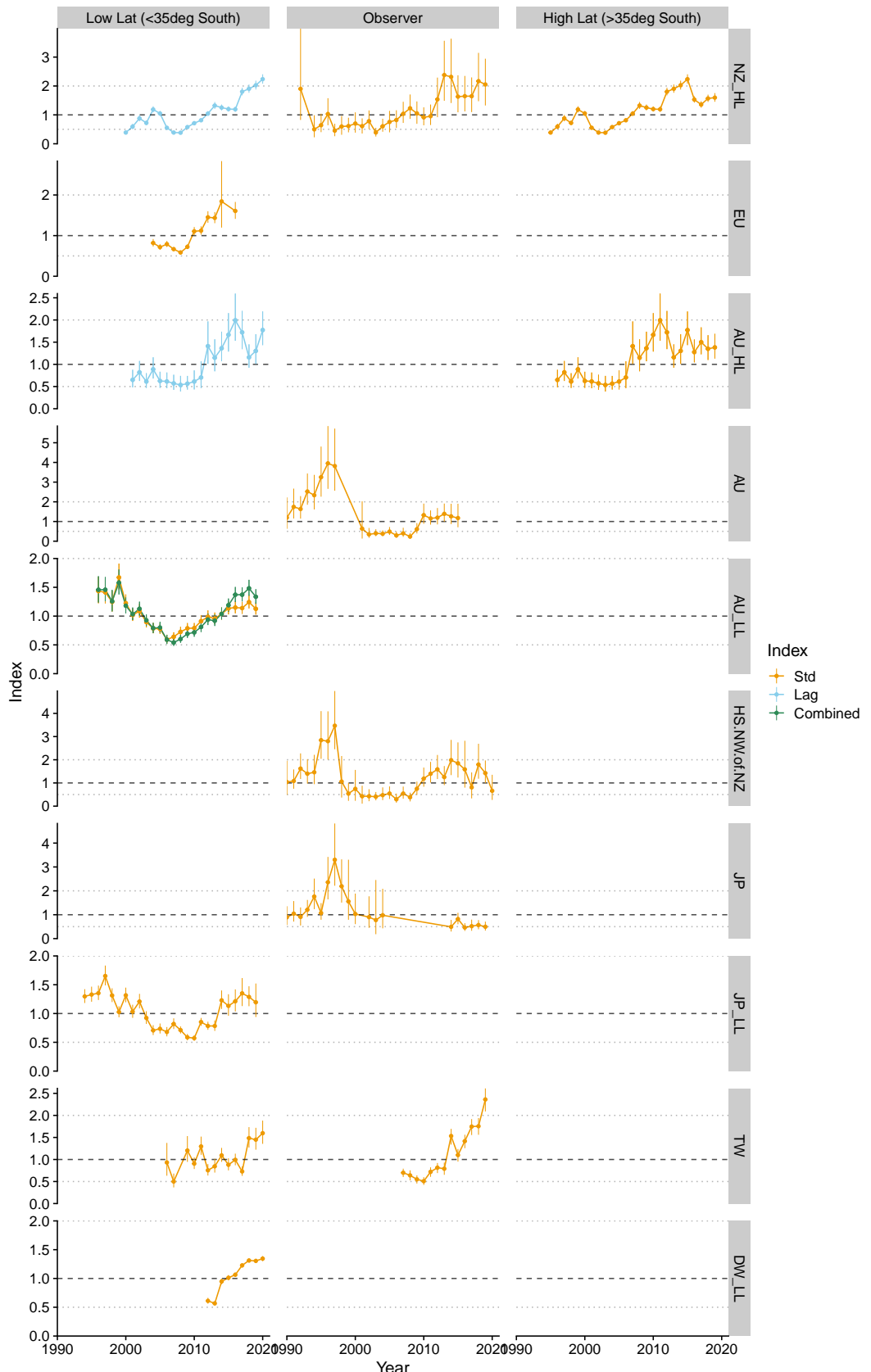


Figure 41: Standardised (circles with standard error) CPUE indices for CCMs included in the log-sheet CPUE analyses. The Chinese-Taipei observer CPUE is included for comparison. To aid comparison between high- and low-latitude CPUE series, the high-latitude indices were lagged by 5 years (dashed CPUE) and plotted alongside the low-latitude indices; 4–5 years is the apparent lag given length frequencies observed in the high latitude fisheries.

APPENDIX A: Observer model diagnostics

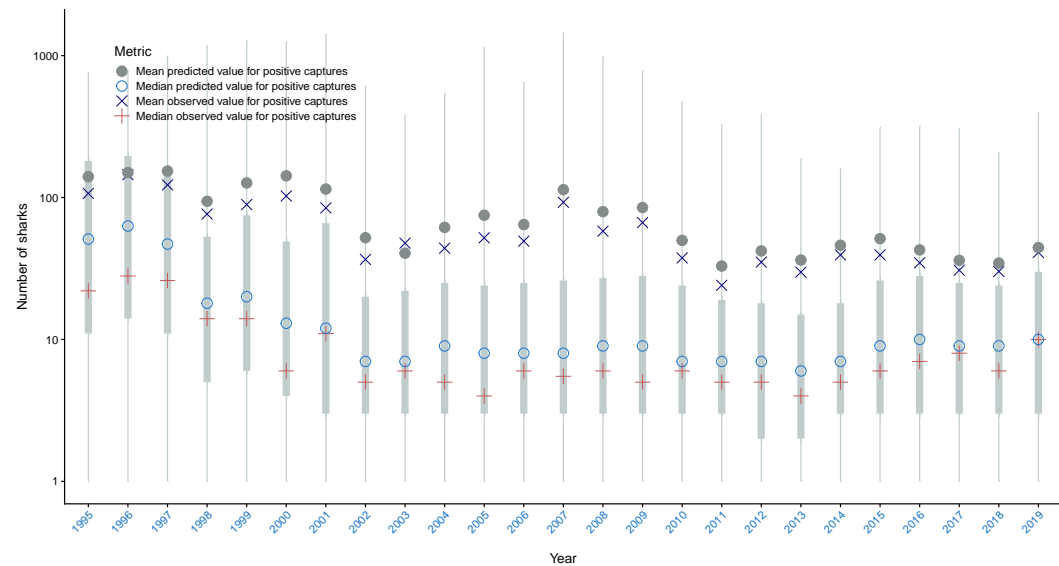


Figure A-1: Diagnostics by model year, with observed and predicted positive captures from a zero-inflated negative binomial model for observed blue shark catch. The negative binomial models were not further pursued due to persistent problems with fitting the data.

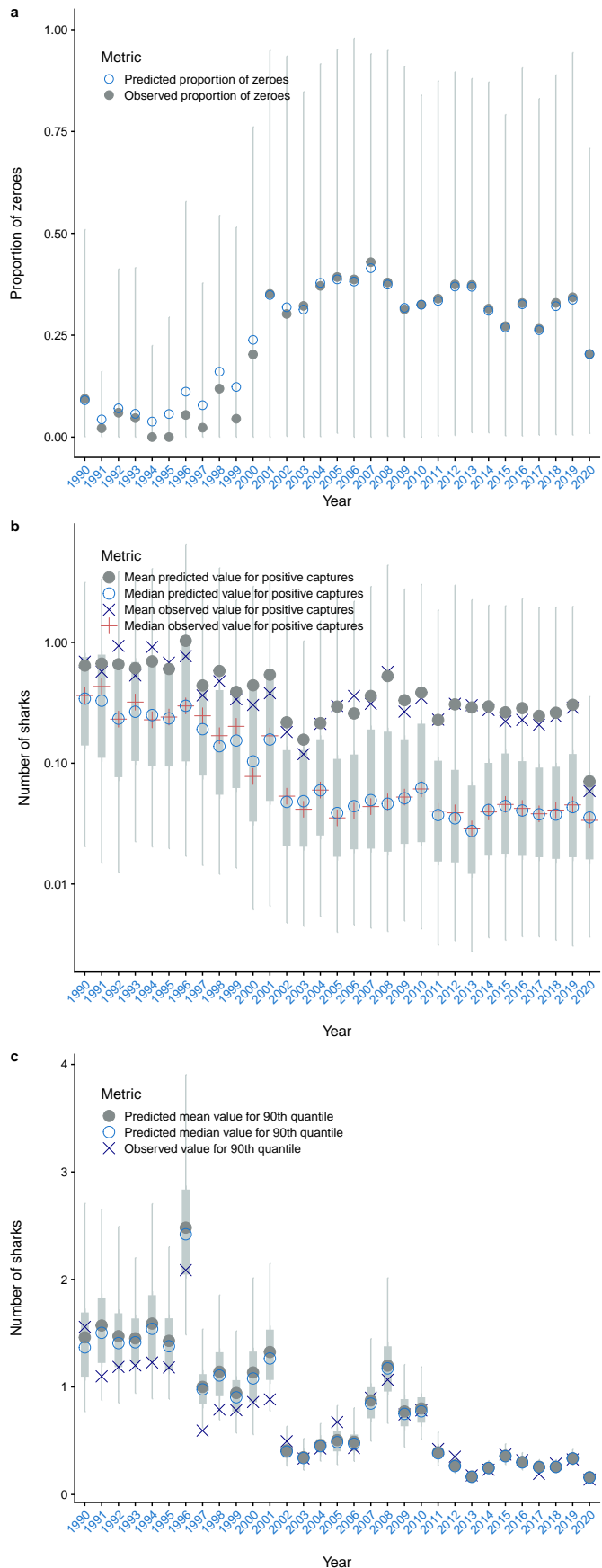


Figure A-2: Diagnostics by model year, with (a) observed and predicted proportion of zero captures, (b) observed and predicted positive captures and (c) dispersion statistics (90% percentile) of observed data and predictions.

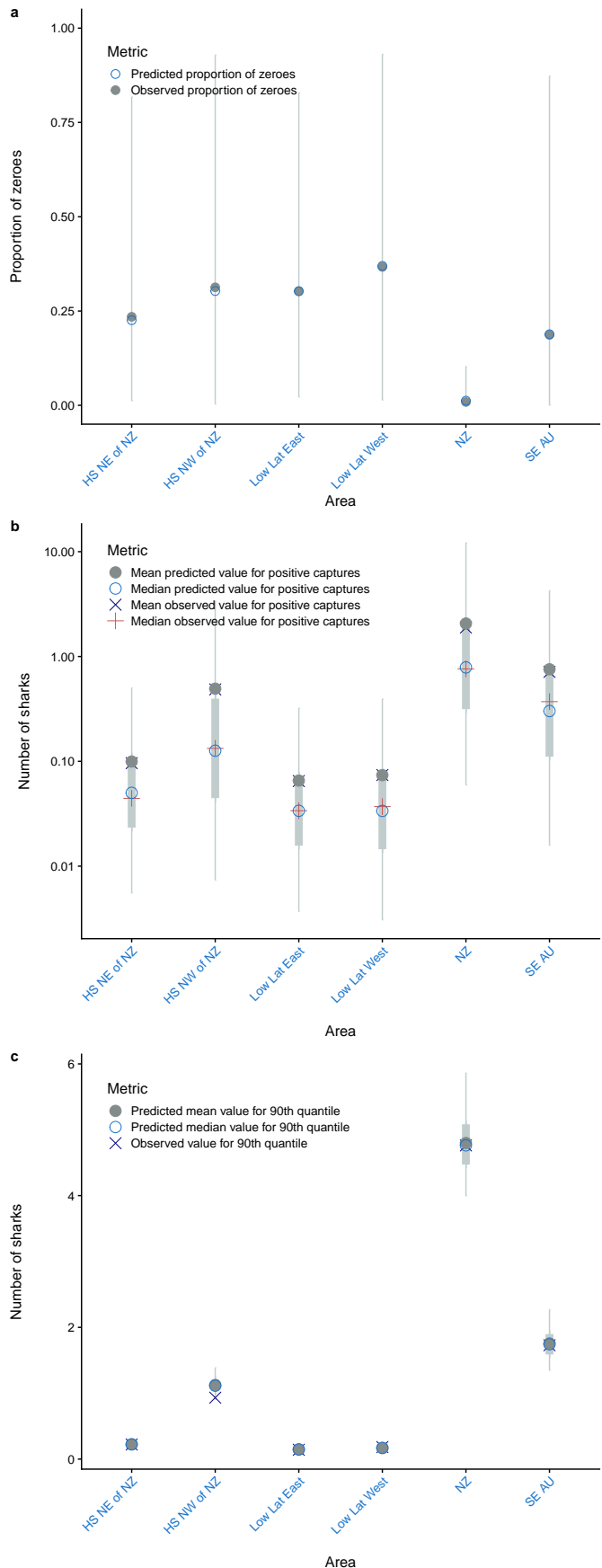


Figure A - 3: Diagnostics by model area, with (a) observed and predicted proportion of zero captures, (b) observed and predicted positive captures and (c) dispersion statistics (90% percentile) of observed data and predictions.

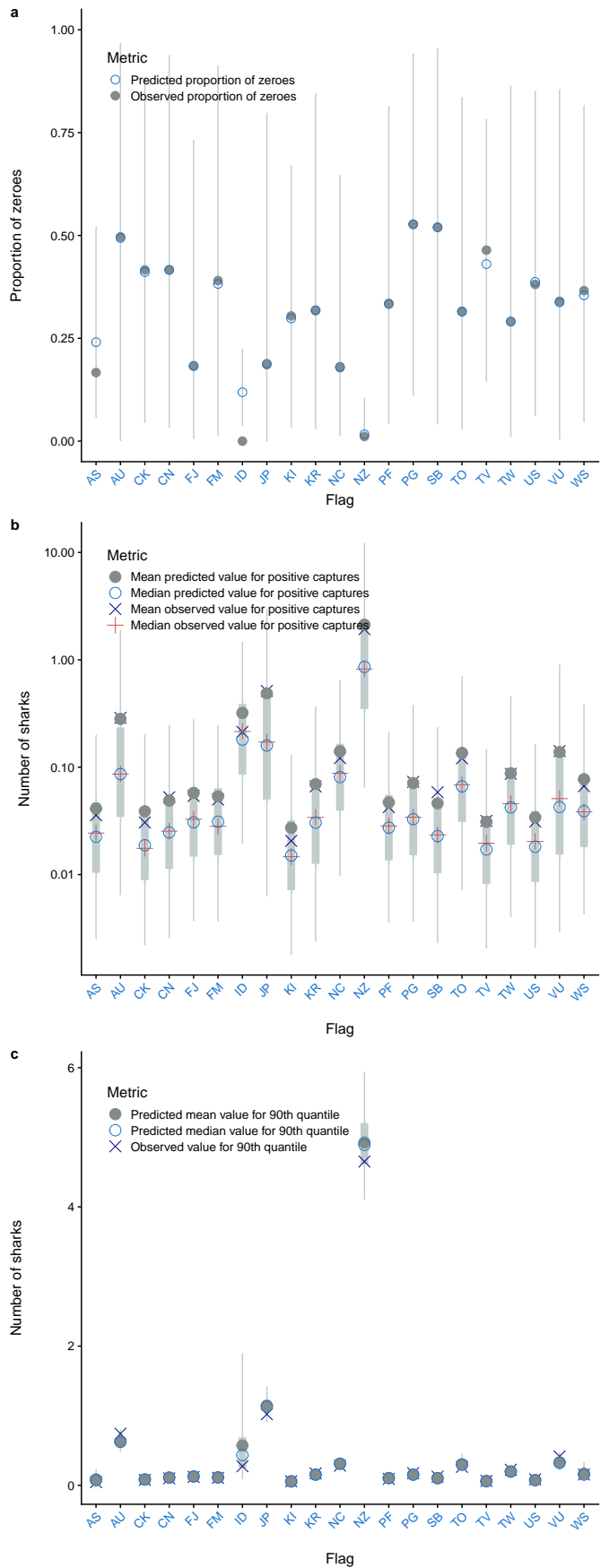


Figure A-4: Diagnostics by flag, with (a) observed and predicted proportion of zero captures, (b) observed and predicted positive captures and (c) dispersion statistics (90% percentile) of observed data and predictions.

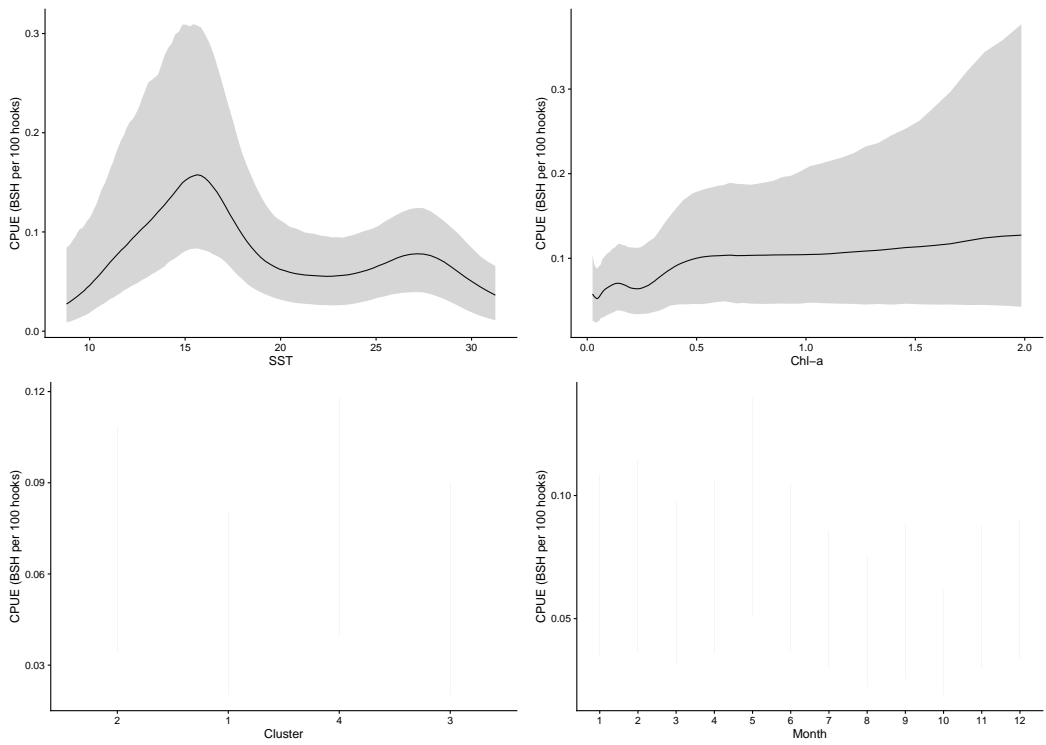


Figure A-5: Conditional effects of SST, chlorophyll-a (CHL-a), targeting cluster and month in the observer catch-prediction model.

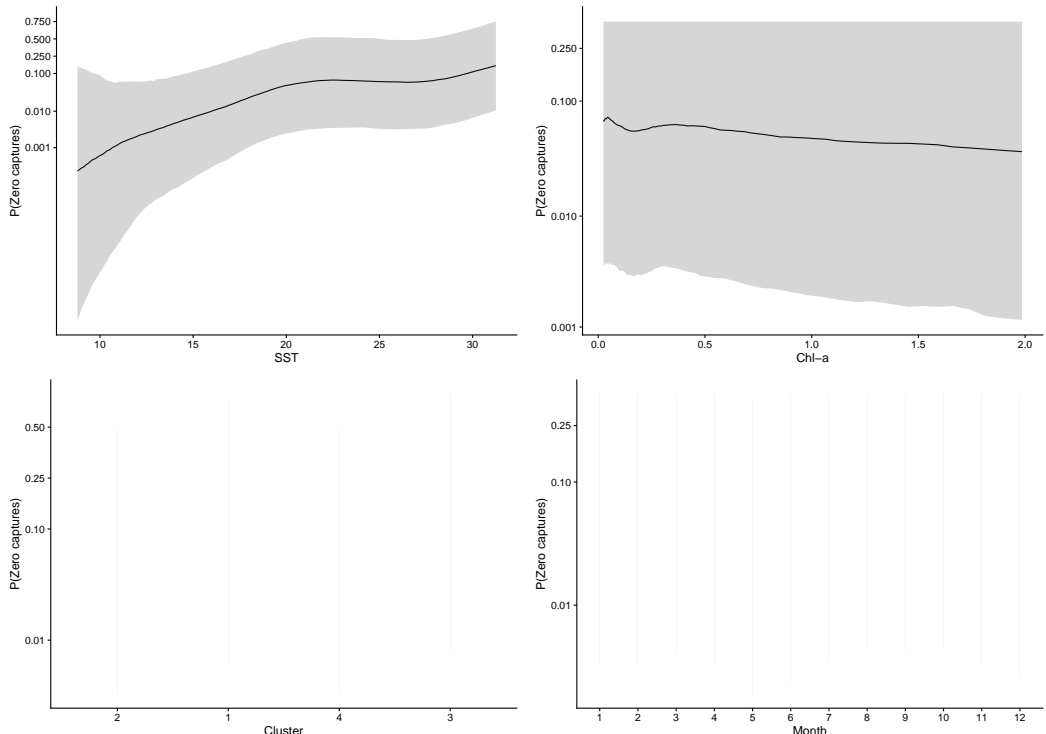


Figure A-6: Conditional effects of SST, chlorophyll-a (CHL-a), targeting cluster and month for the probability of zero catch the observer catch-prediction model.

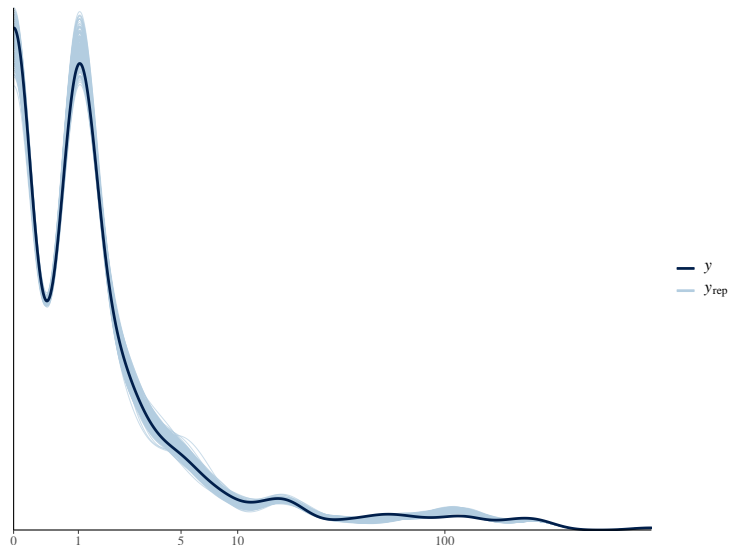


Figure A-7: Posterior predictive check for the release - condition model, showing predicted distribution of number of blue shark in the category dead or alive - dying (blue draws from the posterior distribution), as well as the observed data distribution (black line)

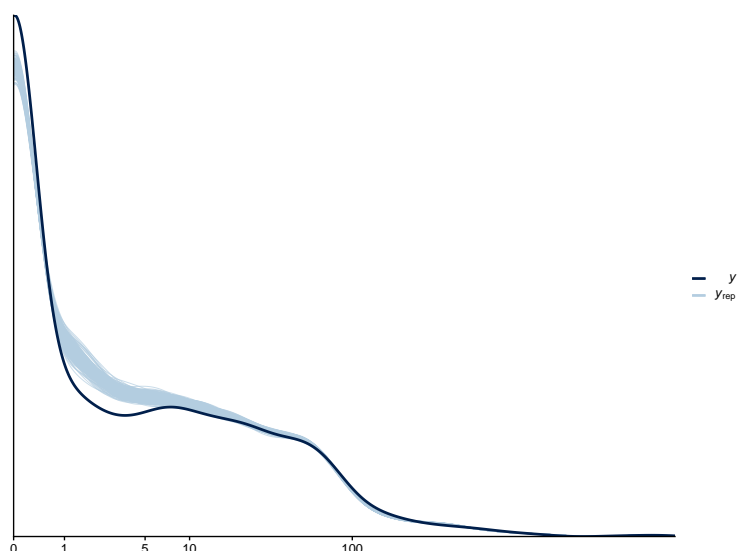


Figure A-8: Posterior predictive check for the fate (discard proportion) model, showing predicted distribution of number of blue shark in the category "discarded alive" (blue draws from the posterior distribution), as well as the observed data distribution (black line).

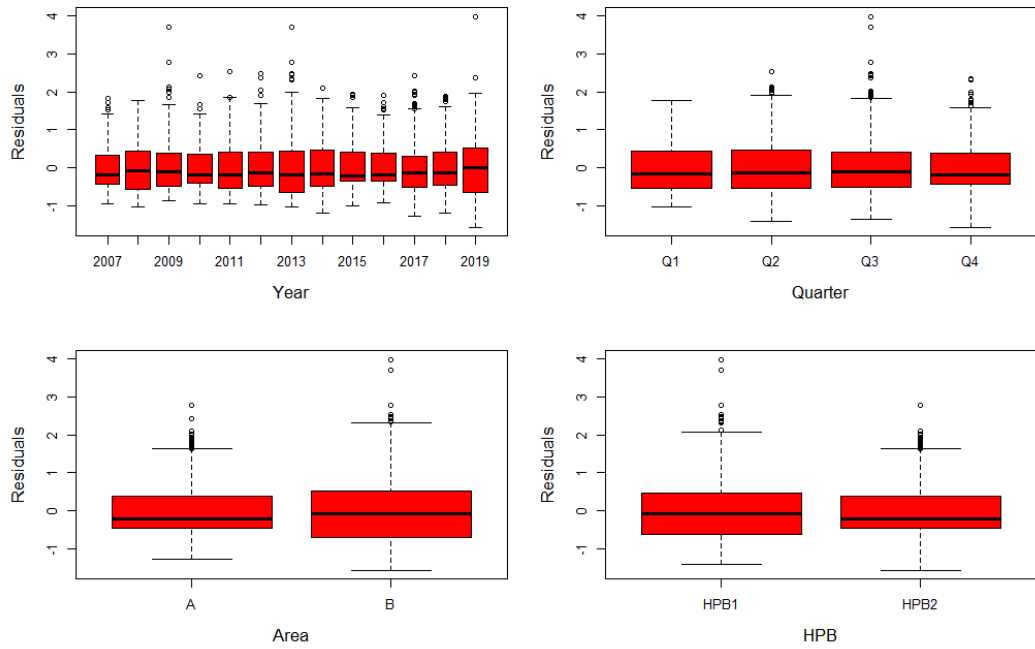


Figure A-9: Residuals from the standardised CPUE from the Chinese - Taipei observer programme.

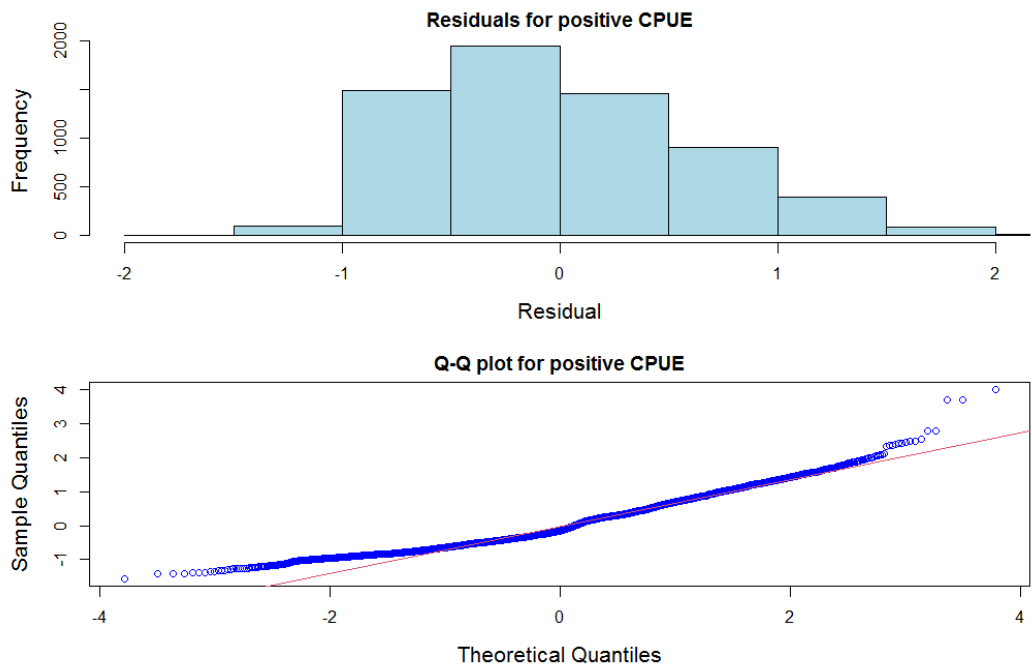


Figure A-10: Residual distribution and quantile - quantile plot from the standardised CPUE from the Chinese - Taipei observer programme.

APPENDIX B: Logsheet CPUE standardisation diagnostics

B.1 New Zealand fleet high latitude CPUE

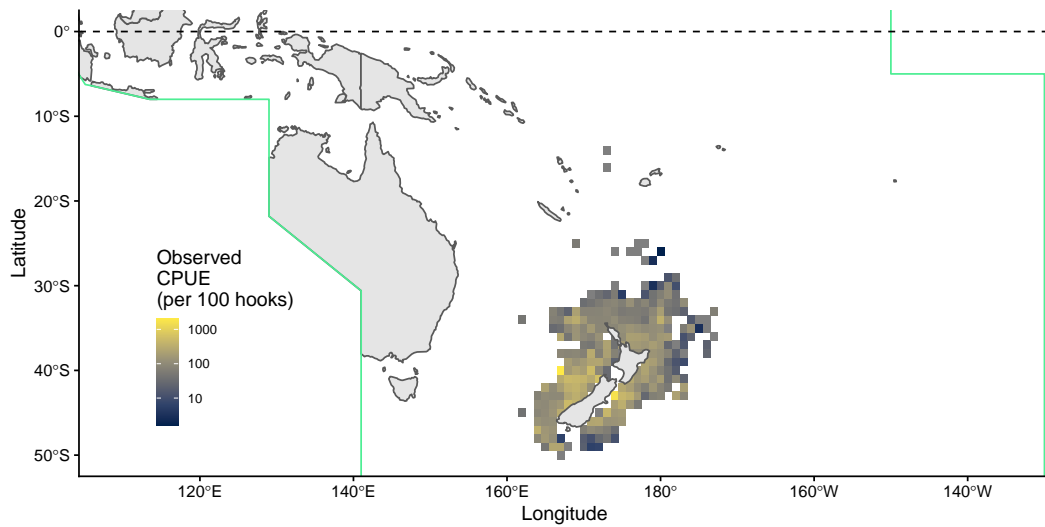


Figure B-11: Maps of average catch rates (CPUE; in number of blue shark per 100 hooks) for the New Zealand longline fleet.

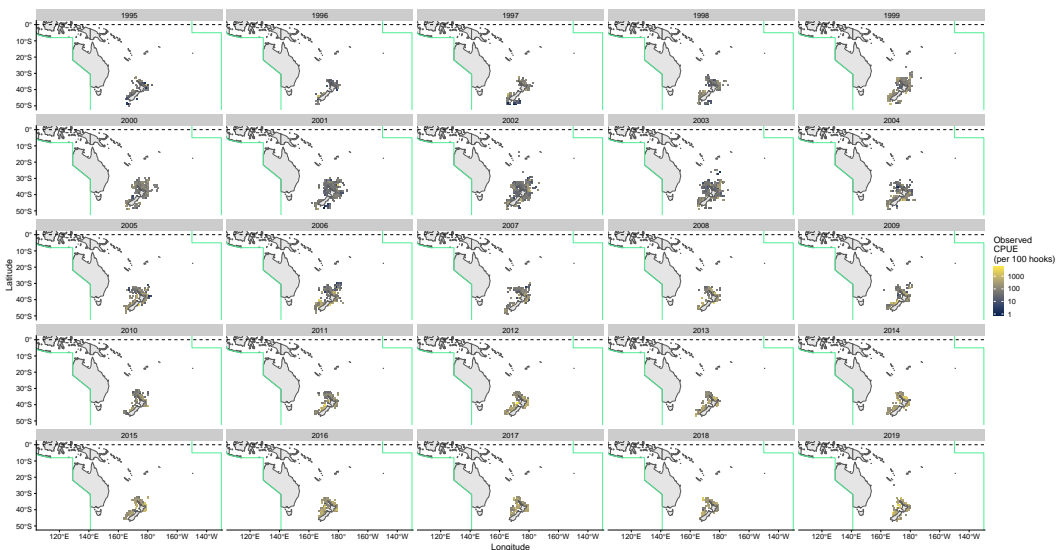


Figure B-12: Maps of average catch rates (CPUE; in number of blue shark per 100 hooks) by year for the New Zealand longline fleet.

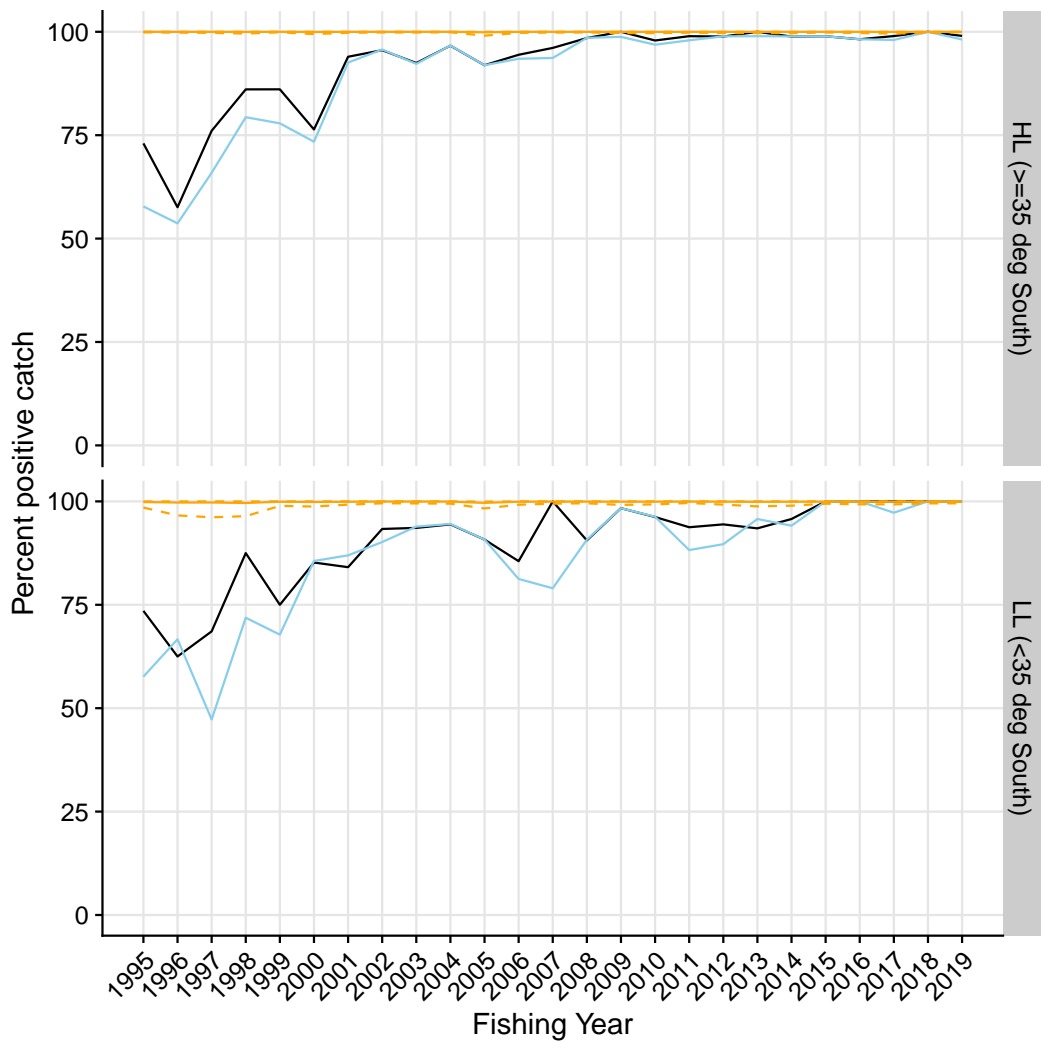


Figure B-13: Proportion of strata for the Zew Zealand fleet with positive catch by latitudinal stratum. Light blue are initial log-sheet records prior to filtering, the black line is the retained dataset after filtering for consistently reporting vessels. Where available, the corresponding values from observed strata is shown in orange.

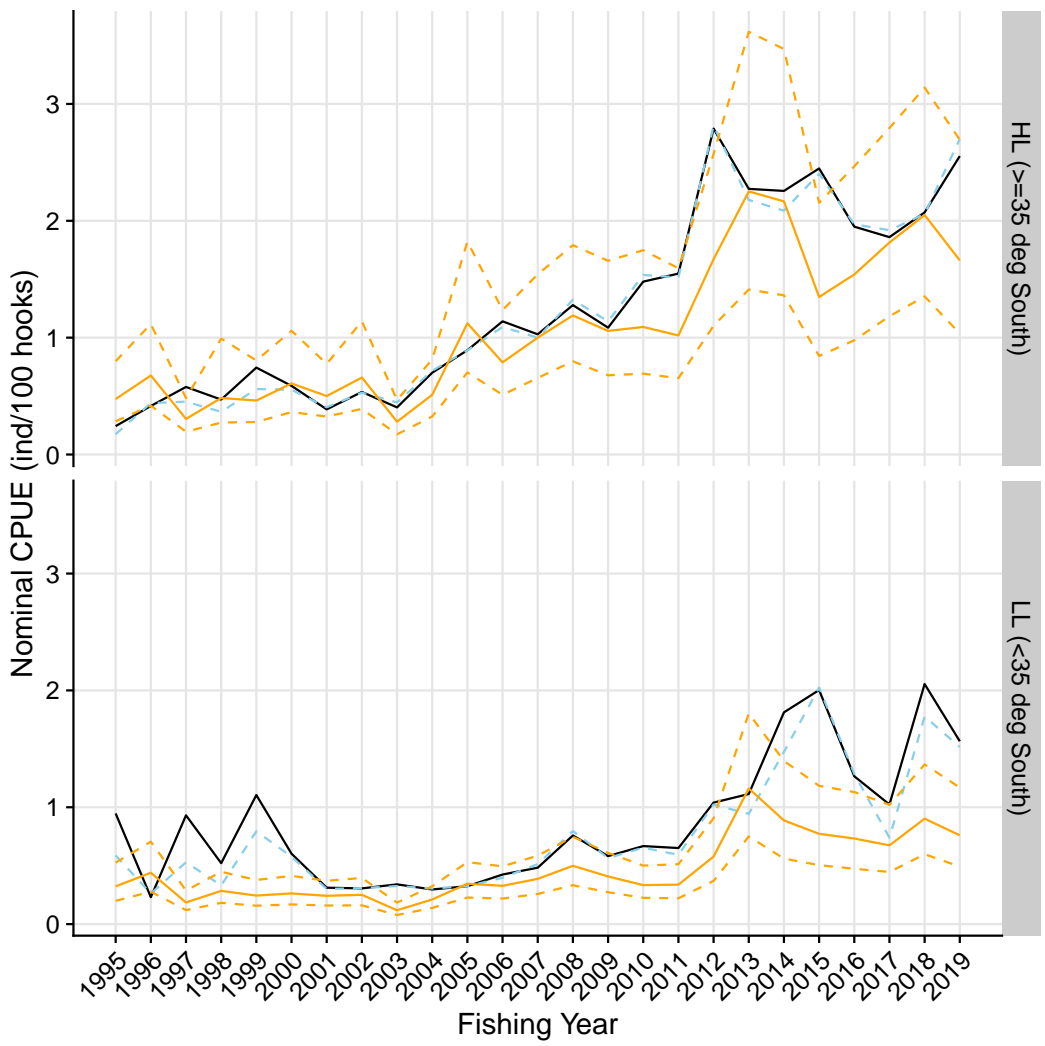


Figure B-14: Nominal CPUE (in number of blue shark per 100 hooks) strata of the Zew Zealand fleet with positive catch by latitudinal stratum. Light blue are initial log-sheet records prior to filtering, the black line is the retained dataset after filtering for consistently reporting vessels. Where available, the corresponding values from observed strata is shown in orange.

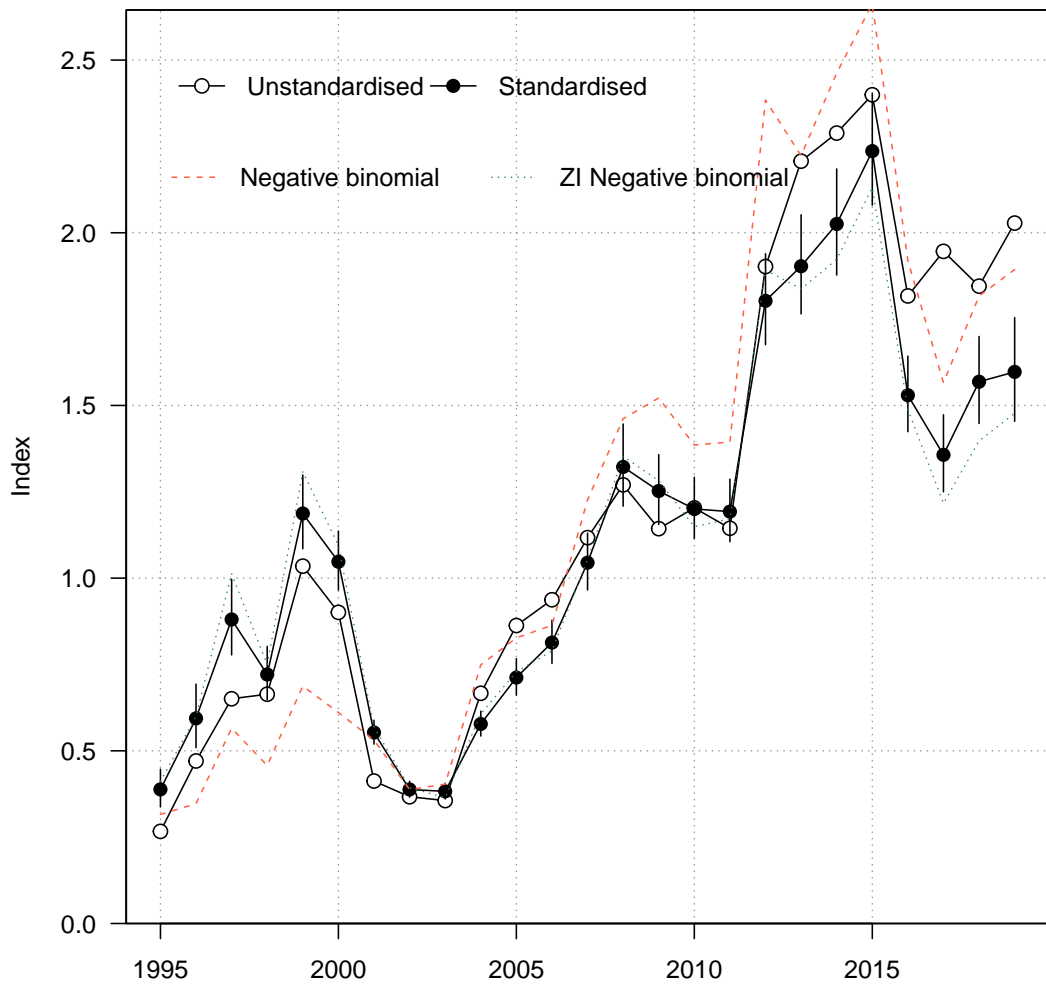


Figure B-15: Standardised (closed black circles with standard error) and unstandardised (open circles) CPUE indices for Zew Zealand fleet strata with positive catch. Where successful (i.e., converged), standardised trends from a negative - binomial and zero - inflated negative binomial model run over the full dataset (including strata with zero values) are also shown for comparison.

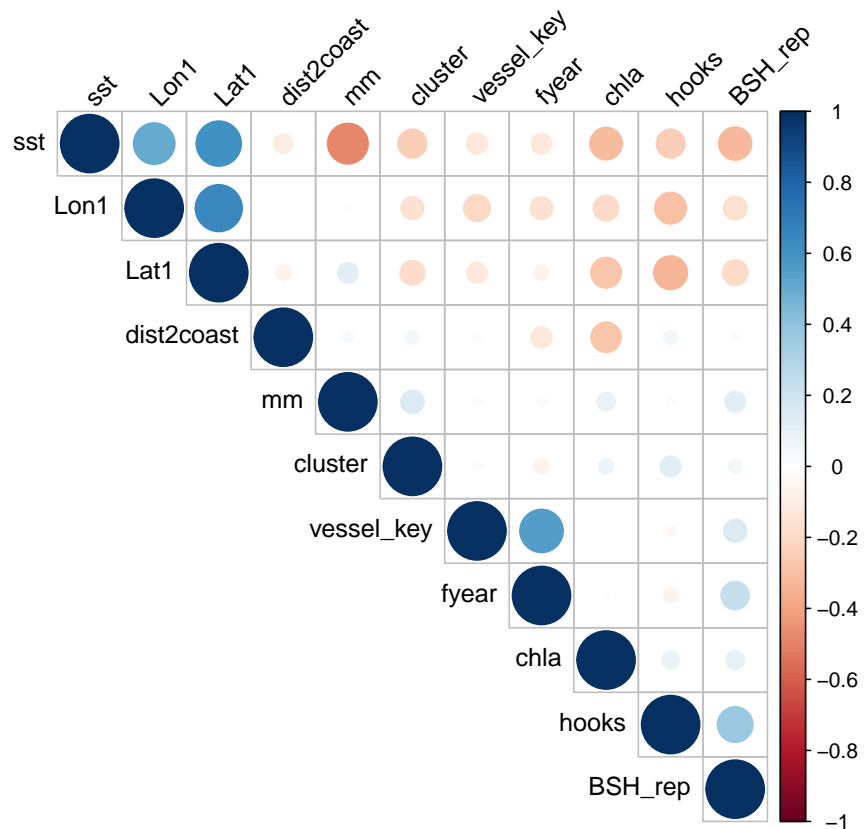


Figure B-16: Correlations amongst potential covariates for CPUE standardisation in the Zew Zealand fleet. Where necessary, variables were removed to reduce redundancy in the models.

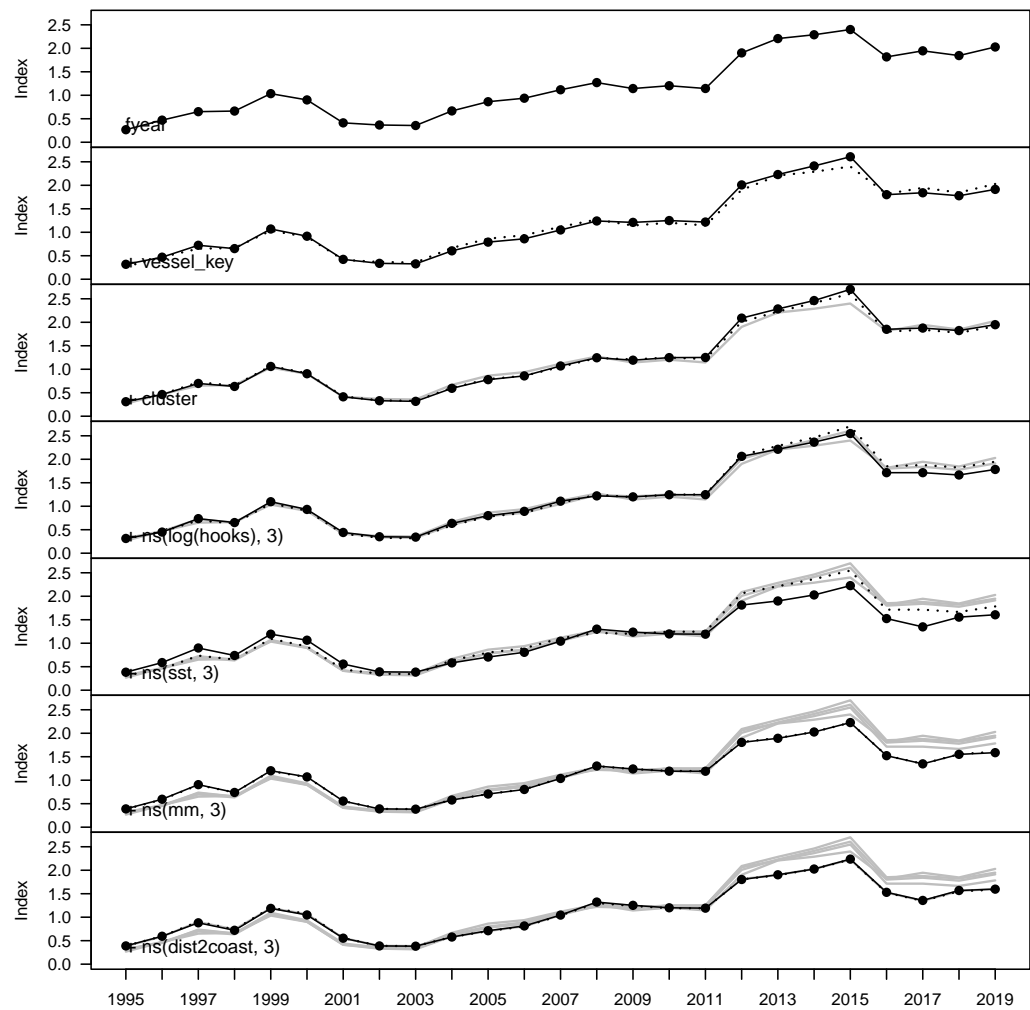


Figure B-17: Step plot for the New Zealand fleet CPUE, showing sequential standardising effects of variables included in the standardisation model.

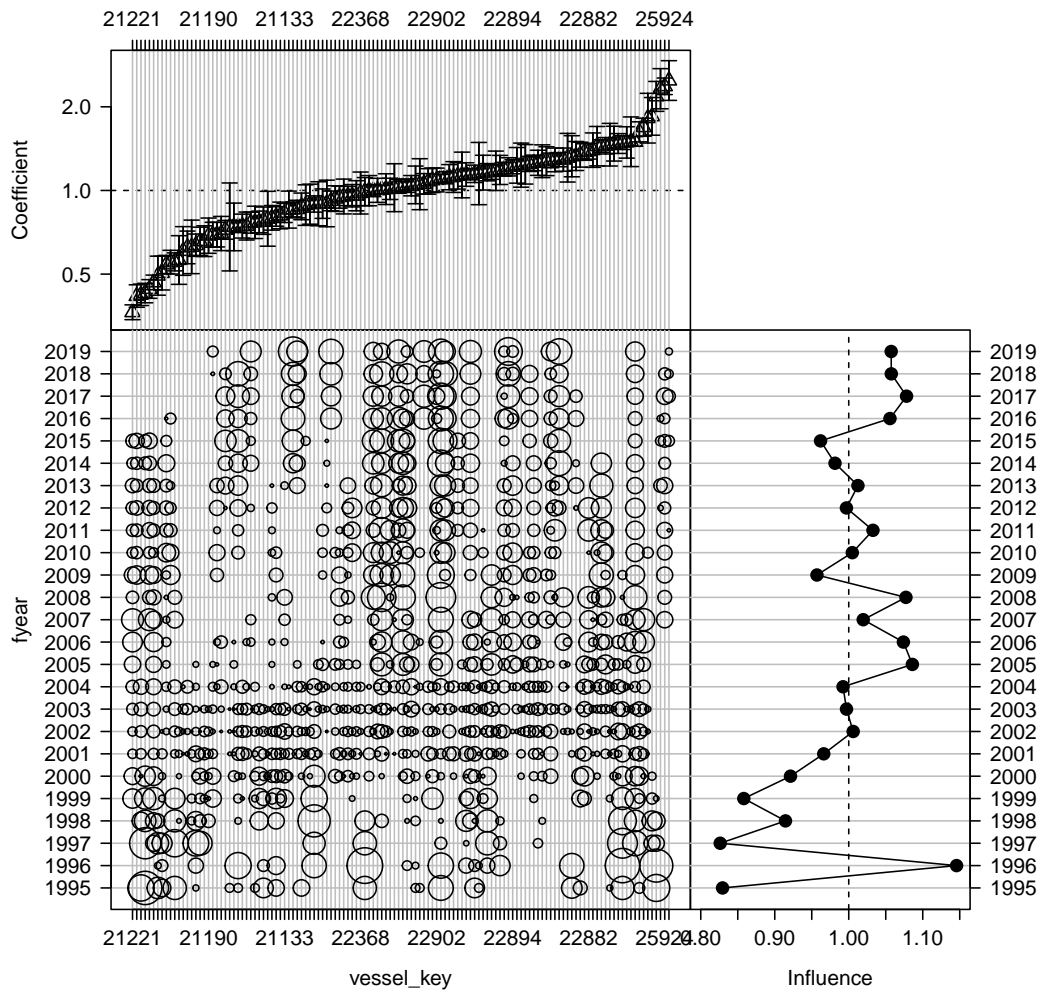


Figure B-18: Influence of fleet composition (vessel keys) for the Zew Zealand fleet (bubble plot; bubbles scales by effort) on CPUE; influence (right hand plot) shows the standardising effect (a positive effect reduces the standardised CPUE by the equivalent amount). Estimated coefficients are given in the top panel.

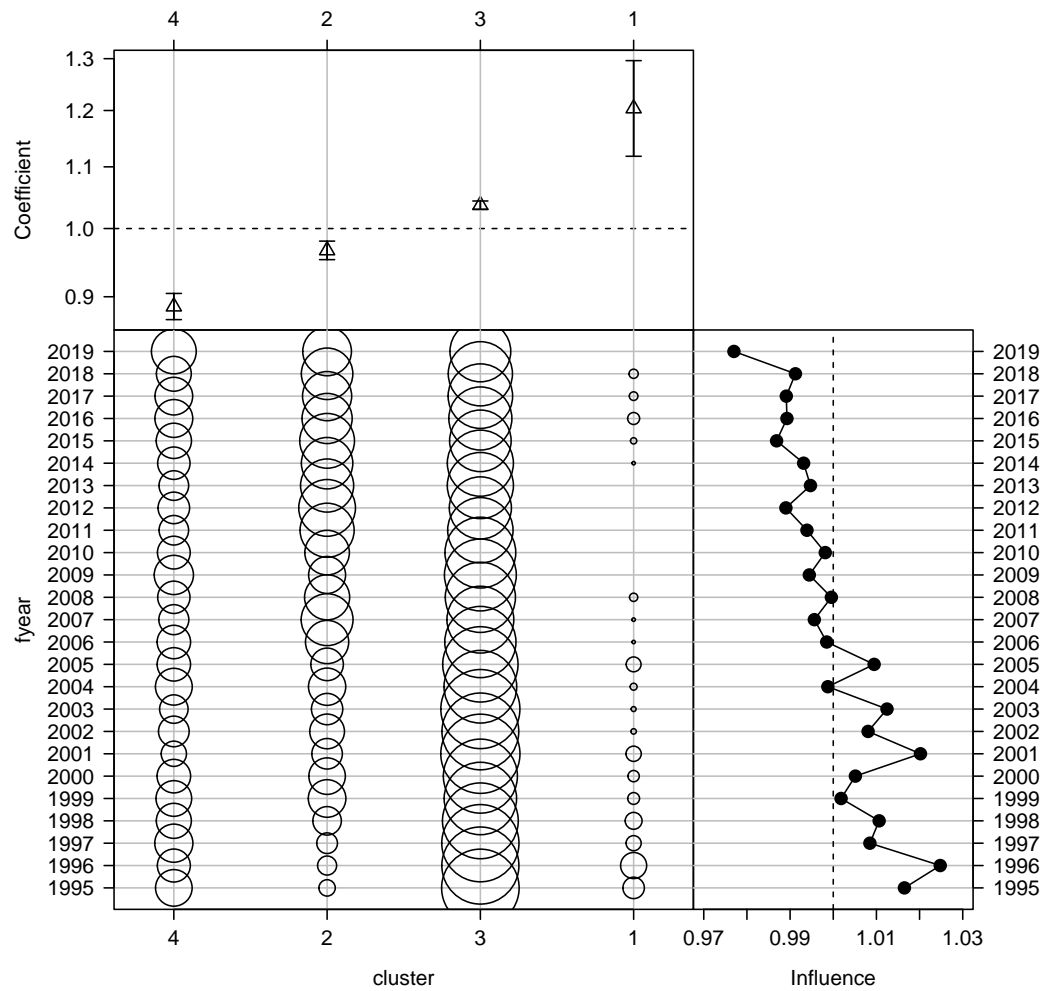


Figure B-19: Influence of targeting cluster for the New Zealand fleet (bubble plot; bubbles scales by effort) on CPUE; influence (right hand plot) shows the standardising effect (a positive effect reduces the standardised CPUE by the equivalent amount). Estimated coefficients are given in the top panel.

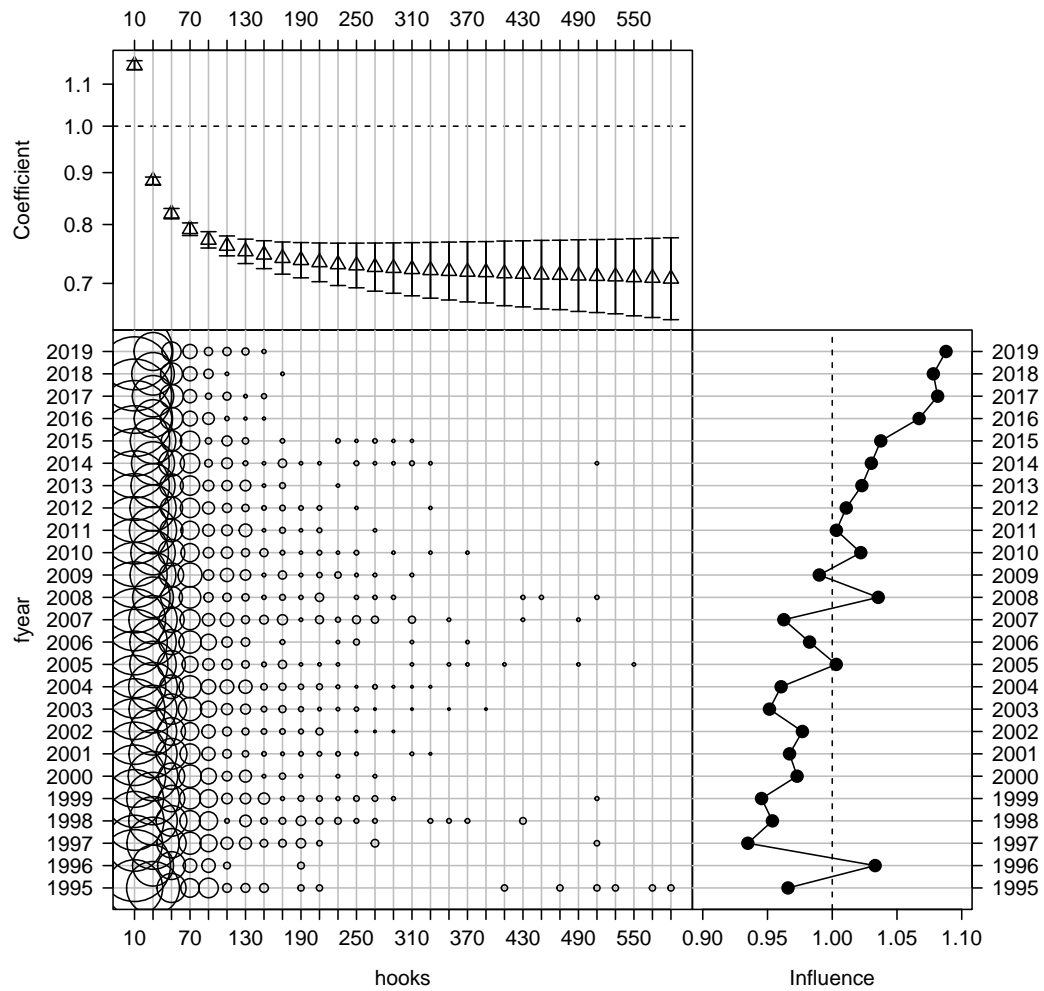


Figure B-20: Influence of number of hooks set per stratum for the Zew Zealand fleet (bubble plot; bubbles scales by effort) on CPUE; influence (right hand plot) shows the standardising effect (a positive effect reduces the standardised CPUE by the equivalent amount). Estimated coefficients are given in the top panel.

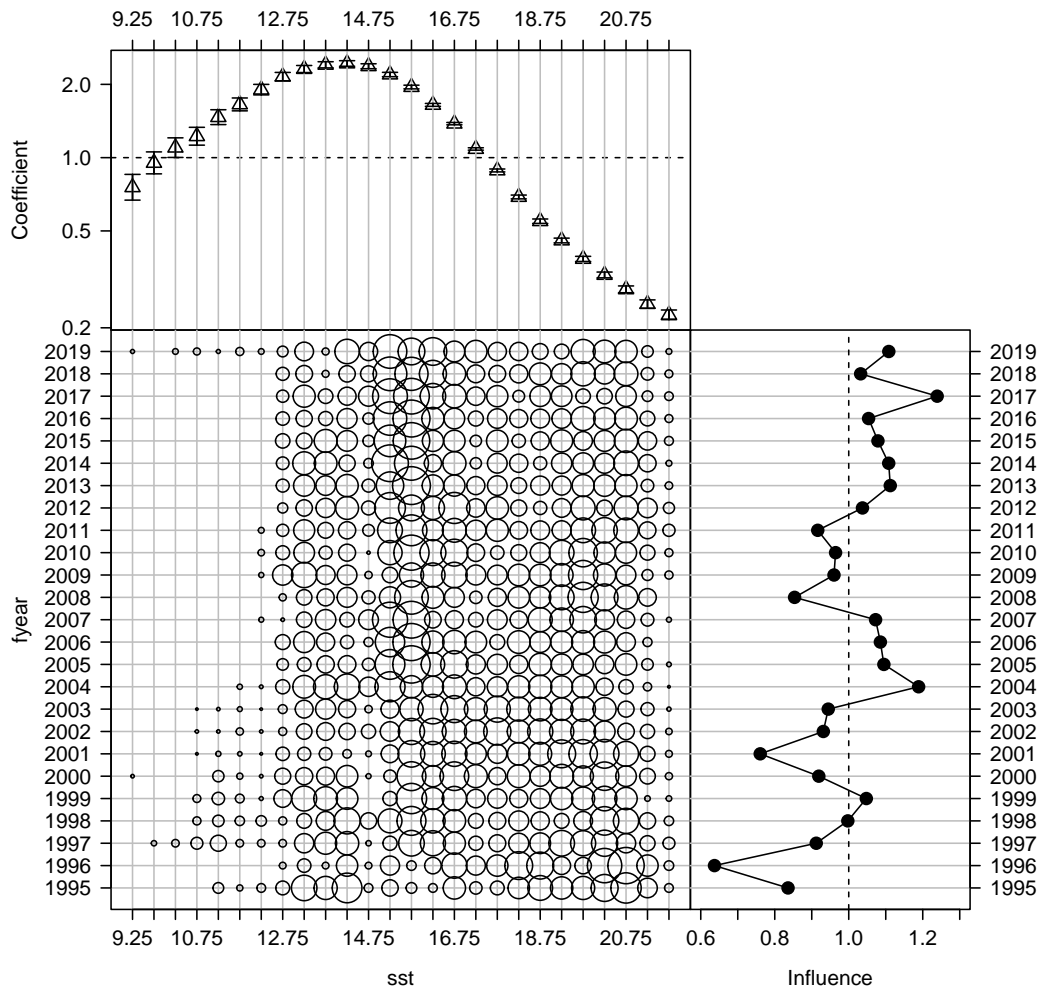


Figure B-21: Influence of sea surface temperature (SST, in degrees Celsius) for the Zew Zealand fleet (bubble plot; bubbles scales by effort) on CPUE; influence (right hand plot) shows the standardising effect (a positive effect reduces the standardised CPUE by the equivalent amount). Estimated coefficients are given in the top panel.

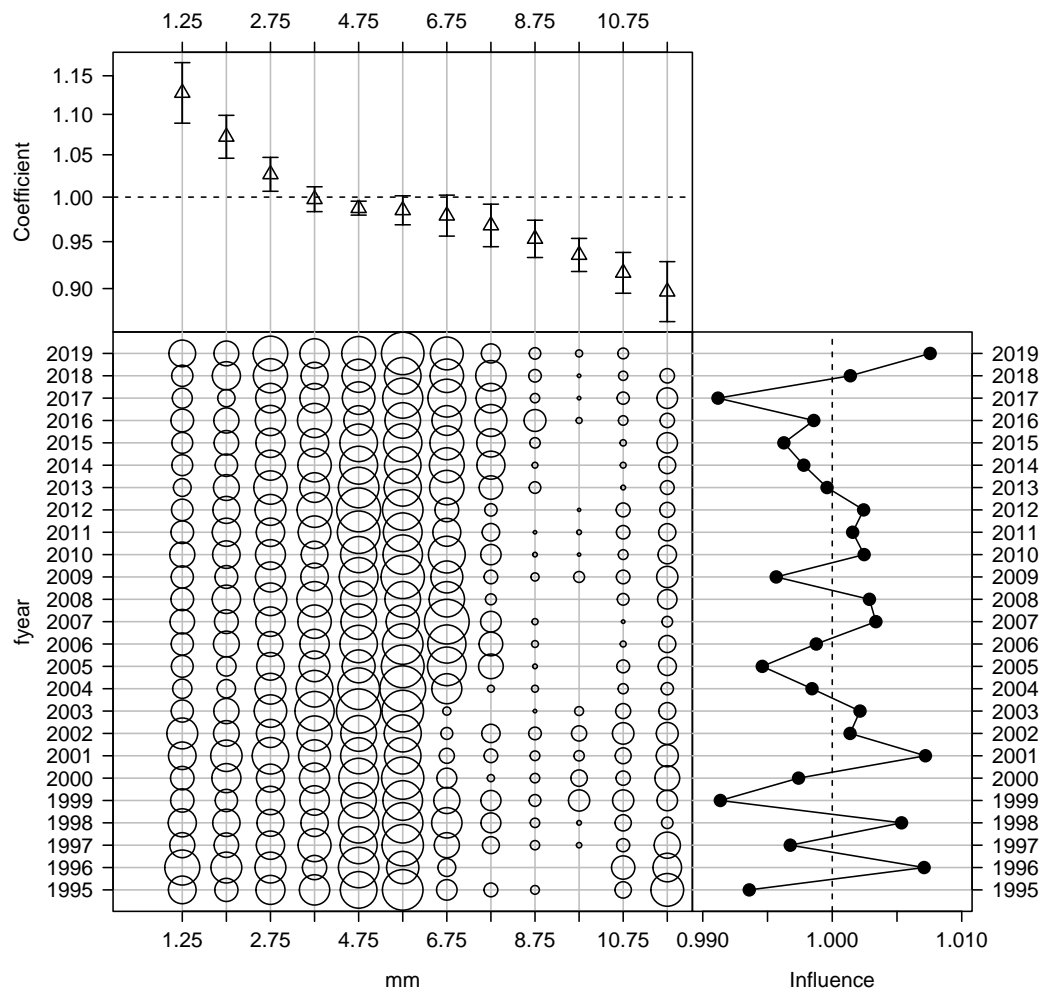


Figure B-22: Influence of month for the New Zealand fleet (bubble plot; bubbles scales by effort) on CPUE; influence (right hand plot) shows the standardising effect (a positive effect reduces the standardised CPUE by the equivalent amount). Estimated coefficients are given in the top panel.

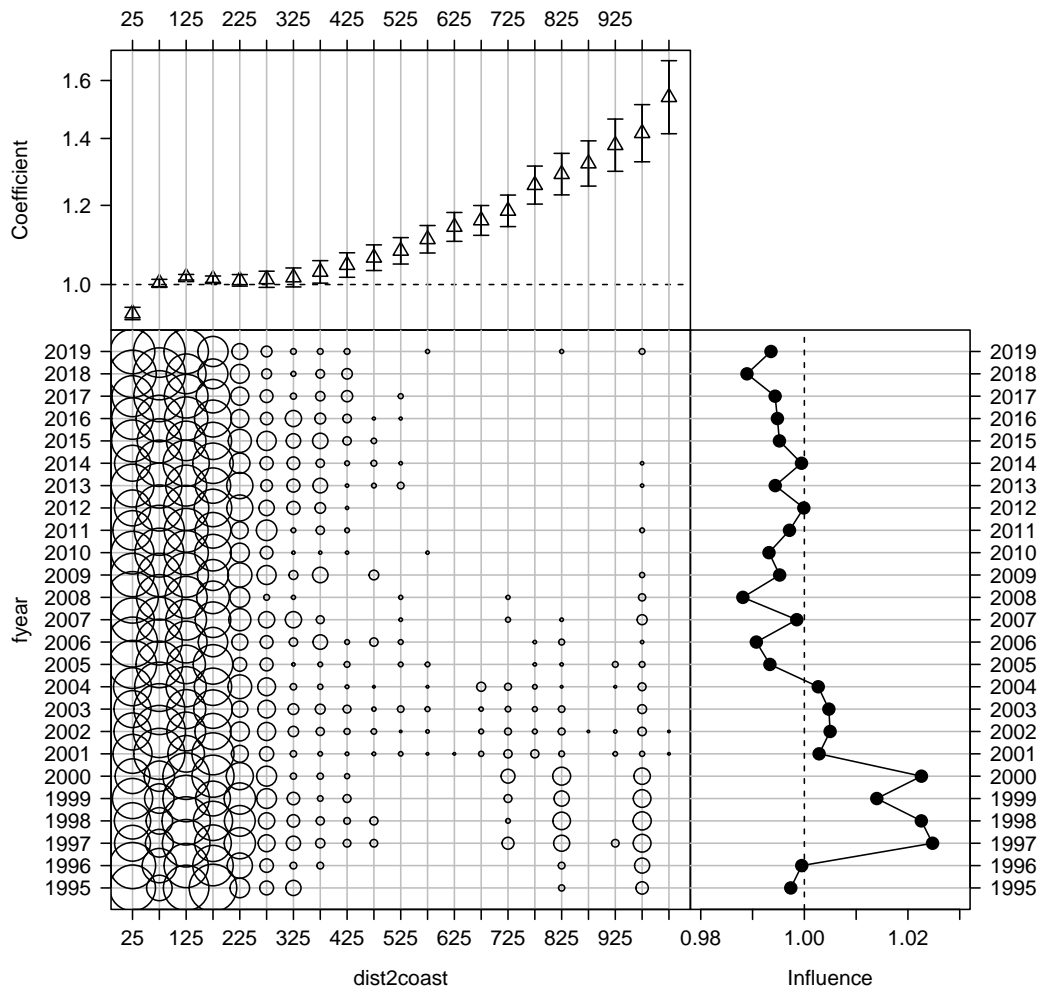


Figure B-23: Influence of distance to coast composition for the Zew Zealand fleet (bubble plot; bubbles scales by effort) on CPUE; influence (right hand plot) shows the standardising effect (a positive effect reduces the standardised CPUE by the equivalent amount). Estimated coefficients are given in the top panel.

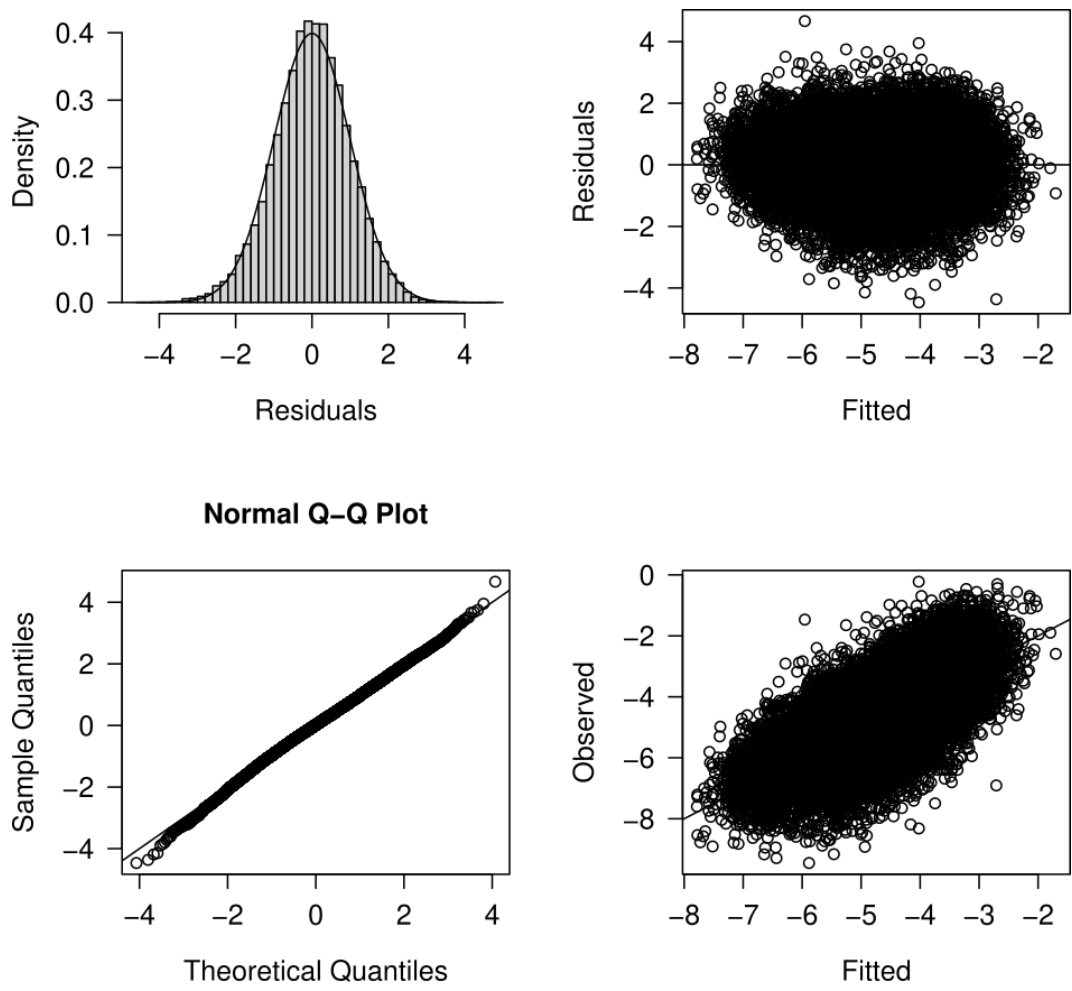


Figure B-24: Diagnostics for the log - normal CPUE standardisation model for Zew Zealand fleet strata with positive catch.

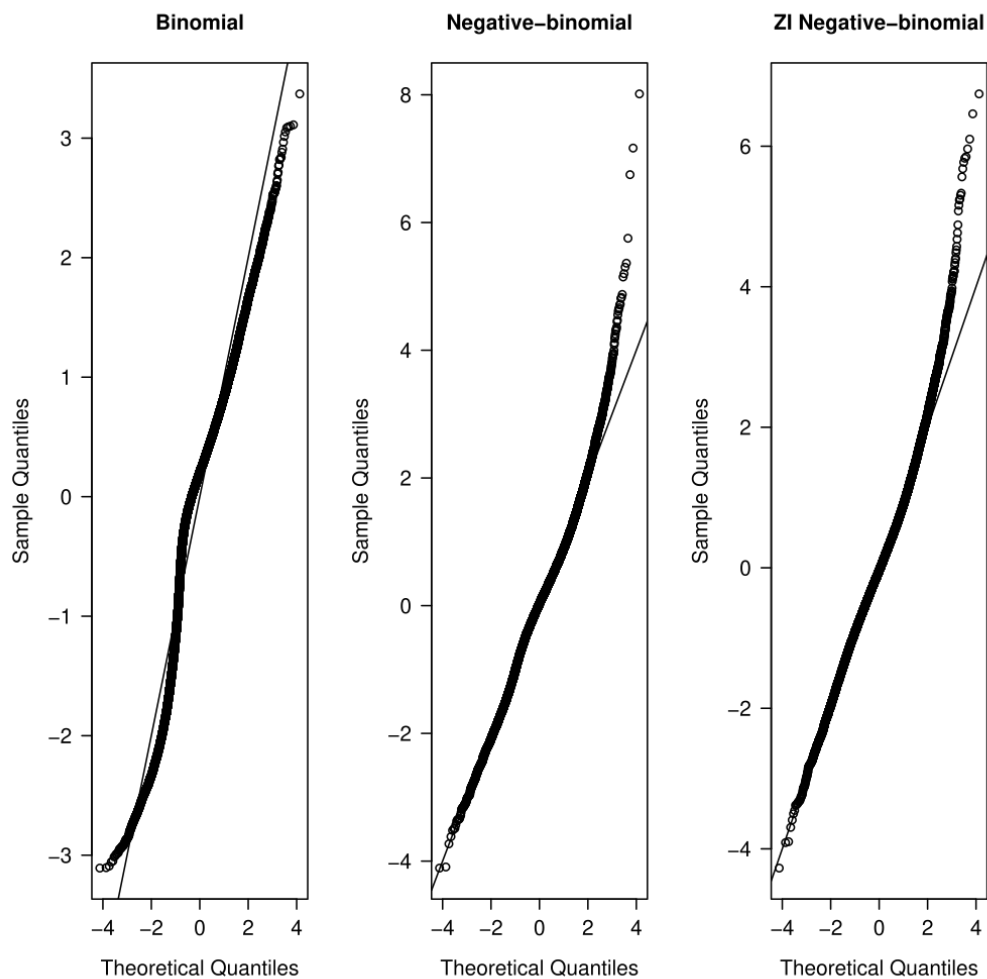


Figure B-25: Quantile residual diagnostics for the binomial component, as well as alternative CPUE standardisation models for Zew Zealand fleet strata with positive catch.

B.2 EU fleet CPUE

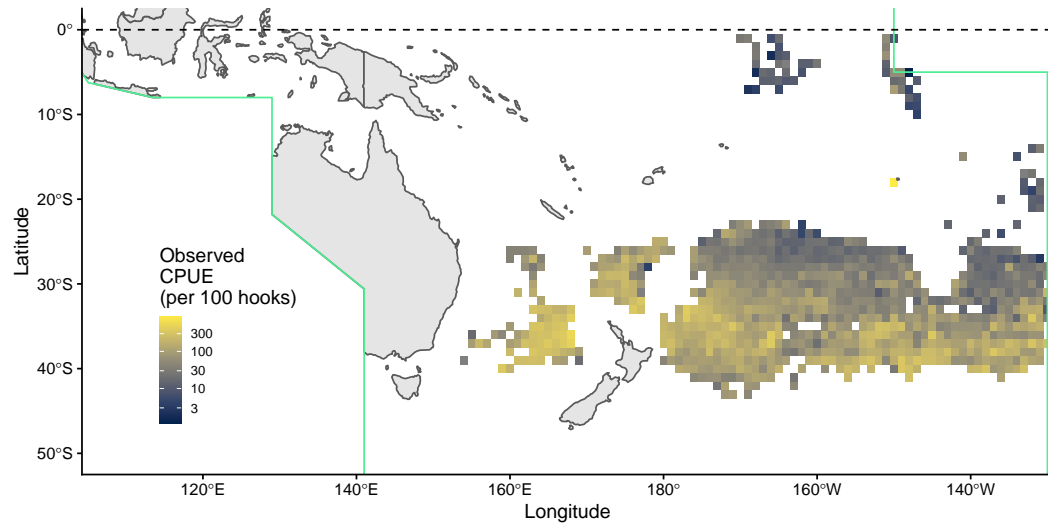


Figure B-26: Maps of average catch rates (CPUE; in kg of blue shark per 100 hooks) for the EU longline fleet.

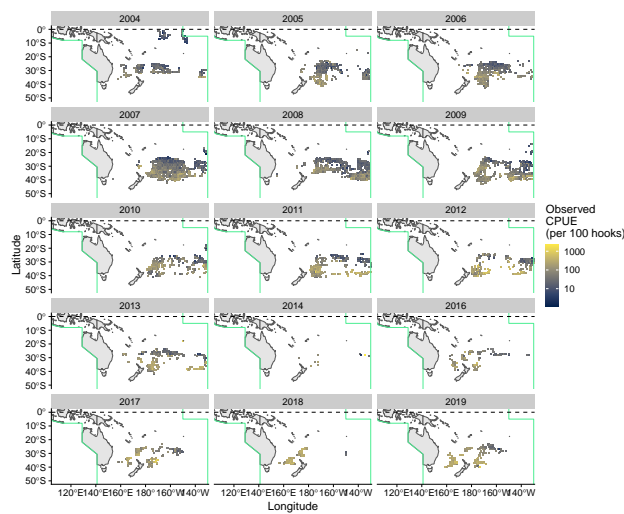


Figure B-27: Maps of average catch rates (CPUE; in kg of blue shark per 100 hooks) by year for the New Zealand longline fleet.

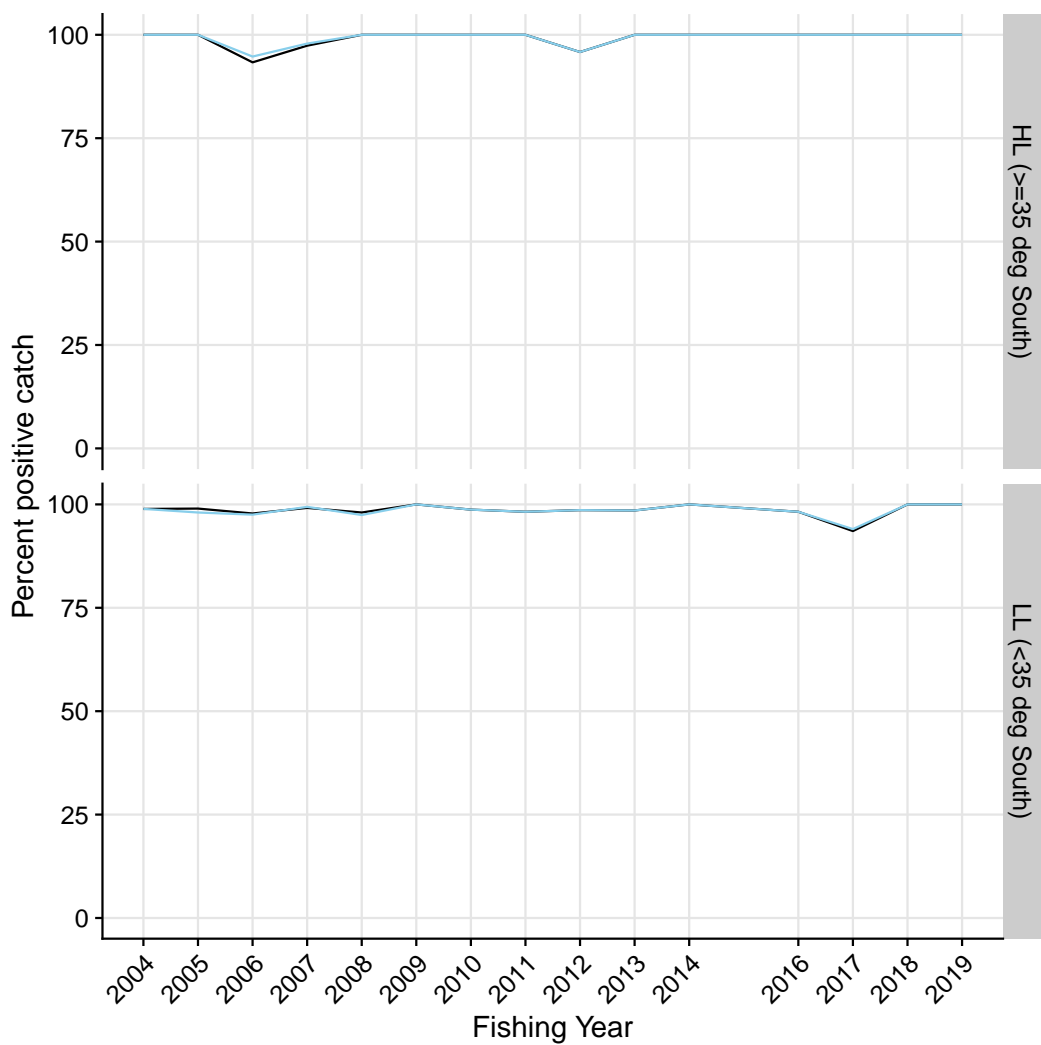


Figure B-28: Proportion of strata for the EU fleet with positive catch by latitudinal stratum. Light blue are initial log-sheet records prior to filtering, the black line is the retained dataset after filtering for consistently reporting vessels. Where available, the corresponding values from observed strata is shown in orange.

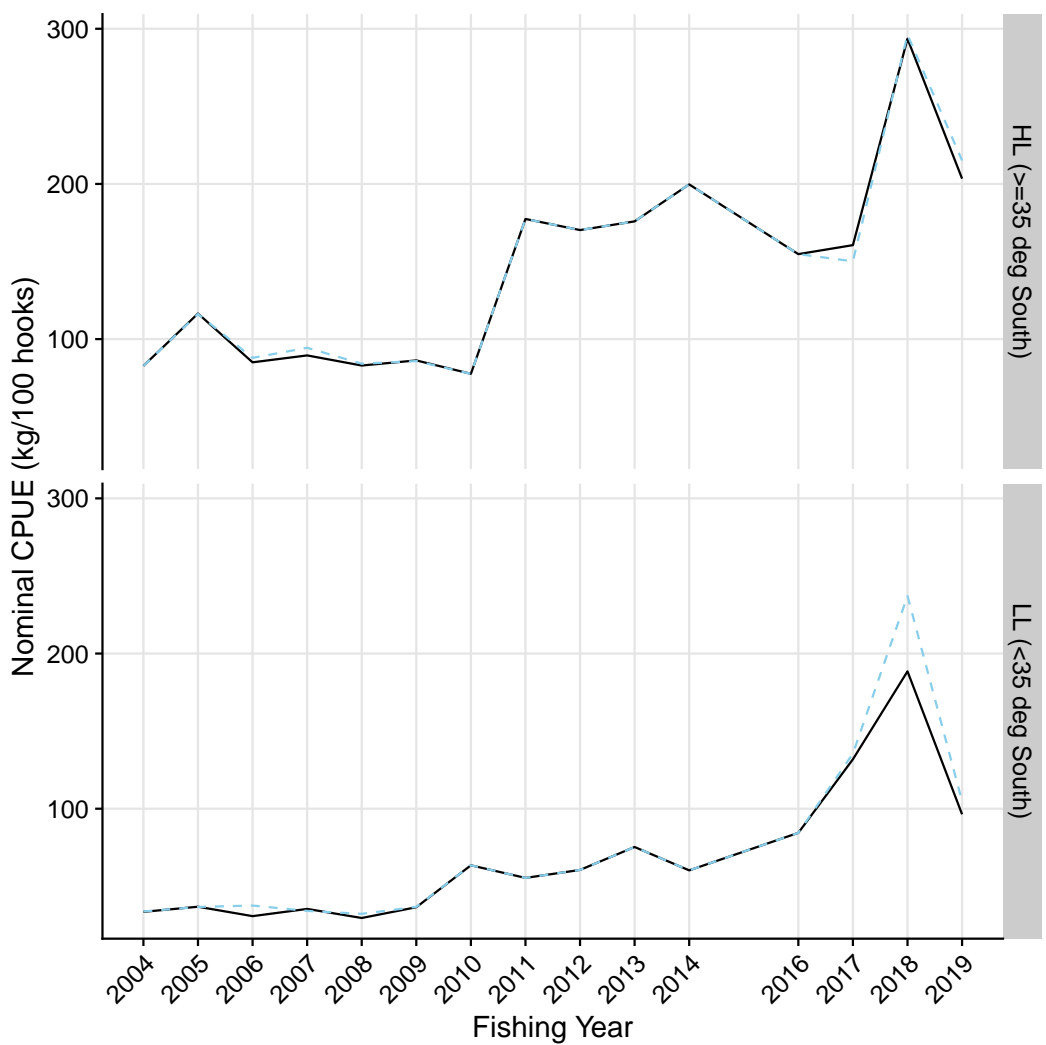


Figure B-29: Nominal CPUE (in number of blue shark per 100 hooks) strata of the EU fleet with positive catch by latitudinal stratum. Light blue are initial log-sheet records prior to filtering, the black line is the retained dataset after filtering for consistently reporting vessels. Where available, the corresponding values from observed strata is shown in orange.

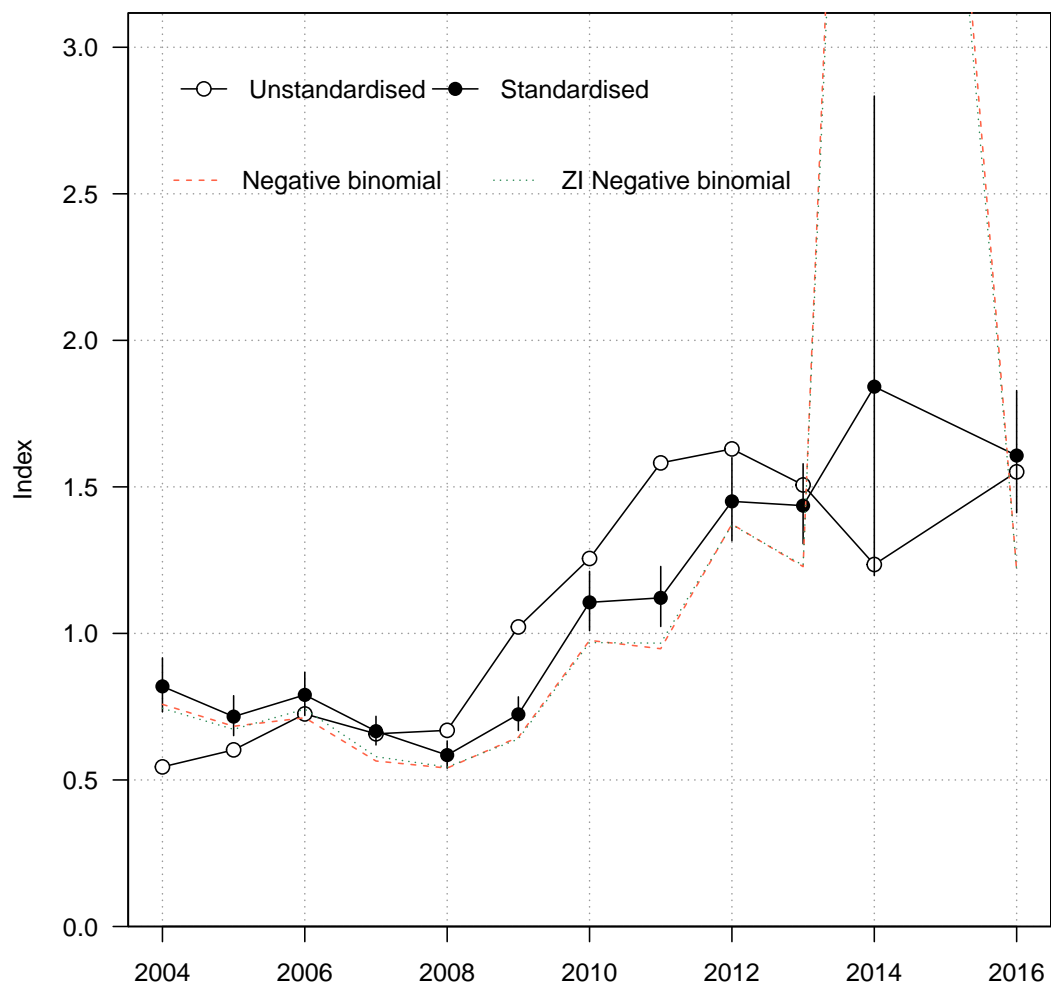


Figure B-30: Standardised (closed black circles with standard error) and unstandardised (open circles) CPUE indices for EU fleet strata with positive catch. Where successful (i.e., converged), standardised trends from a negative - binomial and zero - inflated negative binomial model run over the full dataset (including strata with zero values) are also shown for comparison.

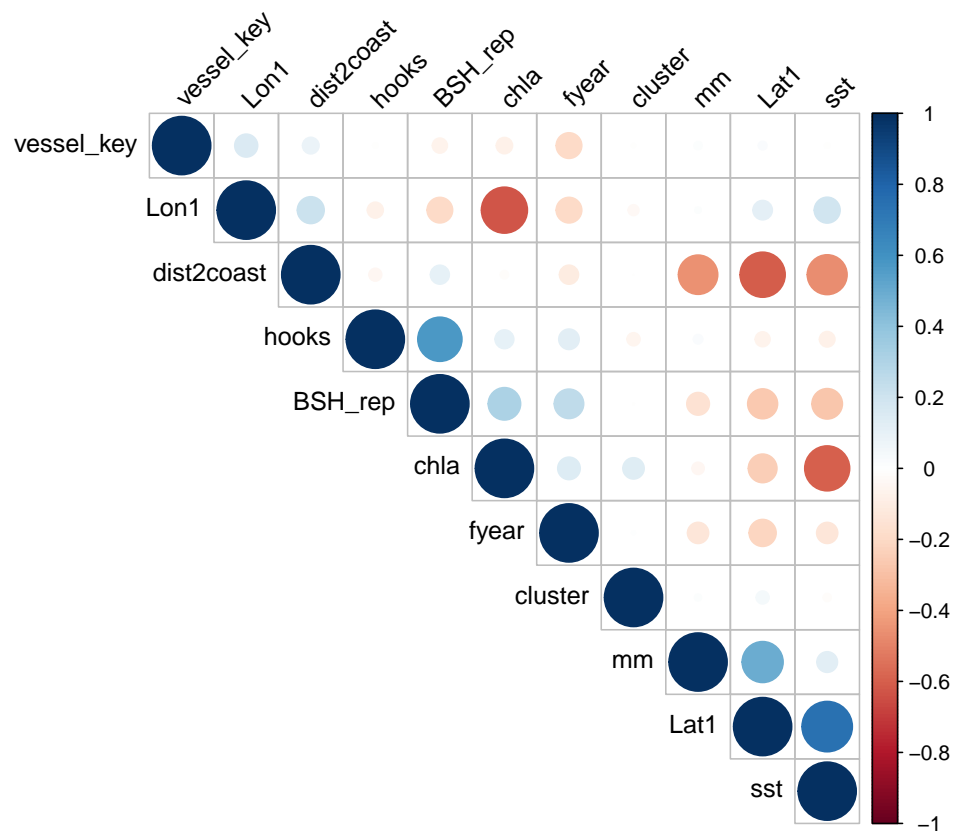


Figure B-31: Correlations amongst potential covariates for CPUE standardisation in the EU fleet. Where necessary, variables were removed to reduce redundancy in the models.

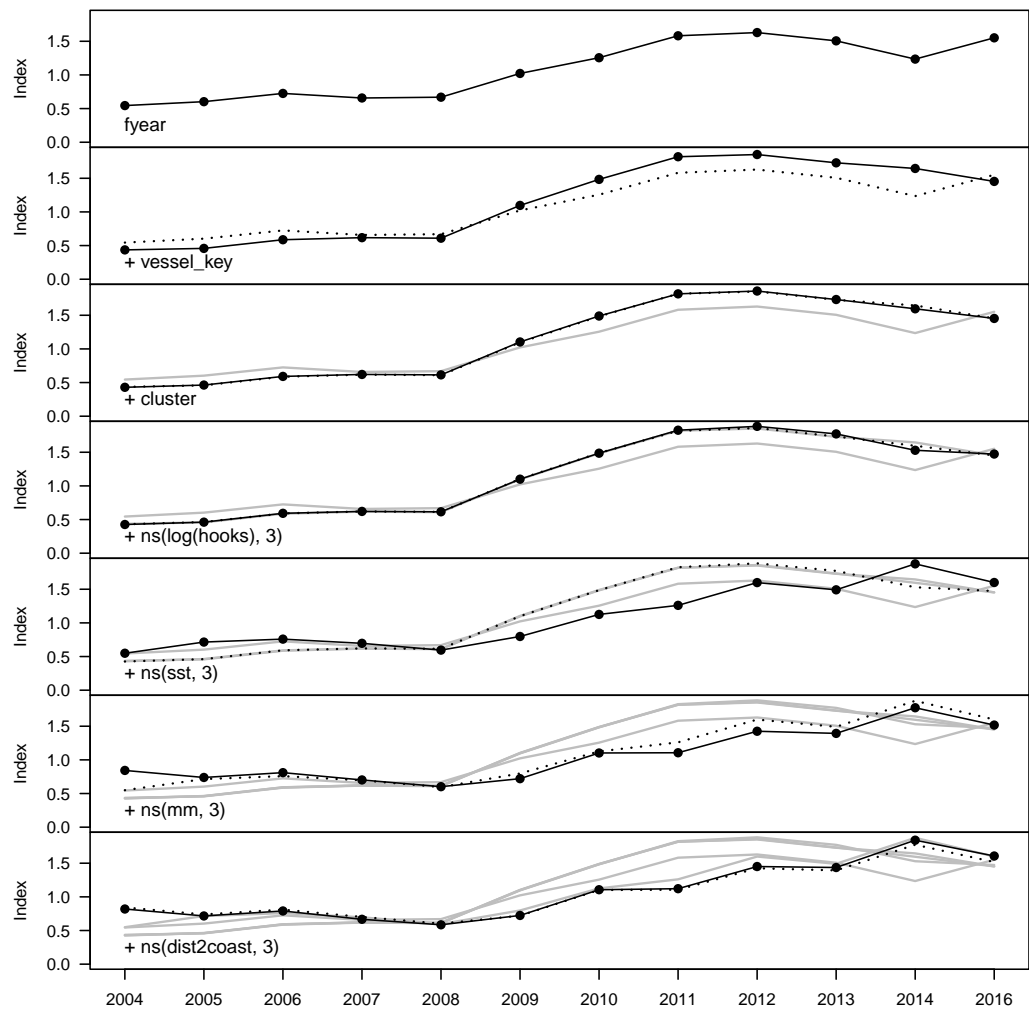


Figure B-32: Step plot for the EU fleet CPUE, showing sequential standardising effects of variables included in the standardisation model.

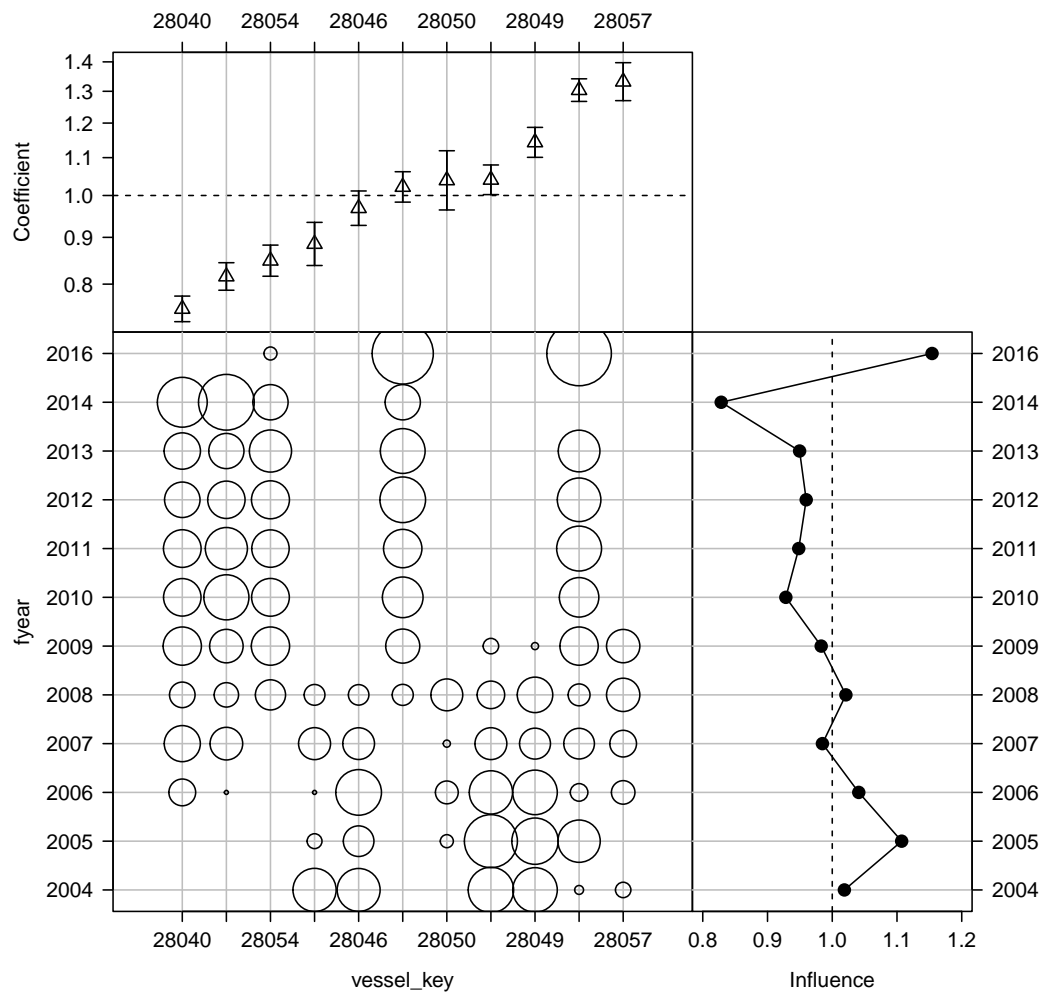


Figure B-33: Influence of fleet composition (vessel keys) for the EU fleet (bubble plot; bubbles scales by effort) on CPUE; influence (right hand plot) shows the standardising effect (a positive effect reduces the standardised CPUE by the equivalent amount). Estimated coefficients are given in the top panel.

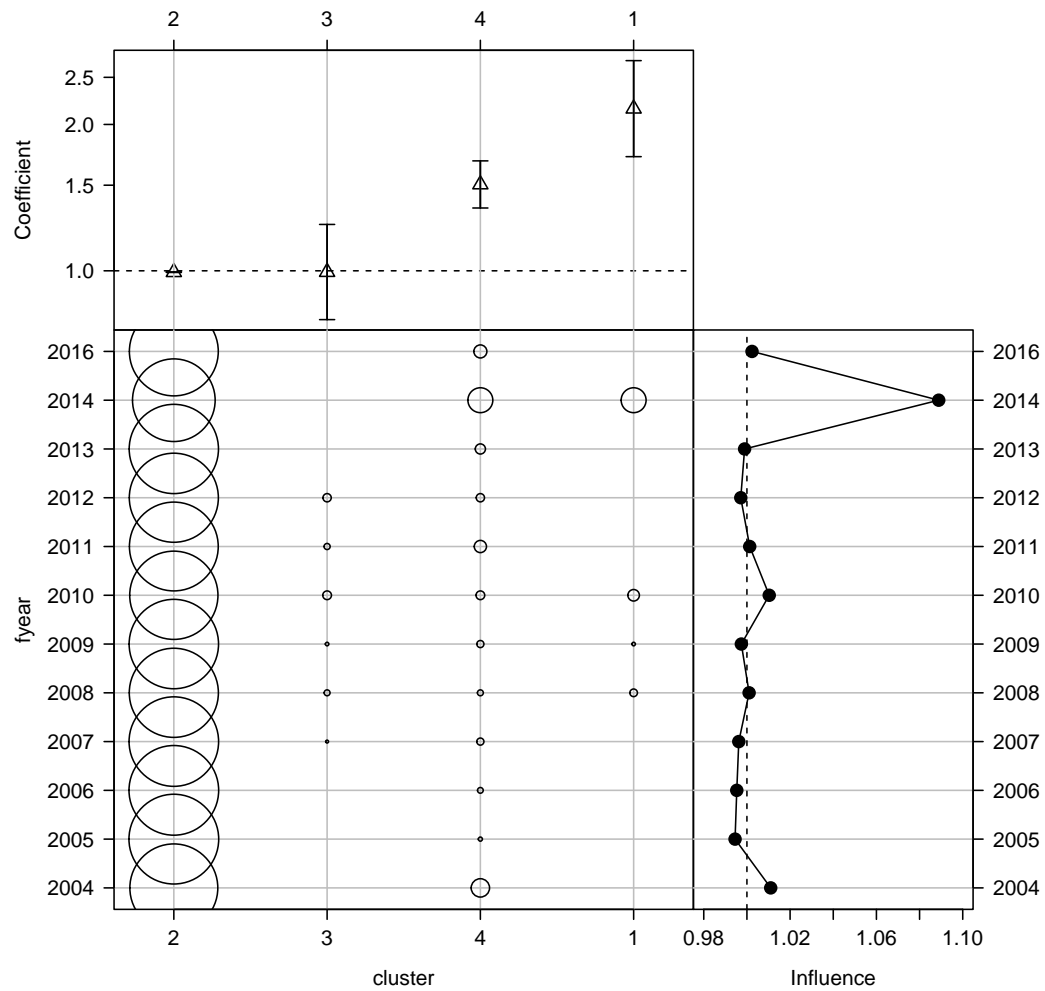


Figure B-34: Influence of targeting cluster for the EU fleet (bubble plot; bubbles scales by effort) on CPUE; influence (right hand plot) shows the standardising effect (a positive effect reduces the standardised CPUE by the equivalent amount). Estimated coefficients are given in the top panel.

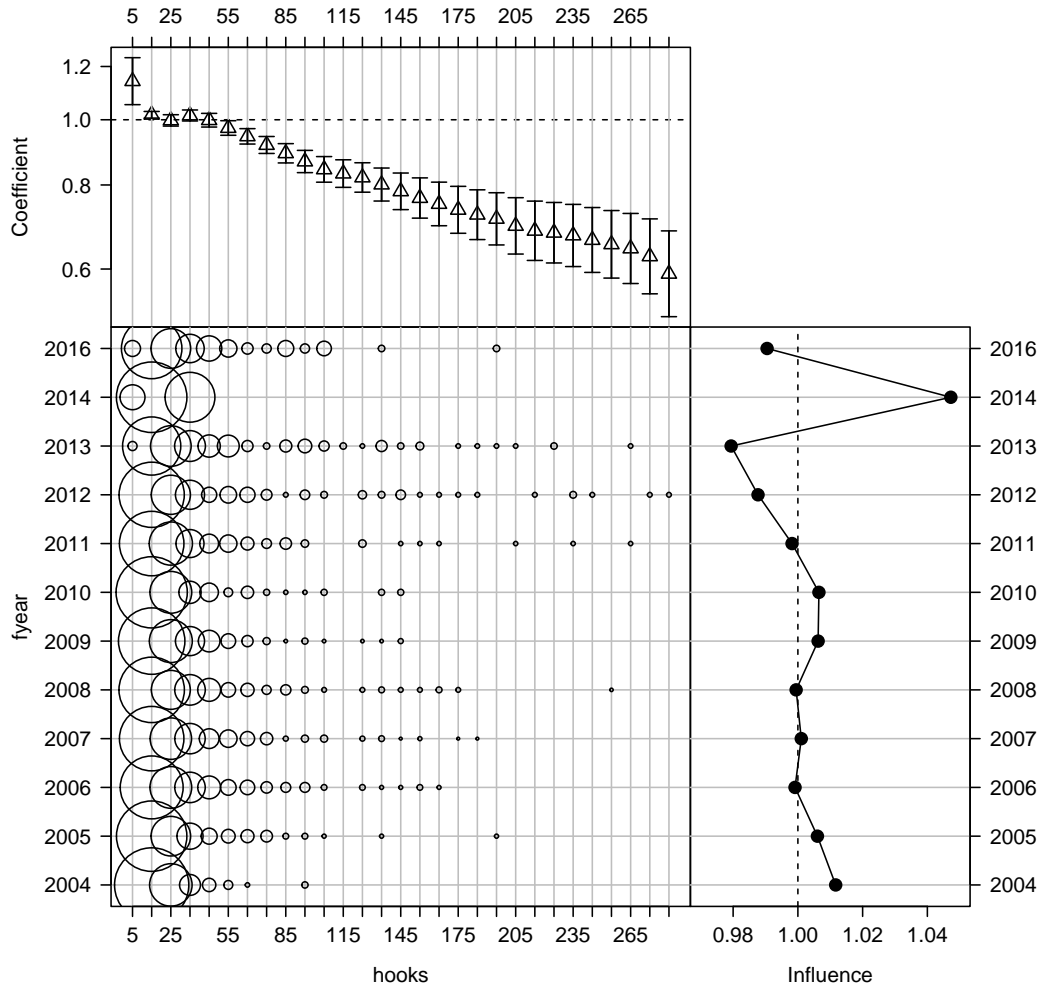


Figure B-35: Influence of number of hooks set per stratum for the EU fleet (bubble plot; bubbles scales by effort) on CPUE; influence (right hand plot) shows the standardising effect (a positive effect reduces the standardised CPUE by the equivalent amount). Estimated coefficients are given in the top panel.

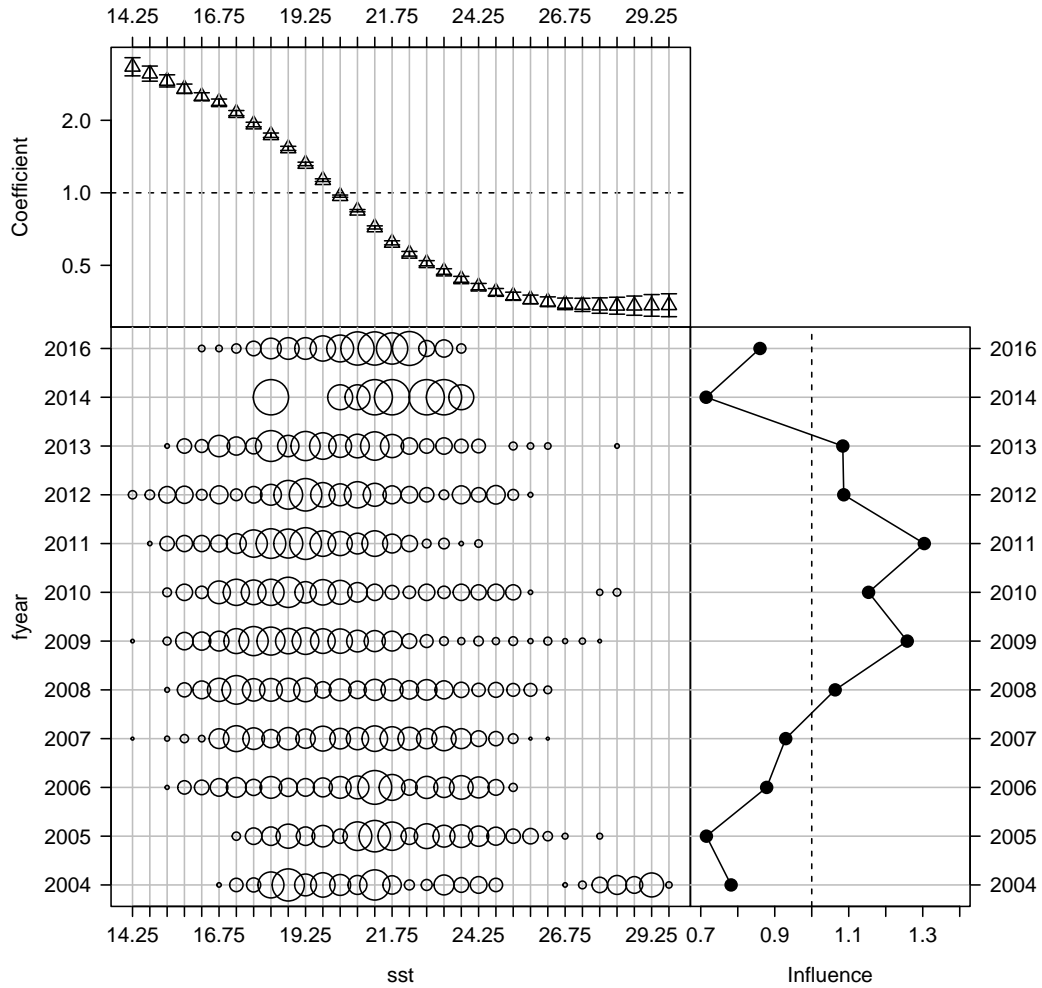


Figure B-36: Influence of sea surface temperature (SST, in degrees Celsius) for the EU fleet (bubble plot; bubbles scales by effort) on CPUE; influence (right hand plot) shows the standardising effect (a positive effect reduces the standardised CPUE by the equivalent amount). Estimated coefficients are given in the top panel.

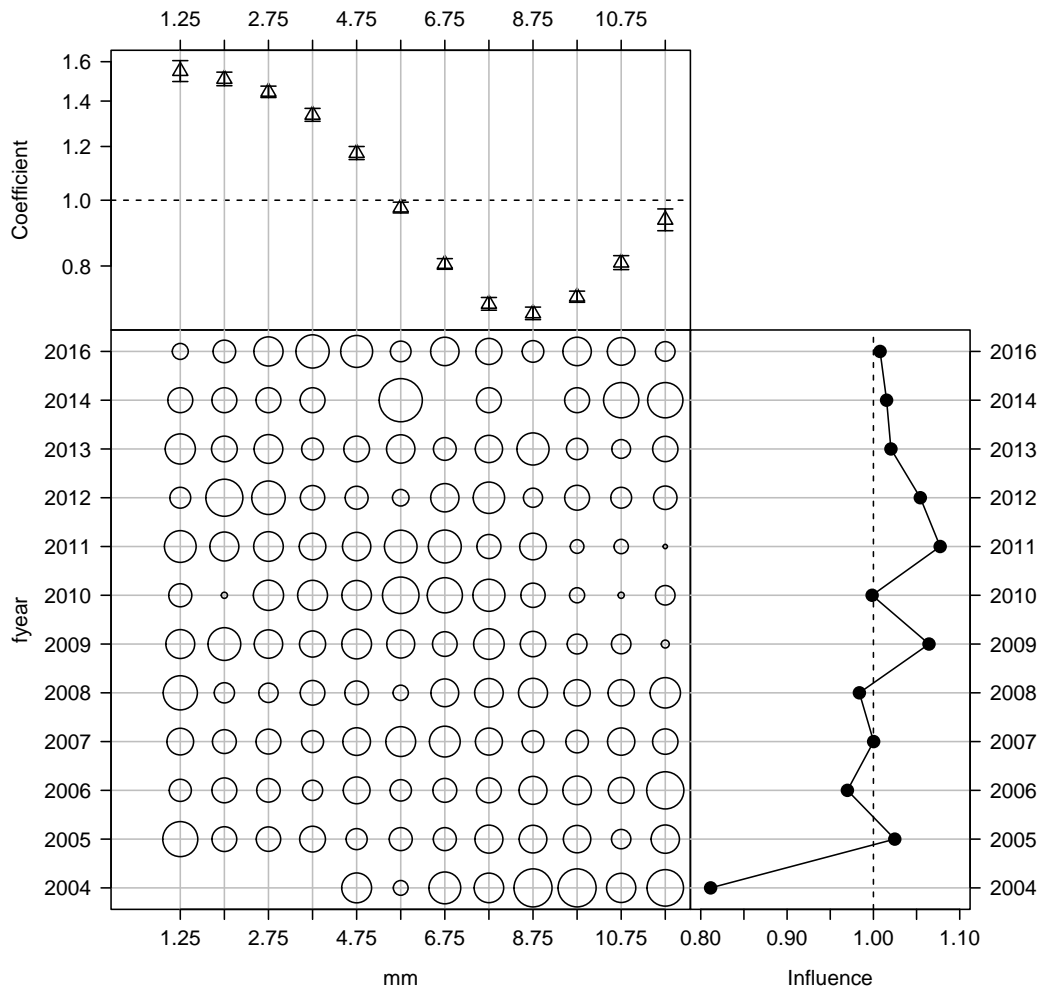


Figure B-37: Influence of month for the EU fleet (bubble plot; bubbles scales by effort) on CPUE; influence (right hand plot) shows the standardising effect (a positive effect reduces the standardised CPUE by the equivalent amount). Estimated coefficients are given in the top panel.

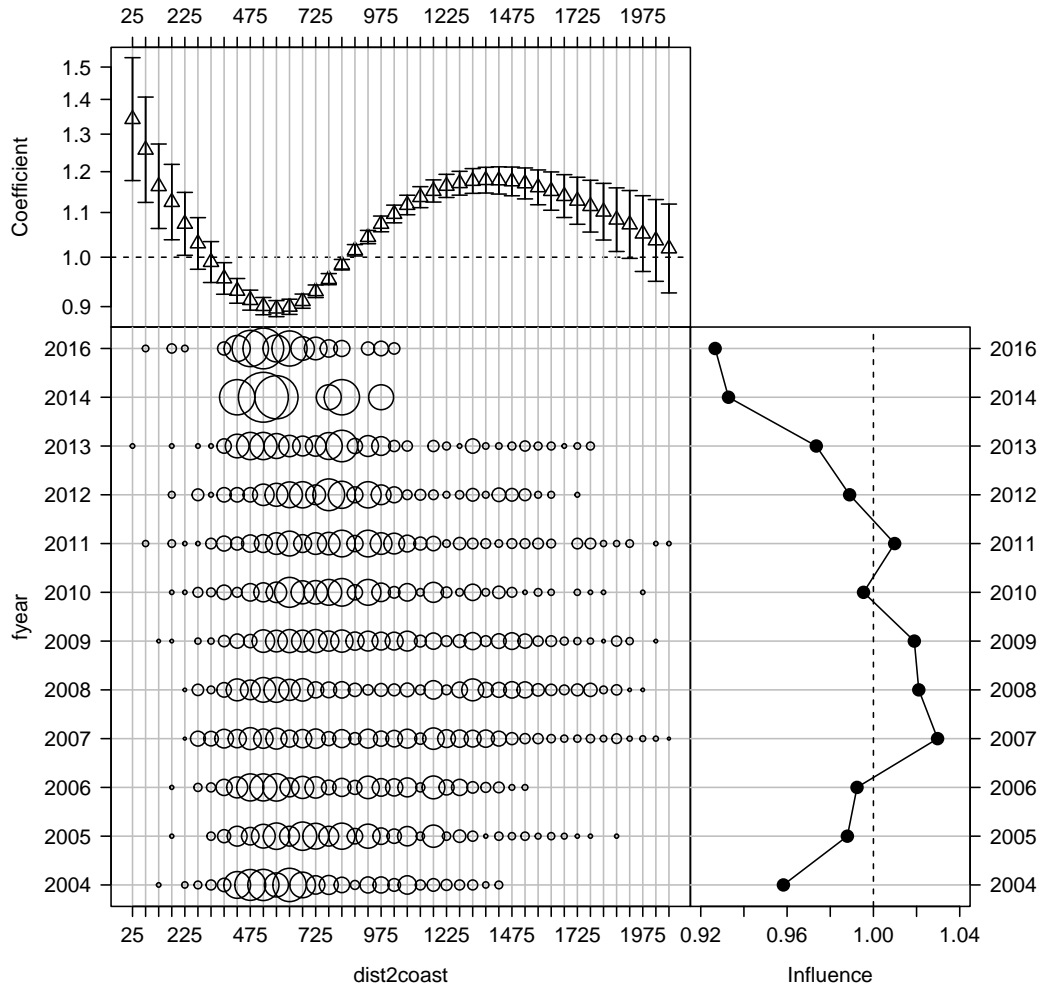


Figure B-38: Influence of distance to coast composition for the EU fleet (bubble plot; bubbles scales by effort) on CPUE; influence (right hand plot) shows the standardising effect (a positive effect reduces the standardised CPUE by the equivalent amount). Estimated coefficients are given in the top panel.

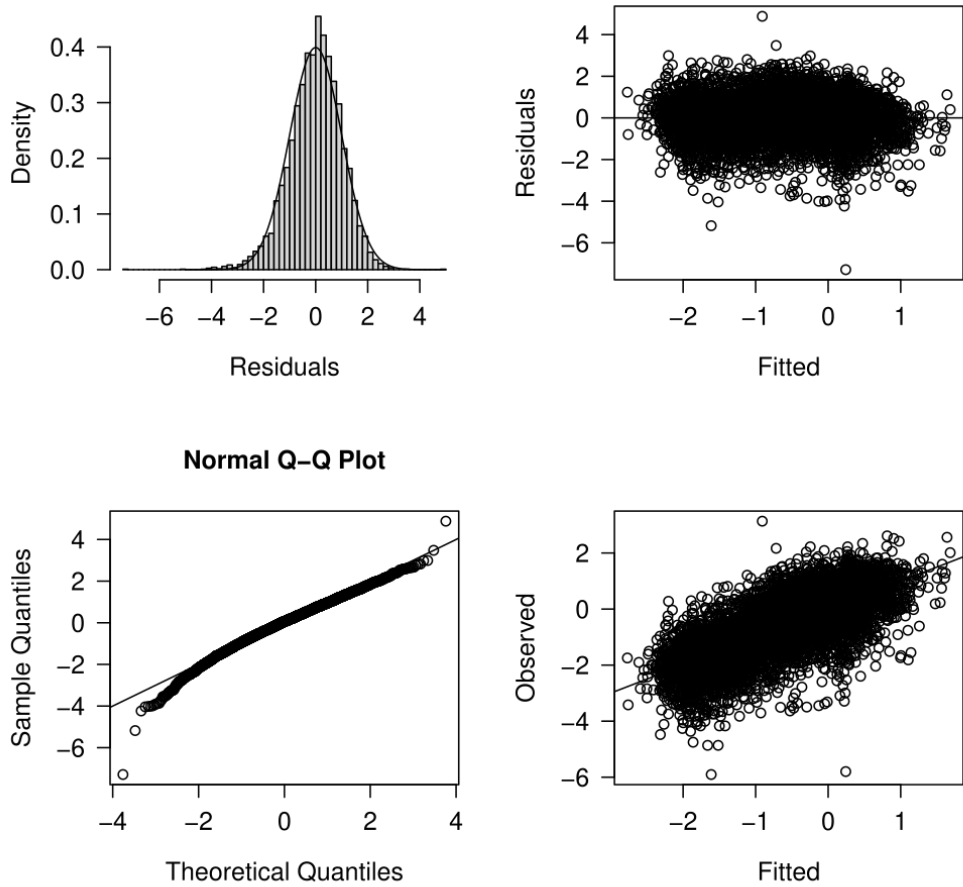


Figure B-39: Diagnostics for the log-normal CPUE standardisation model for EU fleet strata with positive catch.

B.3 Japan low latitude CPUE

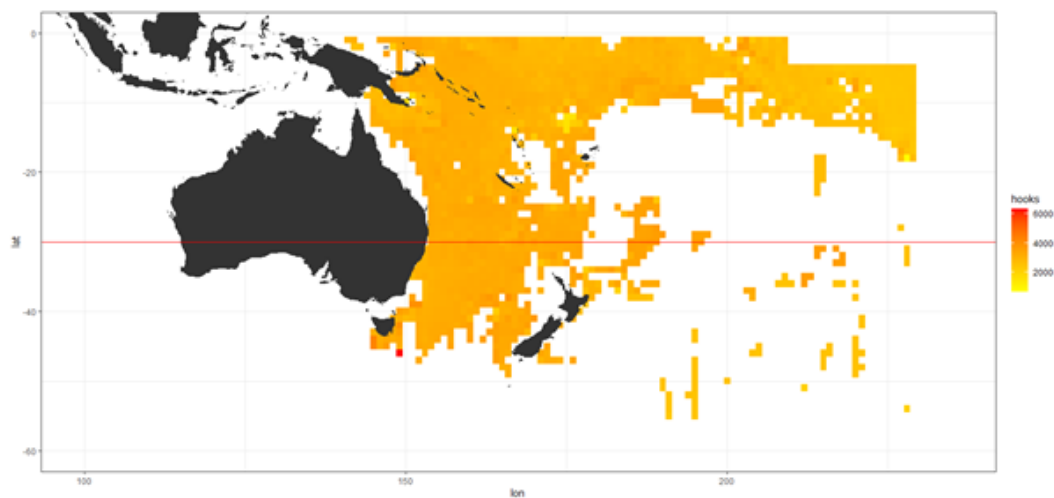


Figure B-40: Operational area of Japanese longline fleets in the southern WCPO from 1994 to 2019 showing the mean number of hooks for 1994-2019.

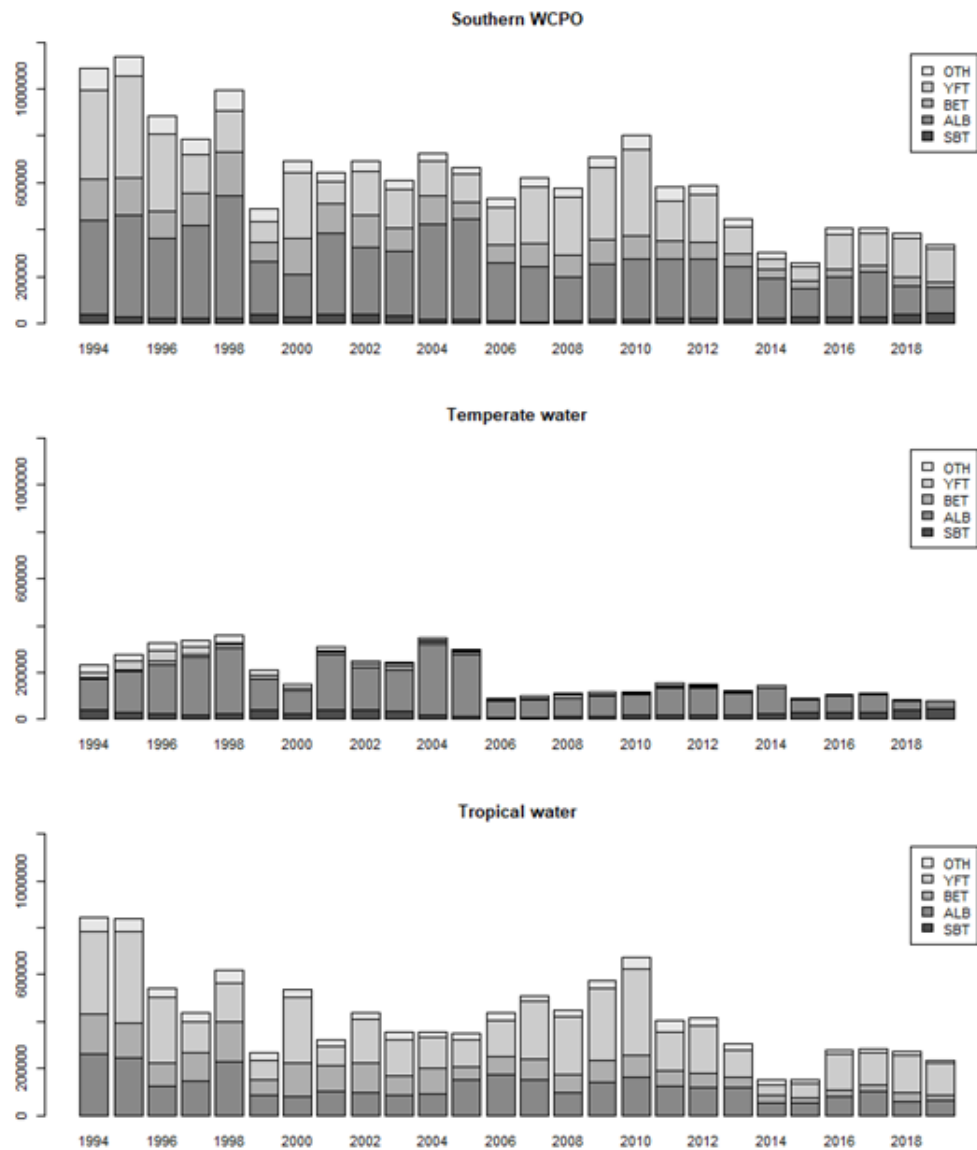


Figure B-41: Annual catch number of target species (OTH: Other species, YFT: Yellowfin tuna, BET: Bigeye tuna, ALB: Albacore, SBT: Southern bluefin tuna) for the Japanese longline fleets in southern WCPO, temperate waters ($30\text{--}60^{\circ}\text{S}$), and tropical waters ($0\text{--}30^{\circ}\text{S}$).

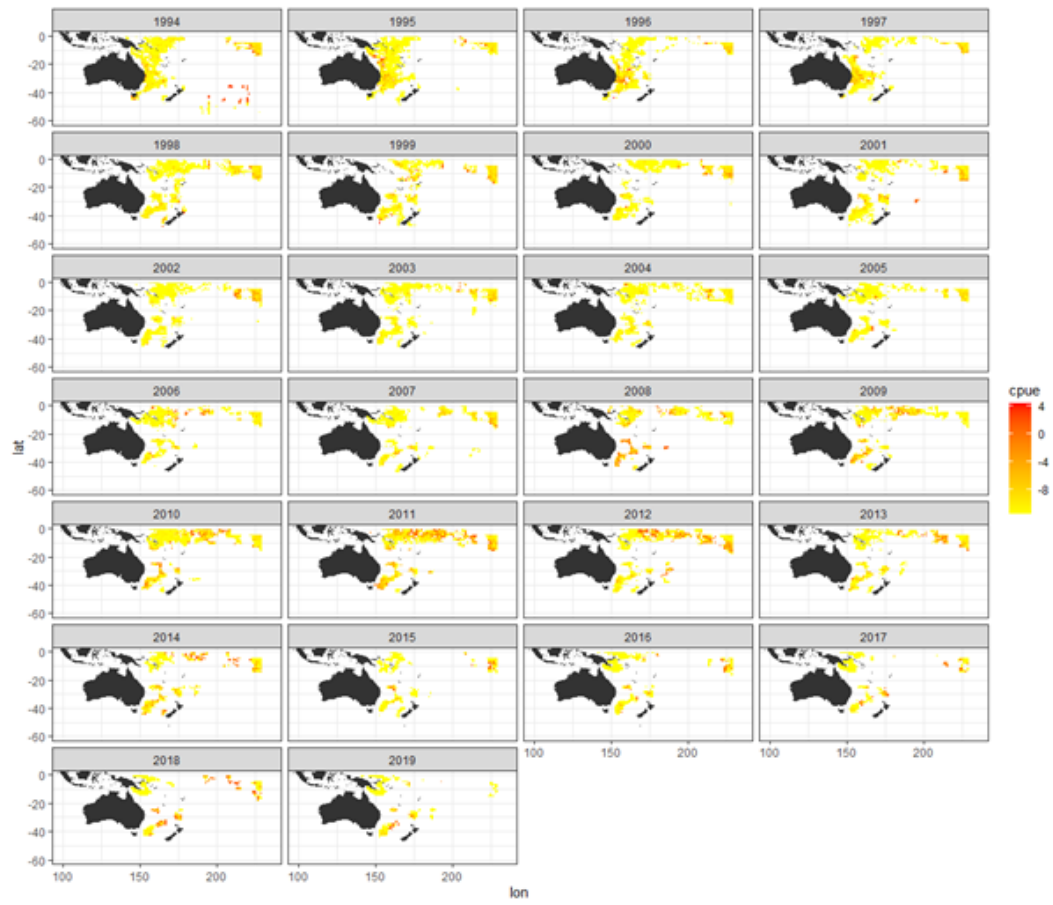


Figure B-42: Operational area of Japanese longline fleets in the southern WCPO from 1994 to 2019 showing the annual changes in the log transformed nominal CPUE of blue shark from 1994 to 2019.

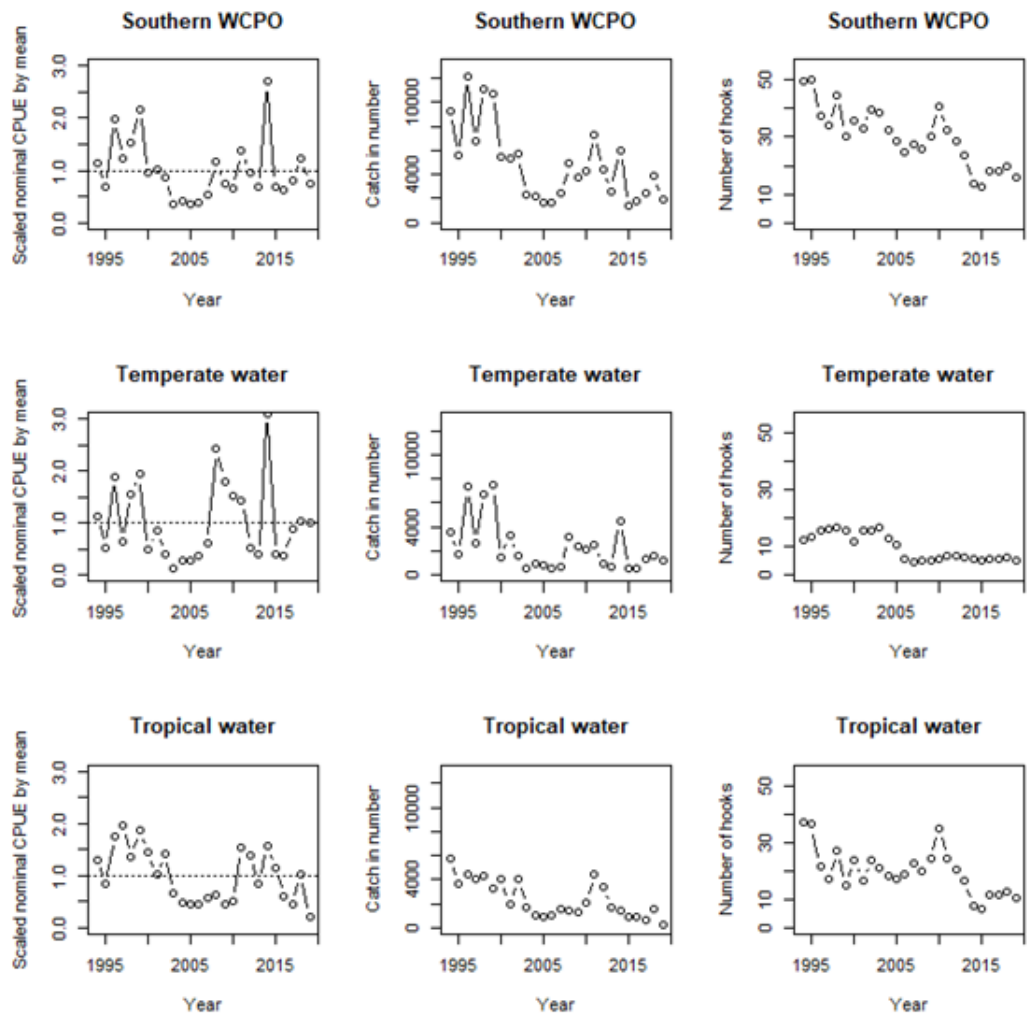


Figure B-43: Annual nominal CPUE of blue shark, annual catch in number of blue shark, annual number of hooks in three areas for the Japanese longline fleets: southern WCPO ($0\text{--}60^{\circ}\text{S}$), temperate waters ($30\text{--}60^{\circ}\text{S}$), and tropics ($0\text{--}30^{\circ}\text{S}$).

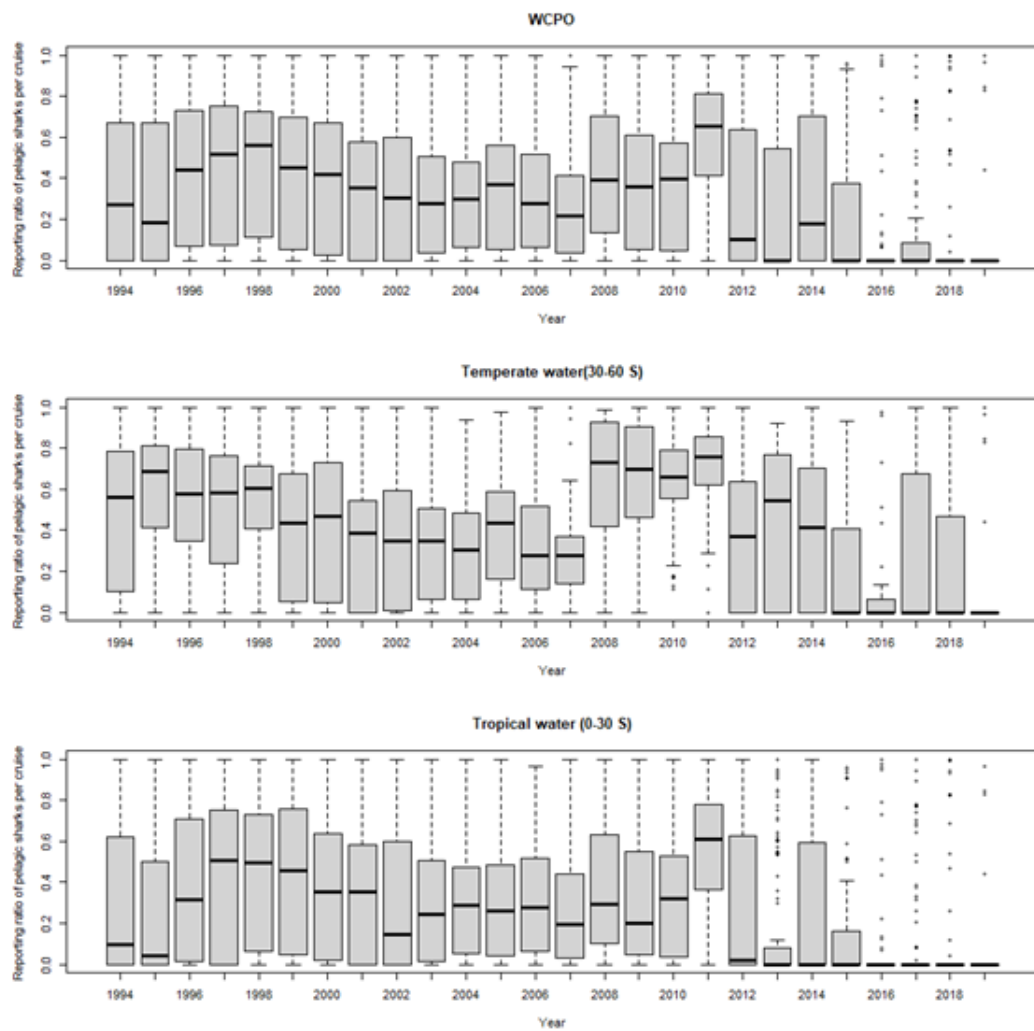


Figure B-44: Annual reporting ratio (RR) of pelagic sharks (blue shark, mako sharks, porbeagle, silky sharks, oceanic whitetip sharks, thresher sharks, other sharks) in southern WCPO for the Japanese longline fleets. RR was calculated using the number of sets with positive catches of pelagic sharks per total number of sets in a cruise of each vessel. Upper panel is RR in whole area in southern WCPO. Middle panel is RR in the temperate waters. Lower panel is RR in the tropics.

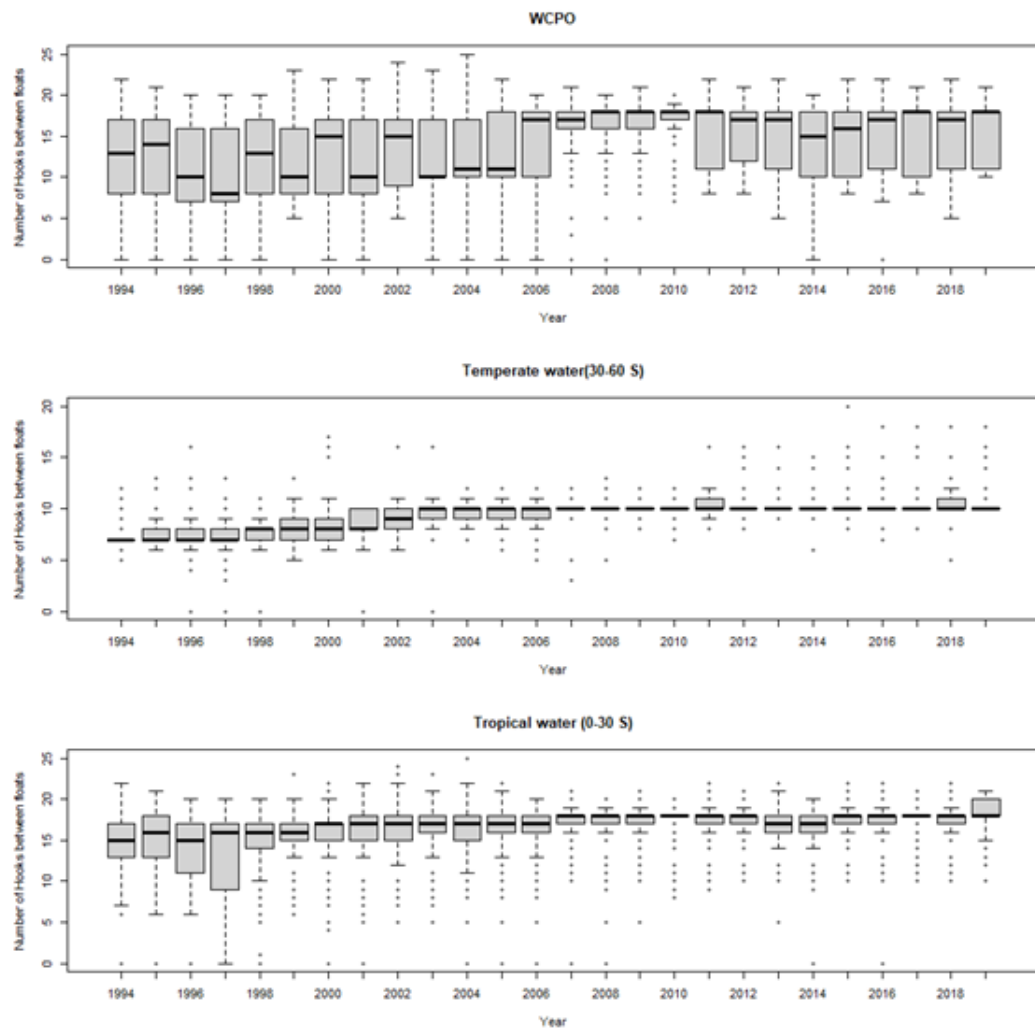


Figure B-45: Annual number of hooks between floats for Japanese fleets in southern WCPO, temperate waters ($30\text{--}60^{\circ}\text{S}$), and tropics ($0\text{--}30^{\circ}\text{S}$).

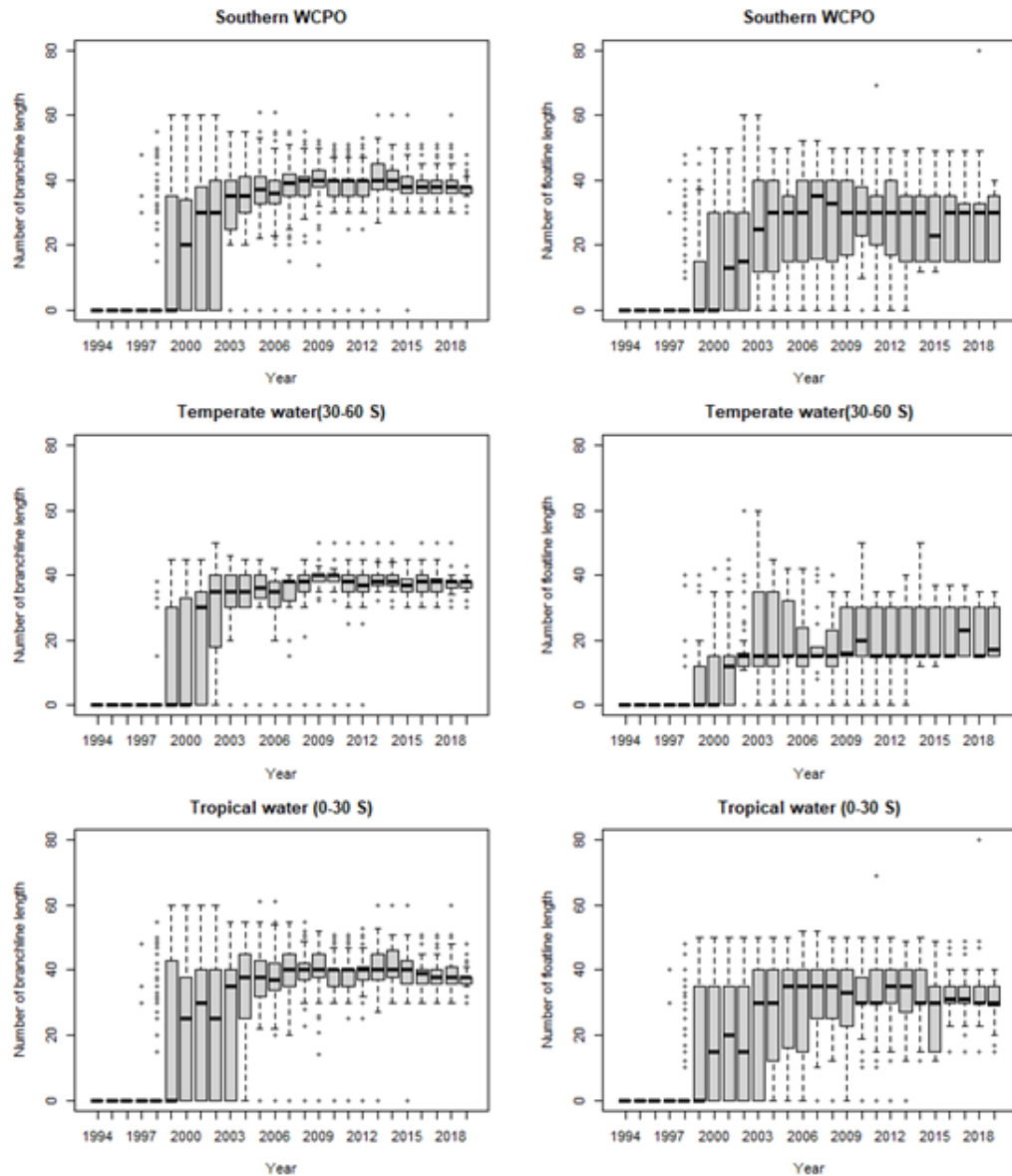


Figure B-46: Annual number of branch-line length (meters) and float-line length (meters) in southern WCPO, temperate waters ($30-60^{\circ}\text{S}$), and tropics ($0-30^{\circ}\text{S}$) for the Japanese longline fleets.

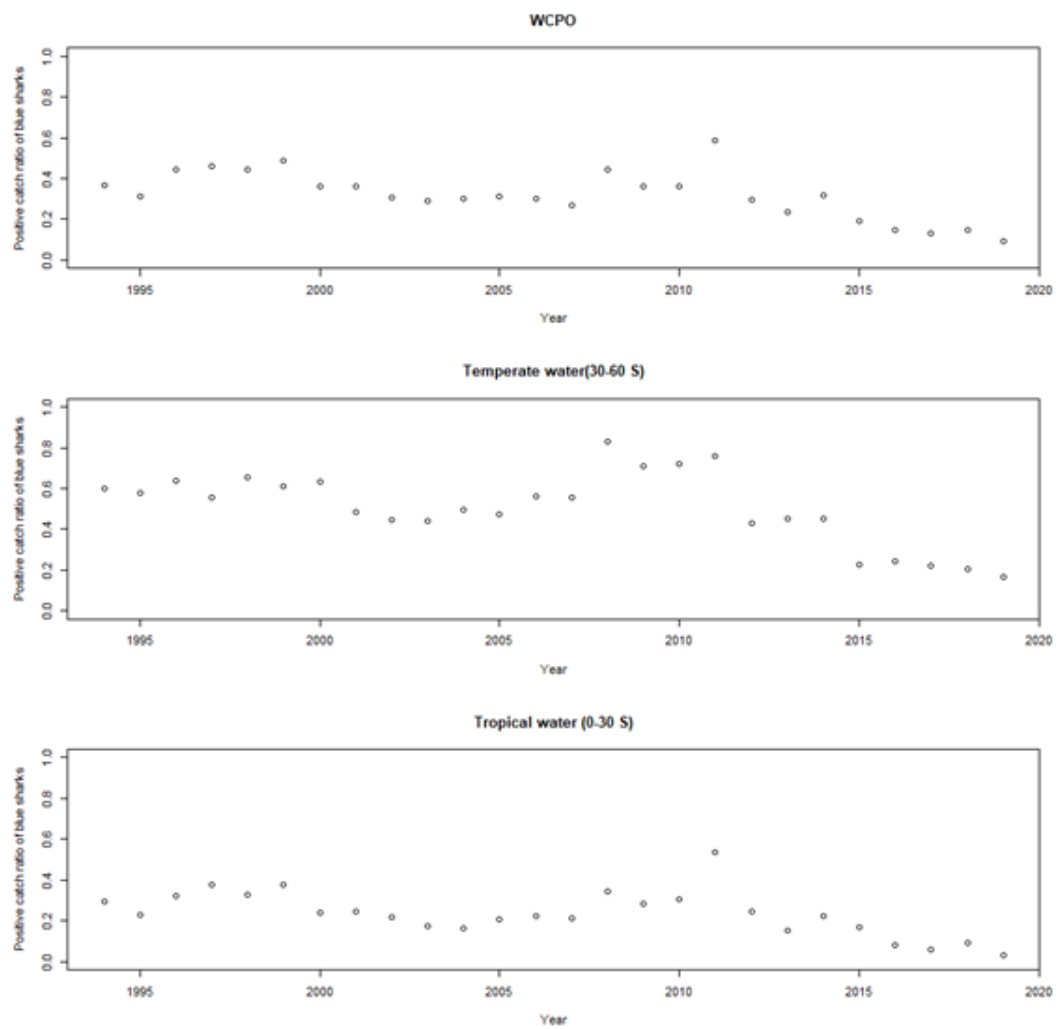


Figure B-47: Annual positive catch ratio of blue sharks (number of sets with positive catch of blue shark to total number of sets) for the Japanese longline fleets in southern WCPO, temperate waters ($30\text{--}60^{\circ}\text{S}$), and tropics ($0\text{--}30^{\circ}\text{S}$).

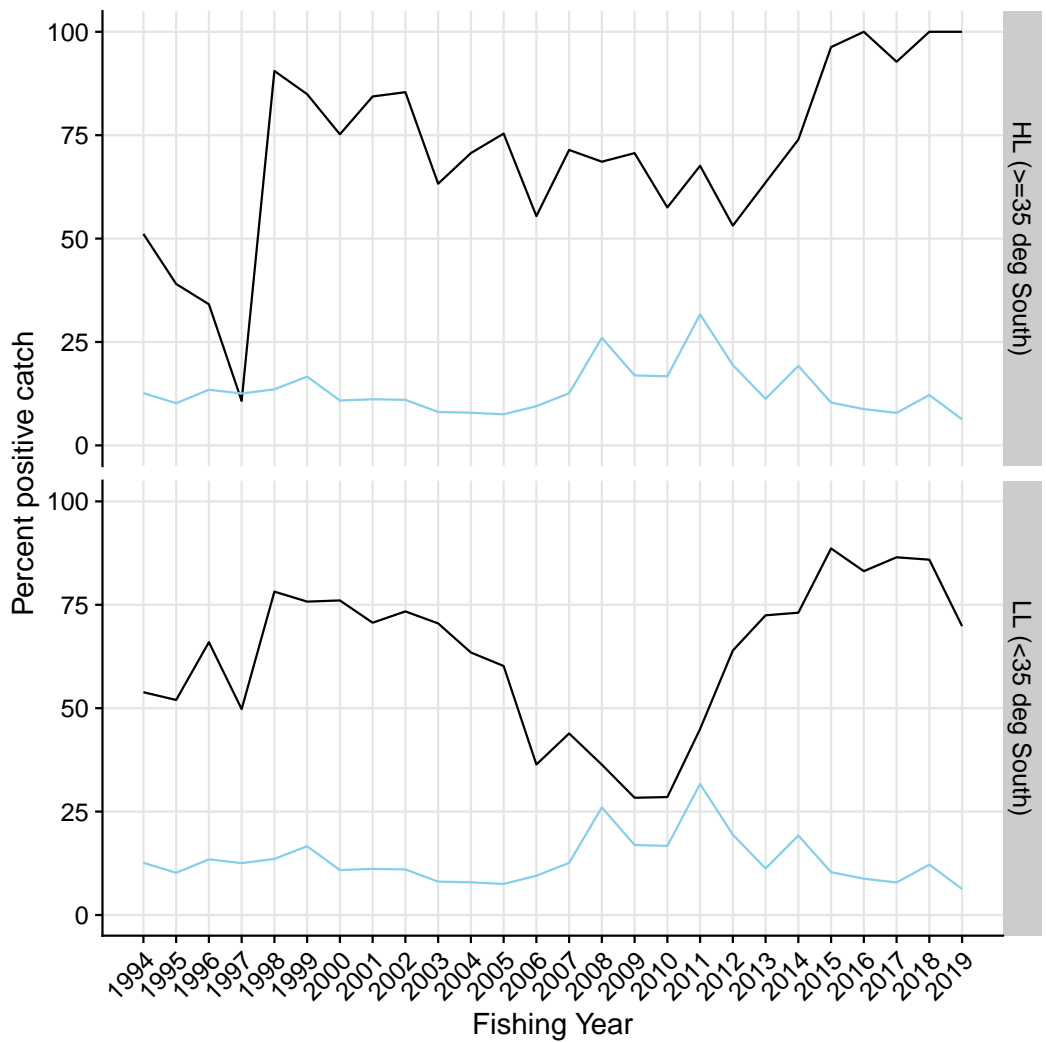


Figure B-48: Proportion of strata for the Japanese fleet with positive catch by latitudinal stratum. Light blue are initial log-sheet records prior to filtering, the black line is the retained dataset after filtering for consistently reporting vessels. Where available, the corresponding values from observed strata is shown in orange.

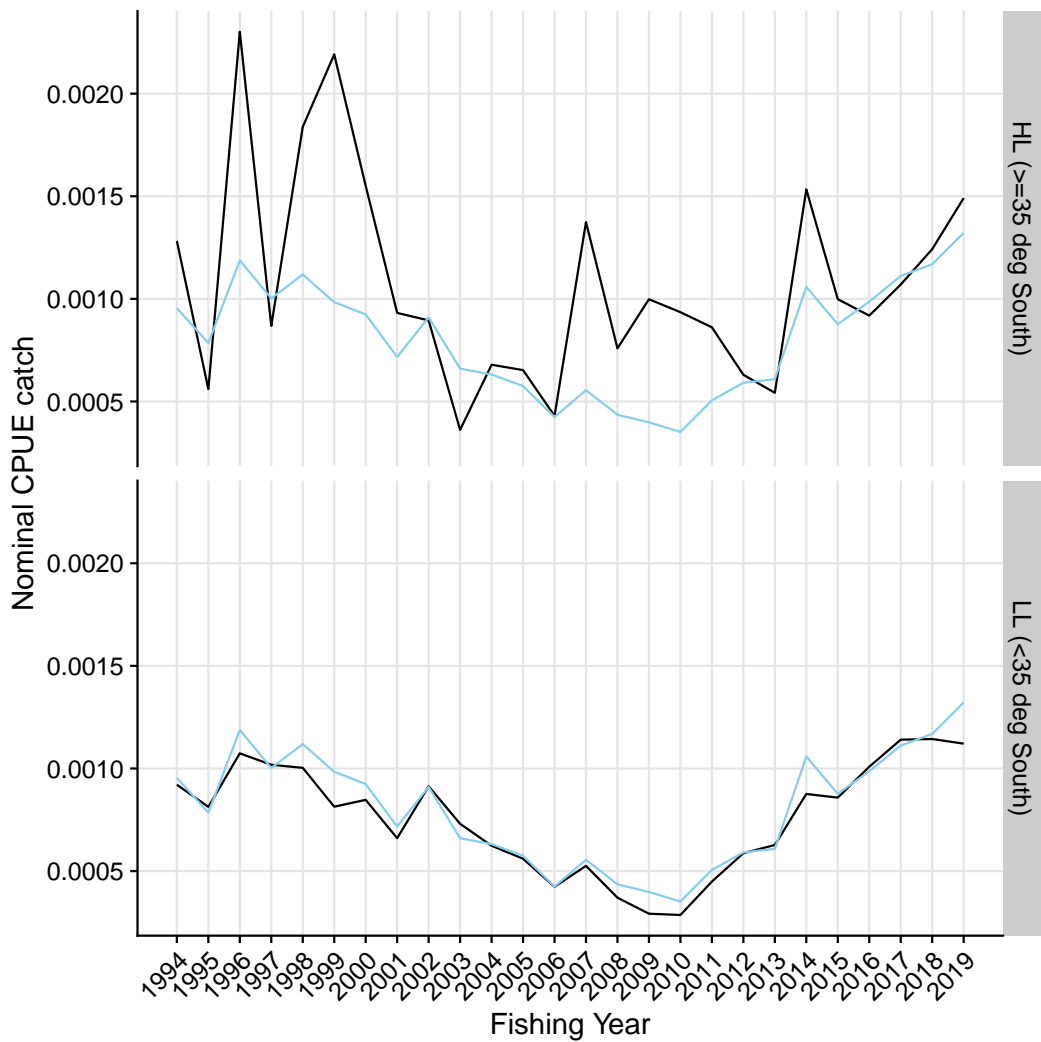


Figure B-49: Nominal CPUE (in number of blue shark per 100 hooks) strata of the Japanese fleet with positive catch by latitudinal stratum. Light blue are initial log-sheet records prior to filtering, the black line is the retained dataset after filtering for consistently reporting vessels. Where available, the corresponding values from observed strata is shown in orange.

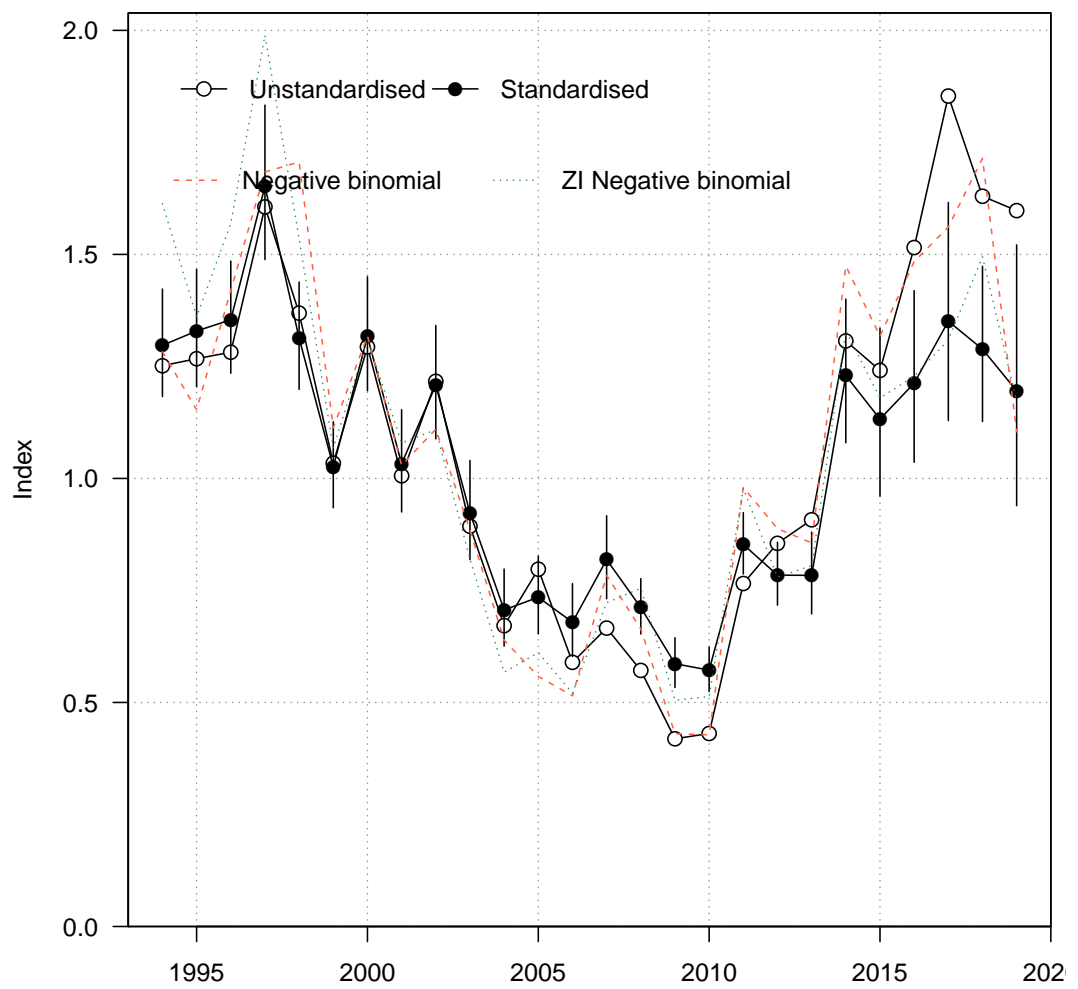


Figure B-50: Standardised (closed black circles with standard error) and unstandardised (open circles) CPUE indices for Japanese fleet strata with positive catch. Where successful (i.e., converged), standardised trends from a negative-binomial and zero-inflated negative binomial model run over the full dataset (including strata with zero values) are also shown for comparison.

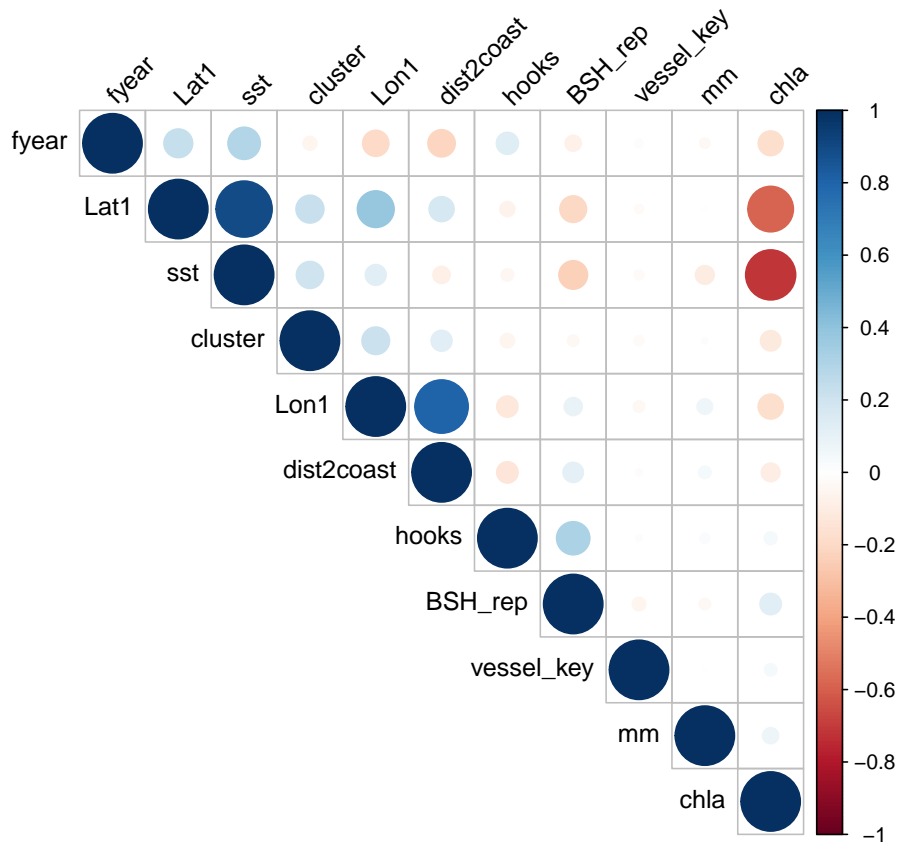


Figure B-51: Correlations amongst potential covariates for CPUE standardisation in the Japanese fleet. Where necessary, variables were removed to reduce redundancy in the models.

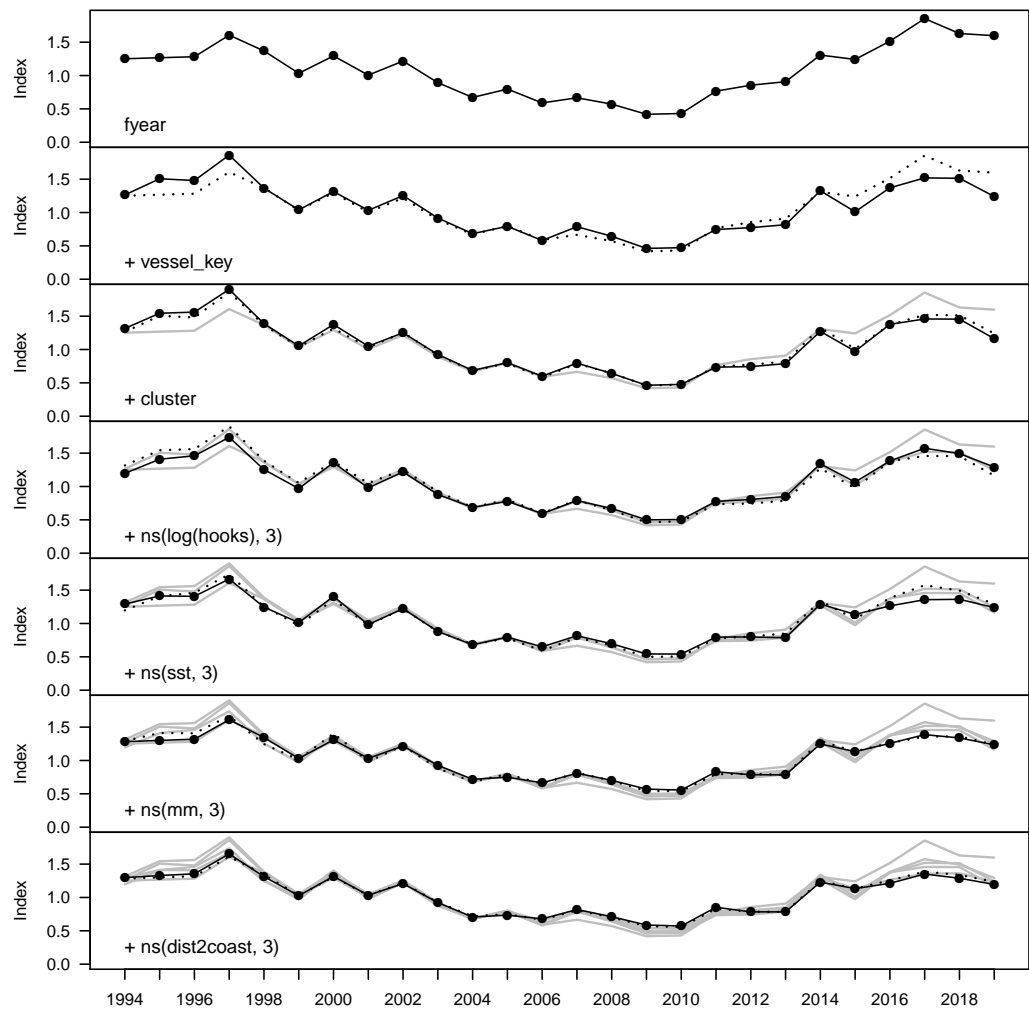


Figure B-52: Step plot for the Japanese fleet CPUE, showing sequential standardising effects of variables included in the standardisation model.

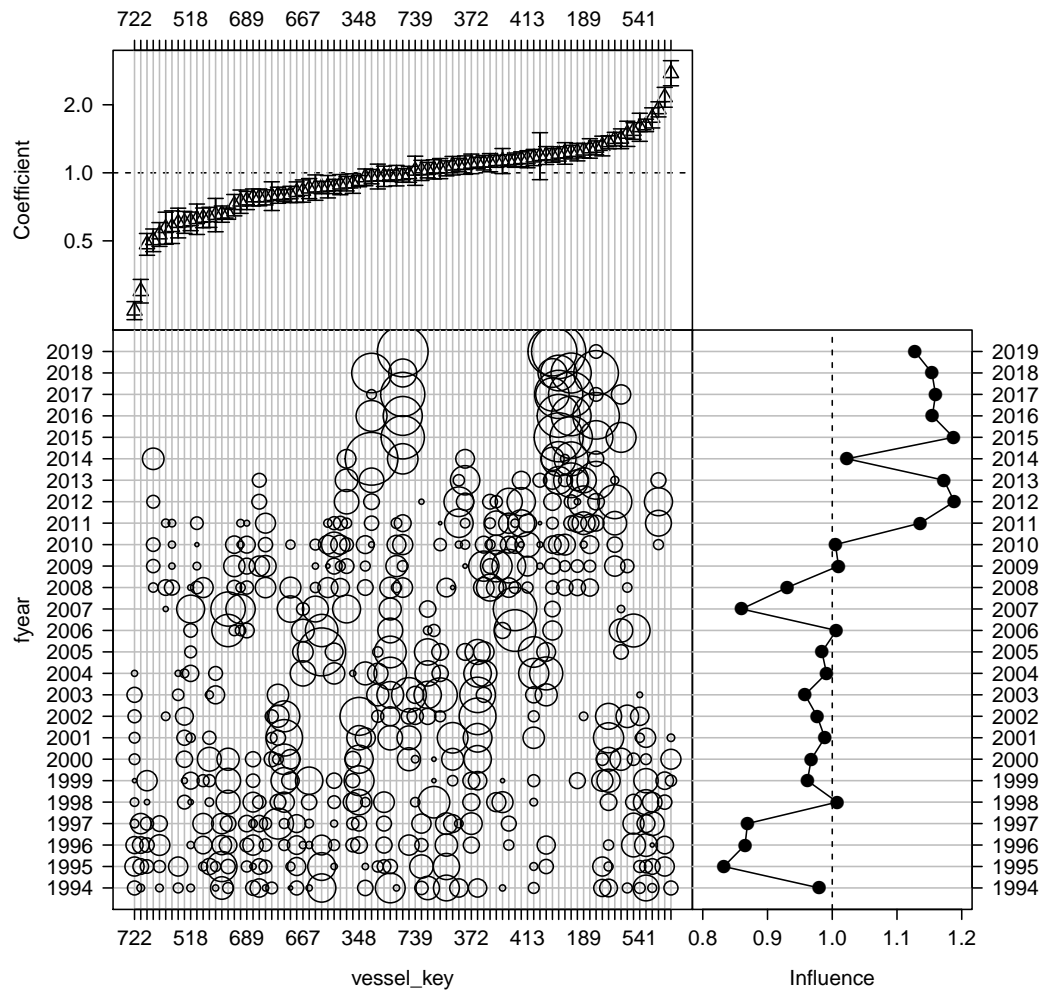


Figure B-53: Influence of fleet composition (vessel keys) for the Japanese fleet (bubble plot; bubbles scales by effort) on CPUE; influence (right hand plot) shows the standardising effect (a positive effect reduces the standardised CPUE by the equivalent amount). Estimated coefficients are given in the top panel.

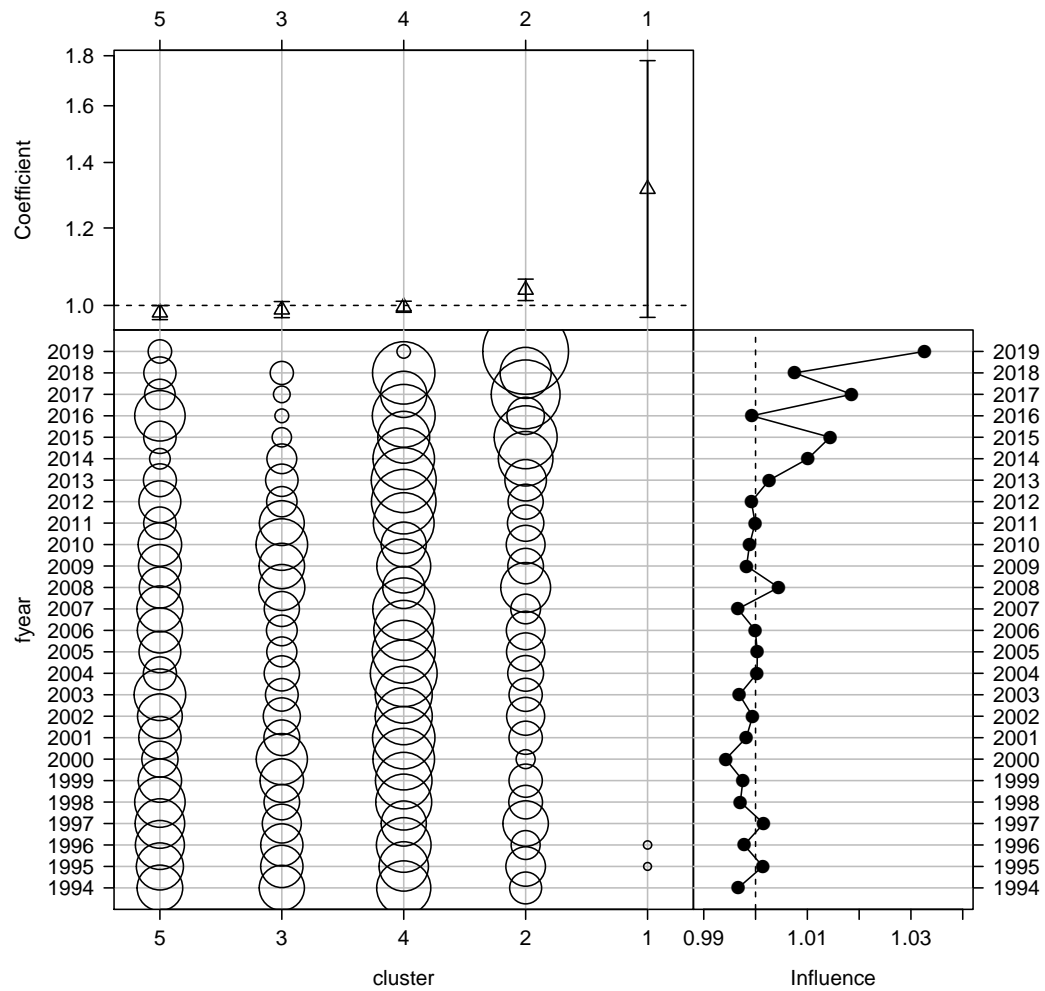


Figure B-54: Influence of targeting cluster for the Japanese fleet (bubble plot; bubbles scales by effort) on CPUE; influence (right hand plot) shows the standardising effect (a positive effect reduces the standardised CPUE by the equivalent amount). Estimated coefficients are given in the top panel.

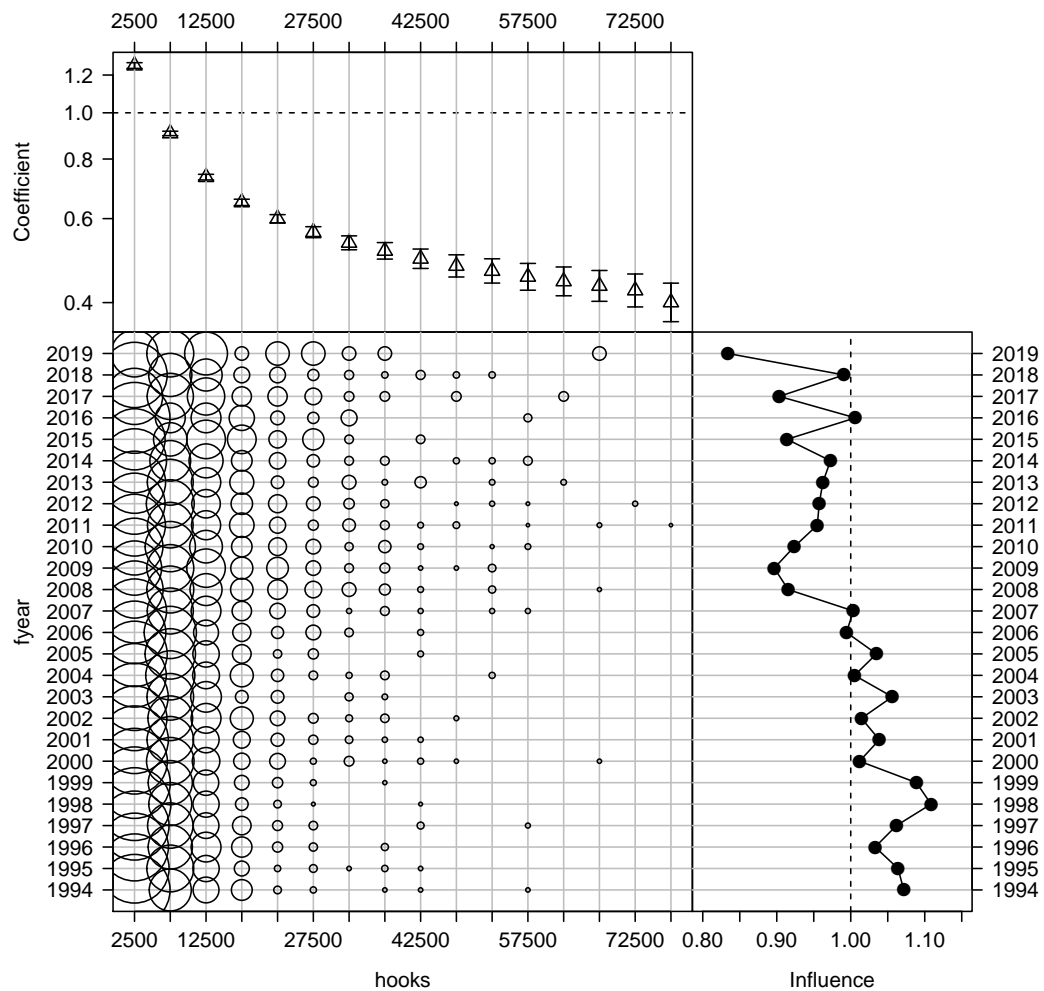


Figure B-55: Influence of number of hooks set per stratum for the Japanese fleet (bubble plot; bubbles scales by effort) on CPUE; influence (right hand plot) shows the standardising effect (a positive effect reduces the standardised CPUE by the equivalent amount). Estimated coefficients are given in the top panel.

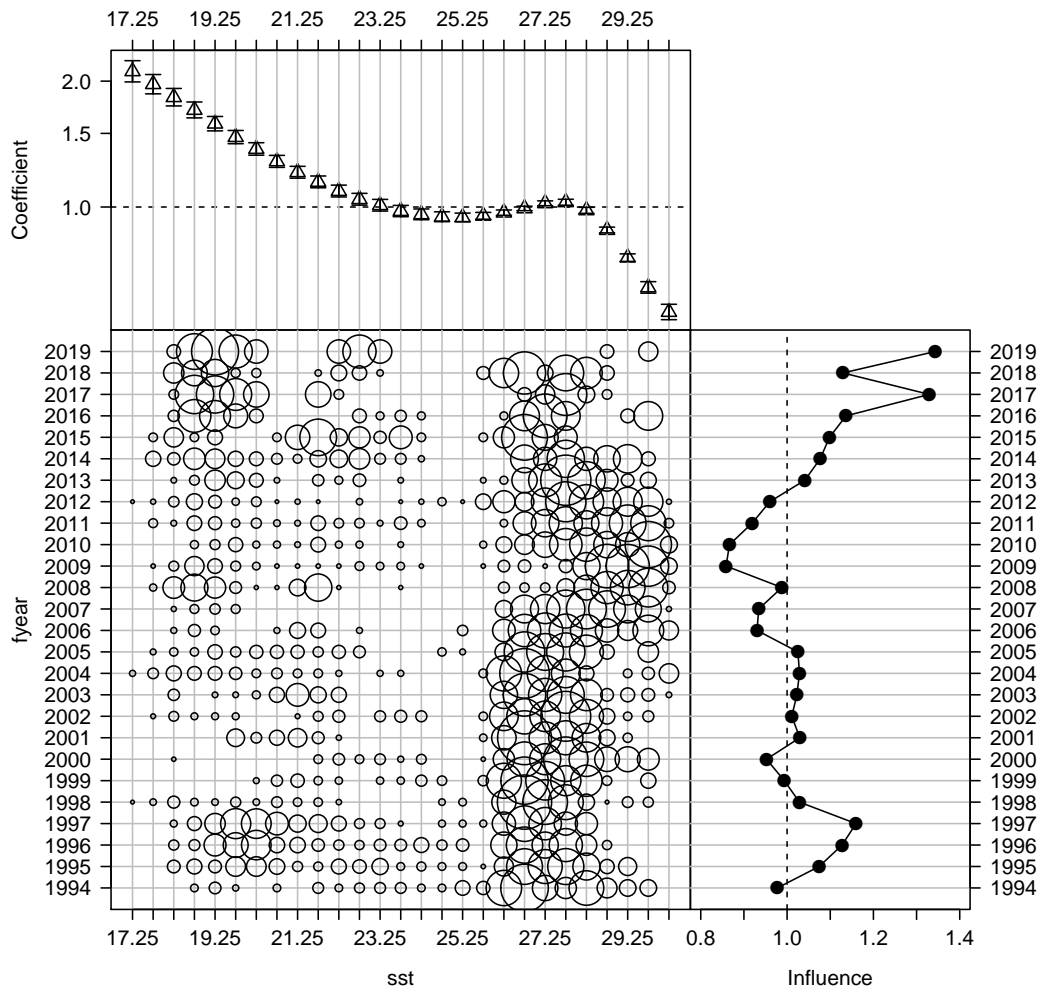


Figure B-56: Influence of sea surface temperature (SST, in degrees Celsius) for the Japanese fleet (bubble plot; bubbles scales by effort) on CPUE; influence (right hand plot) shows the standardising effect (a positive effect reduces the standardised CPUE by the equivalent amount). Estimated coefficients are given in the top panel.

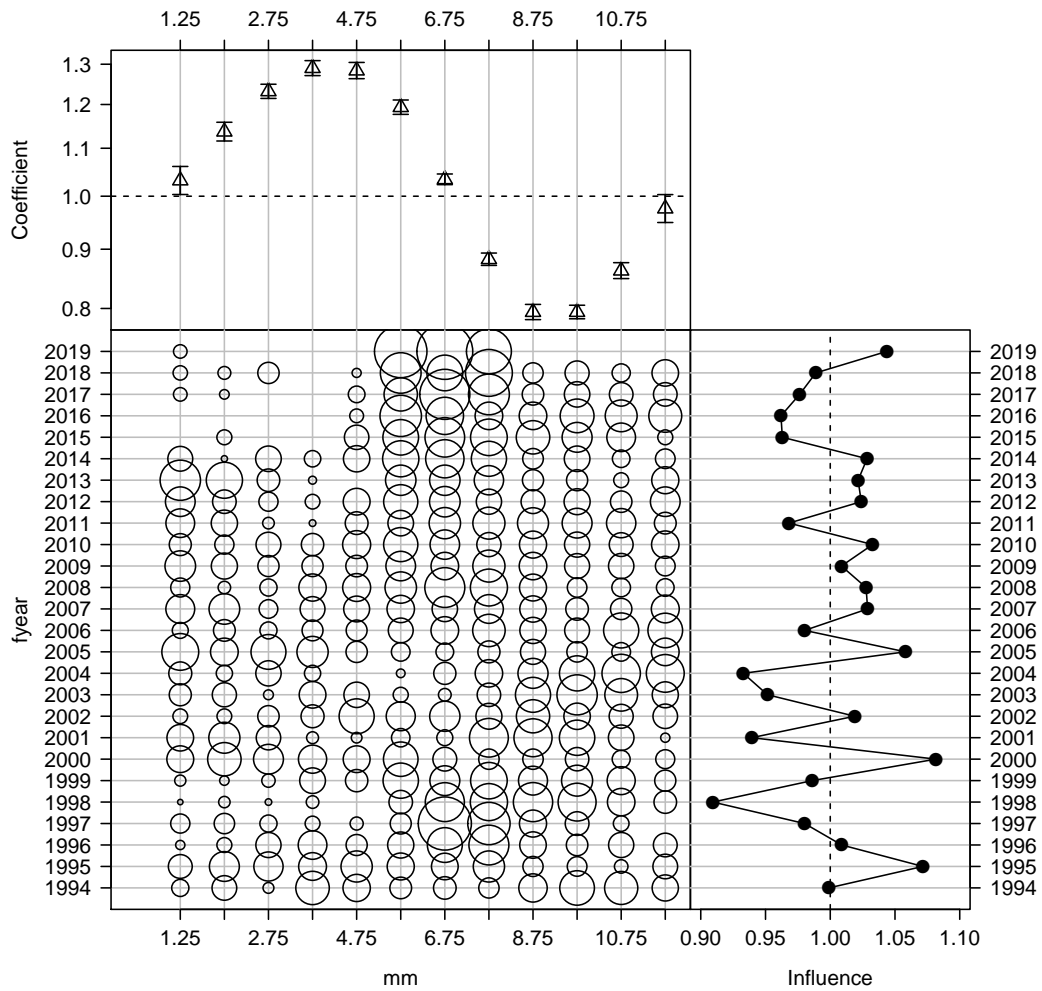


Figure B-57: Influence of month for the Japanese fleet (bubble plot; bubbles scales by effort) on CPUE; influence (right hand plot) shows the standardising effect (a positive effect reduces the standardised CPUE by the equivalent amount). Estimated coefficients are given in the top panel.

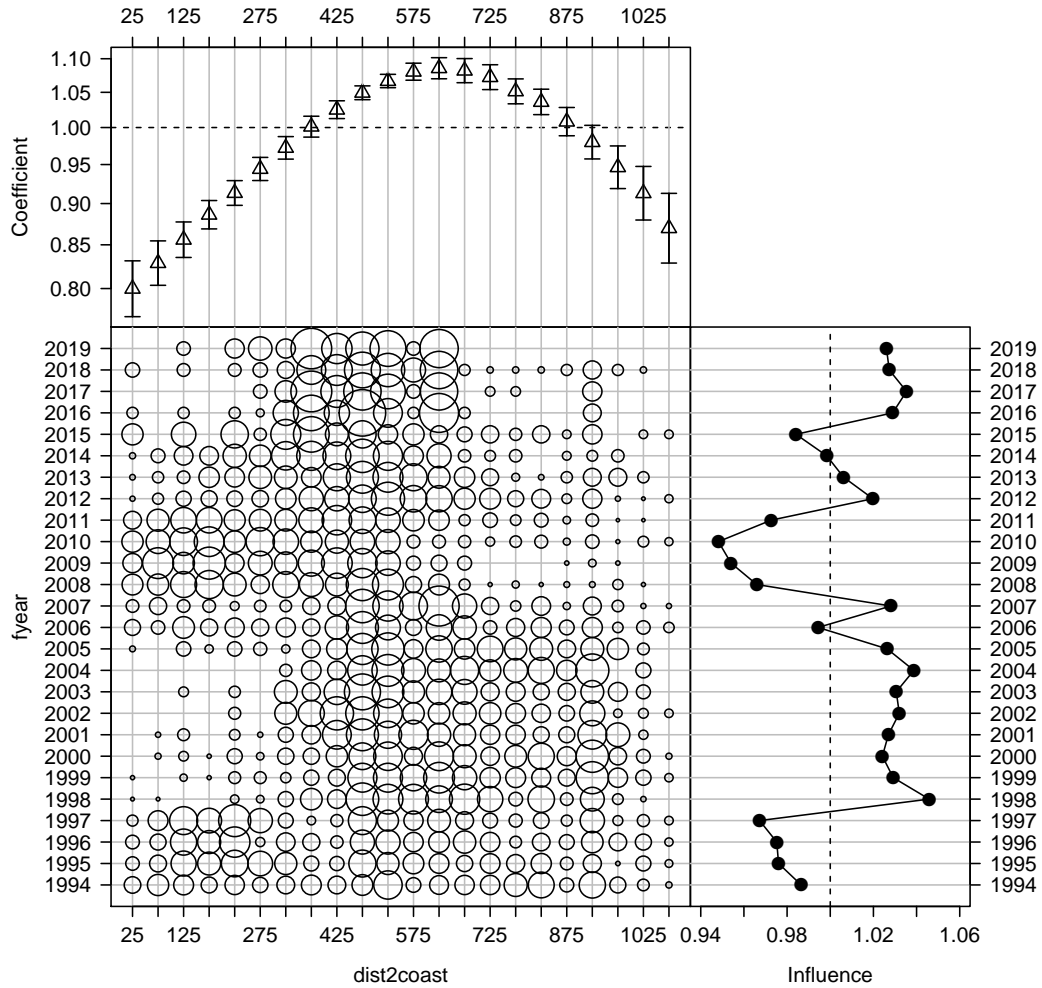


Figure B-58: Influence of distance to coast composition for the Japanese fleet (bubble plot; bubbles scales by effort) on CPUE; influence (right hand plot) shows the standardising effect (a positive effect reduces the standardised CPUE by the equivalent amount). Estimated coefficients are given in the top panel.

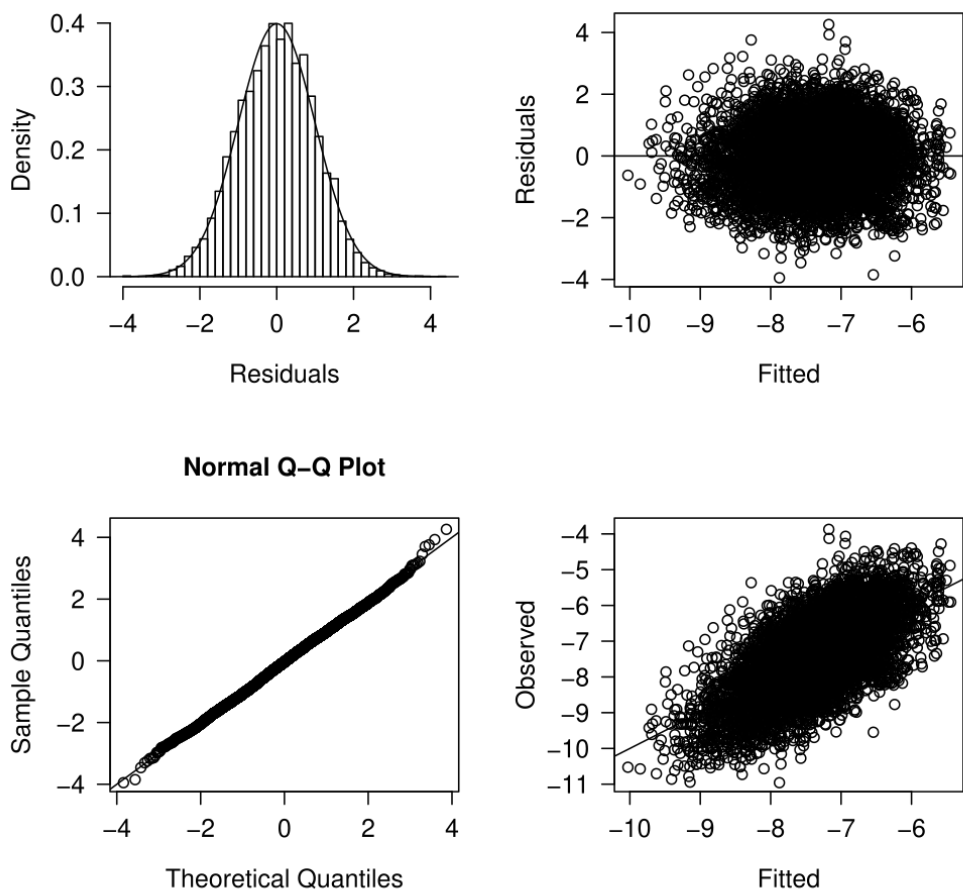


Figure B-59: Diagnostics for the log-normal CPUE standardisation model for Japanese fleet strata with positive catch.

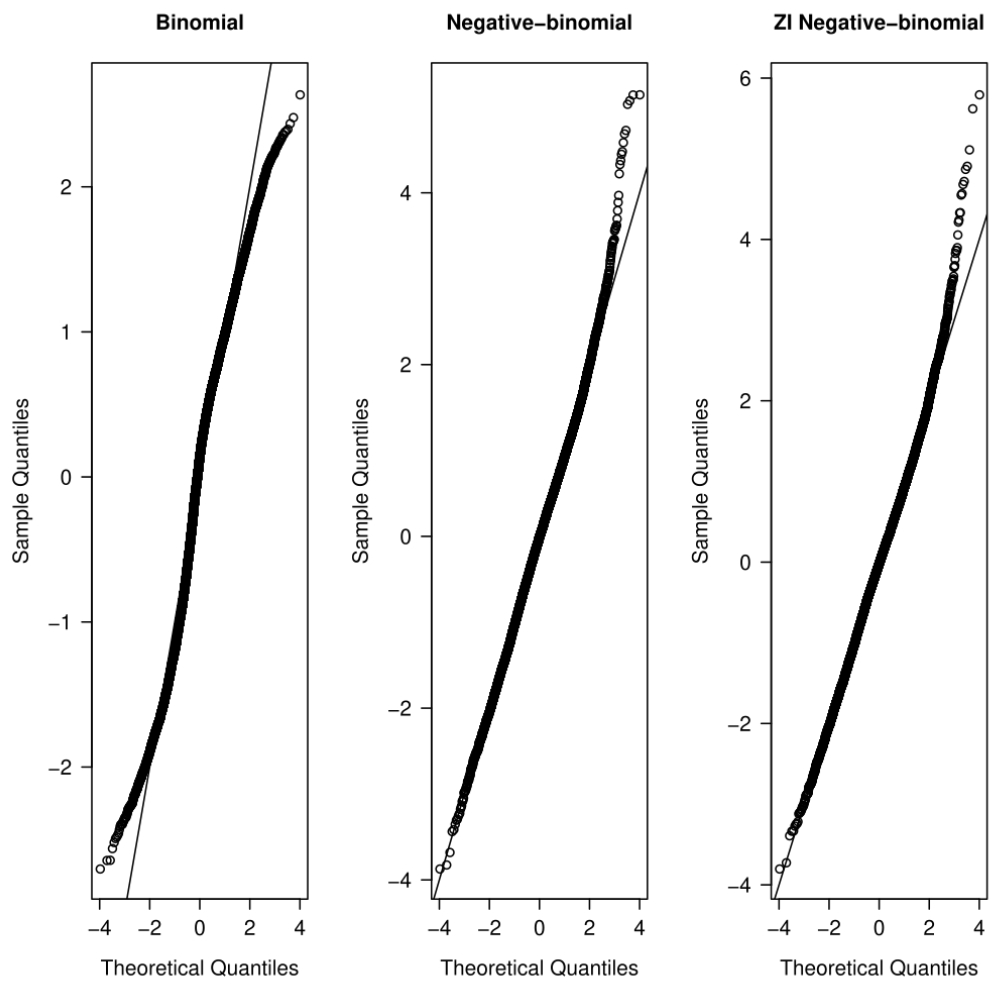


Figure B-60: Quantile residual diagnostics for the binomial component, as well as alternative CPUE standardisation models for Japanese fleet strata with positive catch.

B.4 Alternative CPUE standardisations

B.4.1 Chinese Taipei low latitude CPUE

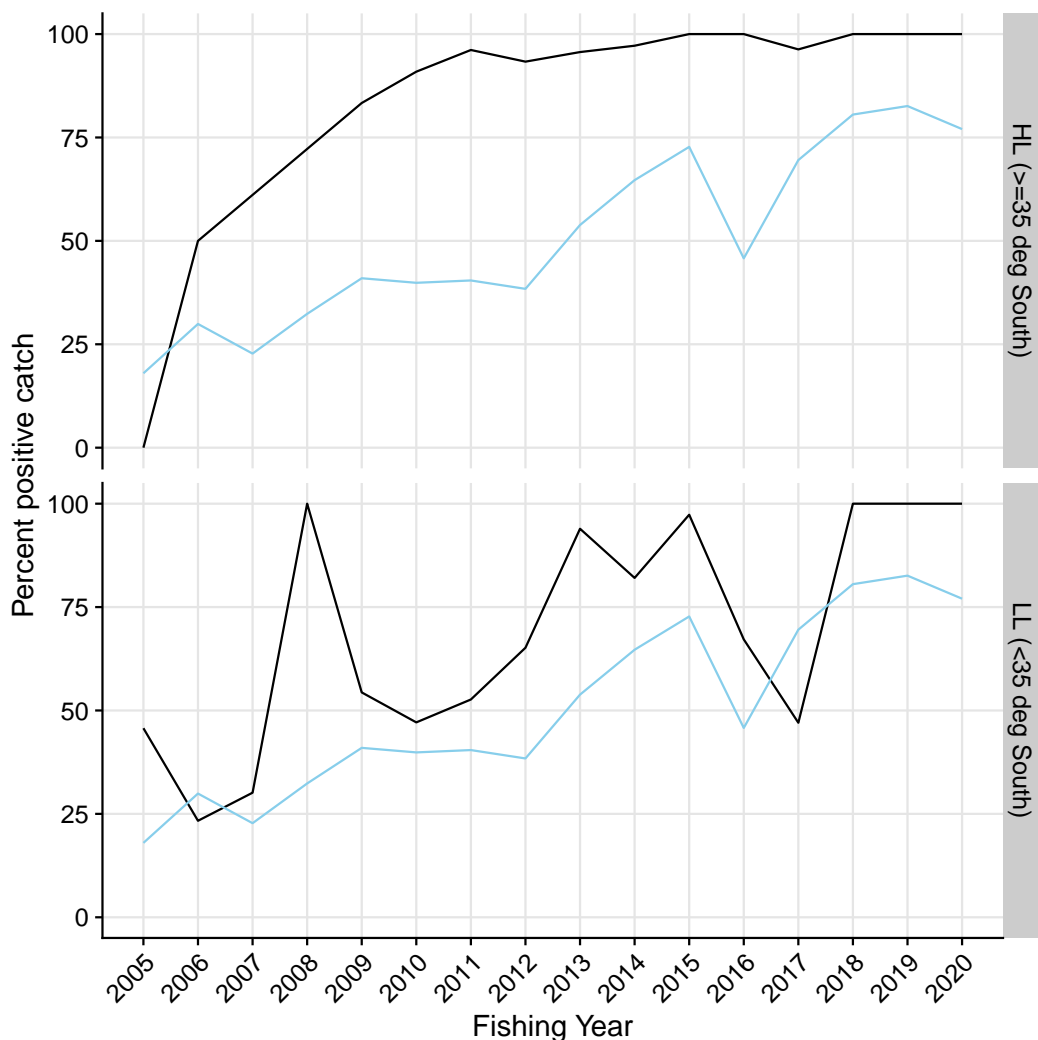


Figure B-61: Proportion of strata for the Chinese Taipei fleet with positive catch by latitudinal stratum. Light blue are initial log-sheet records prior to filtering, the black line is the retained dataset after filtering for consistently reporting vessels. Where available, the corresponding values from observed strata is shown in orange.

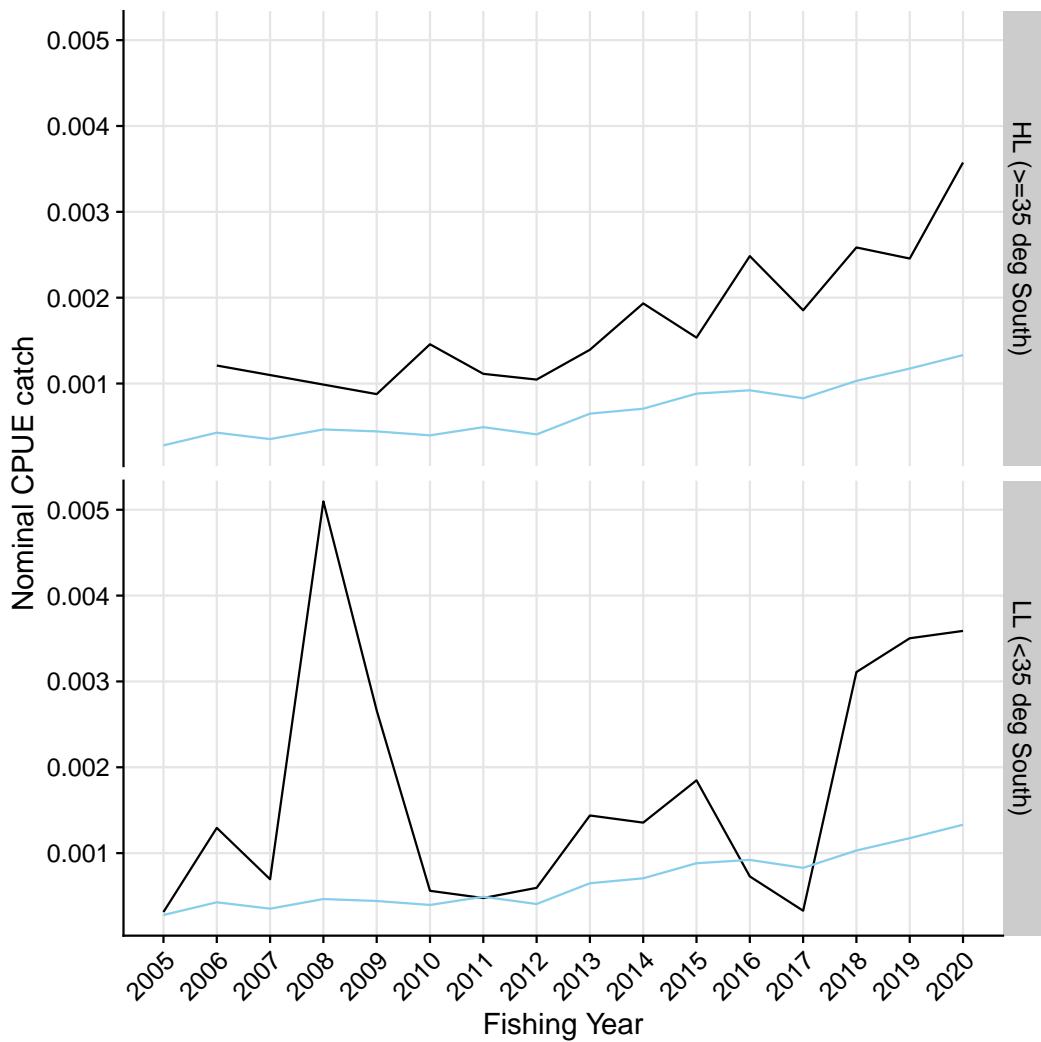


Figure B-62: Nominal CPUE (in number of blue shark per 100 hooks) strata of the Chinese Taipei fleet with positive catch by latitudinal stratum. Light blue are initial log-sheet records prior to filtering, the black line is the retained dataset after filtering for consistently reporting vessels. Where available, the corresponding values from observed strata is shown in orange.

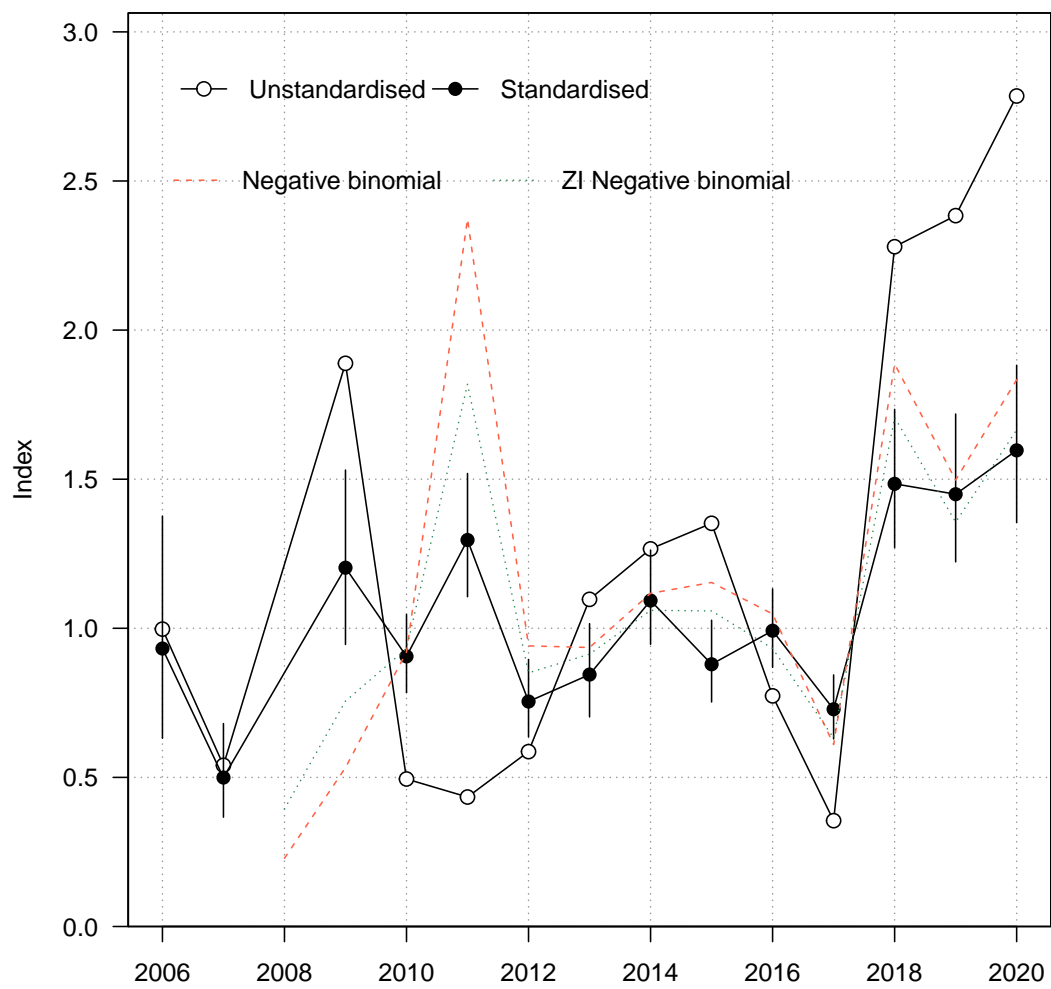


Figure B-63: Standardised (closed black circles with standard error) and unstandardised (open circles) CPUE indices for Chinese Taipei fleet strata with positive catch. Where successful (i.e., converged), standardised trends from a negative - binomial and zero - inflated negative binomial model run over the full dataset (including strata with zero values) are also shown for comparison.

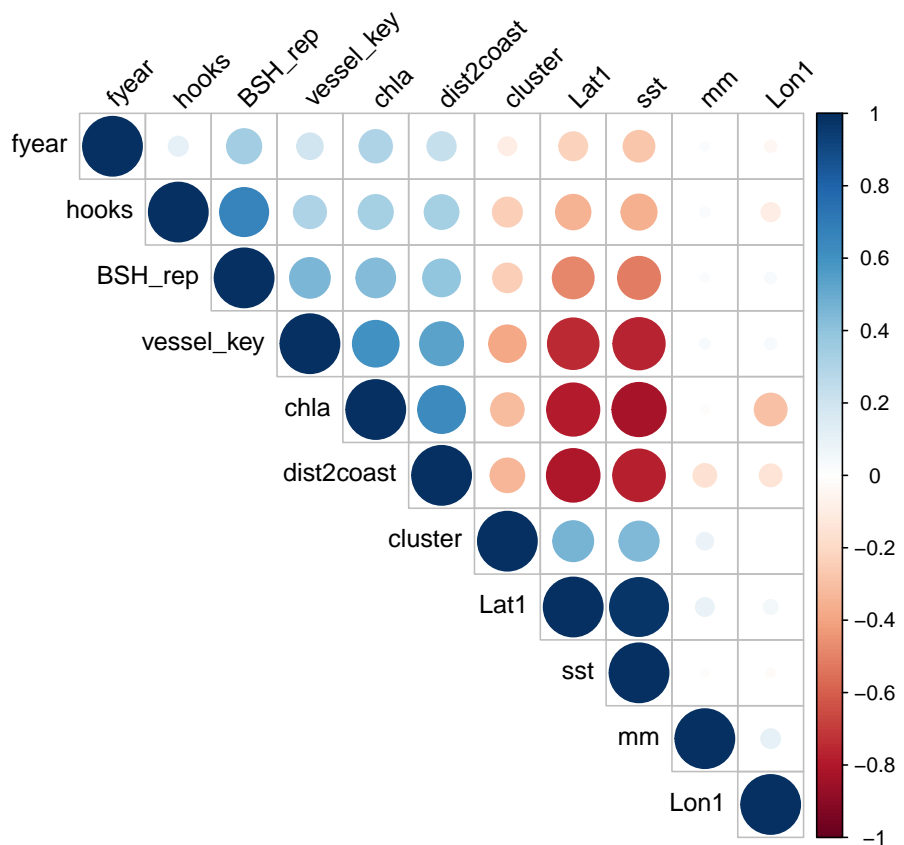


Figure B-64: Correlations amongst potential covariates for CPUE standardisation in the Chinese Taipei fleet. Where necessary, variables were removed to reduce redundancy in the models.

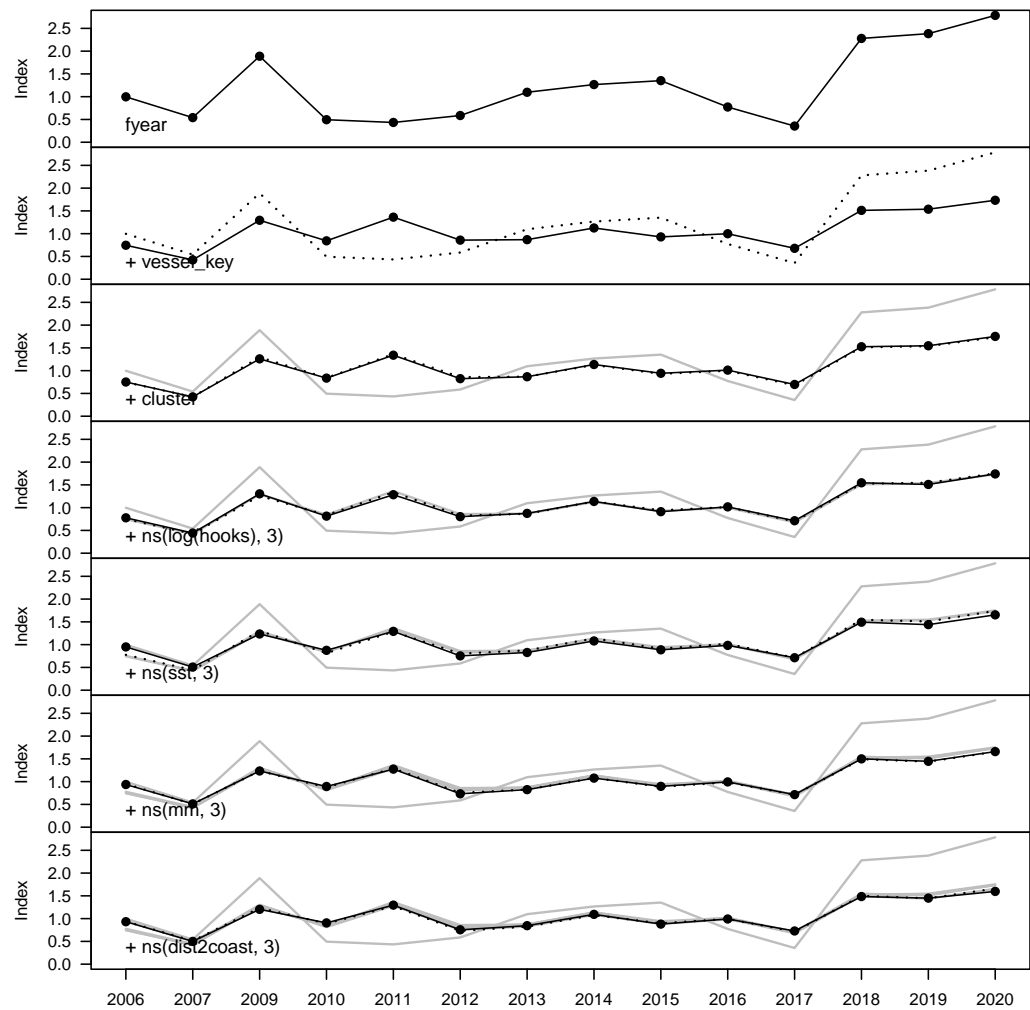


Figure B-65: Step plot for the Chinese Taipei fleet CPUE, showing sequential standardising effects of variables included in the standardisation model.

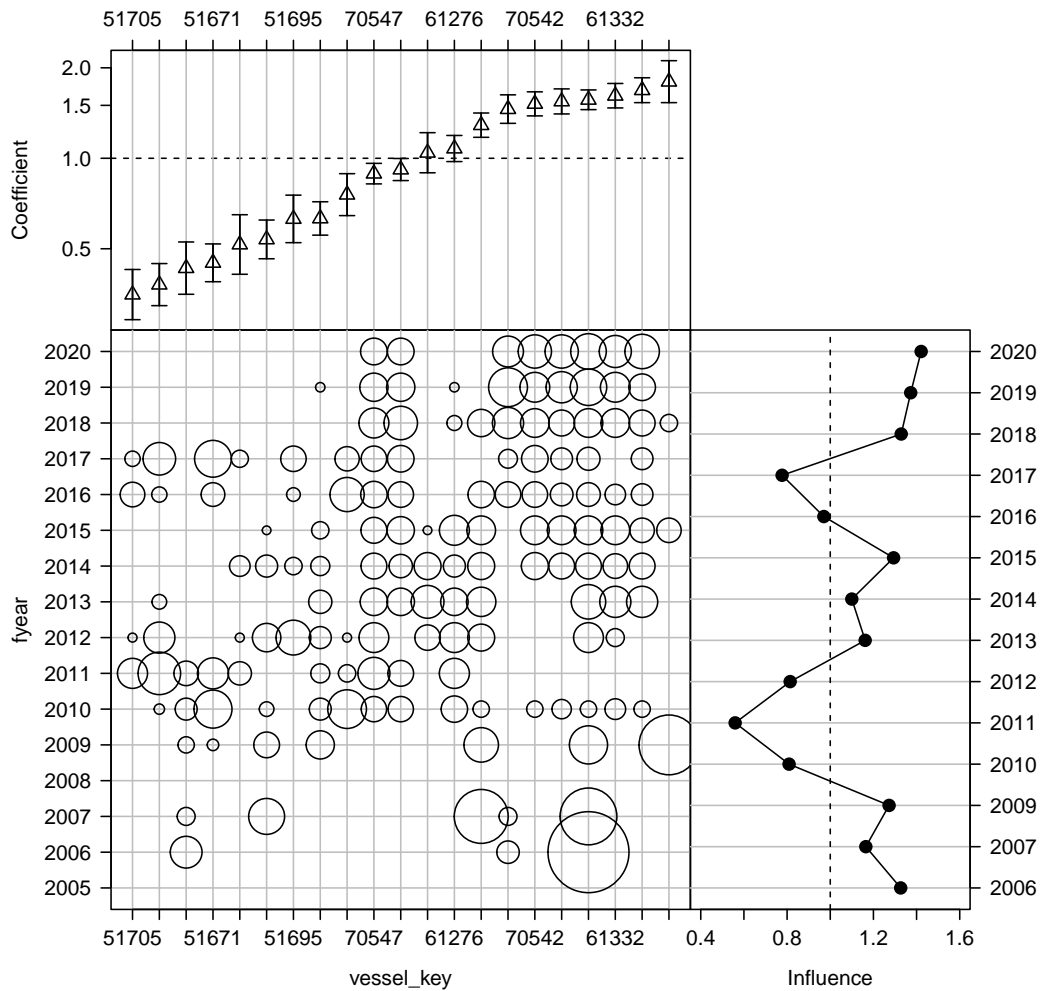


Figure B-66: Influence of fleet composition (vessel keys) for the Chinese Taipei fleet (bubble plot; bubbles scales by effort) on CPUE; influence (right hand plot) shows the standardising effect (a positive effect reduces the standardised CPUE by the equivalent amount). Estimated coefficients are given in the top panel.

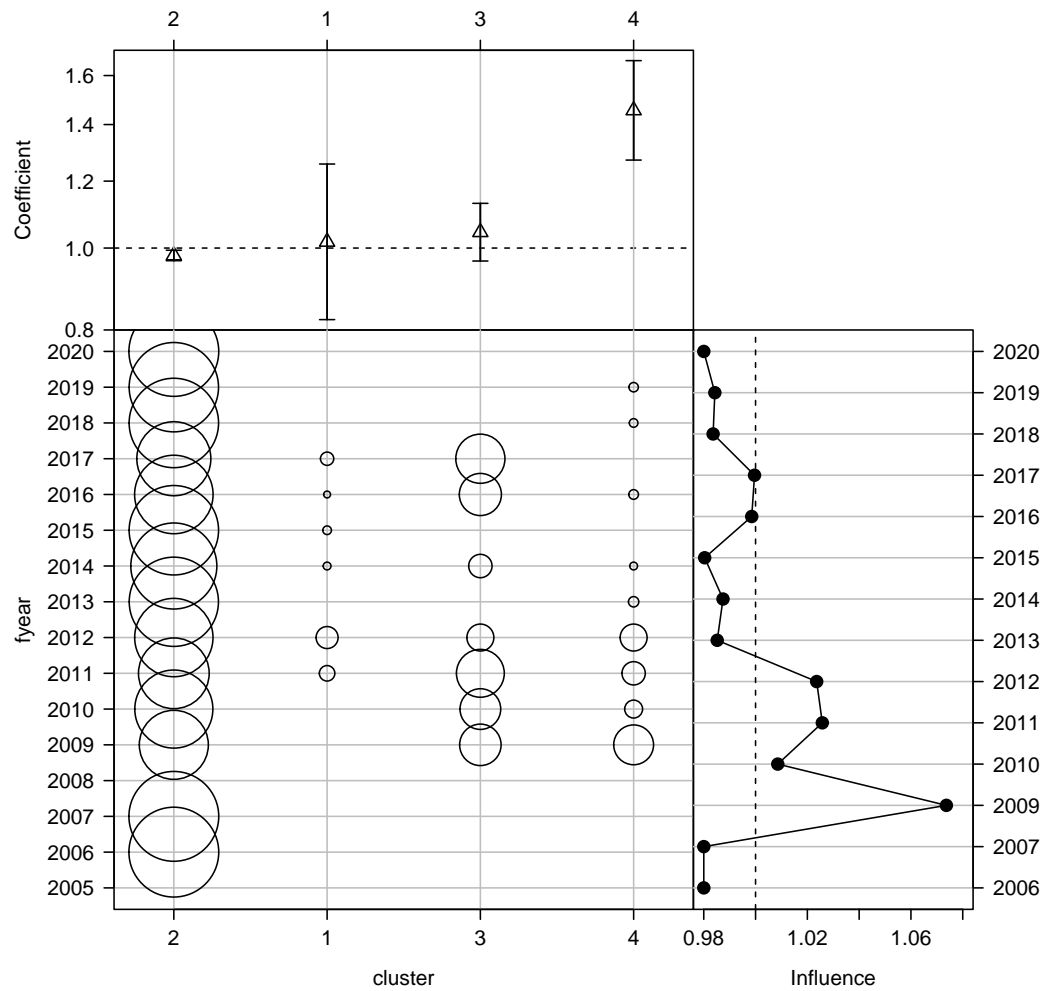


Figure B-67: Influence of targeting cluster for the Chinese Taipei fleet (bubble plot; bubbles scales by effort) on CPUE; influence (right hand plot) shows the standardising effect (a positive effect reduces the standardised CPUE by the equivalent amount). Estimated coefficients are given in the top panel.

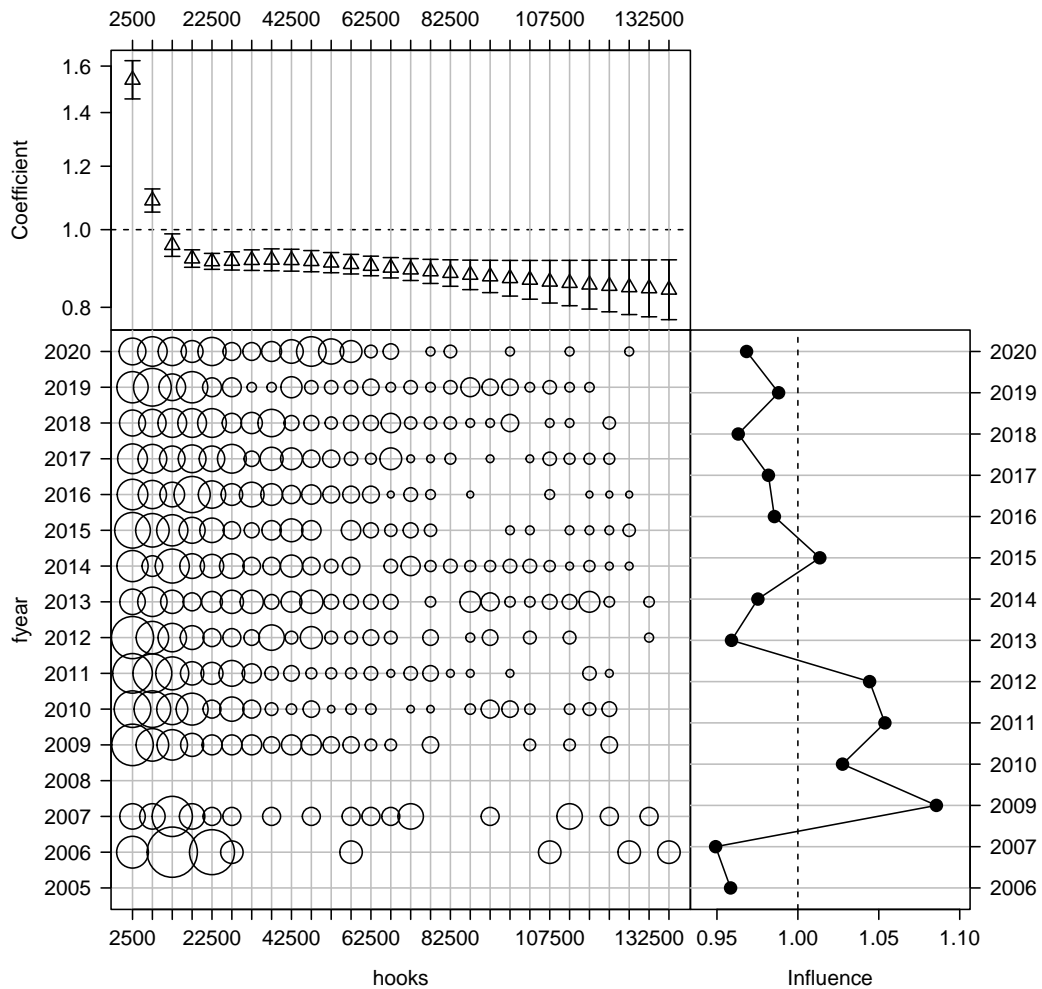


Figure B-68: Influence of number of hooks set per stratum for the Chinese Taipei fleet (bubble plot; bubbles scales by effort) on CPUE; influence (right hand plot) shows the standardising effect (a positive effect reduces the standardised CPUE by the equivalent amount). Estimated coefficients are given in the top panel.

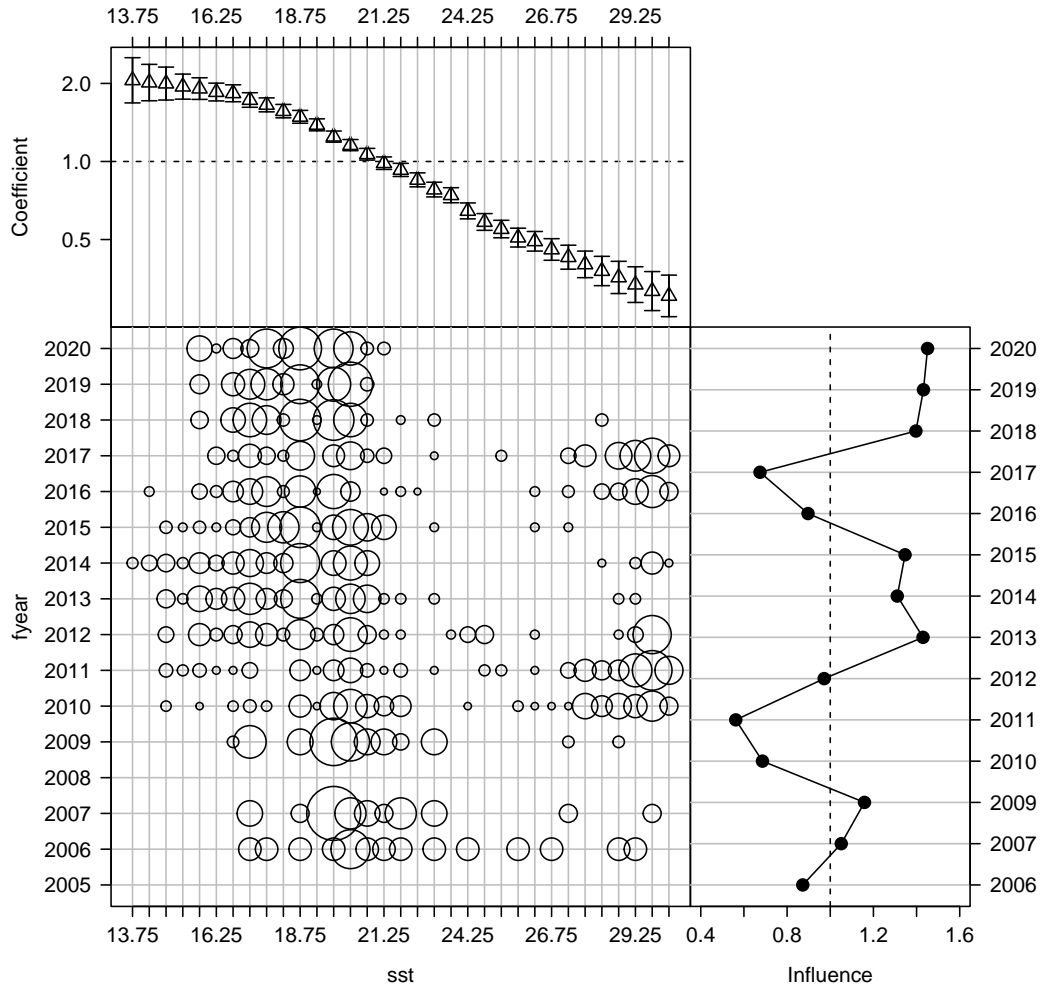


Figure B-69: Influence of sea surface temperature (SST, in degrees Celsius) for the Chinese Taipei fleet (bubble plot; bubbles scales by effort) on CPUE; influence (right hand plot) shows the standardising effect (a positive effect reduces the standardised CPUE by the equivalent amount). Estimated coefficients are given in the top panel.

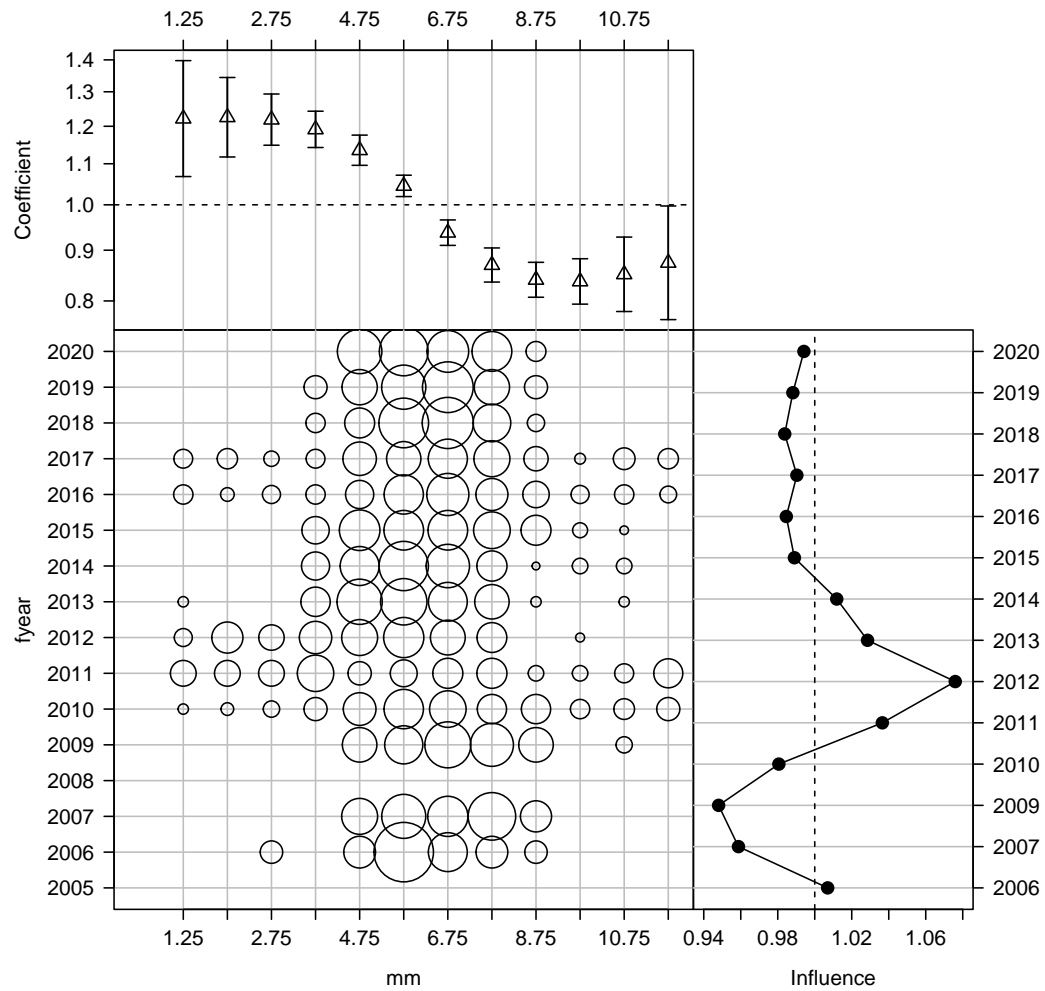


Figure B-70: Influence of month for the Chinese Taipei fleet (bubble plot; bubbles scales by effort) on CPUE; influence (right hand plot) shows the standardising effect (a positive effect reduces the standardised CPUE by the equivalent amount). Estimated coefficients are given in the top panel.

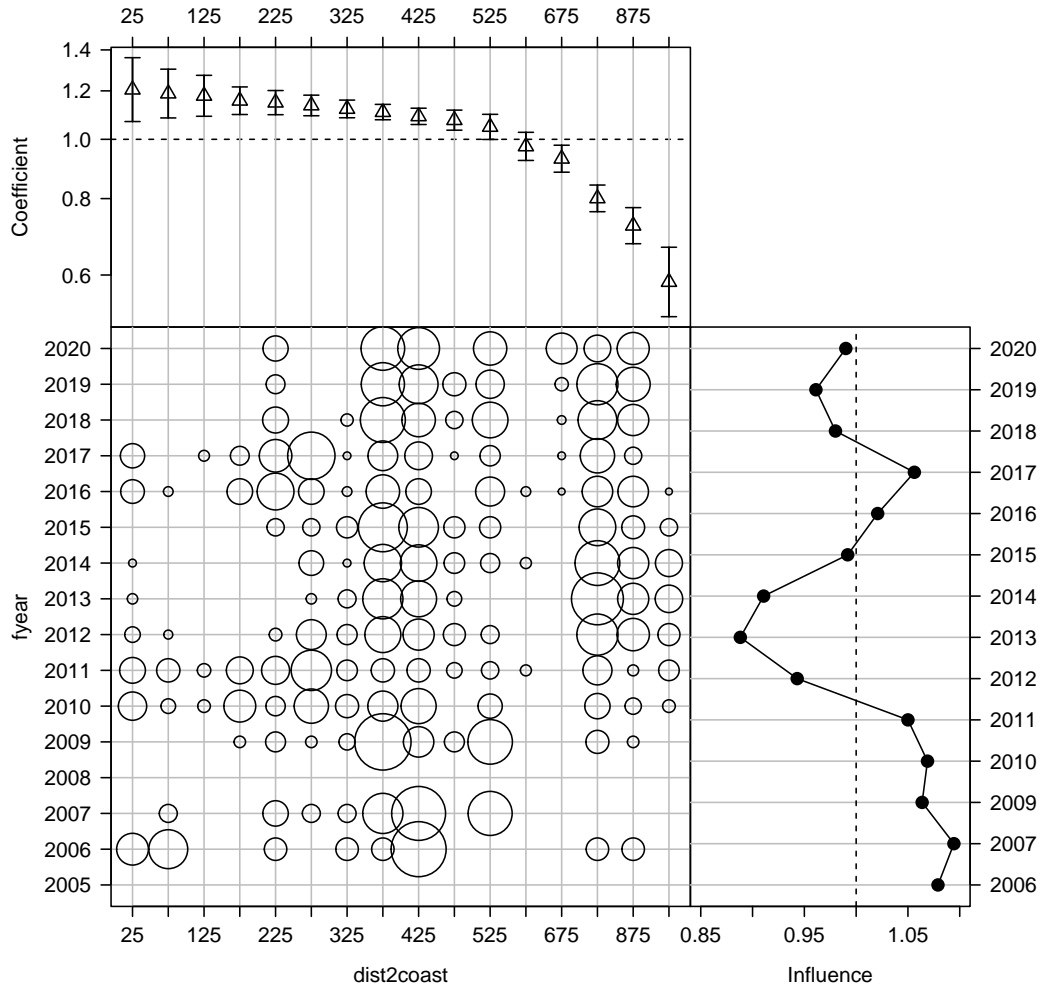


Figure B-71: Influence of distance to coast composition for the Chinese Taipei fleet (bubble plot; bubbles scales by effort) on CPUE; influence (right hand plot) shows the standardising effect (a positive effect reduces the standardised CPUE by the equivalent amount). Estimated coefficients are given in the top panel.

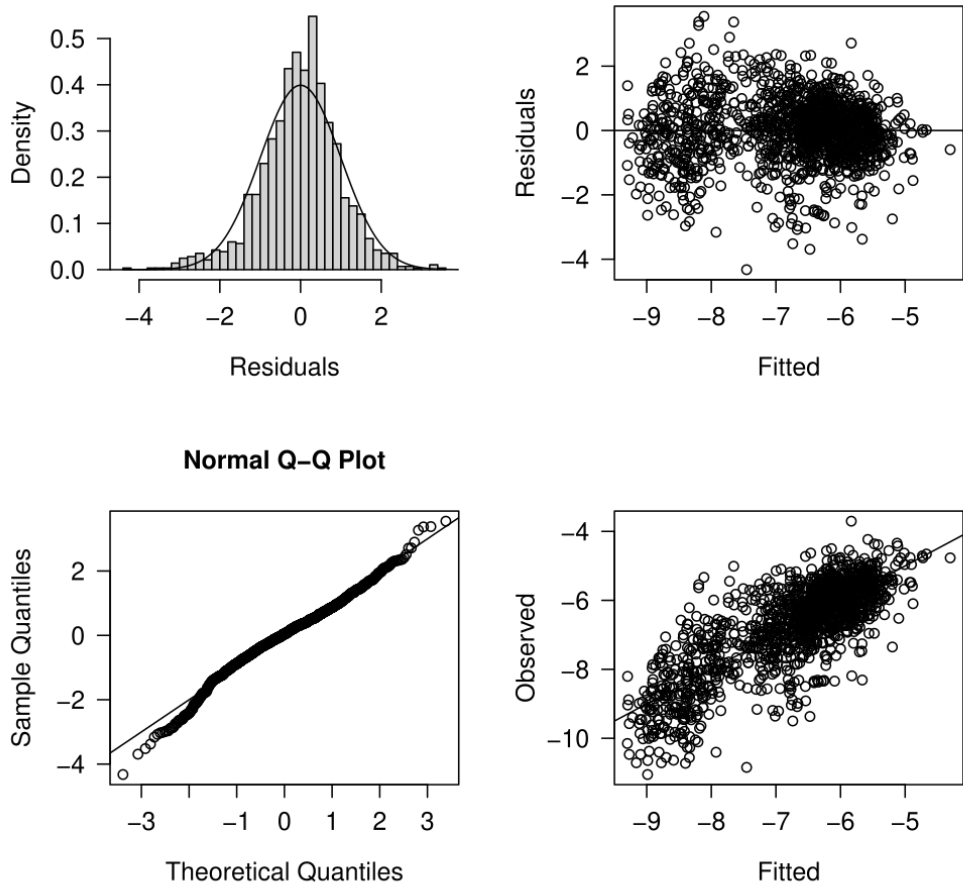


Figure B-72: Diagnostics for the log-normal CPUE standardisation model for Chinese Taipei fleet strata with positive catch.

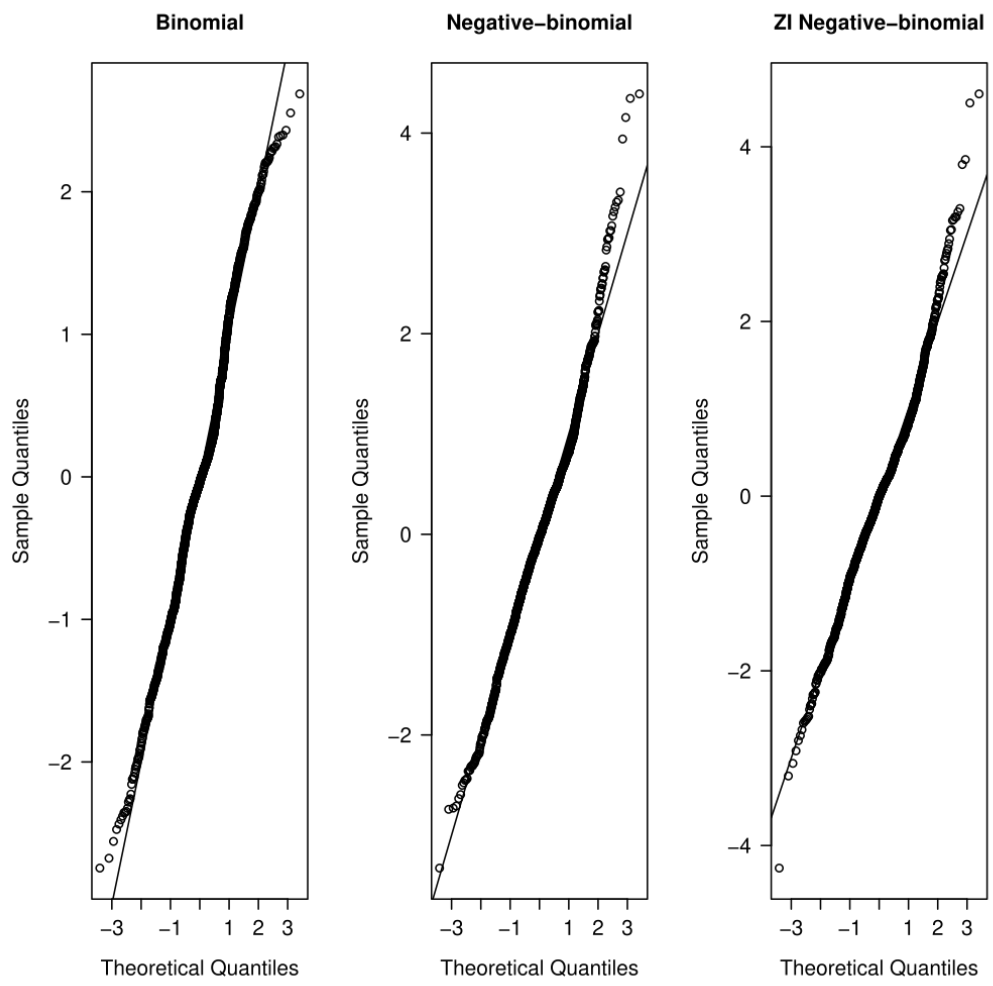


Figure B-73: Quantile residual diagnostics for the binomial component, as well as alternative CPUE standardisation models for Chinese Taipei fleet strata with positive catch.

B.4.2 Australian low latitude CPUE

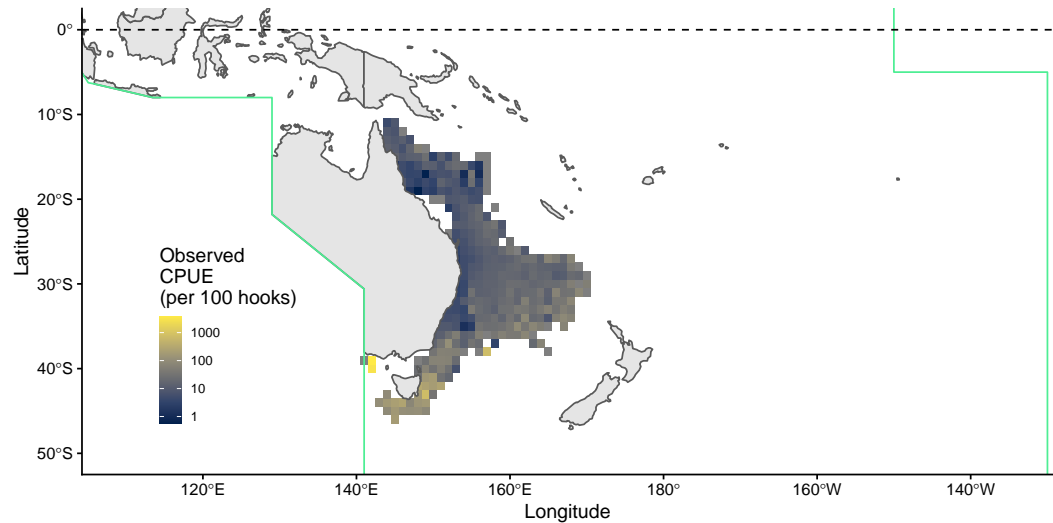


Figure B-74: Maps of average catch rates (CPUE; in number of blue shark per 100 hooks) for the Australian longline fleet.



Figure B-75: Maps of average catch rates (CPUE; in number of blue shark per 100 hooks) by year for the Australian longline fleet.

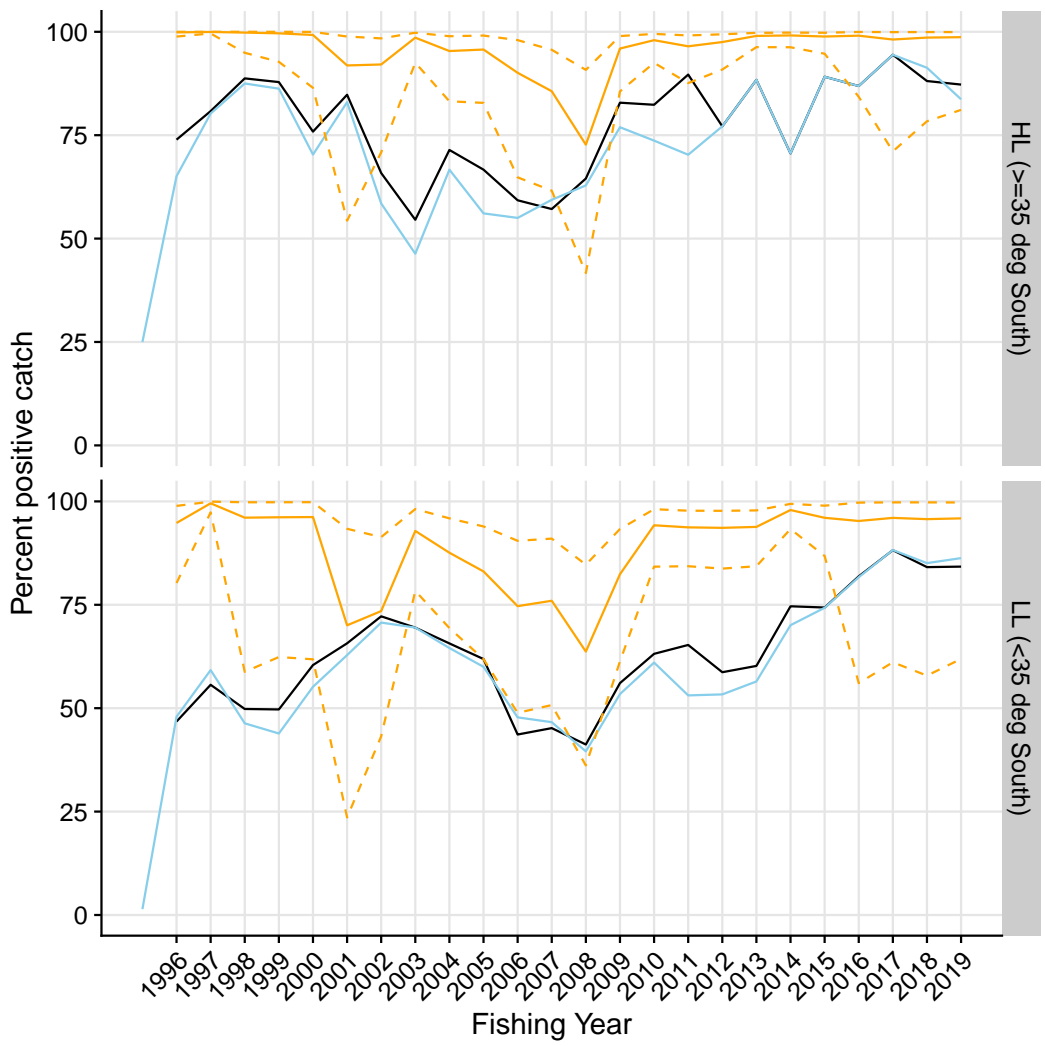


Figure B-76: Proportion of strata for the AU low-latitude fleet with positive catch by latitudinal stratum. Light blue are initial log-sheet records prior to filtering, the black line is the retained dataset after filtering for consistently reporting vessels. Where available, the corresponding values from observed strata is shown in orange.

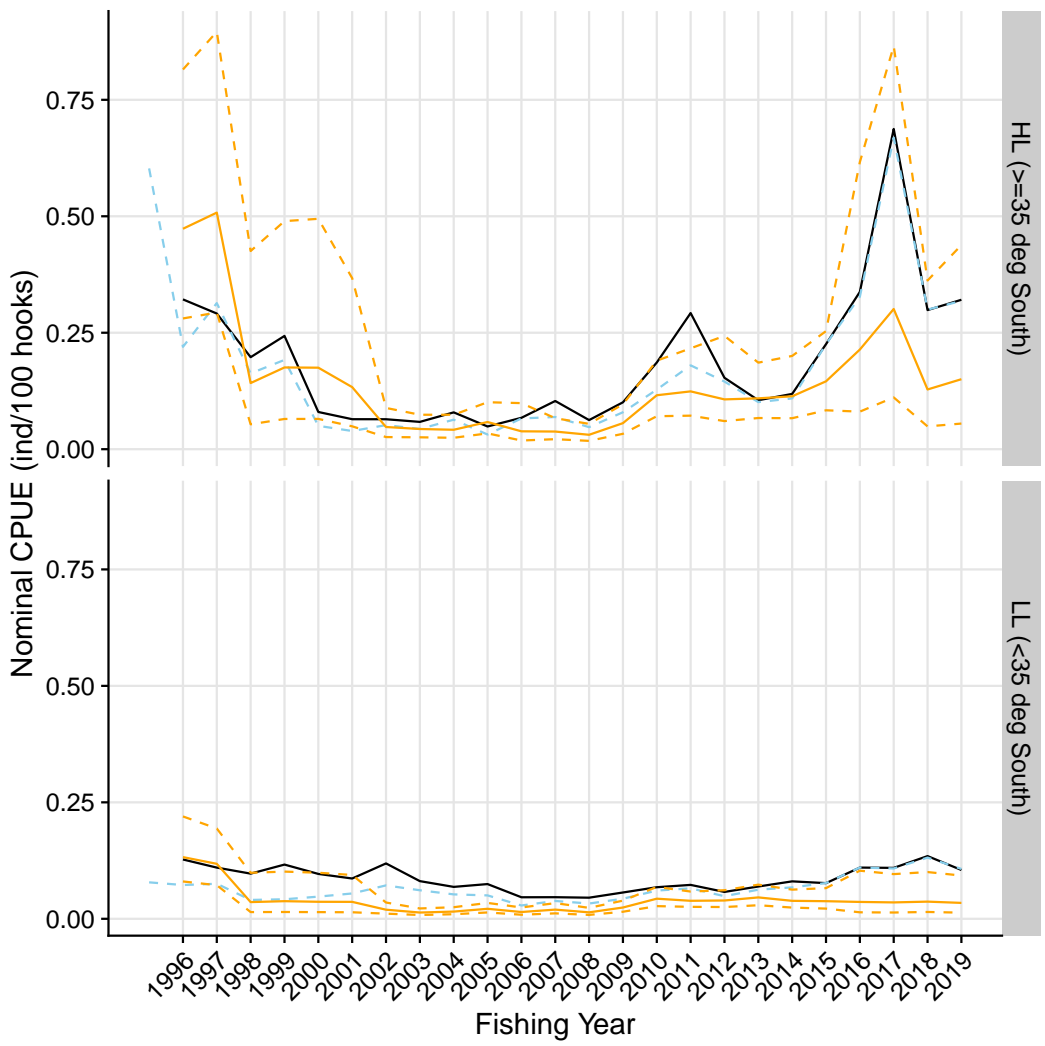


Figure B-77: Nominal CPUE (in number of blue shark per 100 hooks) strata of the AU low-latitude fleet with positive catch by latitudinal stratum. Light blue are initial log-sheet records prior to filtering, the black line is the retained dataset after filtering for consistently reporting vessels. Where available, the corresponding values from observed strata is shown in orange.

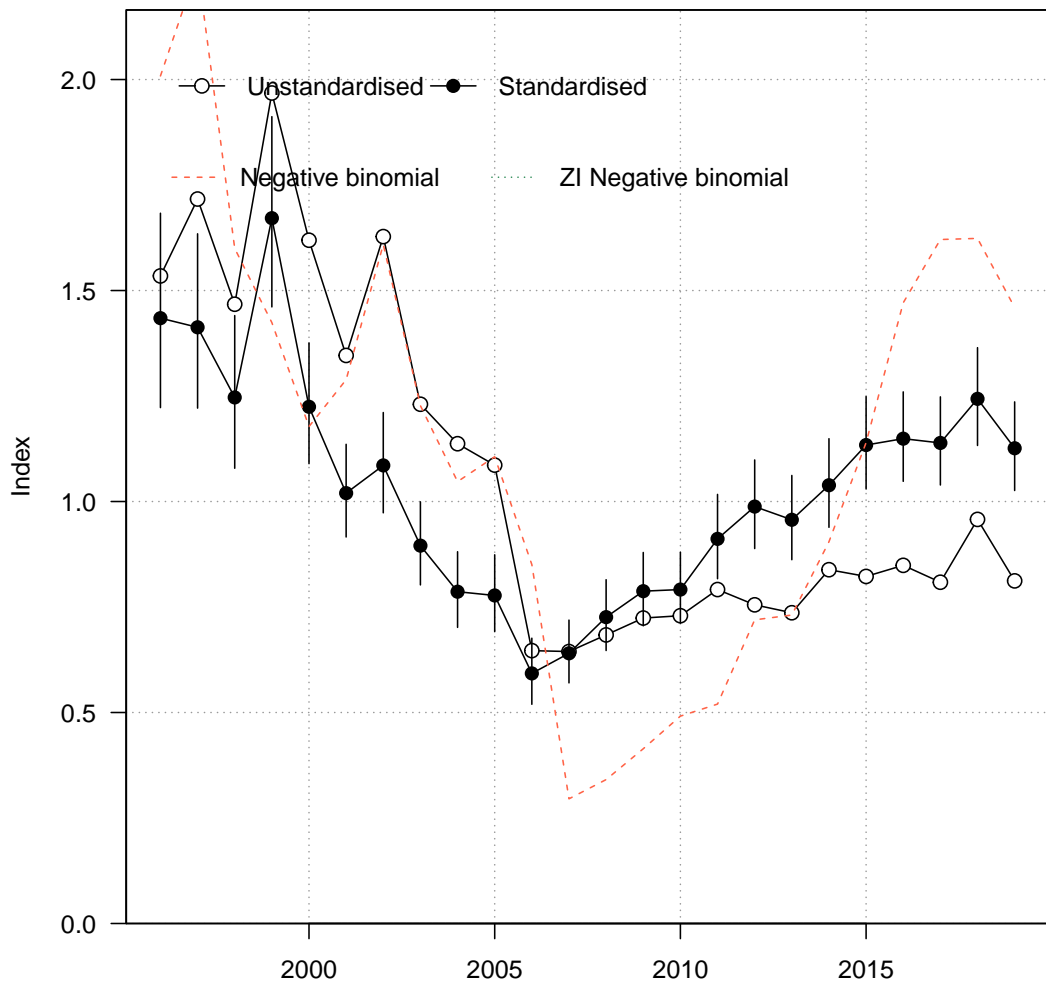


Figure B-78: Standardised (closed black circles with standard error) and unstandardised (open circles) CPUE indices for AU low-latitude fleet strata with positive catch. Where successful (i.e., converged), standardised trends from a negative-binomial and zero-inflated negative binomial model run over the full dataset (including strata with zero values) are also shown for comparison.

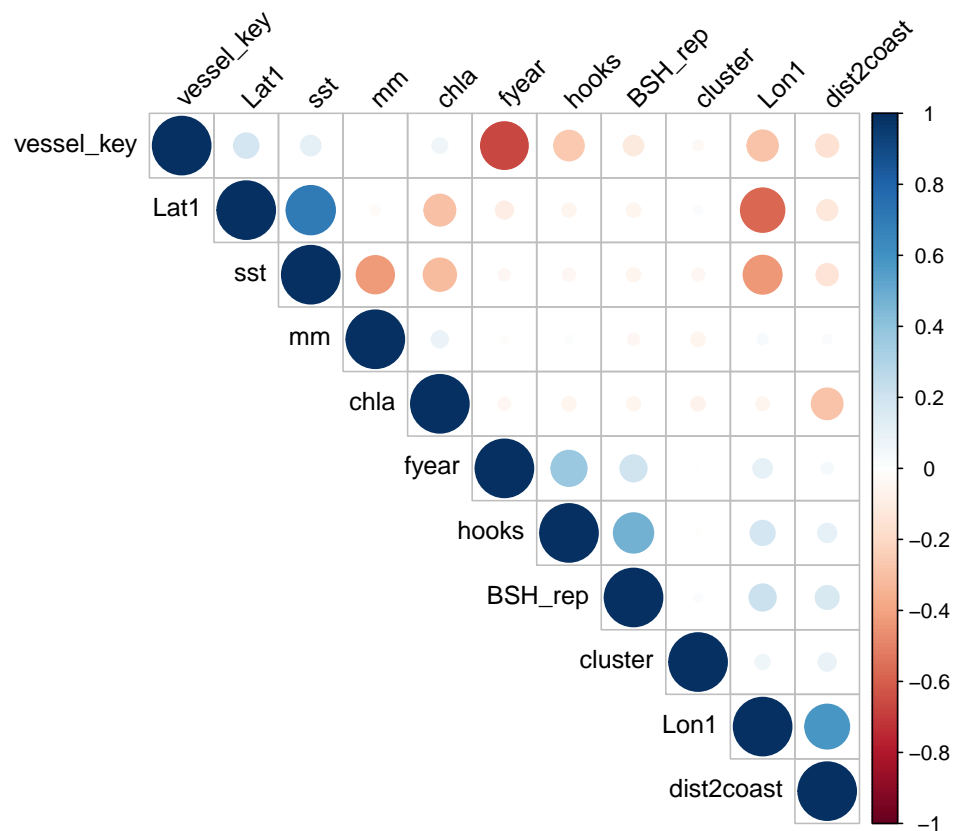


Figure B-79: Correlations amongst potential covariates for CPUE standardisation in the AU low-latitude fleet. Where necessary, variables were removed to reduce redundancy in the models.

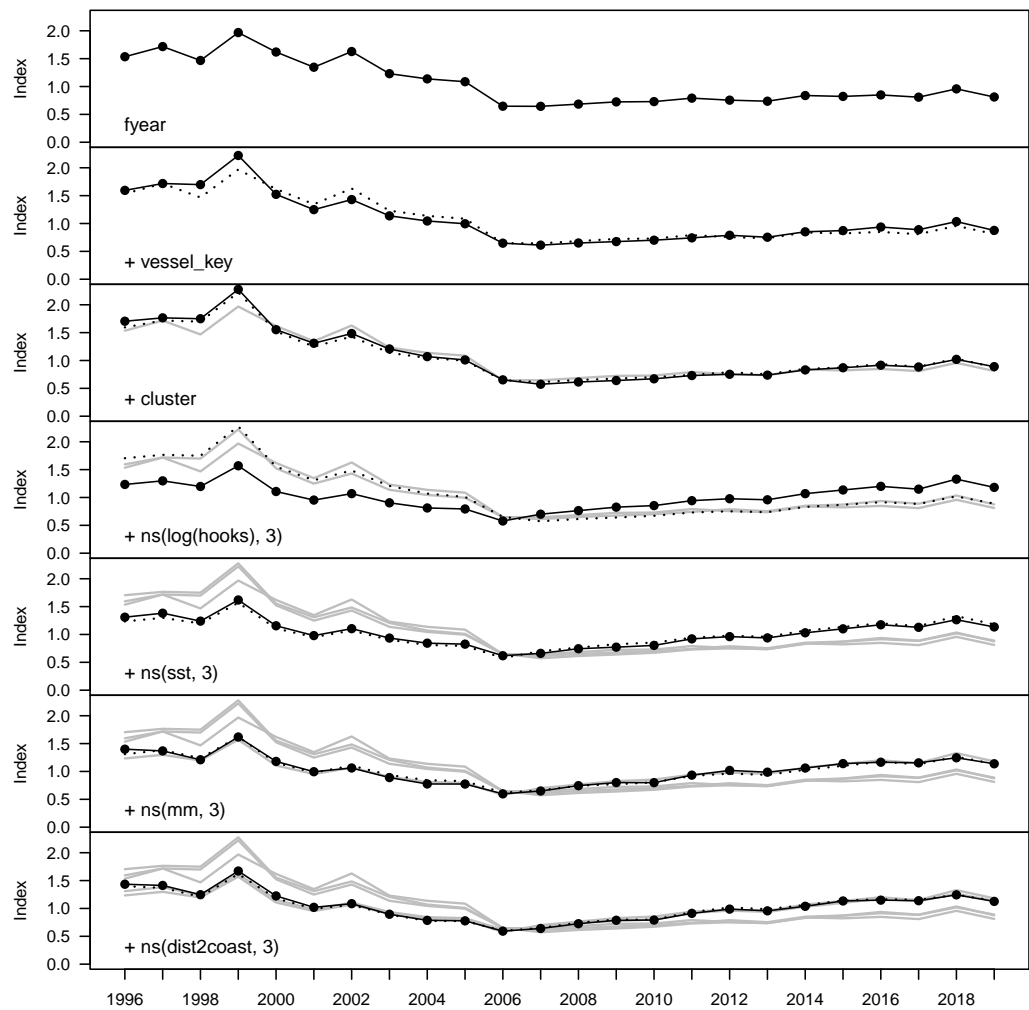


Figure B-80: Step plot for the AU low-latitude fleet CPUE, showing sequential standardising effects of variables included in the standardisation model.

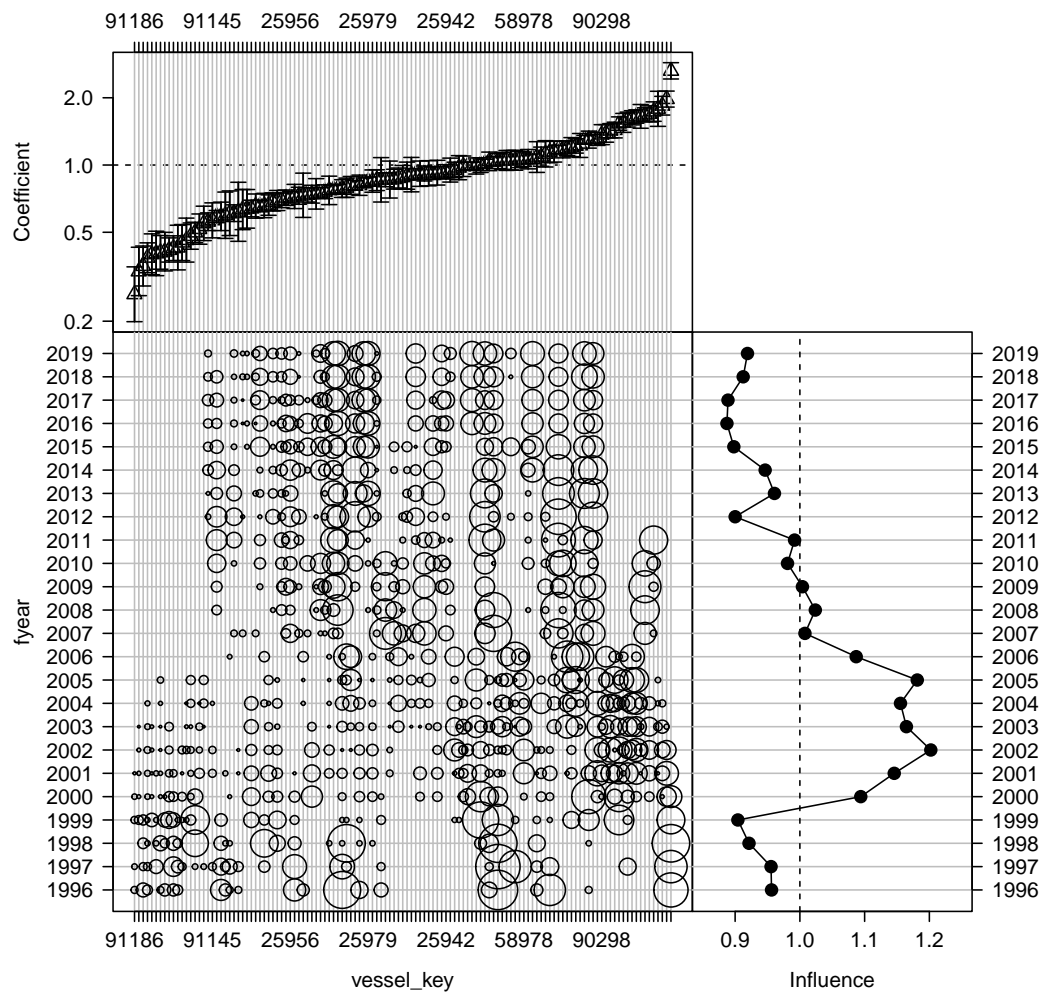


Figure B-81: Influence of fleet composition (vessel keys) for the AU low-latitude fleet (bubble plot; bubbles scales by effort) on CPUE; influence (right hand plot) shows the standardising effect (a positive effect reduces the standardised CPUE by the equivalent amount). Estimated coefficients are given in the top panel.

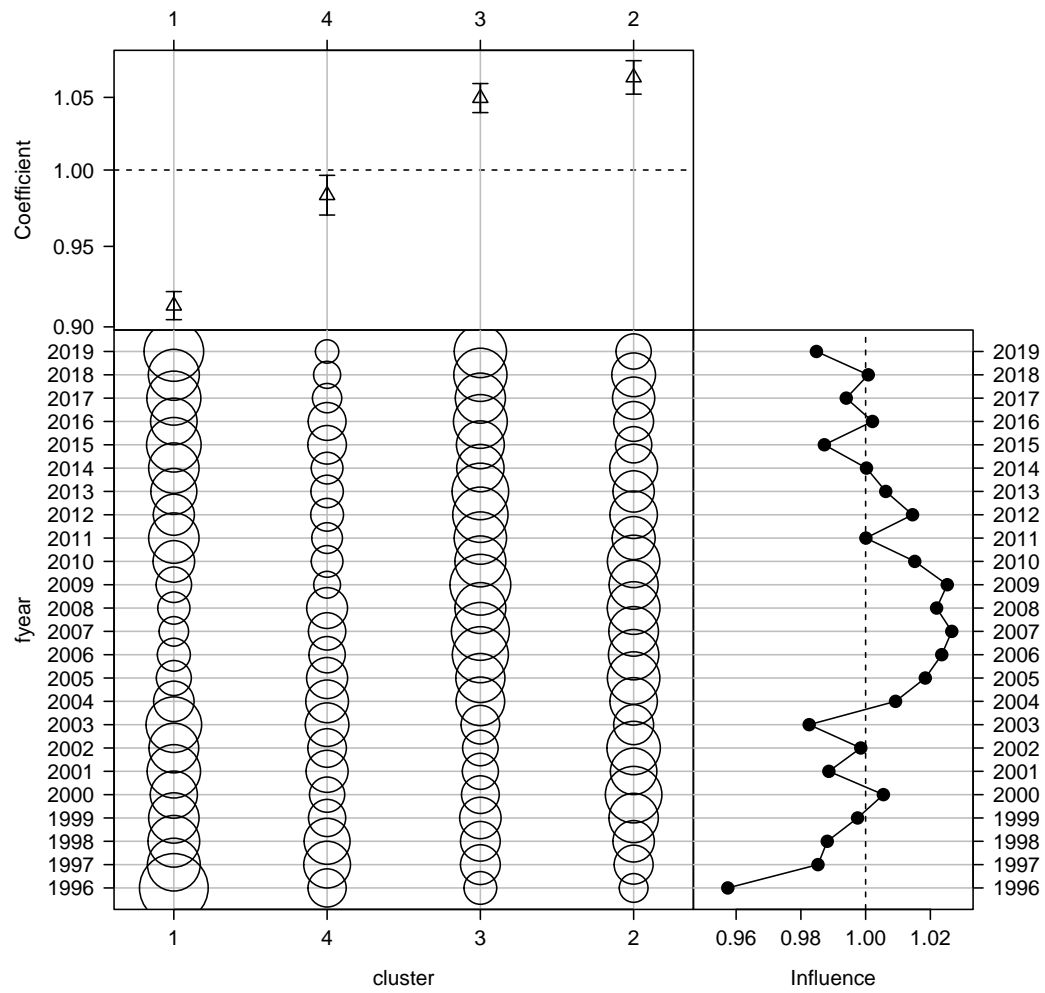


Figure B-82: Influence of targeting cluster for the AU low-latitude fleet (bubble plot; bubbles scales by effort) on CPUE; influence (right hand plot) shows the standardising effect (a positive effect reduces the standardised CPUE by the equivalent amount). Estimated coefficients are given in the top panel.

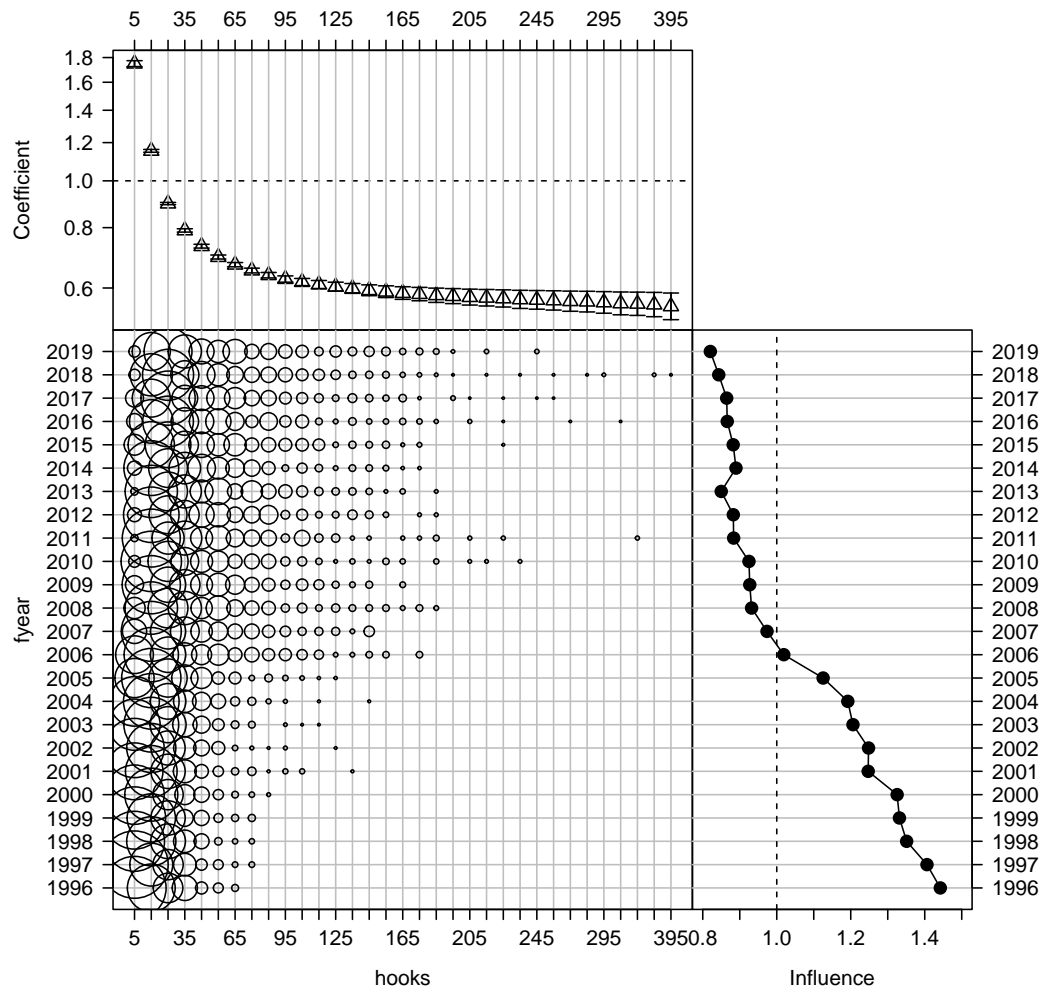


Figure B-83: Influence of number of hooks set per stratum for the AU low-latitude fleet (bubble plot; bubbles scales by effort) on CPUE; influence (right hand plot) shows the standardising effect (a positive effect reduces the standardised CPUE by the equivalent amount). Estimated coefficients are given in the top panel.

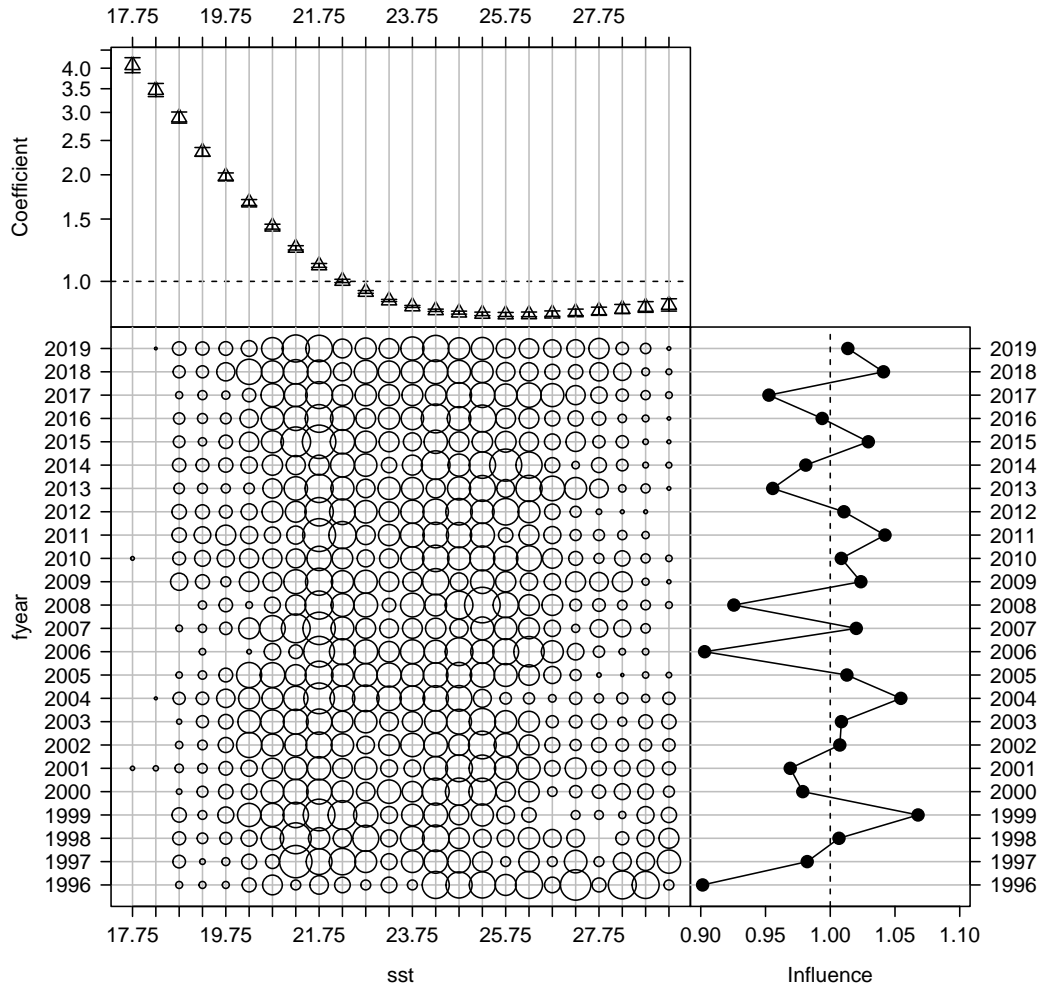


Figure B-84: Influence of sea surface temperature (SST, in degrees Celsius) for the AU low-latitude fleet (bubble plot; bubbles scales by effort) on CPUE; influence (right hand plot) shows the standardising effect (a positive effect reduces the standardised CPUE by the equivalent amount). Estimated coefficients are given in the top panel.

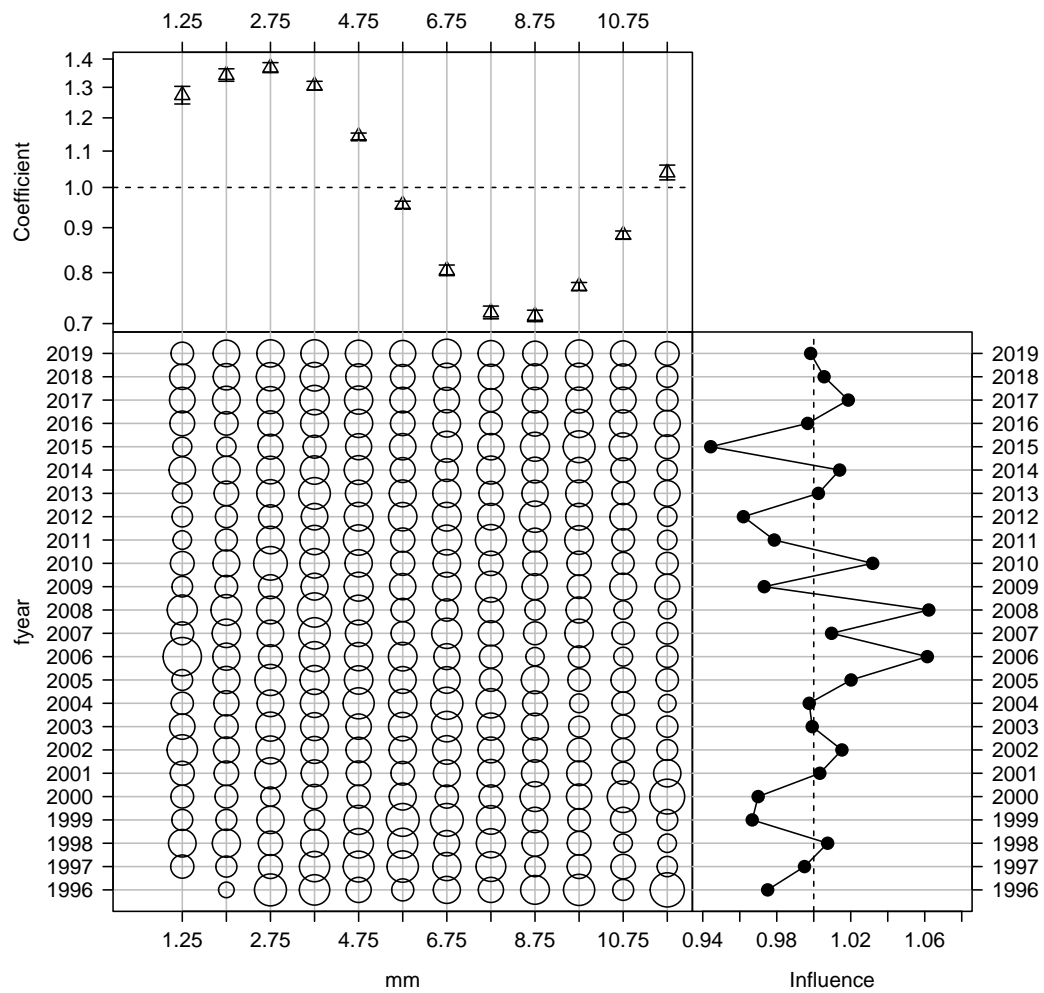


Figure B-85: Influence of month for the AU low - latitude fleet (bubble plot; bubbles scales by effort) on CPUE; influence (right hand plot) shows the standardising effect (a positive effect reduces the standardised CPUE by the equivalent amount). Estimated coefficients are given in the top panel.

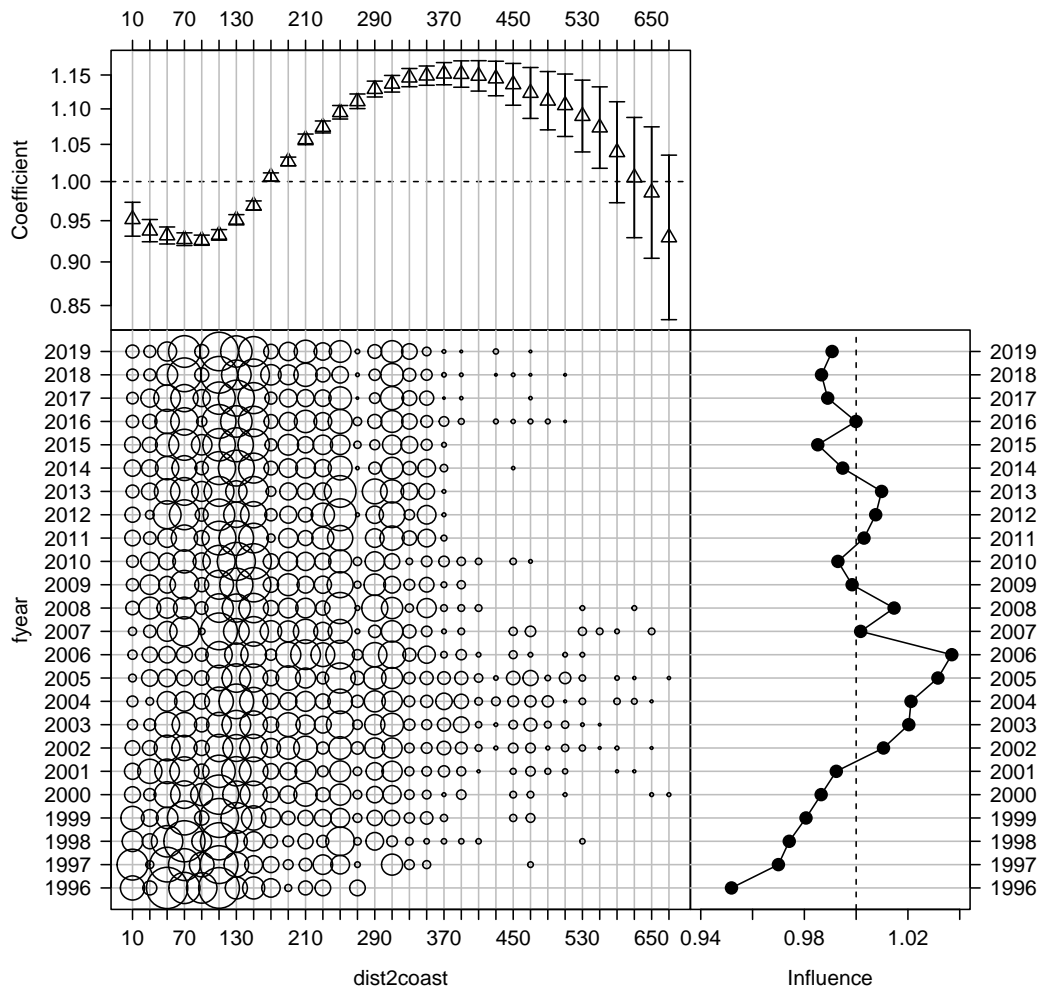


Figure B-86: Influence of distance to coast composition for the AU low-latitude fleet (bubble plot; bubbles scales by effort) on CPUE; influence (right hand plot) shows the standardising effect (a positive effect reduces the standardised CPUE by the equivalent amount). Estimated coefficients are given in the top panel.

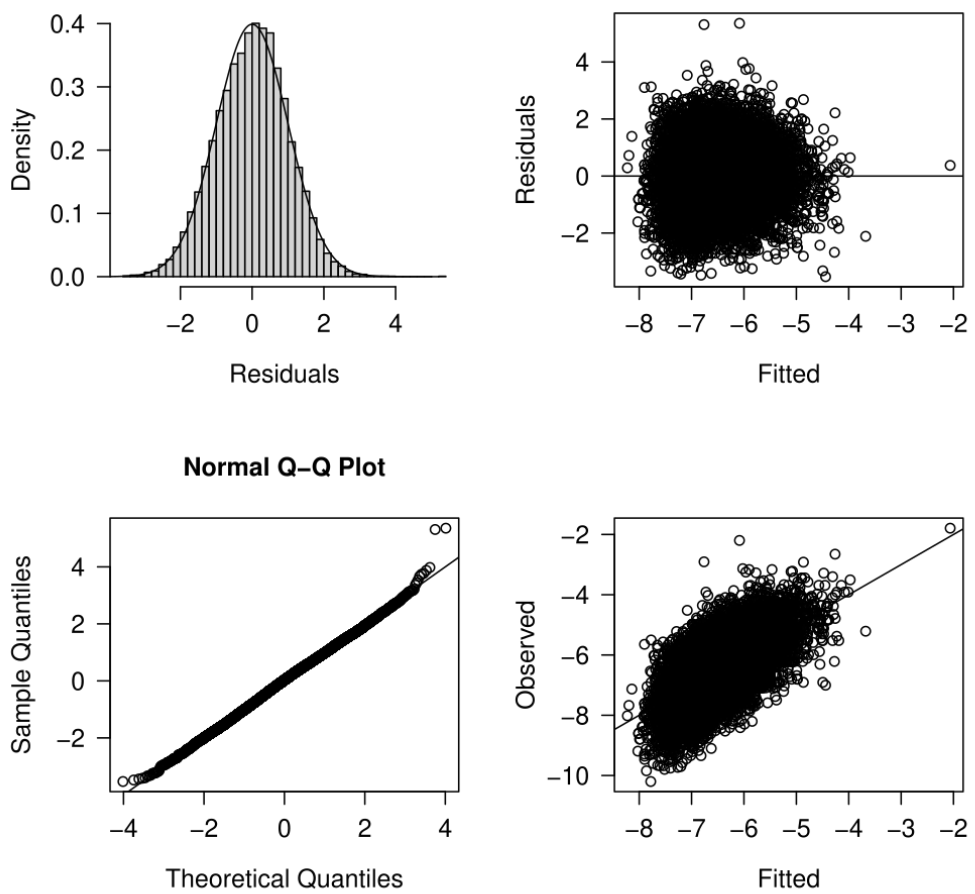


Figure B-87: Diagnostics for the log-normal CPUE standardisation model for AU low-latitude fleet strata with positive catch.

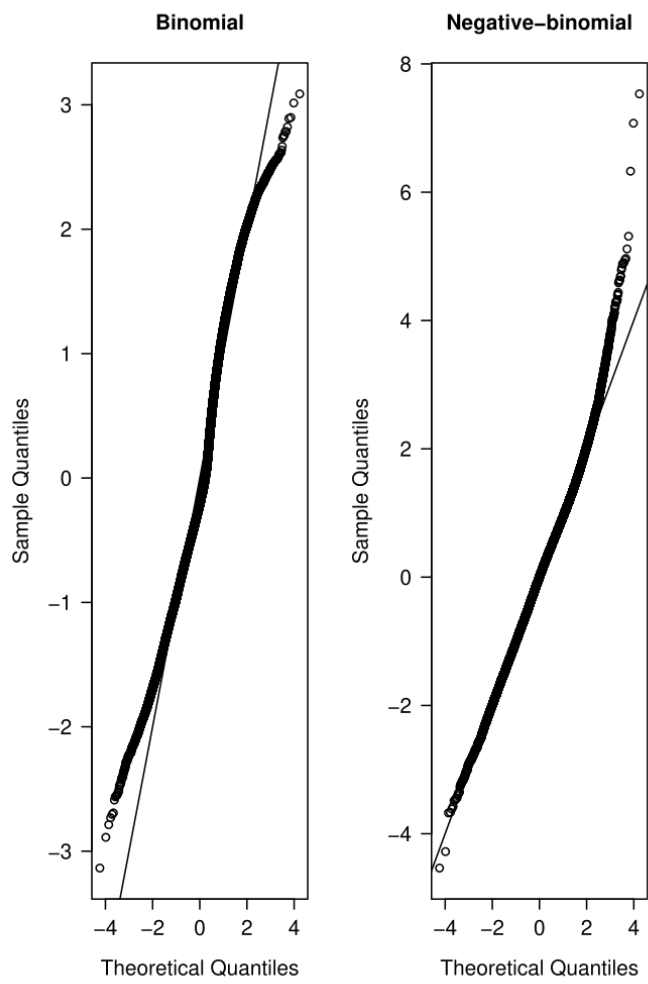


Figure B-88: Quantile residual diagnostics for the binomial component, as well as alternative CPUE standardisation models for AU low-latitude fleet strata with positive catch.

B.4.3 Australian high latitude CPUE

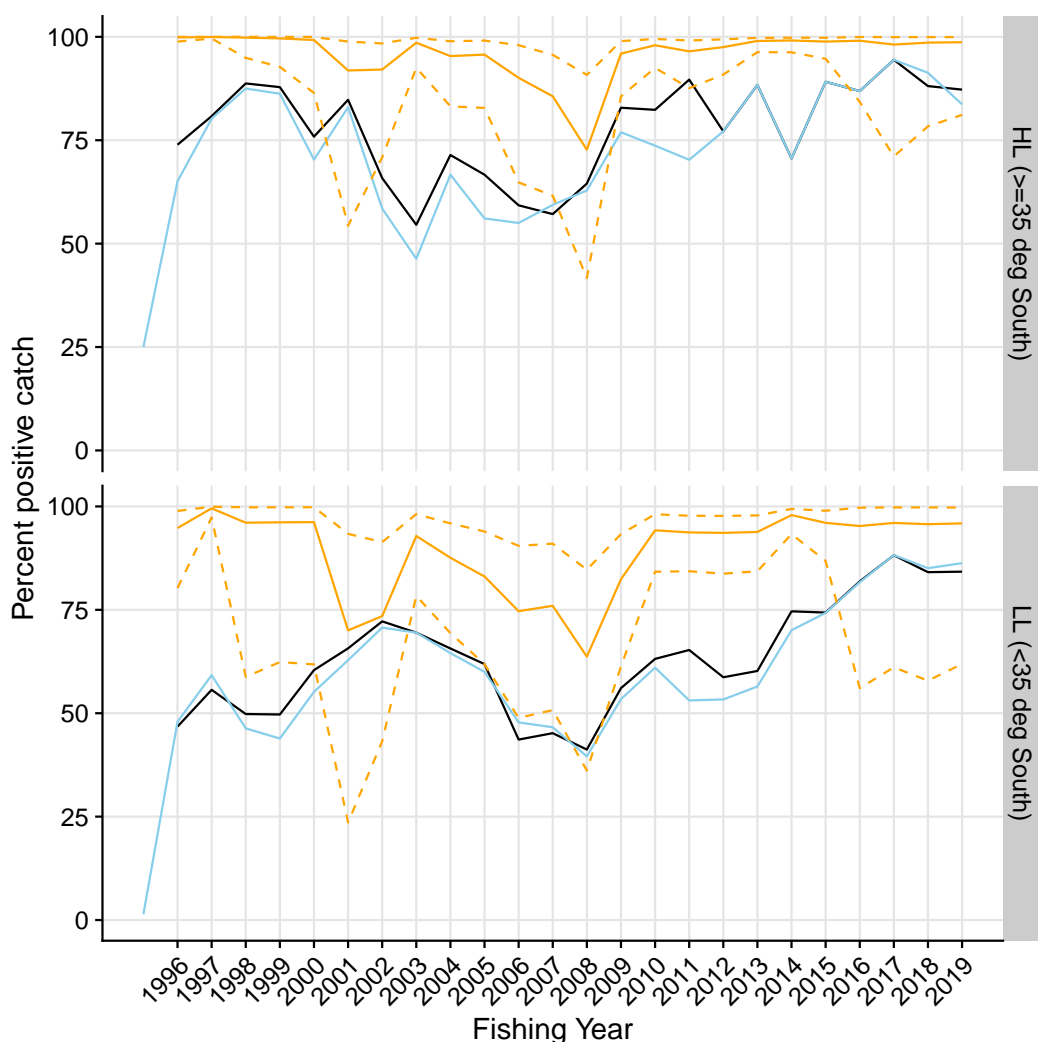


Figure B-89: Proportion of strata for the AU high latitude fleet with positive catch by latitudinal stratum. Light blue are initial log-sheet records prior to filtering, the black line is the retained dataset after filtering for consistently reporting vessels. Where available, the corresponding values from observed strata is shown in orange.

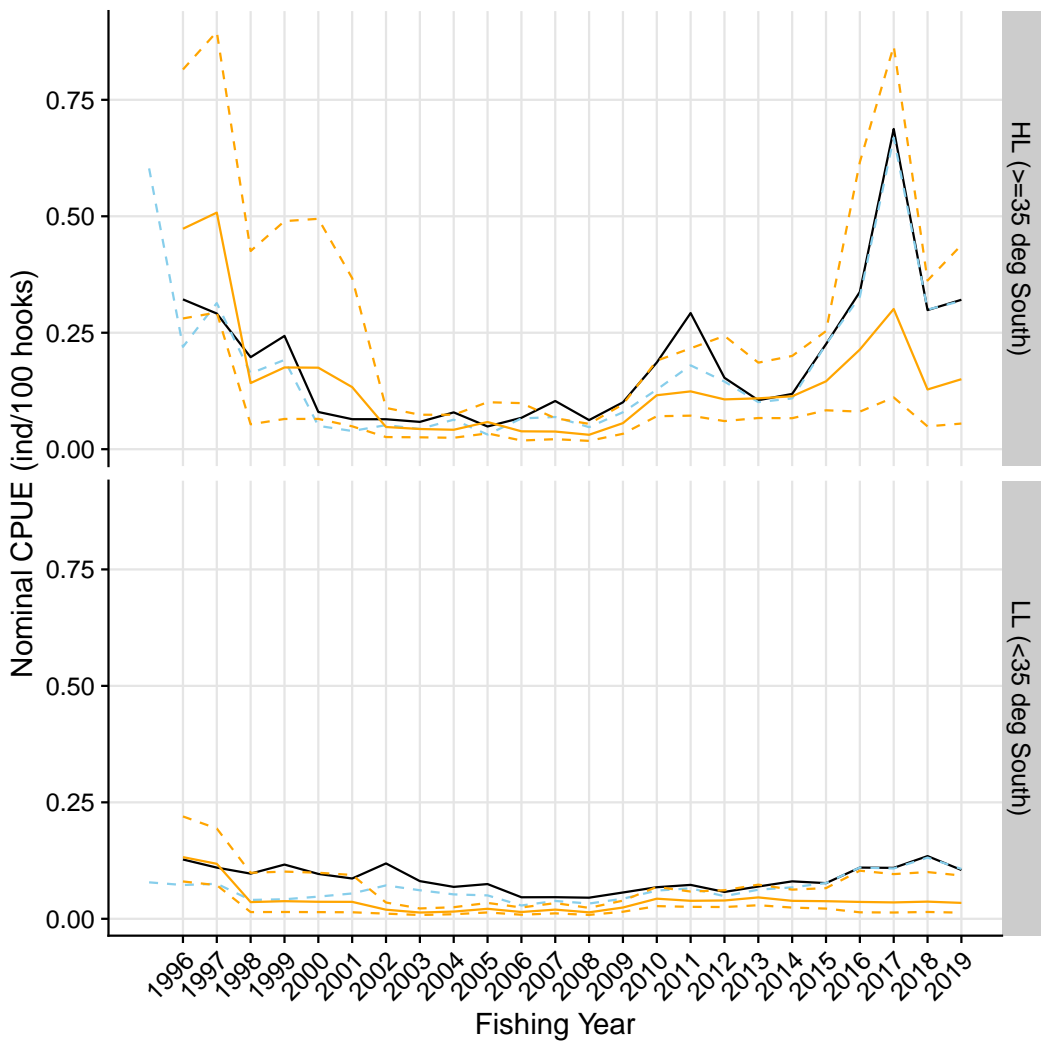


Figure B-90: Nominal CPUE (in number of blue shark per 100 hooks) strata of the AU high latitude fleet with positive catch by latitudinal stratum. Light blue are initial log-sheet records prior to filtering, the black line is the retained dataset after filtering for consistently reporting vessels. Where available, the corresponding values from observed strata is shown in orange.

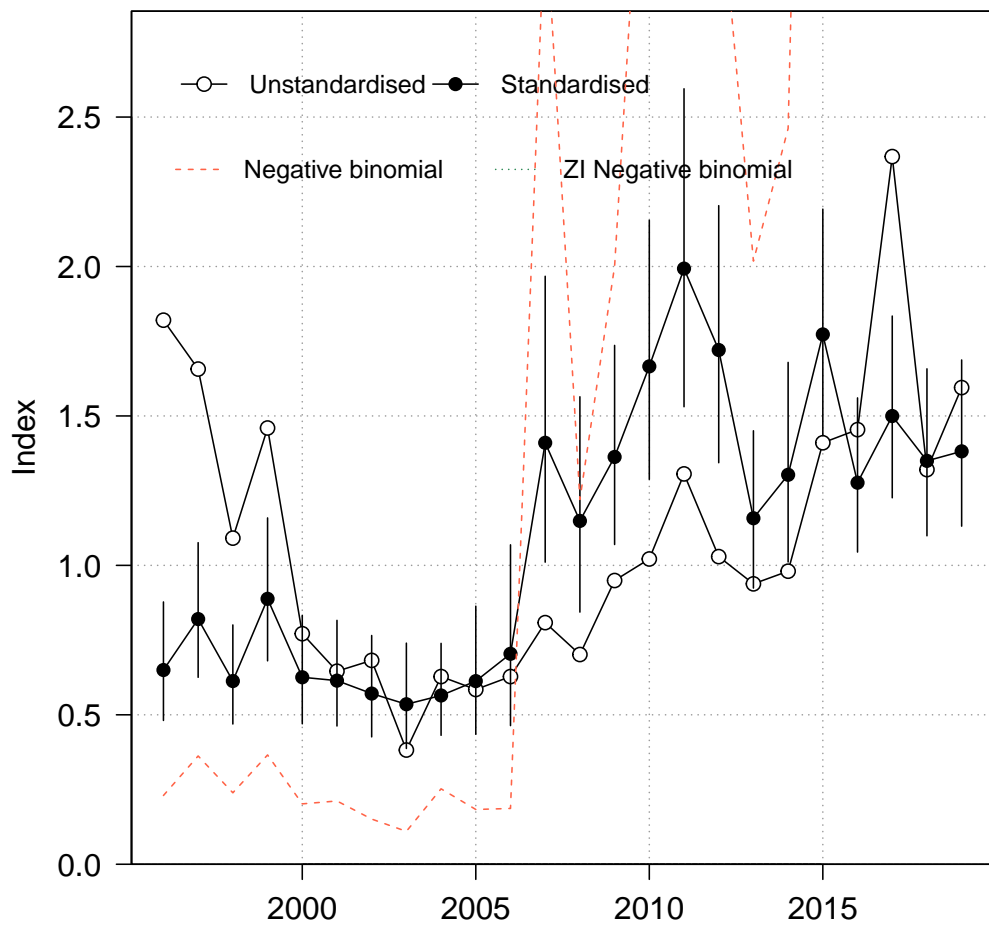


Figure B-91: Standardised (closed black circles with standard error) and unstandardised (open circles) CPUE indices for AU high latitude fleet strata with positive catch. Where successful (i.e., converged), standardised trends from a negative - binomial and zero - inflated negative binomial model run over the full dataset (including strata with zero values) are also shown for comparison.

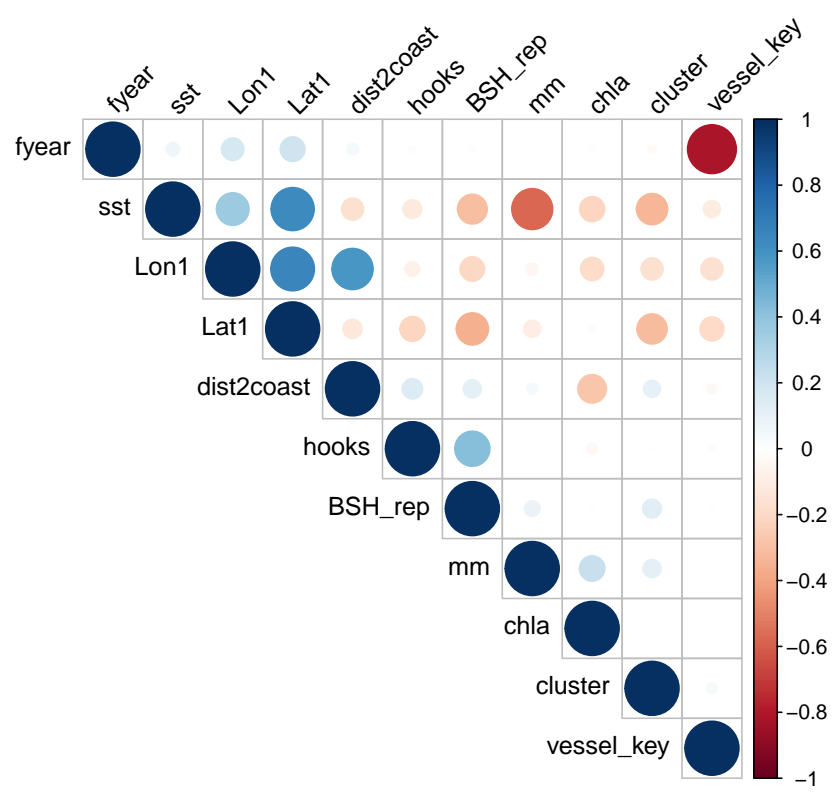


Figure B-92: Correlations amongst potential covariates for CPUE standardisation in the AU high latitude fleet. Where necessary, variables were removed to reduce redundancy in the models.

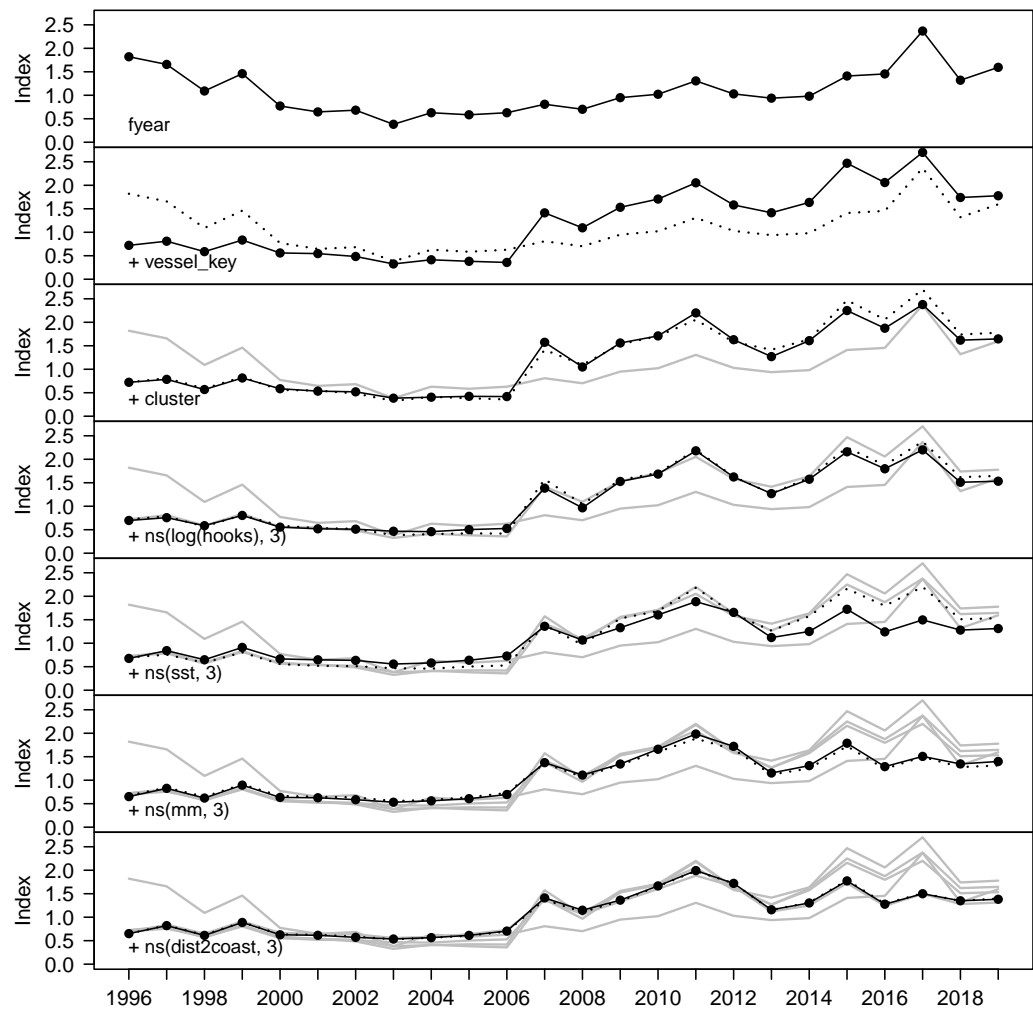


Figure B-93: Step plot for the AU high latitude fleet CPUE, showing sequential standardising effects of variables included in the standardisation model.

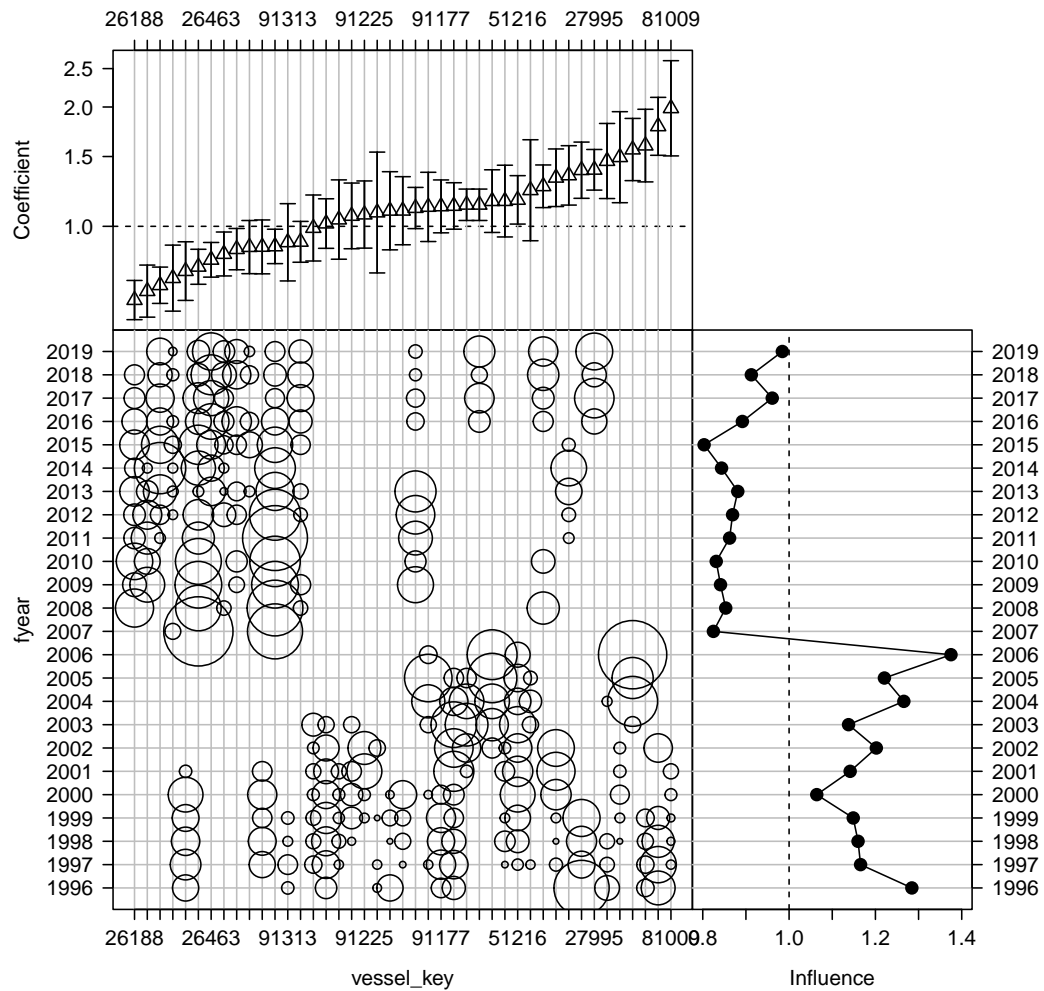


Figure B-94: Influence of fleet composition (vessel keys) for the AU high latitude fleet (bubble plot; bubbles scales by effort) on CPUE; influence (right hand plot) shows the standardising effect (a positive effect reduces the standardised CPUE by the equivalent amount). Estimated coefficients are given in the top panel.

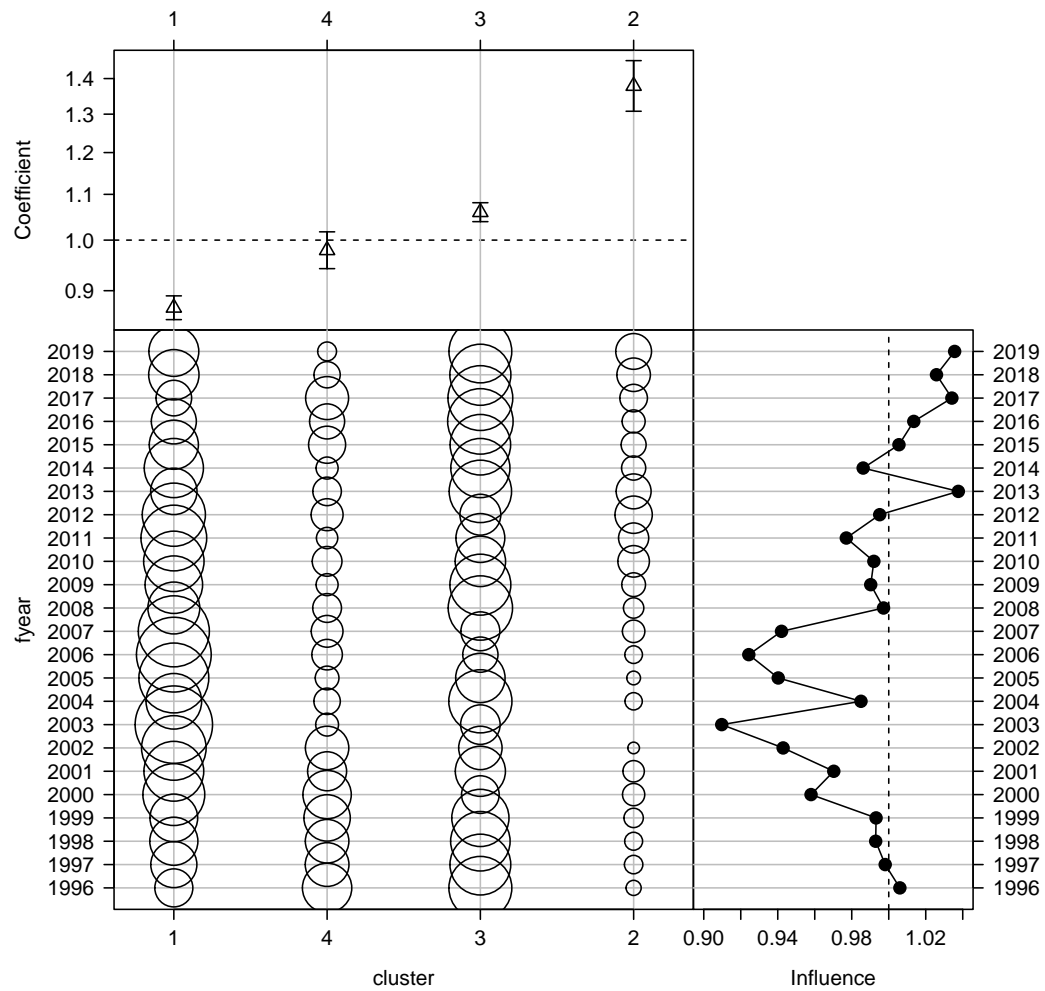


Figure B-95: Influence of targeting cluster for the AU high latitude fleet (bubble plot; bubbles scales by effort) on CPUE; influence (right hand plot) shows the standardising effect (a positive effect reduces the standardised CPUE by the equivalent amount). Estimated coefficients are given in the top panel.

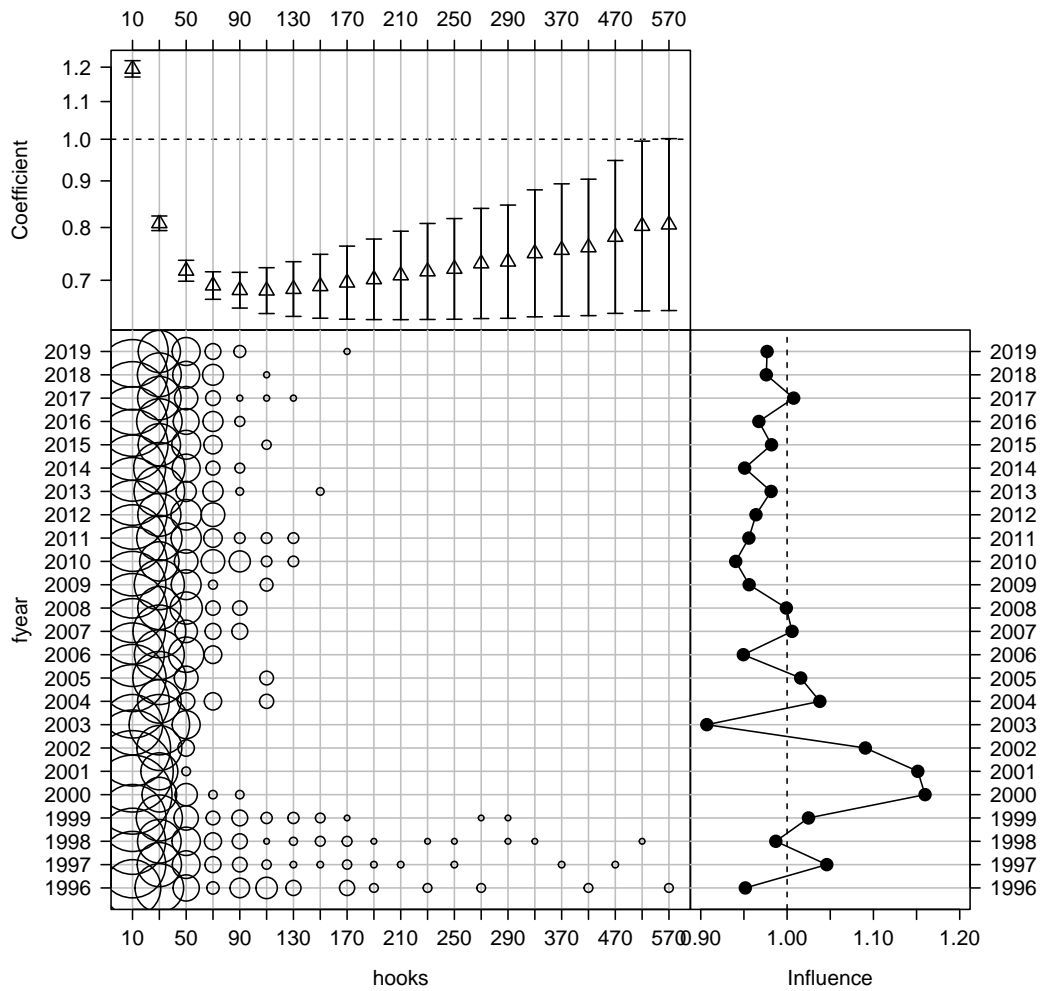


Figure B-96: Influence of number of hooks set per stratum for the AU high latitude fleet (bubble plot; bubbles scales by effort) on CPUE; influence (right hand plot) shows the standardising effect (a positive effect reduces the standardised CPUE by the equivalent amount). Estimated coefficients are given in the top panel.

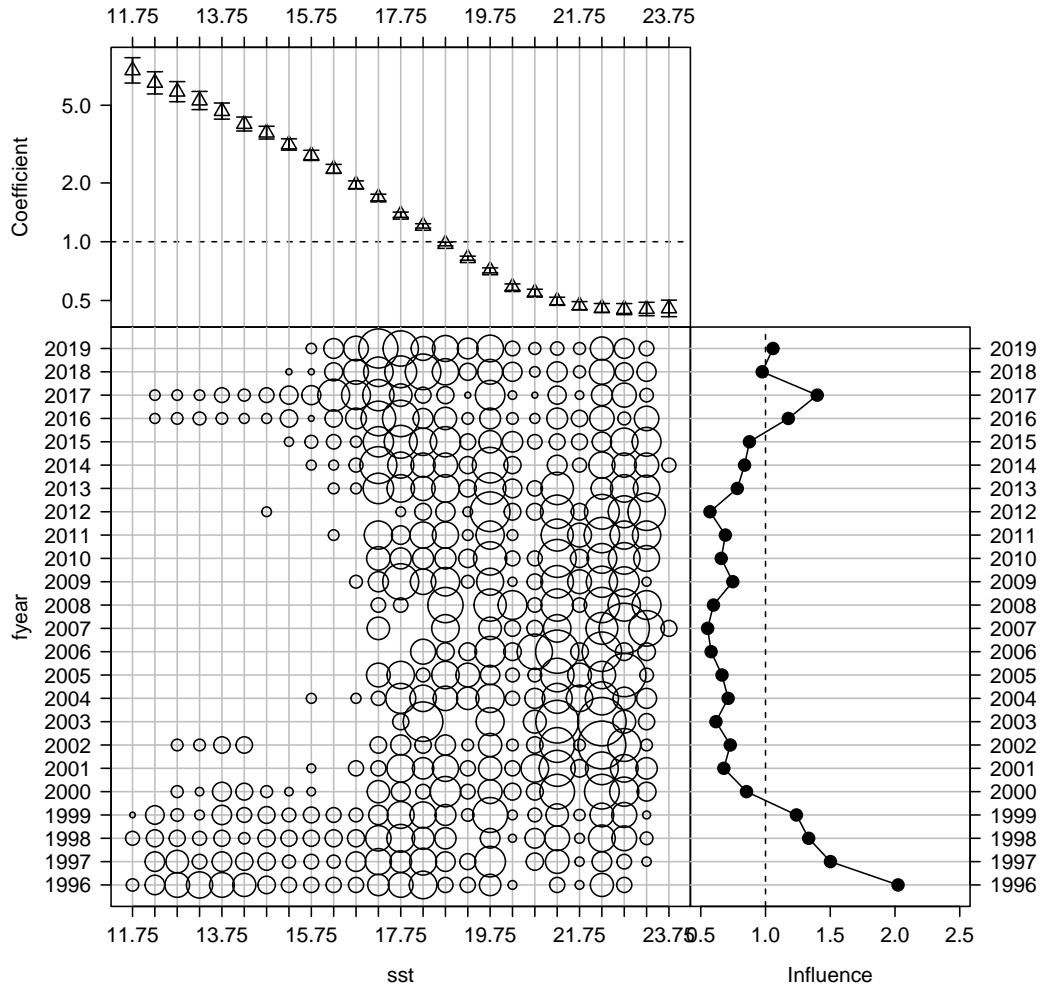


Figure B-97: Influence of sea surface temperature (SST, in degrees Celsius) for the AU high latitude fleet (bubble plot; bubbles scales by effort) on CPUE; influence (right hand plot) shows the standardising effect (a positive effect reduces the standardised CPUE by the equivalent amount). Estimated coefficients are given in the top panel.

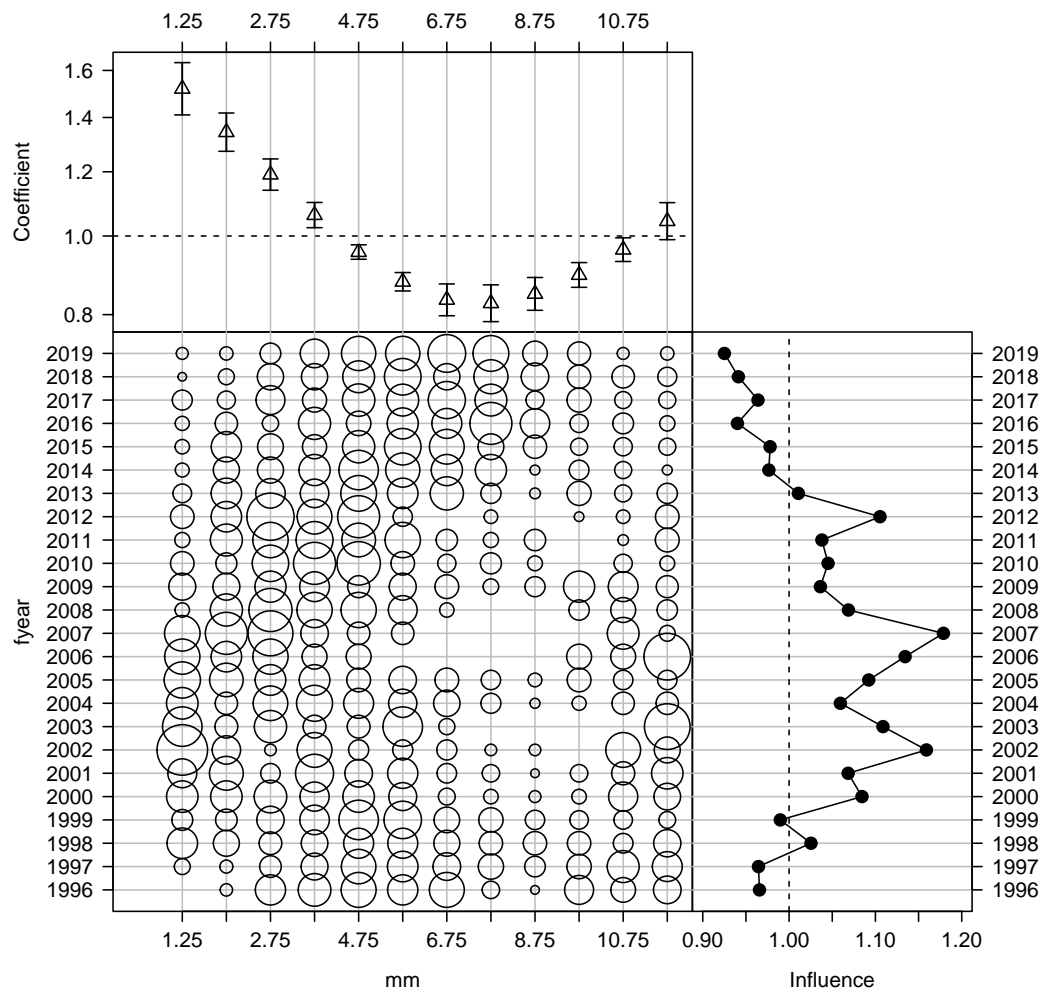


Figure B-98: Influence of month for the AU high latitude fleet (bubble plot; bubbles scales by effort) on CPUE; influence (right hand plot) shows the standardising effect (a positive effect reduces the standardised CPUE by the equivalent amount). Estimated coefficients are given in the top panel.

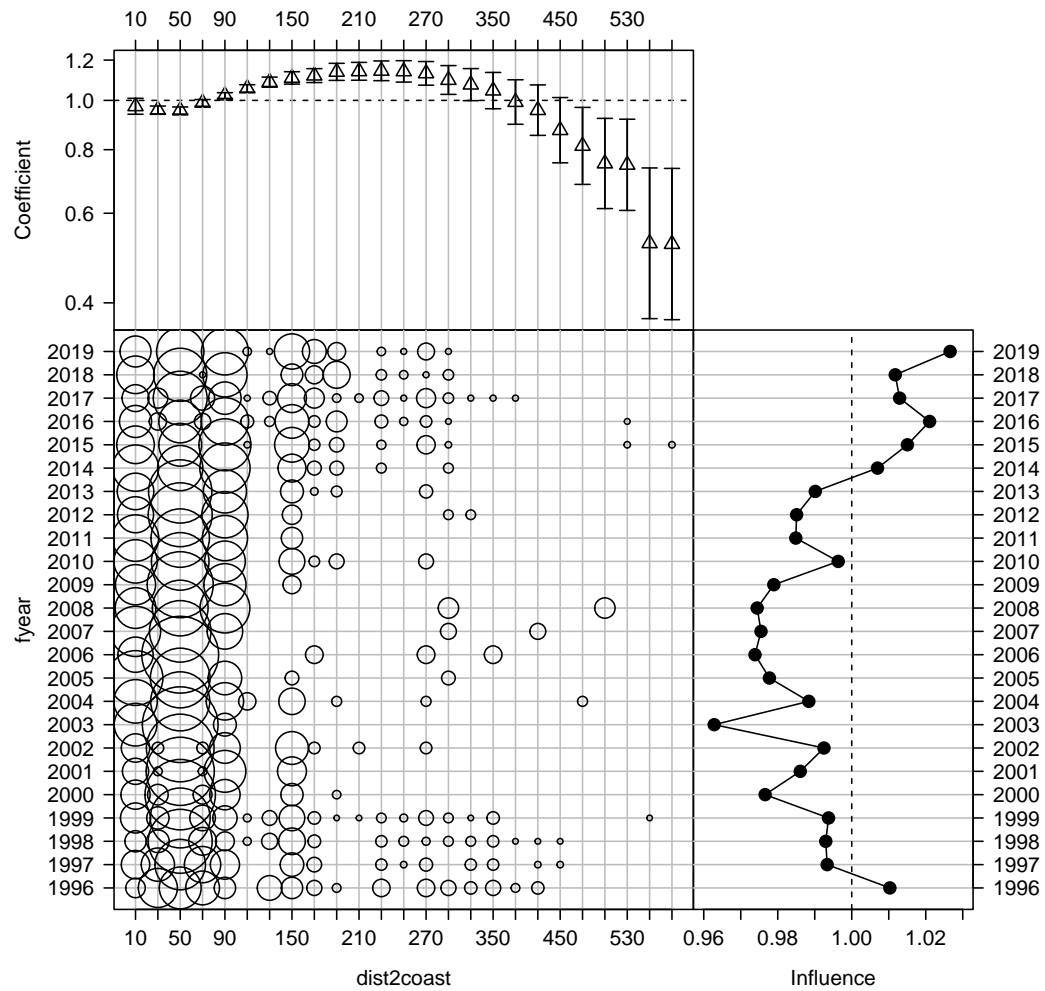


Figure B-99: Influence of distance to coast composition for the AU high latitude fleet (bubble plot; bubbles scales by effort) on CPUE; influence (right hand plot) shows the standardising effect (a positive effect reduces the standardised CPUE by the equivalent amount). Estimated coefficients are given in the top panel.

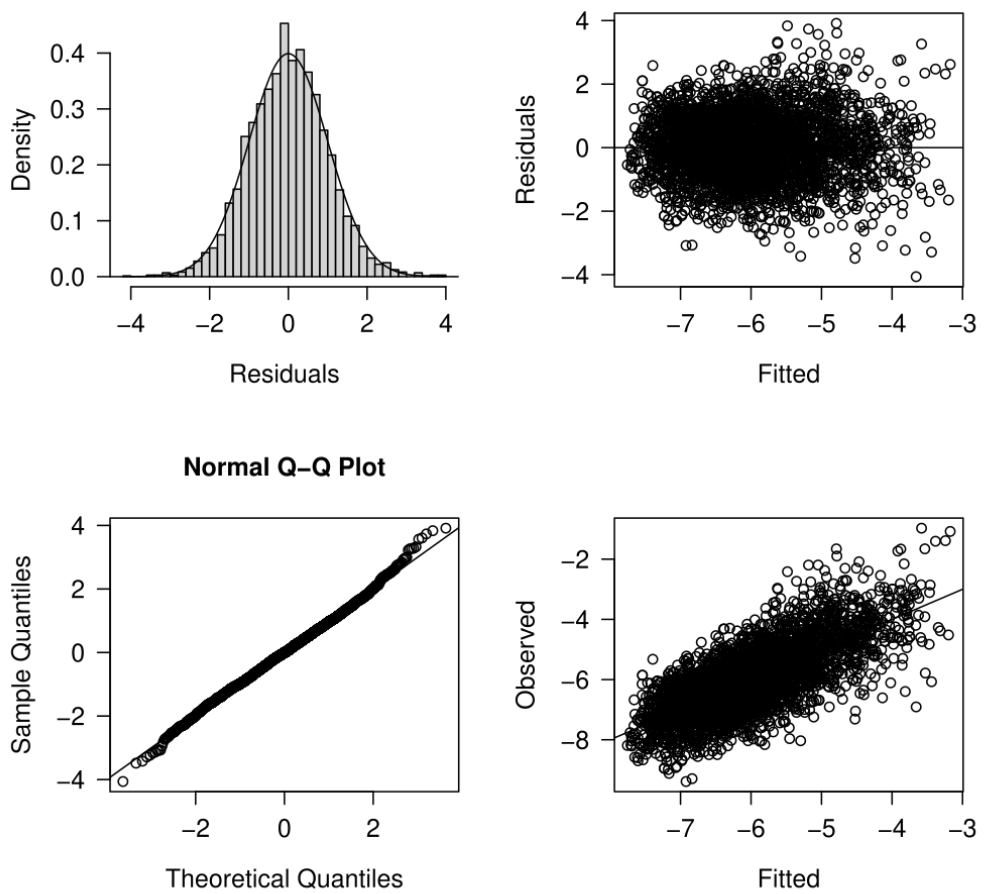


Figure B-100: Diagnostics for the log-normal CPUE standardisation model for AU high latitude fleet strata with positive catch.

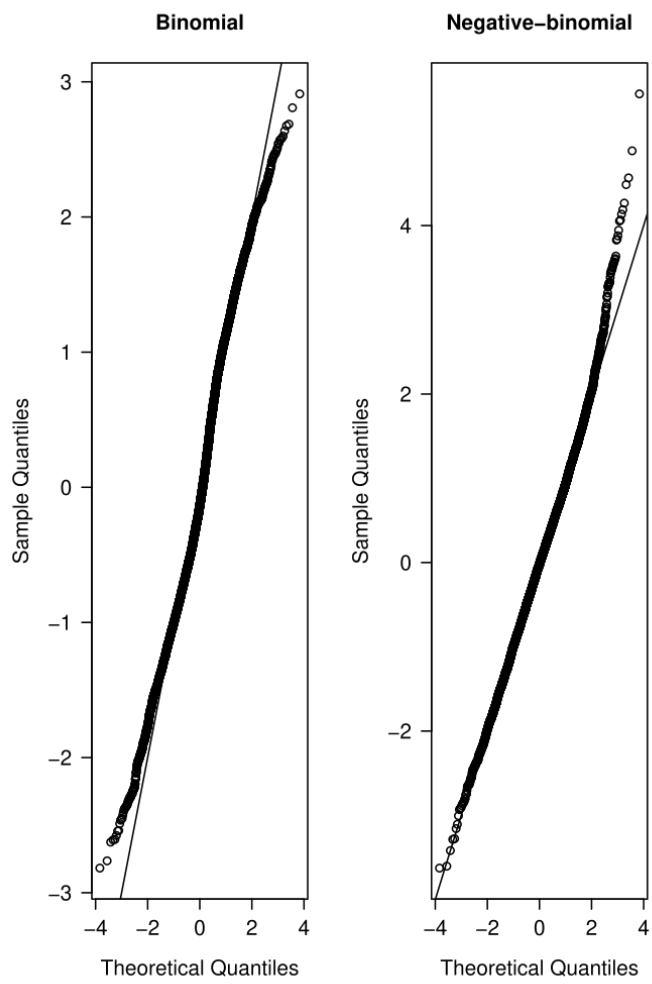


Figure B-101: Quantile residual diagnostics for the binomial component, as well as alternative CPUE standardisation models for AU high latitude fleet strata with positive catch.

B.4.4 Combined low latitude CPUE

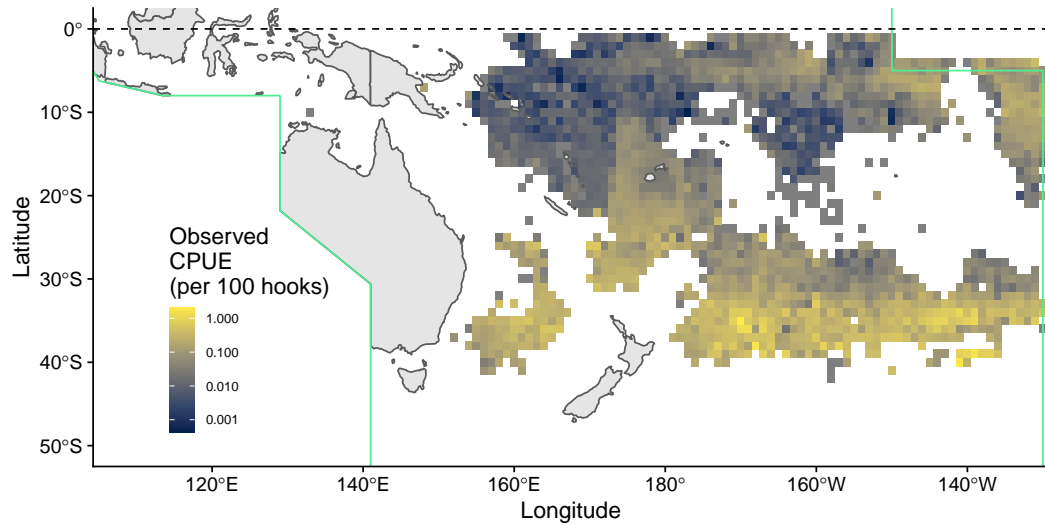


Figure B-102: Maps of average catch rates (CPUE; in number of blue shark per 100 hooks) for the distant water longline fleet.

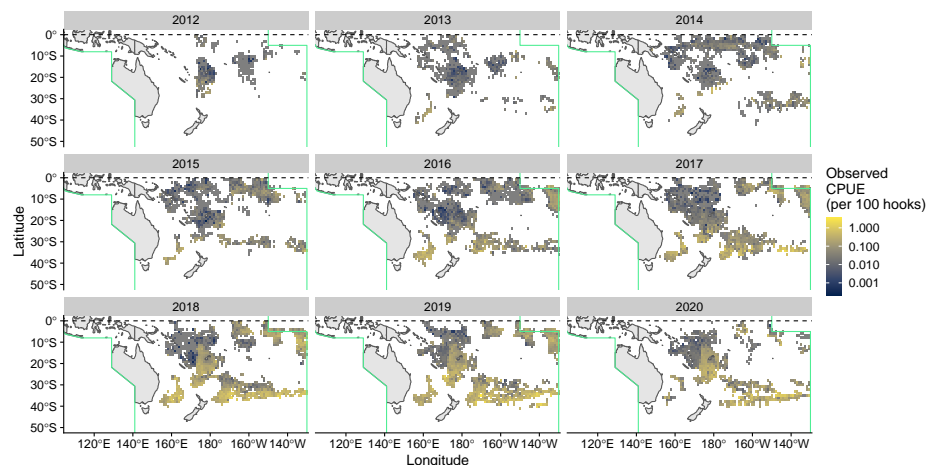


Figure B-103: Maps of average catch rates (CPUE; in number of blue shark per 100 hooks) by year for the distant water longline fleet.

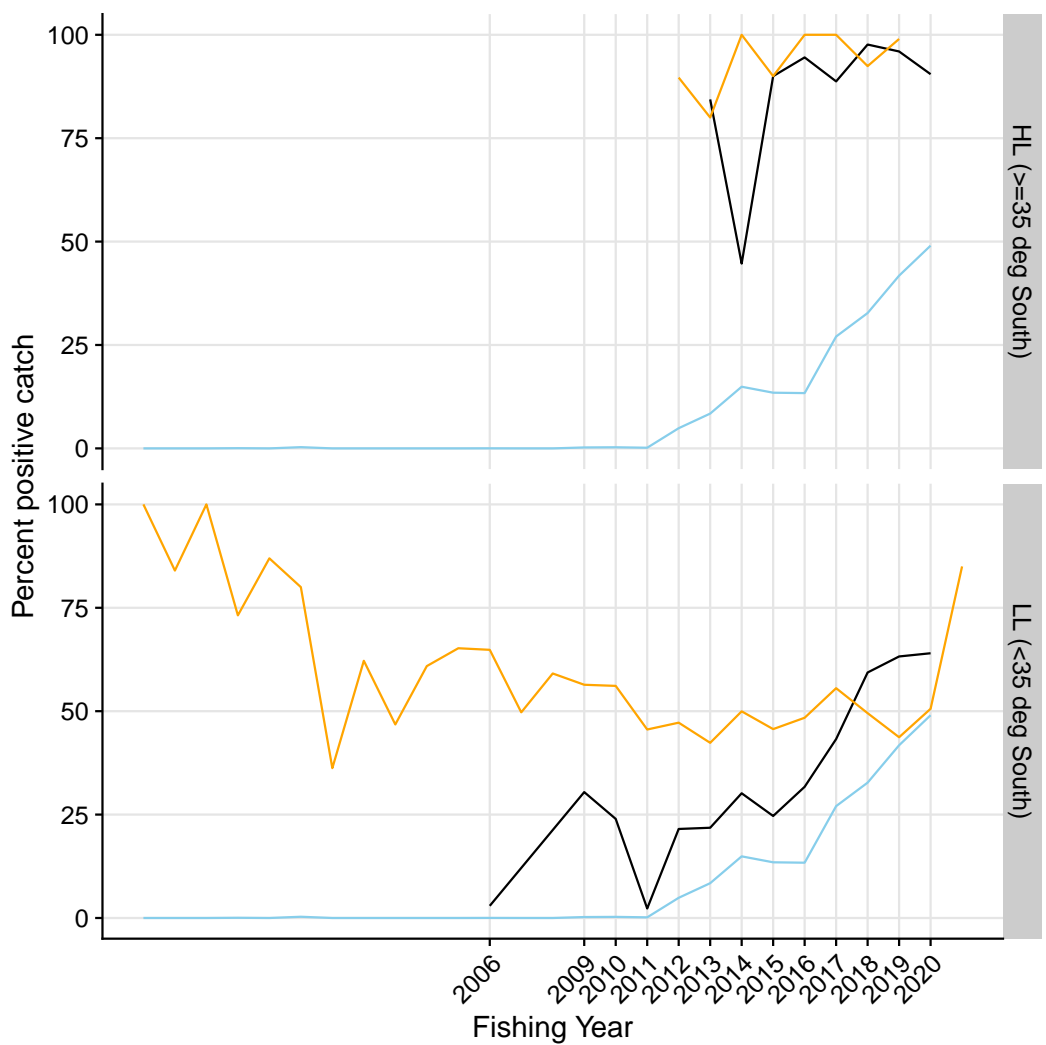


Figure B-104: Proportion of strata for the combined DW low-latitudes (<35 degree South) fleet with positive catch by latitudinal stratum. Light blue are initial log-sheet records prior to filtering, the black line is the retained dataset after filtering for consistently reporting vessels. Where available, the corresponding values from observed strata is shown in orange.

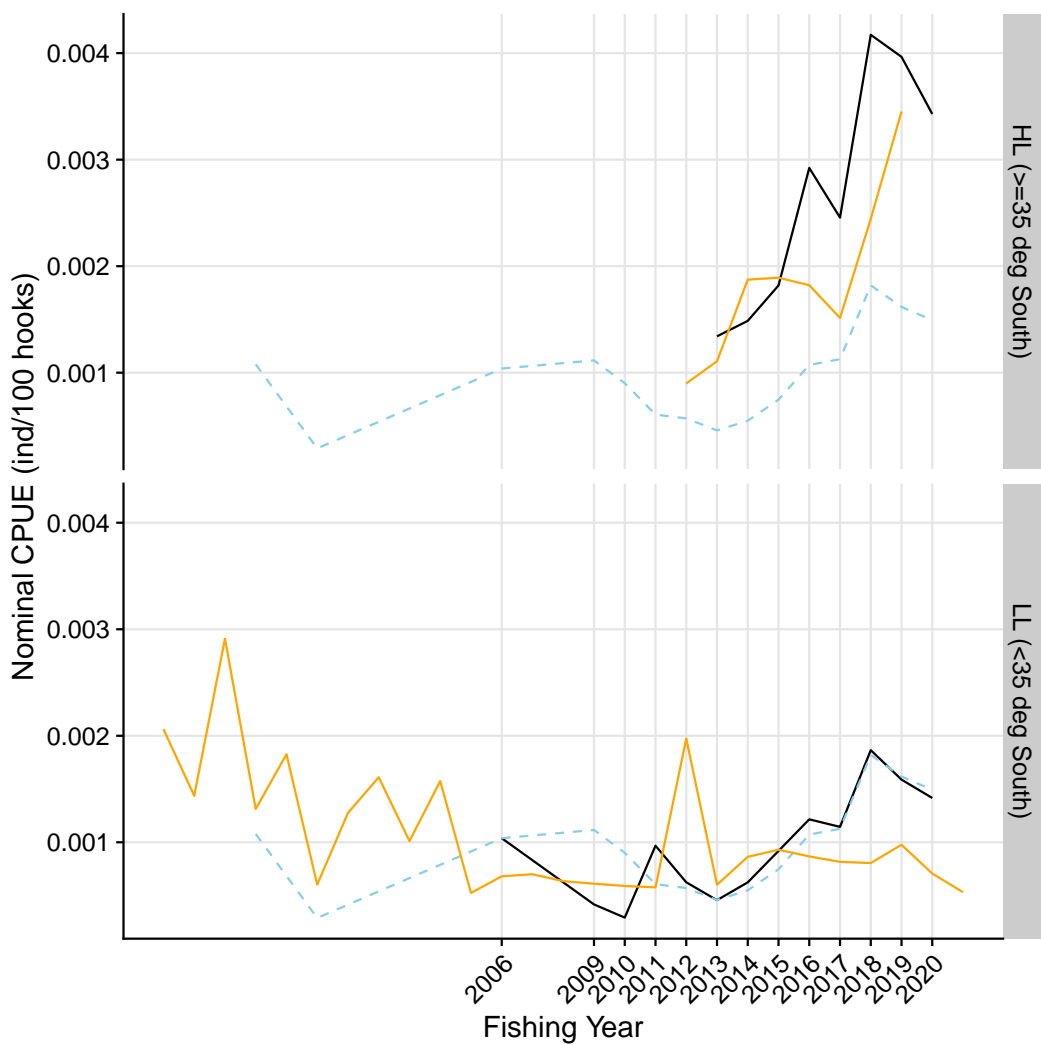


Figure B-105: Nominal CPUE (in number of blue shark per 100 hooks) strata of the combined DW low-latitudes (<35 degree South) fleet with positive catch by latitudinal stratum. Light blue are initial log-sheet records prior to filtering, the black line is the retained dataset after filtering for consistently reporting vessels. Where available, the corresponding values from observed strata is shown in orange.

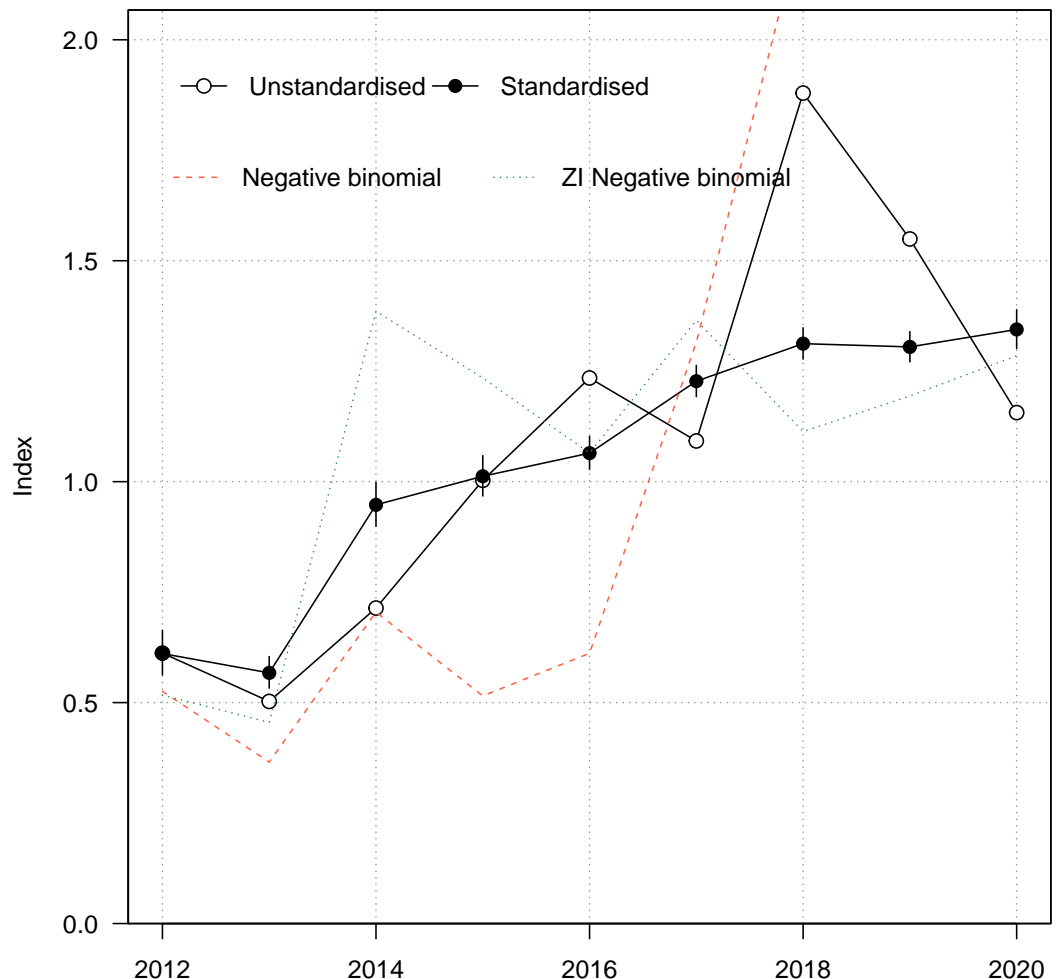


Figure B-106: Standardised (closed black circles with standard error) and unstandardised (open circles) CPUE indices for combined DW low-latitudes (<35 degree South) fleet strata with positive catch. Where successful (i.e., converged), standardised trends from a negative-binomial and zero-inflated negative binomial model run over the full dataset (including strata with zero values) are also shown for comparison.

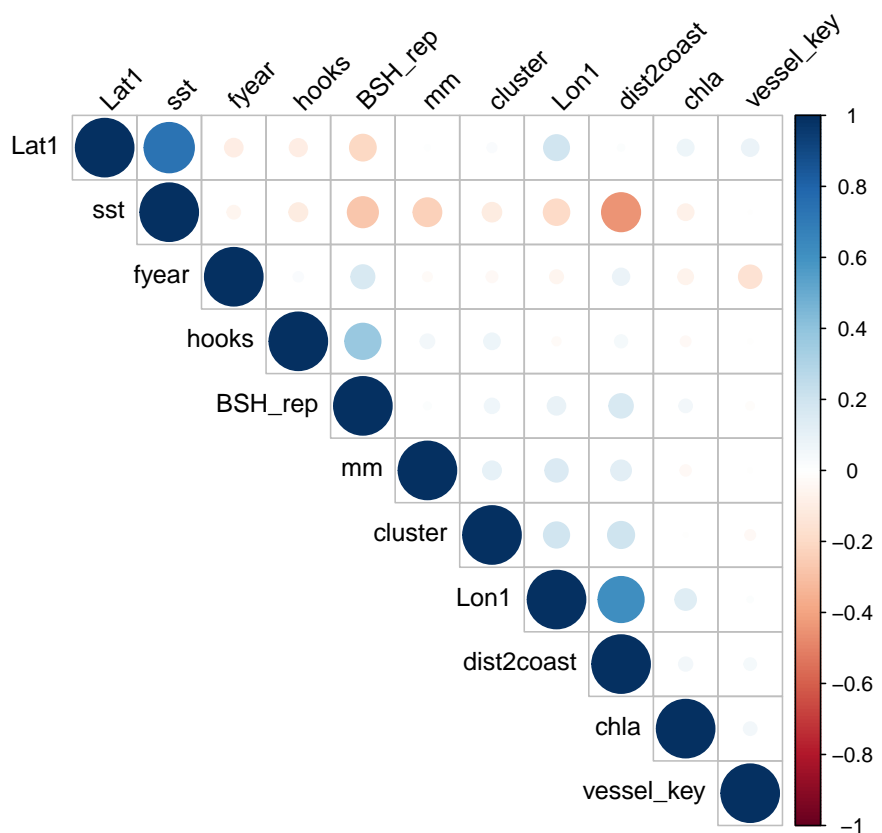


Figure B-107: Correlations amongst potential covariates for CPUE standardisation in the combined DW low-latitudes (<35 degree South) fleet. Where necessary, variables were removed to reduce redundancy in the models.

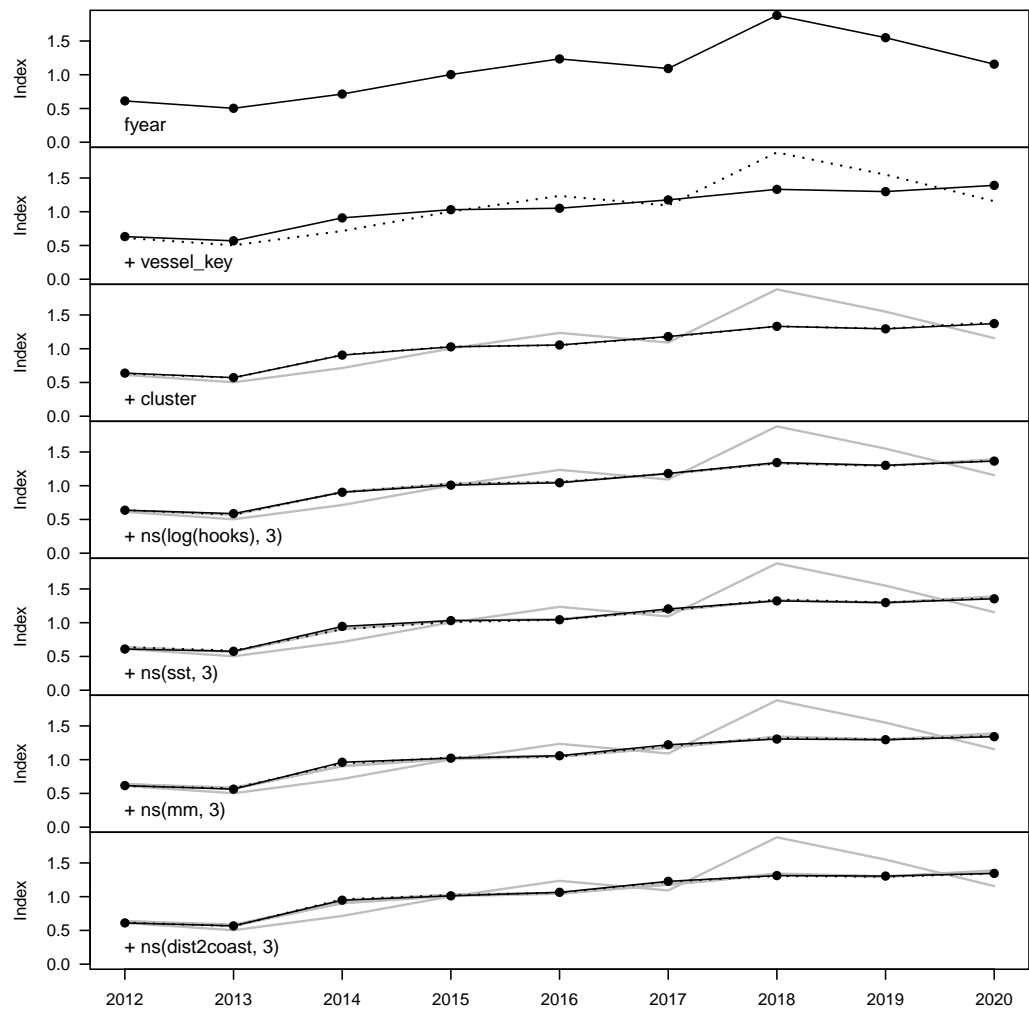


Figure B-108: Step plot for the combined DW low-latitudes (<35 degree South) fleet CPUE, showing sequential standardising effects of variables included in the standardisation model.

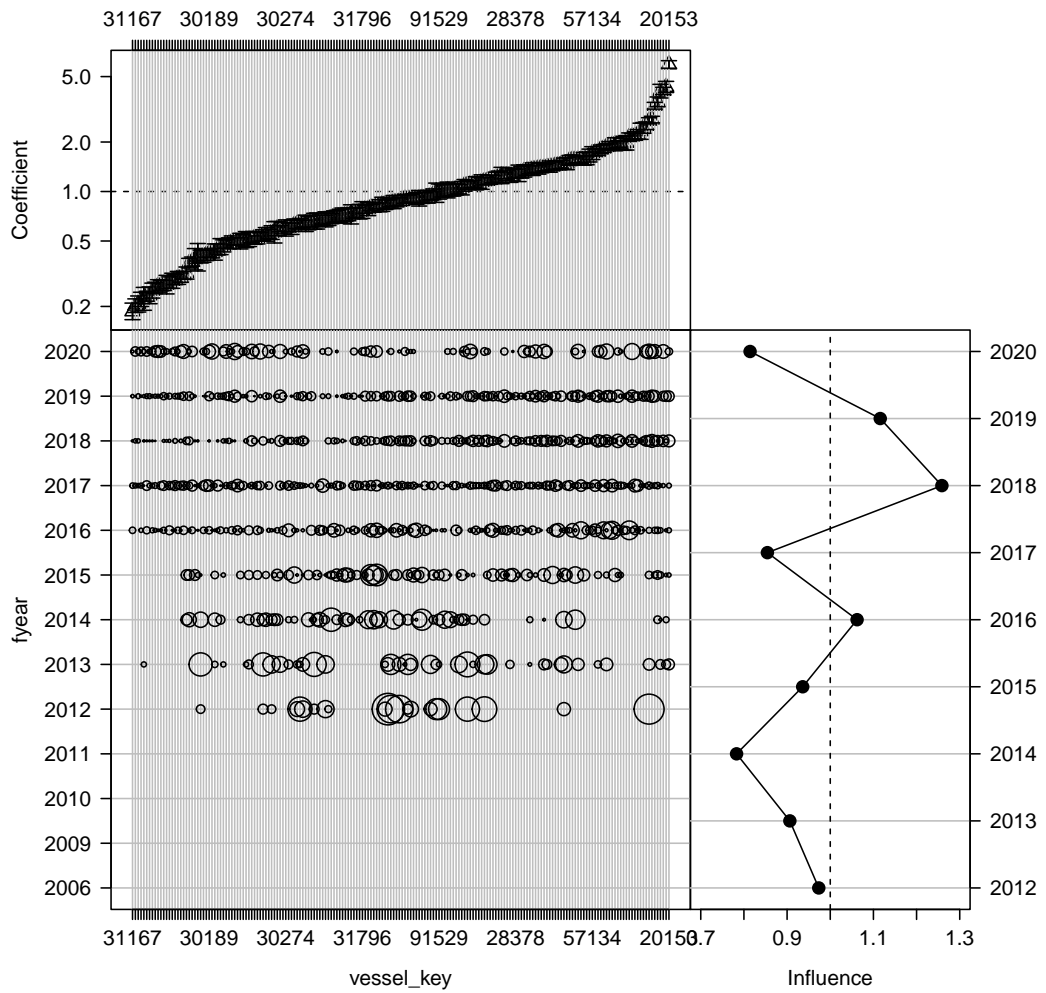


Figure B-109: Influence of fleet composition (vessel keys) for the combined DW low - latitudes (<35 degree South) fleet (bubble plot; bubbles scales by effort) on CPUE; influence (right hand plot) shows the standardising effect (a positive effect reduces the standardised CPUE by the equivalent amount). Estimated coefficients are given in the top panel.

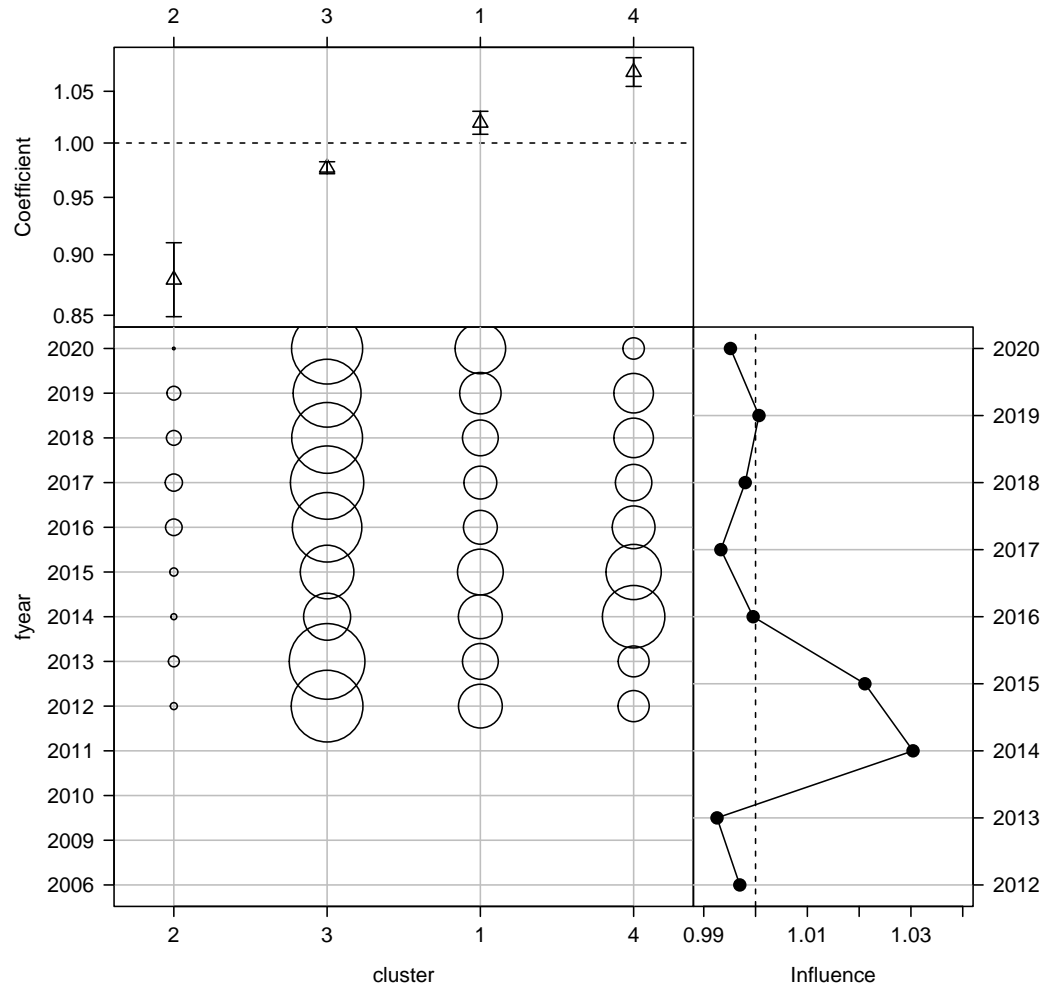


Figure B-110: Influence of targeting cluster for the combined DW low-latitudes (<35 degree South) fleet (bubble plot; bubbles scales by effort) on CPUE; influence (right hand plot) shows the standardising effect (a positive effect reduces the standardised CPUE by the equivalent amount). Estimated coefficients are given in the top panel.

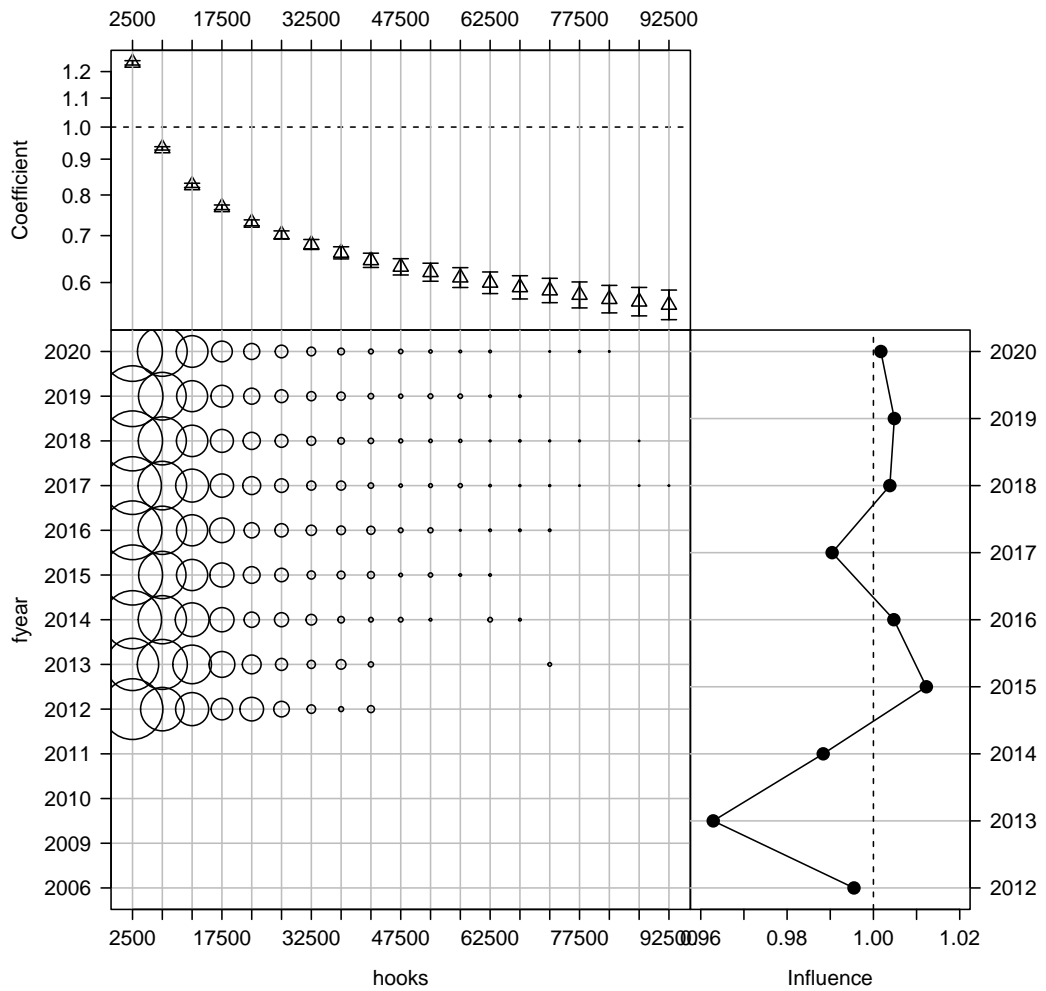


Figure B-111: Influence of number of hooks set per stratum for the combined DW low-latitudes (<35 degree South) fleet (bubble plot; bubbles scales by effort) on CPUE; influence (right hand plot) shows the standardising effect (a positive effect reduces the standardised CPUE by the equivalent amount). Estimated coefficients are given in the top panel.

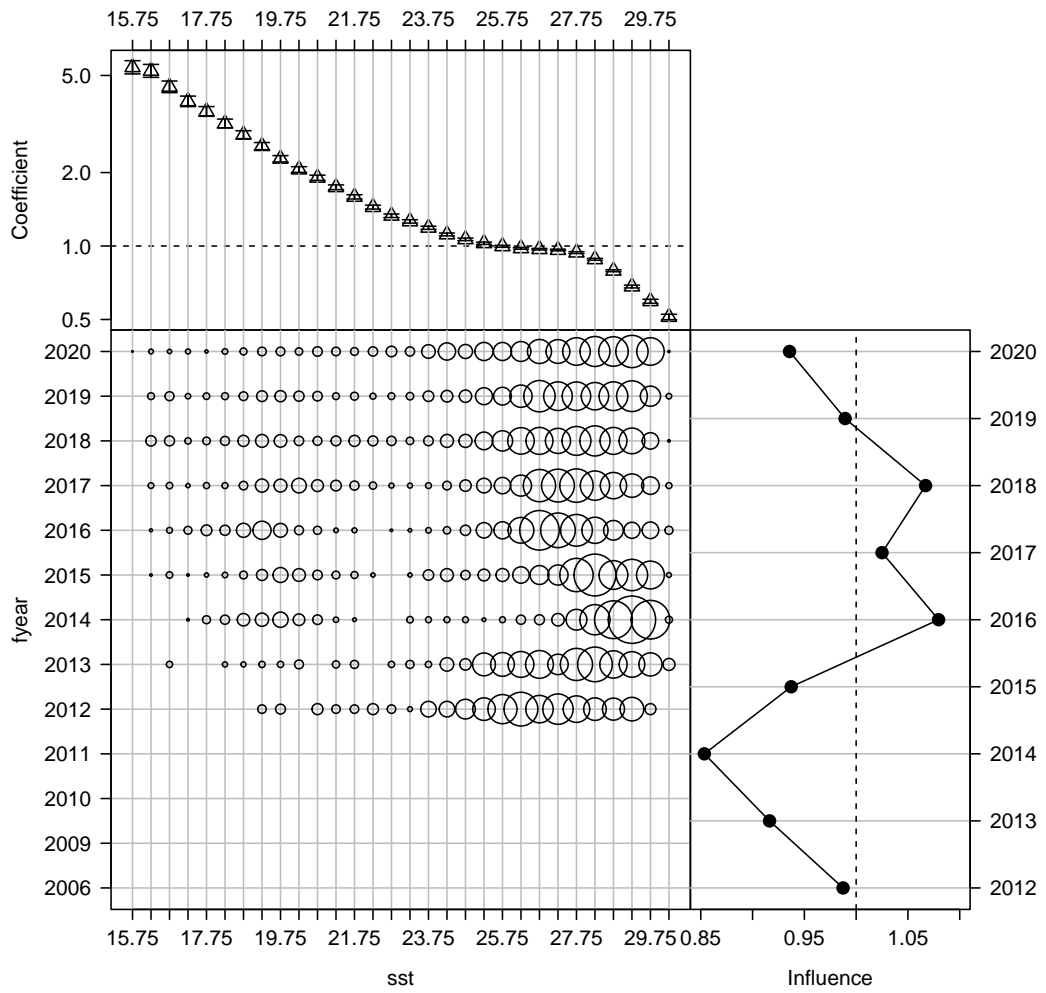


Figure B-112: Influence of sea surface temperature (SST, in degrees Celsius) for the combined DW low-latitudes (<35 degree South) fleet (bubble plot; bubbles scales by effort) on CPUE; influence (right hand plot) shows the standardising effect (a positive effect reduces the standardised CPUE by the equivalent amount). Estimated coefficients are given in the top panel.

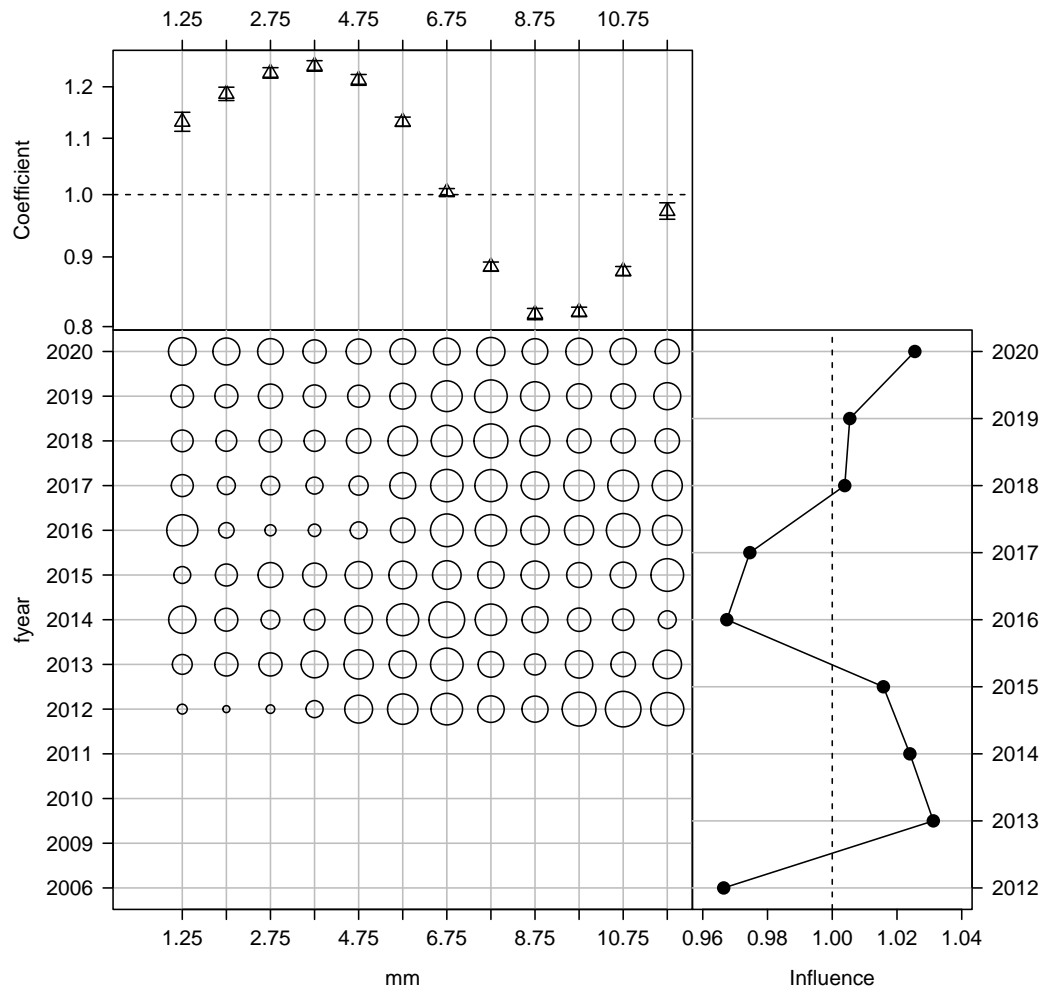


Figure B-113: Influence of month for the combined DW low-latitudes (<35 degree South) fleet (bubble plot; bubbles scales by effort) on CPUE; influence (right hand plot) shows the standardising effect (a positive effect reduces the standardised CPUE by the equivalent amount). Estimated coefficients are given in the top panel.

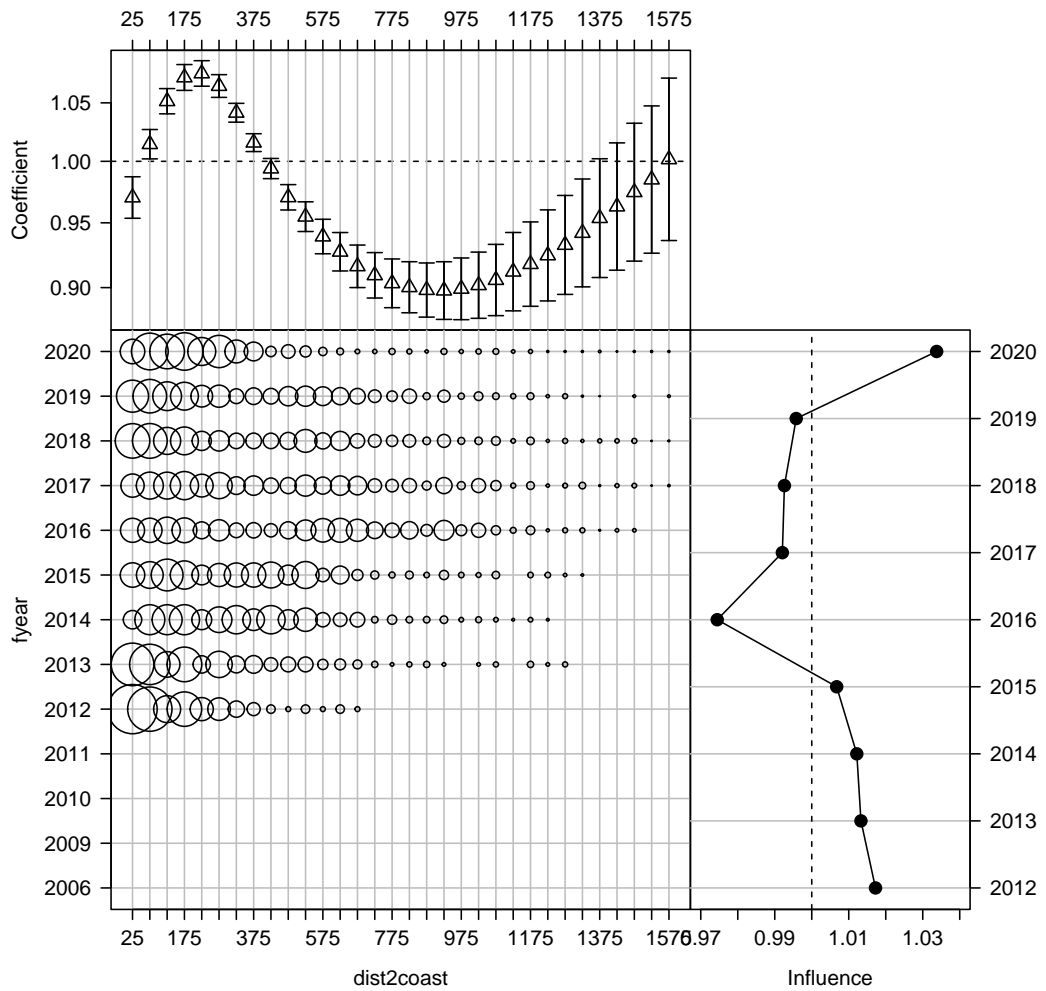


Figure B-114: Influence of distance to coast composition for the combined DW low-latitudes (<35 degree South) fleet (bubble plot; bubbles scales by effort) on CPUE; influence (right hand plot) shows the standardising effect (a positive effect reduces the standardised CPUE by the equivalent amount). Estimated coefficients are given in the top panel.

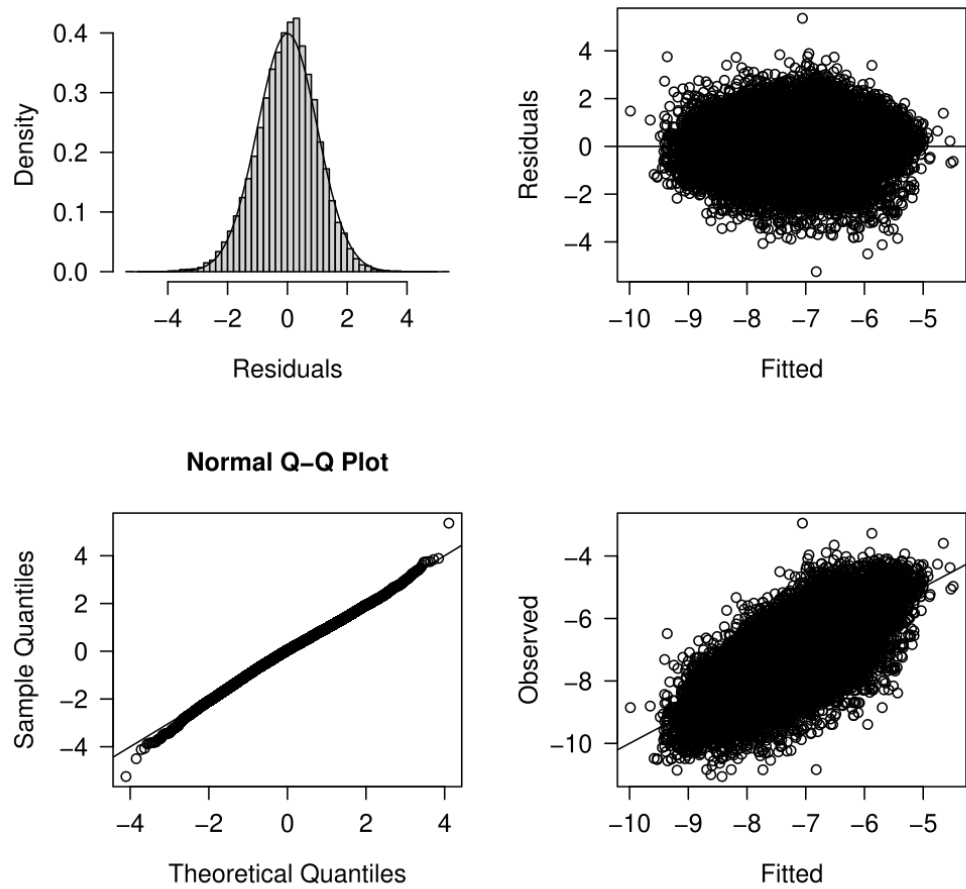


Figure B-115: Diagnostics for the log-normal CPUE standardisation model for combined DW low-latitudes (<35 degree South) fleet strata with positive catch.

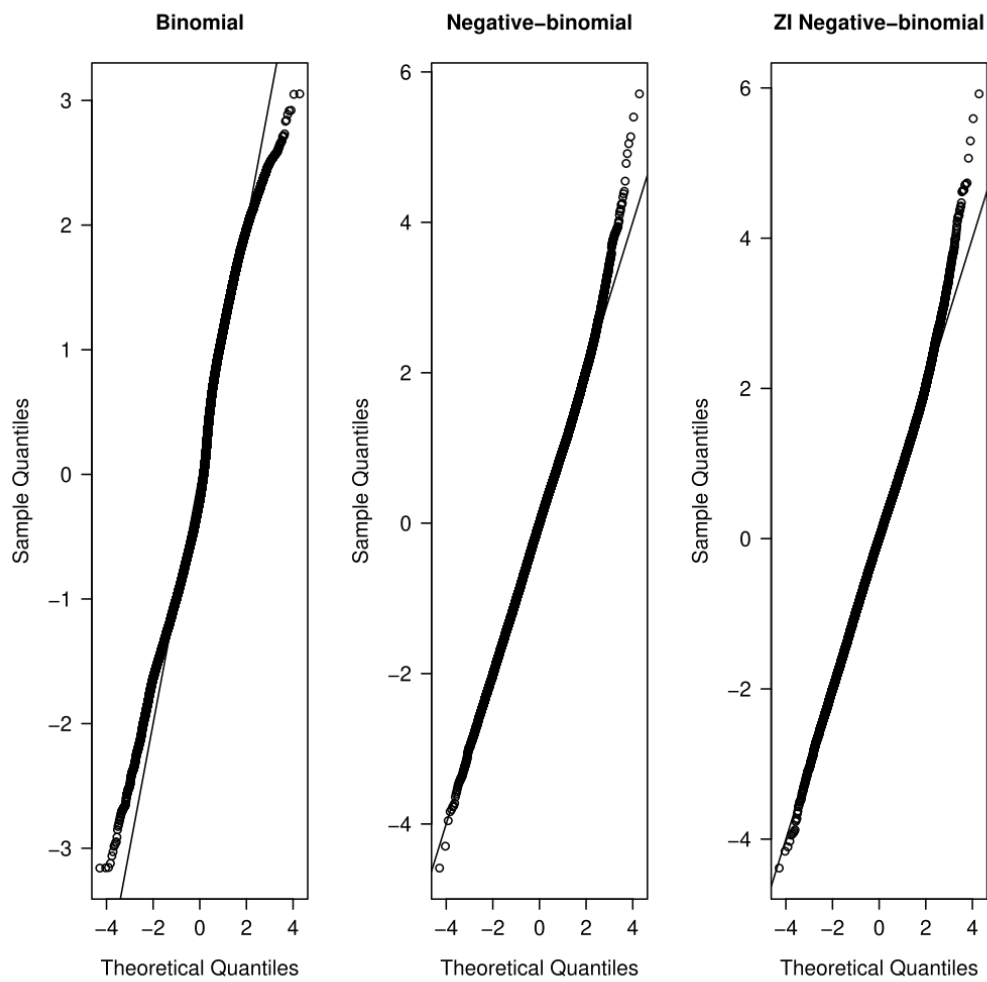


Figure B-116: Quantile residual diagnostics for the binomial component, as well as alternative CPUE standardisation models for combined DW low-latitudes (<35 degree South) fleet strata with positive catch.